UNIVERSIDADE FEDERAL DO RIO GRANDE DO SUL

INSTITUTE OF CHEMISTRY

PROGRAMA DE PÓS-GRADUAÇÃO EM QUÍMICA – PPGQ

ABOUT ALTERNATIVE STRATEGIES IN THE RUTHENIUM-CATALYSED OLEFIN METATHESIS

M.SC. LEONILDO ALVES FERREIRA

PORTO ALEGRE, OCTOBER 2016

UNIVERSIDADE FEDERAL DO RIO GRANDE DO SUL

INSTITUTE OF CHEMISTRY

PROGRAMA DE PÓS-GRADUAÇÃO EM QUÍMICA – PPGQ

M.SC. LEONILDO ALVES FERREIRA

ABOUT ALTERNATIVE STRATEGIES IN THE RUTHENIUM-CATALYSED OLEFIN METATHESIS

Thesis presented as a partial requirement to obtain the PhD degree in Chemistry

PROF. DR. HENRI STEPHAN SCHREKKER

Supervisor

PORTO ALEGRE, OCTOBER 2016

A presente tese foi realizada inteiramente pelo autor, exceto as colaborações as quais serão devidamente citadas nos agradecimentos, no período entre 03/2012 e 10/2016, no Instituto de Química da Universidade Federal do Rio Grande do Sul sob Orientação do Professor Doutor Henri Stephan Schrekker. A tese foi julgada adequada para a obtenção do título de Doutor em Química pela seguinte banca examinadora:

Comissão Examinadora:

Dr. Samuel Dagorne

Prof. Dra. Rosane Angélica Ligabue

Prof. Dr. José Eduardo Damas Martins

Prof. Dr. Osvaldo de Lázaro Casagrande Jr.

Prof. Dr. Henri Stephan Schrekker

M.Sc. Leonildo Alves Ferreira

i

ACKNOWLEDGEMENTS

I'm most grateful to M.Sc. Priscilla de Souza Lima, Ph.D Ricardo Keitel Donato and M.Sc. Renato Figueira da Silva. They were the first to welcome me in the journey that was to begin. Priscilla became one of my dearest friends. Countless were the after-lunch cups of coffee we drunk, and the talks we had about our projects (especially when things weren't working as we expected). These moments I cherish and appreciate.

I'm immensely grateful to my supervisor Henri Schrekker for the trust he has deposited in me, the liberty and the opportunities he bestowed me throughout these years. I would not have finished this work under different circumstances.

Throughout the years I stayed in the Laboratory of Technological Processes and Catalysis, several graduate students and post-doctoral fellows shared their Chemistry enthusiasm and knowledge with me. Most importantly, they tolerated me in my anger moments and made my days more joyful. Needless to say, several cups of coffee and, more recently, glasses of beer were drunk together. They are: Julia Couto, Angela Lopez-Vinasco, Yuri Sokolovicz, Joice Klitzke, Liliana do Amaral Soares, David Rivillo, Larissa Capeletti, Barbara Leal, Priscilla Lima, Ricardo Donato, Kazia Donato, Balaji Selukar, Vinicius Demetrio, Eduardo Karazinski and Juanita van Wyk.

In the period spent in the laboratory I also had the opportunity to work directly with some undergraduate students. Marcos Bergamin, Giulia Santin and Moema Scheffler were the young apprentices for whose I was the "responsible adult" in the laboratory. I hope I succeeded in helping you during your stay in the lab. Certainly, the experience taught me a lot. I include here all other undergraduate students that worked during this period in the laboratory.

During my PhD study, I had the opportunity to develop part of my project at the University of Ottawa, as part of a sandwich exchange program. For this I appreciate the scholarship granted by CAPES and thank Professor Deryn Fogg for receiving me at her laboratory. The period spent in Ottawa was awesome and I learned a lot about ruthenium chemistry and olefin metathesis. I also experienced a different culture which taught me to better enjoy life and its small moments.

I also thank CAPES for the scholarship received and the Chemistry Graduate Program for the opportunities I had during the doctorate period.

I thank all the technicians and employees of the Institute of Chemistry for their valuable assistance in any moment their help was necessary.

I also thank the members of the qualifying exam judging committee, Professor Piet van Leeuwen, Professor José Eduardo Damas and Professor Osvaldo Casagrande, for the valuable contributions they gave that helped to finish this work. I also thank in advance the members of the thesis defense for accepting the invitation.

Above all the acknowledgements, I want to thank all the support my family has been giving me all these years. To them I dedicate this work, because without their trust, teachings and support, this part of my trajectory would not be possible to be concluded.

To my family

ii

PUBLISHED PAPERS

Ferreira, L. A.; Schrekker, H. S. *Catal. Sci. Technol*., **2016**, *6*, 8138-8147.

i ACKNOWLEDGEMENTS v
ii PUBLISHED PAPERS vii
iii CONTENTS ix
iv LIST OF FIGURES xiii
v LIST OF SCHEMES xvii
vi LIST OF TABLES xxi
vii LIST OF ABBREVIATIONS AND SYMBOLS xxiii
viii LIST OF COMPOUNDS xxvii
xi ABSTRACT xxix
x RESUMO xxxi
1 INTRODUCTION 1
2 STATE OF THE ART 7
  2.1 OLEFIN METATHESIS 7
    2.1.1 Olefin cross-metathesis 10
  2.2 SYNTHESES OF COMPLEXES 11
    2.2.1 Benzylidene-type (pre)-catalysts 12
    2.2.2 Indenylidene-type (pre)-catalysts 15
  2.3 OLEFIN METATHESIS MECHANISMS 18
    2.3.1 Initiation mechanism 19
    2.3.2 Propagation 21
    2.3.3 Deactivation and decomposition 22
    2.3.4 Regeneration 25
  2.4 α,β-UNSATURATED CARBONYL COMPOUNDS 28
    2.4.1 Enoic-carbene complexes relevant to olefin metathesis 28

2.4.2 Other Metal-enoic carbene complexes 33
2.5 INDUSTRIAL OLEFIN METATHESIS 34
2.6 RENEWABLE OLEFIN METATHESIS 36
2.7 GENERAL CONSIDERATIONS ON CARBENES AND ALKYLIDENES 41
3 RESULTS AND DISCUSSION 43
3.1 CROSS-METATHESIS WITH MALEIC ACID 43
3.1.1 System optimization 43
3.1.2 Maleic acid vs maleates 54
3.1.3 Maleic acid versus acrylic acid 57
3.1.4 Vegetable oils as substrate 59
3.1.5 Monitoring the formation of a Ru-enoic carbene from the reaction of GII with MA-H 61
3.2 DEVELOPMENT OF A PHOSPHINE-FREE STRATEGY FOR THE SYNTHESIS OF RU-ALKYLIDENE COMPLEXES 75
3.2.1 *trans*-Dichlorotetrakis(pyridine)ruthenium(II) (*trans*-$RuCl_2(py)_4$) 75
3.2.2 Dichloro(*p*-cymene)ruthenium(II) dimer ([$RuCl_2$(*p*-cymene)]$_2$) 77
3.2.3 *cis*-Dichloro*tetrakis(*dimethylsulfoxide)ruthenium(II) (*cis*-$RuCl_2(DMSO)_4$) 85
4 CONCLUSIONS 93
4.1 CROSS-METATHESIS WITH MALEIC ACID 93
4.2 DEVELOPMENT OF A PHOSPHINE-FREE STRATEGY FOR THE SYNTHESIS OF RU-ALKYLIDENE COMPLEXES 95
5 EXPERIMENTAL 97
5.1 CROSS-METATHESIS WITH MALEIC ACID 97
5.2 MONITORING THE FORMATION OF A RU-ENOIC CARBENE FROM THE REACTION OF GII WITH MA-H 99
5.3 DEVELOPMENT OF A PHOSPHINE-FREE STRATEGY FOR THE SYNTHESIS OF RU-ALKYLIDENE COMPLEXES 100
6 APPENDICES 111

Appendix I Summary of different classes of alkylidenes 111

Appendix II Characteristic chemical shifts (^{13}C, ^{1}H and ^{31}P NMR) of selected 1,1-diphenylpropargyl alcohol derived ruthenium complexes. 112

Appendix III Selected Chromatograms 114

Appendix IV Formulae used to calculate the yield of CM products in reactions with vegetable oils 118

Appendix V Spectra 120

Appendix VI Manuscript published in *Catalysis Science and Technology* 129

7 REFERENCES 131

iv

LIST OF FIGURES

Figure 1 Effect of the addition of a catalyst to a hypothetical (R → P) reaction. In the catalysed reaction (dashed line) the largest free energy of activation ($\Delta G^{\ddagger}$) is much smaller than the free energy of activation for the uncatalysed reaction (continuous line). 1

Figure 2 Second-generation Grubbs (**GII**) and Hoveyda-Grubbs (**HGII**) metathesis (pre)-catalysts. 3

Figure 3 Selected examples of olefin metathesis (pre)-catalysts. 9

Figure 4 General trends in the functional group tolerance of titanium-, tungsten-, molybdenum- and ruthenium-based alkylidenes. 10

Figure 5 Olefin categorization and rules for selectivity in cross-metathesis. 11

Figure 6 Experiment used to demonstrate the validity of the *boomerang* mechanism. a) CM of anethole with methyl acrylate catalysed by **HGII** in the presence of ^{i}**PrOstyr***. b) Time scale equilibration of ^{i}**PrOstyr*** in the absence of substrate. 27

Figure 7 Selected examples of compounds prepared using olefin cross-metathesis with acrylates. 29

Figure 8 Free Gibbs reaction energy profiles of the RCM of cyclohexene by complexes **GII** (top) and **Ru-18** (bottom, bold lines). 31

Figure 9 a) CM of *cis*-4-octene with **MA-H** promoted by **GII**; b) the two possible alkylidene intermediates generated in the reaction. c) SM of **MA-H**. 32

Figure 10 Examples of some isolated enoic carbene complexes. 33

Figure 11 Structure of the Hepatitis C Virus (HCV) drug Simeprevir developed by Medivir and Johnson & Johnson and sold under the name of Olysio^{TM}. Inside the box, the conditions used in the metathesis step. 36

Figure 12 General properties of Schrock and Fischer alkylidenes and NHC carbenes. 42

Figure 13 Time-dependent plots of the effect of the **MO** purification procedure on the product distribution in the CM of **MO** with **MA-H** catalyzed by **GII**. 46

Figure 14 Effect of the substrates concentration on the cross-metathesis of **MO** with **MA-H** using (pre)-catalyst **GII**. 49

Figure 15 Effect of the temperature on the CM of **MO** with **MA-H**. 50

Figure 16 (Pre)-Catalysts employed in the CM of **MO** with maleic and acrylic acid derivatives. 51

Figure 17 Influence of the (pre)-catalyst on the CM of **MO** with **MA-H** a); and time-dependent plots of: b) the conversion of **MO** and c) the yield of the CM products. 53
Figure 18 Cross-metathesis partner scope. 54
Figure 19 a) Influence of the CM partner on the conversion (blue bars) and yields of CM (dashed green bars) and SM (dashed red bars) of the reaction with **MO** – **MA-H** vs **MA-Me** and **MA-^{i}Pent**. b) Time-dependent plots using **GII** and **HGII**, respectively. 56
Figure 20 a) Influence of the CM partner on the conversion (blue bars) and yields of CM (dashed green bars) and SM (dashed red bars) of the reaction with **MO** – **MA-H** vs **AA-H** and **AA-Me**. b) Time-dependent plots using **GII** and **HGII**, respectively. 58
Figure 21 General structure of a triglyceride with the most common fatty acid side chains and the global market consumption of vegetable oils in 2014/15 (100 % = 175.65 million metric tons). 60
Figure 22 Effect of the vegetable oil composition on the yield of the CM products. 61
Figure 23 ^{1}H NMR spectra (300 MHz, THF-d_8, 20 °C) of the reaction of **GII** (10 mg, 0.0118 mmol) and **MA-H** (0.07 mmol). 62
Figure 24 a) Staggered ^{1}H NMR spectra (300 MHz, THF-d_8, 20 ºC) of the alkylidene region in the reaction of **GII** with **MA-H**; **b)** time-dependant plot of the variation of the alkylidenic signals in the ^{1}H spectra; **c)** plot of the ln of %**GII** versus time. 64
Figure 25 Examples of second-generation ruthenium alkylidene complexes exhibiting a small coupling $^{3}J_{P,H}$. 65
Figure 26 Staggered ^{1}H NMR spectra (300 MHz, THF-d_8, 20 ºC) of the aromatic and olefinic regions in the reaction of **GII** and **MA-H**. 65
Figure 27 a) Staggered ^{31}P{^{1}H} NMR spectra (121.5 MHz, THF-d_8, 20 °C) in the reaction of **GII** with **MA-H**; **b)** time-dependant plot of the variation of intensity of the signals in the ^{31}P{^{1}H} spectra; and **c)** plot of the ln of %**GII** versus time..........................67
Figure 28 ^{31}P{^{1}H} NMR spectrum (101 MHz, THF-d_8) of the reaction between **MA-H** and PCy_3. 67
Figure 29 ^{1}H NMR spectrum (300 MHz, THF-d_8) of the reaction between **MA-H** and PCy_3. The ^{1}H NMR spectrum of PCy_3 is shown in the inset at the top. 68
Figure 30 ^{13}C{^{1}H} NMR spectrum (100 MHz, THF-d_8) of the compound **Ru-CHCO$_2$H**. 71
Figure 31 Characteristic ^{13}C resonances observed for the compound **Ru-CHCO$_2$H** and examples of other complexes with similar ligands. 72
Figure 32 Expansion of the ^{1}H-^{13}C HSQC spectrum showing the correlation of the alkylidenic hydrogen signal at 18.61 ppm with the carbon resonance at 290.11 ppm. ..73

Figure 33 Expansion of the ^1H-^{13}C HMBC spectrum showing the correlation of the alkylidenic hydrogen signal at 18.61 ppm with the carbon resonance at 169.42 ppm....74

Figure 34 ^1H NMR spectra ($CDCl_3$, 300 MHz) of *trans*-$RuCl_2(py)_4$ (left) and after heating overnight at 55 °C with 1,1-diphenylpropargyl alcohol (right)...77

Figure 35 ^1H NMR spectrum ($CDCl_3$, 300 MHz) of the dimer [$RuCl_2$(*p*-cymene)]$_2$.........78

Figure 36 ^1H NMR spectra ($CDCl_3$, 300 MHz) of $RuCl_2$(*p*-cymene)(IMes) (a) and $RuCl_2$(*p*-cymene)(H_2IMes) (b). 80

Figure 37 Loss of *p*-cymene in the complex $RuCl_2$(*p*-cymene)(H_2IMes) in the presence of light. Asterisks (*) indicate the signals from free *p*-cymene. 81

Figure 38 Loss of *p*-cymene in the complex $RuCl_2$(*p*-cymene)(H_2IMes) in the absence of light. Asterisks (*) indicate the signals from free *p*-cymene. 81

Figure 39 ^1H NMR spectra of the reaction between $RuCl_2$(*p*-cymene)(IMes) and 1,1-diphenylpropargyl alcohol in CD_3OD at room temperature. 83

Figure 40 Inset of the ^1H NMR spectra of the reaction between $RuCl_2$(*p*-cymene)(IMes) and 1,1-diphenylpropargyl alcohol in CD_3OD at room temperature showing the aliphatic region..84

Figure 41 ^1H NMR spectrum ($CDCl_3$, 300 MHz) of *cis*-$RuCl_2(DMSO)_4$ showing the signals of *S*-coordinated, *O*-coordinated and free DMSO. 86

Figure 42 ^1H NMR spectra ($CDCl_3$; 300 MHz) of the reaction between *cis*-$RuCl_2(DMSO)_4$ and 1,1-diphenylpropargyl alcohol. Full spectra (a) and inset of the region containing the signals from DMSO and propargyl alcohol methynic (2.88 ppm) protons (b). 88

Figure 43 Insets of the ^1H (300 MHz, $CDCl_3$ - left) and ^{13}C (75.5 MHz, $CDCl_3$ - right) NMR spectra showing resonances that are likely from a mixture of alkenylcarbyne complexes...89

Figure 44 Insets of the ^1H (left) and $^{13}C\{^1H\}$ (right) NMR spectra of the crude mixture obtained in the reaction of *cis*-$RuCl_2(DMSO)_4$ and 1,1-diphenylpropargyl alcohol in boiling THF in the presence of 20 mol% (vs [Ru]) of HCl. 91

Figure 45 Insets from the ^1H-^{13}C HMQC (a) and ^1H-^{13}C HMBC (b) spectra of the crude mixture obtained in the reaction of *cis*-$RuCl_2(DMSO)_4$ and 1,1-diphenylpropargyl alcohol with 20 mol% of HCl (vs [Ru]), showing the correlations of the singlet at $\delta = 5.36$ ppm with the carbon resonances at 113.4 and 186.8 ppm, respectively. 91

Figure 46 Chromatogram of methyl oleate. 114

Figure 47 Typical chromatograms obtained in the cross-metathesis of **MO** with **MA-H** (after derivatization). 116

Figure 48 Typical ^{1}H NMR spectrum of a vegetable oil with the signal attributions and the formulae used to calculate the molecular weight and number of C=C double bonds per triglyceride. 118

Figure 49 Inset of the olefinic region of a typical ^{1}H NMR spectrum of the CM of vegetable oils with **MA-H** with the signal attributions and the formula used to calculate the yield of cross-metathesis products. 119

V

LIST OF SCHEMES

Scheme 1 Olefin metathesis of a generic olefin promoted by a metal-alkylidene catalyst (a) and the generally accepted mechanism of the reaction (for simplification, a non-productive cycle is depicted) (b). 2

Scheme 2 Schematic representation of the general objectives of this work. Cross-metathesis of vegetable oil derivatives with **MA-H** (a) and the development of a phosphine-free strategy for the synthesis of **HGII**. 5

Scheme 3 Simplistic representation of the olefin metathesis mechanism. 7

Scheme 4 Different types of transformations in olefin metathesis (with selected examples) and the driving force(s) for each transformation. 8

Scheme 5 Different synthetic routes to prepare ruthenium alkylidene complexes structurally similar to the first-generation Grubbs metathesis (pre)-catalyst (**GI**). 12

Scheme 6 General synthetic route used for the preparation of ruthenium-benzylidene complexes active in olefin metathesis. 14

Scheme 7 Selected examples of variations of the **HGII** complex resulting in improved activity/stability (top) or enantio- and regioselectivity (bottom). 15

Scheme 8 General synthetic route employing 1,1-diphenylpropargyl alcohol as alkylidene source in the synthesis of ruthenium-indenylidene complexes active in olefin metathesis. 16

Scheme 9 Two-step synthesis and possible transformations of ‘third-generation’ indenylidene complexes (**IndIII`**). 17

Scheme 10 Main steps involved in the formation of ruthenium-indenylidene complexes from 1,1-diphenylpropargyl alcohol. 18

Scheme 11 Steps involved in the olefin metathesis reaction catalyzed by ruthenium complexes. 19

Scheme 12 Initiation mechanism for the ruthenium-based metathesis catalysts of the a) Grubbs and b) Hoveyda-Grubbs types. 20

Scheme 13 Propagation mechanism of the ruthenium-based olefin metathesis catalysts. 22

Scheme 14 Decomposition of **GIIm** into a dinuclear complex. Inside the dashed box, the proposed decomposition mechanism. 24

Scheme 15 Michael addition chemistry that results in the decomposition of **HGII** in the presence of added PCy_3. 25
Scheme 16 Fortuitous discovery of chelating etherbenzylidene ruthenium metathesis (pre)-catalyst **HGI**. a) RO/CM of ^{i}**PrOstyr** with 3-phenoxy-*cis*-cyclooctene; b) synthesis of **HGI**. 26
Scheme 17 The release-return (*boomerang*) mechanism for chelating ether-benzylidene ruthenium complexes. 26
Scheme 18 Synthesis of ruthenium enoic carbene complexes by double oxidative addition reported by Grubbs and the decomposition constants (k_{dec}) in C_6D_6 at room temperature. 29
Scheme 19 Speculative initial step in the decomposition of the Ru-enoic carbene complexes reported by Grubbs. 30
Scheme 20 Decomposition of diazocompounds in the preparation of enoic carbene complexes and the use of *in situ* generated complexes for ROMP (**a**); olefin cyclopropanation (**b**) and carbonyl olefination (**c**). 34
Scheme 21 Biorefinery process developed by Elevance Renewable Sciences® using olefin metathesis as key step in the valorization of bio-oils. 35
Scheme 22 ROMP of the sesquiterpenes caryophyllene and humulene. 37
Scheme 23 Metathesis transformations of lactonic sophorolipid. 38
Scheme 24 ROMP of an itaconic acid derived norbornene. 38
Scheme 25 Synthesis of the monomer 1,3-hexadiene from plant oils. 39
Scheme 26 Cross metathesis of fatty acid derivatives with acrylates, acrolein and acrylonitrile. 40
Scheme 27 CM of essential oils with acrylate esters. 40
Scheme 28 CM of methyl oleate (**MO**) with maleic acid (**MA-H**). 43
Scheme 29 CM of **MO** with **MA-H**. 47
Scheme 30 Proposed reaction that occurred between **MA-H** and PCy_3. 69
Scheme 31 Schematic representation of the reaction between **GII** and **MA-H** resulting in the formation of the Ru-enoic carbene complex. 70
Scheme 32 Two-step synthesis and possible transformations of 'third-generation' indenylidene complexes (**IndIII`**). 75
Scheme 33 Synthesis of half-sandwich $RuCl_2$(*p*-cymene)(NHC) complexes. 78
Scheme 34 Cationic RuCl(*p*-cymene)(diphenylallenylidene)(NHC) complexes. 82
Scheme 35 Attempted one pot synthesis of **HGII** from $RuCl_2$(*p*-cymene)(NHC). 85

Scheme 36 Attempted synthesis of an indenylidene complex from *cis*-$RuCl_2(DMSO)_4$. 87

Scheme 37 Ruthenium allenylidene-to-indenylidene rearrangement via the formation of an alkenylcarbyne intermediate. 90

LIST OF TABLES

Table 1 Selected examples of industrially relevant applications of olefin metathesis. ...35

Table 2 Influence of the **MO** purification method on the **GII**-catalyzed CM of **MO** with **MA-H**. 45

Table 3 Effect of the **MO**:**MA-H** molar ratio on the **GII**-catalyzed CM of **MO** with **MA-H**. 48

Table 4 Effect of the catalyst on the CM of **MO** with **MA-H**. 52

Table 5 ^{13}C NMR chemical shifts of the olefinic ($\delta_{C=C}$) and carbonylic ($\delta_{C=O}$) carbons of **MA-H**, **MA-Me** and **Ma-^{i}Pent**....................55

Table 6 Composition of the vegetable oils used. 59

Table 7 Conditions tested to prepare a Ru-indenylidene complex from *trans*-$RuCl_2(py)_4$. 76

vii

LIST OF ABBREVIATIONS AND SYMBOLS

Abbreviations of compounds are repeated in the list of compounds (page xxvii).

□ – Vacant site, available for coordination of a ligand or substrate.

α - First position in relation to a specific group or atom.

β - Second position in relation to a specific group or atom.

γ - Third position in relation to a specific group or atom.

δ - Chemical shift, given in ppm (parts per million - NMR).

η - Hapticity, refers to the number of donor atoms coordinated to a metal center

μ - Bridging, refers to a same donor atom coordinated to two or more metal centers.

$\boldsymbol{\Delta_r G^\circ}$ - General standard Gibbs-free energy.

$\Delta G^\ddagger$ - Free energy of activation.

ω - Last position in relation to a specific group or atom.

AA-H - Acrylic acid.

AA-Me - Methyl acrylate.

ADMET - Acyclic diene metathesis polymerization.

ATR - Attenuated total reflectance (Infrared).

CM - Cross-metathesis.

$^{13}C\{^1H\}$ NMR - Hydrogen decoupled, carbon^{13} nuclear magnetic resonance.

d - Doublet (NMR).

dd - Double doublet (NMR).

dt - Double triplet (NMR).

e^- - Electron.

E - Refers to the arrangement of the two groups of higher priority in a C=C bond displaced in opposite sides to each other.

ESI - Electrospray ionization.

FAME - Fatty acid methyl ester.

FID - Flame ionization detector.

GC - Gas chromatography.

GI - First-generation Grubbs metathesis (pre)-catalyst.

GII - Second-generation Grubbs metathesis (pre)-catalyst.

H$_2$IMes - 1,3-Bis(2,4,6-trimethylphenyl)-4,5-dihydroimidazol-2-ylidene.

HGI - First-generation Hoveyda-Grubbs metathesis (pre)-catalyst.

HGII - Second-generation Hoveyda-Grubbs metathesis (pre)-catalyst.

^{1}H NMR – Hydrogen^{1} nuclear magnetic resonance.

^{1}H-^{13}C HMBC - ^{1}H-^{13}C heteronuclear multiple bond correlation.

^{1}H-^{13}C HMQC - ^{1}H-^{13}C heteronuclear multiple quantum coherence.

^{1}H-^{13}C HSQC - ^{1}H-^{13}C heteronuclear single quantum coherence.

IMes - 1,3-Bis(2,4,6-trimethylphenyl)imidazol-2-ylidene.

IndI - Dichloro(3-phenyl-1H-inden-1-ylidene) bis(tricyclohexylphosphine)ruthenium(II).

IndII - [1,3-Bis(2,4,6-trimethylphenyl)-2-imidazolidinylidene] dichloro(3-phenyl-1H-inden-1-ylidene)(tricyclohexylphosphine)ruthenium(II).

IUPAC - International Union of Pure and Applied Chemistry (International federation that standardizes nomenclature in chemistry and other fields of science).

J - Coupling constant, given in Hz (NMR).

L - General representation of a neutral ligand that donates 2 electrons to a metal center.

Litre.

m - multiplet (NMR).

MA-H - Maleic acid.

MA-Me - Dimethyl maleate.

MA-^{i}Pent - Diisopentyl maleate.

MO - Methyl oleate.

MPI - 1-Methylene-3-phenyl-1H-indene.

MS - Mass spectrometry.

NHC - *N*-Heterocyclic carbene.

^{31}P{^{1}H} NMR - Hydrogen decoupled, phosphorus^{31} Nuclear Magnetic Resonance;

^{i}PrOstyr - 2-isopropoxystyrene.

PTFE - Polytetrafluorethylene.

q - Quartet (NMR).

qd - Quadruple doublet (NMR).

RCM - Ring-closing metathesis.

R_f - Retention factor.

RO/CM - Ring-opening/cross-metathesis.

ROMP - Ring-opening metathesis polymerization.

s - Singlet (NMR).

sept - Septet (NMR).

SM - Self-metathesis.

t - Triplet (NMR).

TON - Turnover number. Measurement of the productivity of a catalyst. Defined as the average number of catalytic cycles per catalytic specie. Dimensionless.

Um42 - [1,3-Bis(2,4,6-trimethylphenyl)-2-imidazolidinylidene]-[2-[[(2-methylphenyl) imino]methyl]-phenolyl]-[3-phenyl-1H-inden-1-ylidene](chloro)ruthenium(II).

Z - refers to the arrangement of the two groups of higher priority in a C=C bond displaced at the same side.

viii LIST OF COMPOUNDS

List of selected compounds mentioned throughout the thesis.

Abbreviation / Symbol	**Name**	**Structure**
1	1,1-Diphenylpropargyl alcohol	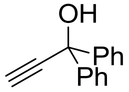
AA-H	Acrylic acid	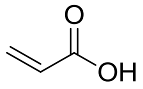
AA-Me	Methyl acrylate	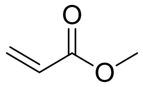
GI	First-generation Grubbs metathesis (pre)-catalyst	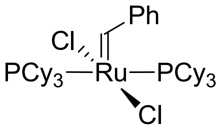
GII	Second-generation Grubbs metathesis (pre)-catalyst	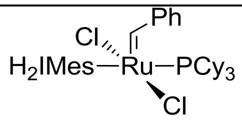
HGI	First-generation Hoveyda-Grubbs metathesis (pre)-catalyst	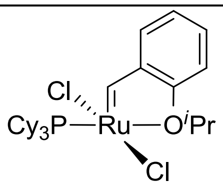
HGII	Second-generation Hoveyda-Grubbs metathesis (pre)-catalyst	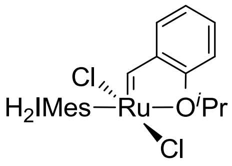
H_2IMes	1,3-Bis(2,4,6-trimethylphenyl)-4,5-dihydroimidazol-2-ylidene	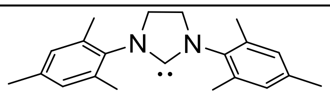

IndII	[1,3-Bis(2,4,6-trimethylphenyl)-2-imidazolidinylidene] dichloro(3-phenyl-1H-inden-1-ylidene)(tricyclohexylphosphine)ruthenium(II)	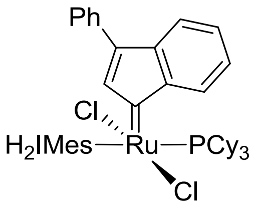
MA-H	Maleic acid	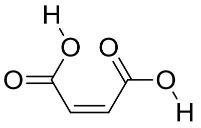
MA-Me	Dimethyl maleate	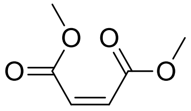
MA-*i*Pent	Diisopentyl maleate	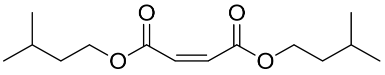
MO	Methyl oleate	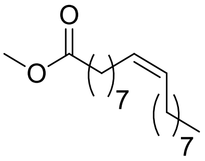
P1	11-Methoxy-11-oxoundec-2-enoic acid	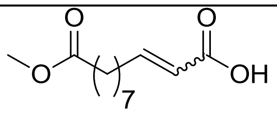
P2	2-Undecenoic acid	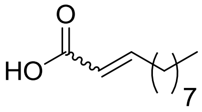
***i*PrOstyr**	2-Isopropoxystyrene	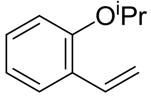
Um42	[1,3-Bis(2,4,6-trimethylphenyl)-2-imidazolidinylidene]-[2-[[(2-methylphenyl) imino]methyl]-phenolyl]-[3-phenyl-1H-inden-1-ylidene](chloro)ruthenium(II)	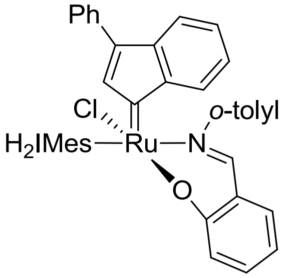

The versatility of the olefin metathesis reaction was explored in the work described herein, pursuing two different strategies for new alternatives in the ruthenium-catalyzed reaction. In the first part is described the use of maleic acid (**MA-H**) as an alternative to the use of acrylate esters in the cross-metathesis (CM) to produce α,β-unsaturated carboxylic compounds. Therefore, the reaction of methyl oleate (**MO**) with **MA-H** was investigated, optimizing a series of parameters such as the **MO** purification method, **MO**:**MA-H** ratio, temperature, time, and concentration. All reactions were monitored over the course of 70 minutes. Commercially available ruthenium metathesis (pre)-catalysts were employed. The second-generation Grubbs (**GII**) and Hoveyda-Grubbs (**HGII**) metathesis (pre)-catalysts displayed the best results. The CM of **MO** with **MA-H** using 0.05 mol% of **GII** or **HGII** resulted in conversions of 92 and 88 % and selectivity towards the CM products of 89 and 78%, respectively. Further studies employing acrylic acid (**AA-H**) and methyl acrylate (**AA-Me**) with the phosphine-containing (pre)-catalyst **GII** showed that the formation of a ruthenium-methylidene propagating specie has a detrimental effect on the outcome of the reaction. Such specie is completely avoided when **MA-H** is used as CM-partner. Moreover, bulkier alkoxy-substituents also jeopardize both conversion and yield of the reaction. Additionally, the use of unsaturated vegetable oils was investigated as an alternative to the direct use of **MO** in the reaction with **MA-H**. The use of vegetable oils as substrates was found to have no detrimental effect on the reaction.

The reaction of **GII** with **MA-H** was investigated by NMR spectroscopy (^{1}H and ^{31}P{^{1}H}) in THF-d_8 at 20 ºC, which proceeded slowly over the course of 7 hours with observed first order kinetics. Disappearance of **GII** with concomitant formation of a new alkylidenic complex was observed. ^{13}C{^{1}H} NMR and 2D techniques (^{1}H-^{13}C HSQC and ^{1}H-^{13}C HMBC) confirmed the formation of a ruthenium-enoic carbene complex. A ruthenium-enoic carbene intermediate is the propagating specie of the CM reaction of **MO** with **MA-H** and also of other olefin metathesis reactions involving acrylates. This was the first time such specie could be observed and characterized spectroscopically.

The second part of this work investigated alternative synthetic routes to the second-generation Hoveyda-Grubbs (pre)-catalyst (**HGII**) that avoid the use of sacrificial phosphines and diazo compounds as the alkylidene source. Three different ruthenium

precursors were applied in the reaction with 1,1-diphenylpropargyl alcohol (source of the alkylidene ligand). The precursor *trans*-$RuCl_2(py)_4$ was found to be inert towards the reaction with the propargylic alcohol. Reaction of the dimeric precursor [$RuCl_2$(*p*-cymene)$]_2$ with the *N*-heterocyclic carbenes **IMes** (1,3-bis(2,4,6-trimethylphenyl)imidazol-2-ylidene) and **H_2IMes** (1,3-bis(2,4,6-trimethylphenyl)-4,5-dihydroimidazol-2-ylidene) afforded the corresponding monomeric complexes $RuCl_2$(*p*-cymene)IMes (**Ru-35a**) and $RuCl_2$(*p*-cymene)H_2IMes (**Ru-35b**), which decompose in solution with loss of the *p*-cymene ligand. Both compounds **Ru-35a,b** reacted with 1,1-diphenylpropargyl alcohol but decomposition occurred during the reaction, which circumvented the isolation of the corresponding products. The precursor *cis*-$RuCl_2(DMSO)_4$ reacted with 1,1-diphenylpropargyl alcohol but formed a complex mixture of products, which did not allow the isolation of the desired compound. Independent of the ruthenium precursor, none of the routes investigated resulted in the development of a new synthetic strategy for the synthesis of **HGII**.

X

RESUMO

A versatilidade da reação de metátese de olefinas foi explorada no presente trabalho de duas formas diferentes. Em ambas as formas buscou-se novas alternativas para a metátese de olefinas catalisada por complexos de rutênio. Na primeira parte do trabalho, ácido maleico (**MA-H** – do inglês *Maleic acid*) é descrito como uma alternativa ao uso de ésteres de acrilato na metátese cruzada (CM – do inglês *cross-metathesis*) para preparar compostos carboxílicos α,β-insaturados. Portanto, a reação entre oleato de metila (**MO** – do inglês *methyl oleate*) com **MA-H** foi investigada, otimizando diversos parâmetros de reação como o método de purificação do **MO**, razão **MO**:**MA-H**, temperatura, tempo, concentração e tipo de (pre)-catalisador. Todas as reações foram monitoradas por um período de 70 minutos. Quatro (pré)-catalisadores de rutênio comercialmente disponíveis foram utilizados. Os (pré)-catalisadores de Grubbs (**GII**) e Hoveyda-Grubbs (**HGII**) de segunda geração apresentaram os melhores resultados. Reações de CM entre **MO** e **MA-H** usando 0.05 mol% de **GII** ou **HGII** resultaram em conversões de 92 e 88 % e seletividade para os produtos de metátese cruzada de 89 e 78 %, respectivamente. Estudos adicionais utilizando ácido acrílico (**AA-H** – do inglês *acrylic acid*) e acrilato de metila (**AA-Me** – do inglês *methyl acrylate*) foram efetuados e mostraram que para o complexo **GII**, o qual dissocia um ligante fosfina (PCy_3) em sua etapa de iniciação, a formação de espécies propagantes do tipo rutênio-metilideno acarretam em um efeito detrimental para a reação (a formação de espécies propagantes rutênio-metilideno é totalmente evitada utilizando **MA-H** como substrato). Além disso, para os respectivos ésteres, grupos alcóxidos volumosos prejudicam ambos os rendimento e conversão da reação. Posteriormente, óleos vegetais insaturados foram investigados como alternativa ao uso de **MO** na reação com **MA-H**. Nas reações utilizando óleos vegetais observou-se que o uso de tais substratos não acarretam efeitos detrimentais para a reação.

A reação entre **GII** com **MA-H** foi investigada por espectroscopia de ressonância magnética nuclear (RMN de ^{1}H e de $^{31}P\{^{1}H\}$) em THF-d_8 à 20 ºC. A reação ocorreu lentamente por um período de 7 horas com cinética observada de primeira ordem. O consumo de **GII** com a formação concomitante de um novo complexo alquilidênico foi observado. Os espectros de RMN $^{13}C\{^{1}H\}$, ^{1}H-^{13}C HSQC e ^{1}H-^{13}C HMBC claramente mostraram a formação de um complexo rutênio-carbeno enoico. A espécie rutênio-

carbeno enoico é a espécie propagante da reação de CM entre **MO** e **MA-H** e também de outras reações de metátese de olefinas envolvendo acrilatos. Esta foi a primeira vez que tal espécie foi observada via reação de metátese e caracterizada espectroscopicamente

Na segunda parte do trabalho, rotas sintéticas alternativas para a síntese do (pré)-catalisador de Hoveyda-Grubbs de segunda geração (**HGII**) que não envolve o uso de fosfinas de sacrifício e diazo compostos foi investigada. Três precursores de rutênio foram estudados na reação com álcool 1,1-difenilpropargílico como fonte do alquilideno. O precursor *trans*-$RuCl_2(py)_4$ mostrou-se inerte frente à reação com o álcool propargílico. A reação do precursor dimérico de rutênio $[RuCl_2($*p*-cimeno$)]_2$ com os carbenos *N*-heterocíclos **IMes** (1,3-bis(2,4,6-trimetilfenil)imidazol-2-ilideno) e **H_2IMes** (1,3-bis(2,4,6-trimetilfenil)-4,5-dihidroimidazol-2-ilideno) resultou na formação dos complexos monoméricos $RuCl_2$(*p*-cimeno)IMes (**Ru-35a**) e $RuCl_2$(*p*-cimeno)H_2IMes (**Ru-35b**), respectivamente, os quais decompôem-se em solução com perda do ligante *p*-cimeno. Os compostos **Ru-35a,b** reagem com álcool 1,1-difenilpropargílico, porém, observou-se que os produtos se decompuseram durante a reação, impossibilitando a isolação dos produtos. O precursor *cis*-$RuCl_2(DMSO)_4$ reagiu com álcool 1,1-difenilpropargílico resultando em uma mistura complexa de produtos, a qual não foi possível isolar e analisar adequadamente. Nenhuma das rotas usando os três precursores de rutênio investigados resultou no desenvolvimento de uma nova estratégia sintética para a síntese de **HGII**.

“It has the words *Don`t Panic* inscribed in large friendly letters on its cover”

Douglas Adams

“The Hitch Hiker`s Guide to the Galaxy”

The fast growing population and its consequent increasing consumption of raw materials for chemicals, energy and materials demands the search for alternative sources and the better usage of the existing ones. Nowadays, this is a constant concern that likely tends to persist in the future.[1] In the context of better use of the existing raw materials, catalysis plays a key role. The use of a catalyst allows novel transformations and to obtain a target compound in shorter periods, resulting in overall energy economy. Besides, selectivity towards a sole product (chemo-, regio-, stereoselectivity) can be achieved.[2]

Catalysis is the increase in the reaction rate promoted by the use of a specific substance, defined as the catalyst. The catalyst does not change the reaction general standard Gibbs-free energy ($\Delta_r G°$). This increase in the reaction rate occurs due to a decrease in the free energy of activation ($\Delta G^‡$) (**Figure 1**).[3]

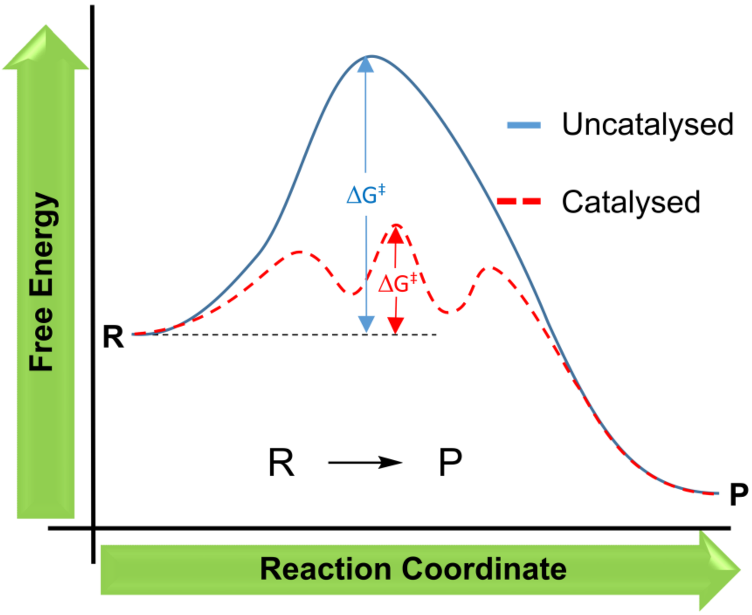

Figure 1 Effect of the addition of a catalyst to a hypothetical (R → P) reaction. In the catalysed reaction (dashed line) the largest free energy of activation (ΔG‡) is much smaller than the free energy of activation for the uncatalysed reaction (continuous line).

Olefins are probably the most important building blocks in industry for the manufacturing of commodities, specialties and fine chemicals, as these can be converted by several catalytic transformations (hydroformylation, oligo- and polymerization, olefin metathesis, epoxidation, hydrogenation, among others), resulting in a large variety of compounds with applications in basically everything the modern society demands. Amongst these transformations, the olefin metathesis is a very versatile reaction from both academic and industrial point of view. Olefin metathesis has revolutionized the way chemists create carbon-carbon bonds.[4-6] The reaction is formally an alkylidene scrambling promoted by a metal-alkylidene (metal = W, Mo, Re, Ru) and proceeds through a metallacyclobutane intermediate as proposed by Hérisson and Chauvin in 1971 (**Scheme 1a**).[7] The main steps involved in the olefin metathesis mechanism are (i) olefin coordination to an unsaturated metal-alkylidene (**1-B**); (ii) [2 + 2] cycloaddition to form a metallacyclobutane intermediate (**1-C**); (iii) cycloreversion of the metallacyclobutane to form either a new olefin and metal-alkylidene (productive metathesis) or regenerate the original species (non-productive metathesis) (**1-B'**); and (iv) dissociation of the (newly) formed olefin from the metal-alkylidene (**Scheme 1b**).

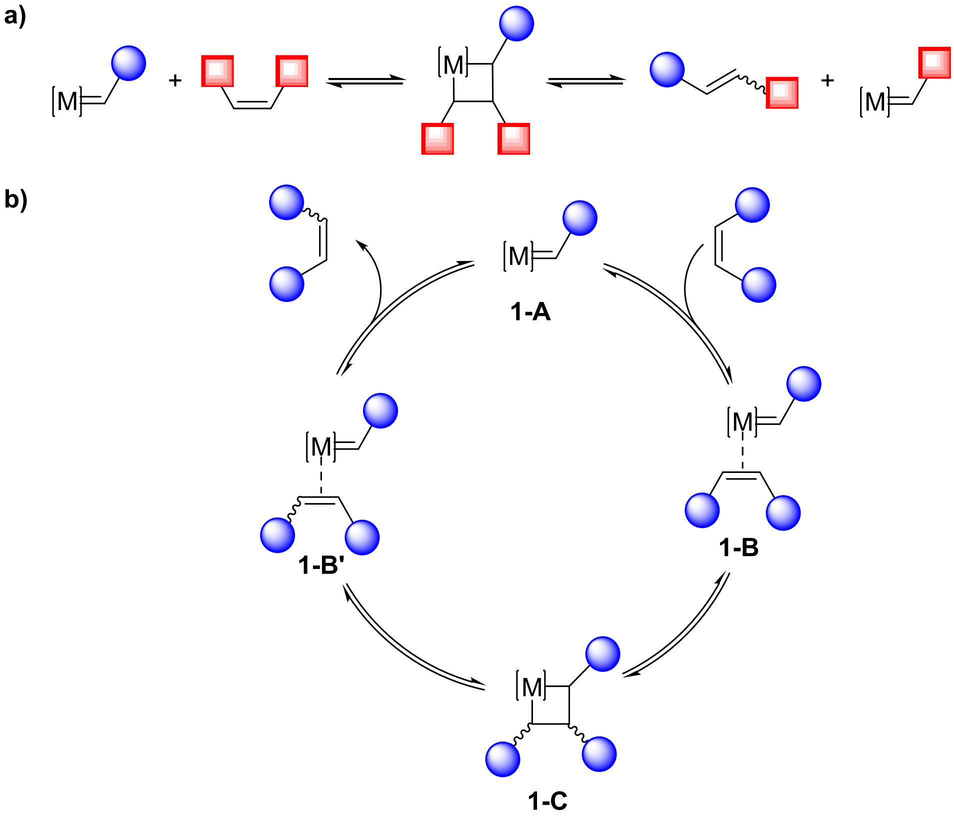

Scheme 1 Olefin metathesis of a generic olefin promoted by a metal-alkylidene catalyst (a) and the generally accepted mechanism of the reaction (for simplification, a non-productive cycle is depicted) (b).

Driven by the proposal of the metal-alkylidene mechanism, molecular well-defined catalysts were developed shortly after by Richard Schrock`s (Mo- and W-based)[8, 9] and Robert Grubbs` (Ru-based)[10] groups, resulting in the synthesis of a large variety of complexes active in olefin metathesis (some commercially available). Several of these complexes (most of them Ru-based) are very robust towards functional groups containing oxygen and (in a few cases) some nitrogen-containing functional groups,[11] allowing their use in the transformation of naturally occurring substrates such as unsaturated fatty acids (and the corresponding esters), [12-14] essential oils (e.g. eugenol, isoeugenol), [15] terpenes (e.g. limonene, pinenes),[16,17] among others.

The use of vegetable oil derivatives as substrates for olefin metathesis has gained attention for several years, especially after the development of the robust ruthenium (pre)-catalysts. The metathesis reactions mostly studied using vegetable oils derivatives include ethenolysis, self-metathesis and cross-metathesis (CM) of methyl oleate with α-functionalized terminal olefins. Recently, Elevance Renewable Sciences® announced the beginning of operation of an industrial plant based on the self-metathesis of fatty acid derivatives to produce olefins, specialty chemicals and oleochemicals.[18]

Although a large variety of ruthenium metathesis (pre)-catalysts has been reported so far, few are the ones that exhibit remarkable activity and robustness to varying reaction conditions. Amongst these complexes, two are noteworthy: the second-generation Grubbs metathesis (pre)-catalyst (**GII**) and the analogous second-generation Hoveyda-Grubbs metathesis (pre)-catalyst (**HGII**) (**Figure 2**).[i]

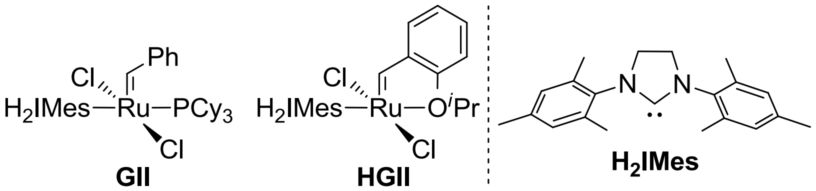

Figure 2 Second-generation Grubbs (**GII**) and Hoveyda-Grubbs (**HGII**) metathesis (pre)-catalysts.

For benchmark substrates (e.g. diethyl diallylmalonate) both **GII** and **HGII** show a similar catalytic performance, nevertheless, exceptions have been reported for both complexes.[19] A noteworthy exception is the CM of acrylates. **HGII** is found to be a much more effective (pre)-catalyst in a number of reactions involving the cross-metathesis with acrylate esters. For instance, Meier reported that the CM of methyl oleate (**MO**) with methyl acrylate is more efficient with **HGII**, resulting only in the formation of the target cross-metathesis products (methyl 2-undecenoate and dimethyl 2-undecenoate), while **GII** is less selective and the self-metathesis (SM) products of **MO** (9-octadecene and dimethyl 9-octadecenoate) were also observed.[13] The α,ω-diester, dimethyl 2-undecenedioate, and the monoester, methyl 2-undecenoate, are useful substrates in the chemical industry as monomers for the synthesis of polycondensation polymers (e.g. polyesters) and as starting material for detergents, respectively.

---

[i] All catalysts/pre-catalysts mentioned in this thesis will be referred to as (pre)-catalysts.

A main limitation in the use of acrylate esters in CM is the need to use large excesses to achieve high selectivity and drive the reactions to completion. Moreover, ethenolysis can occur as side reaction if the ethylene co-product is not efficiently removed.[20] Besides the formation of fumarates, the direct consequence of the excess of acrylate is that it may influence in the decomposition of the catalyst, promoting the formation of methylidene and enoic carbene intermediates (see **Appendix I** for generic representations of these alkylidenes).

One major limitation in the use of **HGII** is its cost, which is high due to the low atom-economy of its synthesis. Because of the linear approach used in the synthesis, **HGII** is more expensive than the analogous phosphine-containing **GII**. Although the cost difference of the two complexes has considerably decreased in recent years, the synthesis of **HGII** still relies on the use of phosphine-containing precursors.

Based on the aforementioned, this work aims to find two possible solutions to overcome the limitations in the acrylate cross-metathesis. Firstly, the use of maleic acid - **MA-H** - (instead of acrylates) could allow the use of phosphine-containing complexes such as **GII** (**Scheme 2a**). Secondly, the synthesis of **HGII** using a phosphine-free strategy would allow its preparation in a more atom-economically manner, resulting in a decrease of its final cost (**Scheme 2b**). Moreover, the use of toxic and unstable alkylidene sources will be avoided by exploring the reactivity of 1,1-diphenylpropargyl alcohol (**1**) with ruthenium(II) precursors.

a) Cross-Metathesis of MO with Maleic Acid

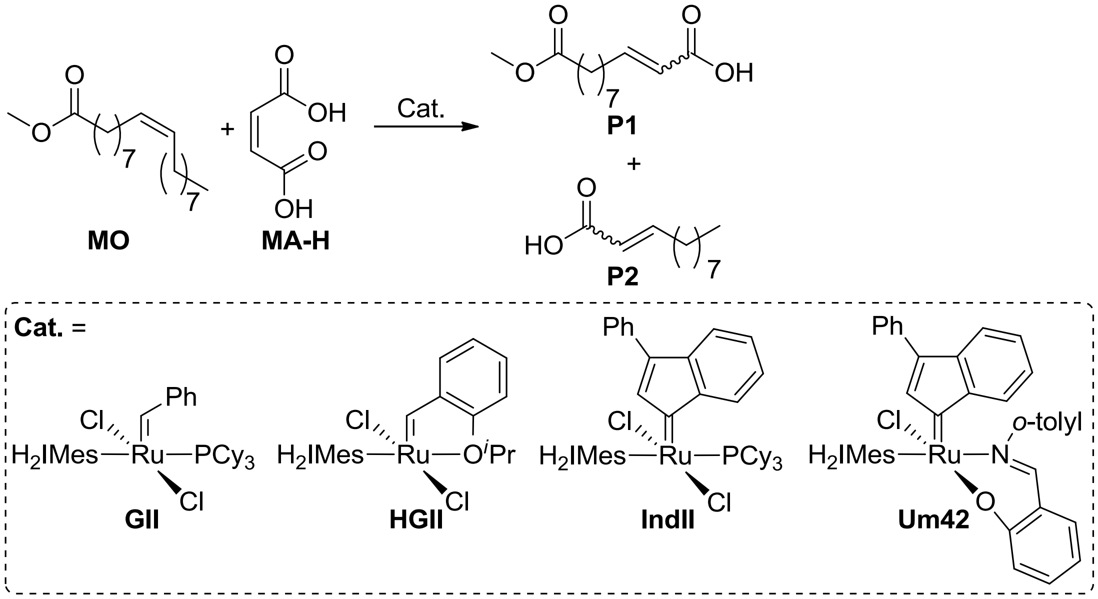
Cat.
MO
MA-H
P1
P2
Cat. =
GII
HGII
IndII
Um42

b) Proposed phosphine-free route to the 2nd generation Hoveyda-Grubbs catalyst (HGII)

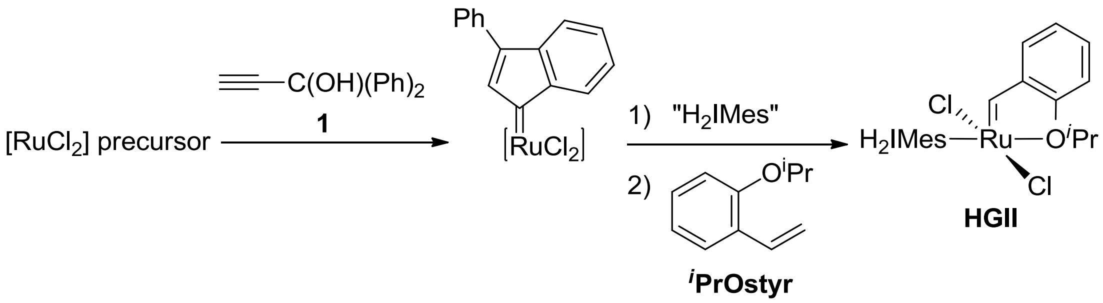
[RuCl2] precursor
C(OH)(Ph)2
1
[RuCl2]
1) "H2IMes"
2)
iPrOstyr
HGII

Scheme 2 Schematic representation of the general objectives of this work. Cross-metathesis of vegetable oil derivatives with **MA-H** (a) and the development of a phosphine-free strategy for the synthesis of **HGII**.

2.1 OLEFIN METATHESIS

The *dance of olefins* (as described by Ives Chauvin) is one of the splendid examples of serendipity in Chemistry. Discovered during attempts to find new catalytic systems for olefin polymerization in the years that succeed the Second World War, the olefin scrambling reaction gained rapid interest in academia and industry. In 1967 Calderon coined the term *Olefin Metathesis* (from the Greek put in different order, change of position) and a few years later (1971) Hérisson and Chauvin proposed the elegant, non-pairwise, metallacyclobutane mechanism for the reaction (**Scheme 3**). The proposal of the olefin metathesis mechanism by Chauvin paved the way for the development of well-defined catalytic systems, following the postulated metal-alkylidene complex as active specie. Since then, a diverse plethora of complexes have been synthesized, characterized and evaluated catalytically; the mechanisms for the most successful complexes have been investigated in detail along with very informative reports on decomposition/deactivation pathways; intermediate species, such as the key metallacyclobutane, have been spectroscopycally observed; the well-defined complexes have been used for the preparation of substances with varied complexity and applications; and the industry has embraced the reaction for the production of commodities and fine chemicals.

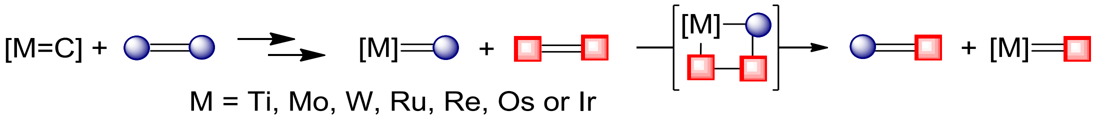

Scheme 3 Simplistic representation of the olefin metathesis mechanism.

One of the most striking and unique characteristic of the olefin metathesis reaction is its ability to be employed in a different set of transformations. The simple variation in the reaction conditions may result in the formation of a polymer or a low strain cycle (via acyclic diene metathesis polymerization – ADMET, or ring-closing metathesis – RCM, of dienes, respectively) for instance (**Scheme 4**).

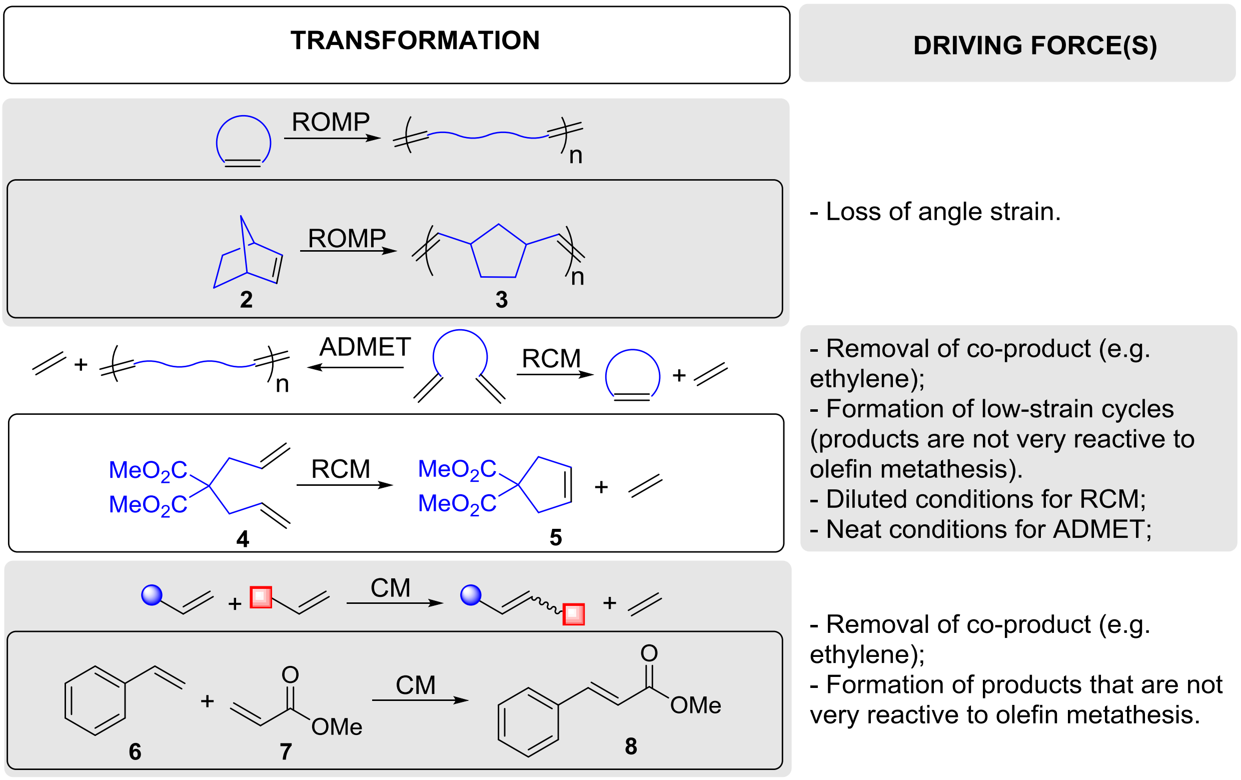

DRIVING FORCE(S)

- Loss of angle strain.

- Removal of co-product (e.g. ethylene);
- Formation of low-strain cycles (products are not very reactive to olefin metathesis).
- Diluted conditions for RCM;
- Neat conditions for ADMET;

- Removal of co-product (e.g. ethylene);
- Formation of products that are not very reactive to olefin metathesis.

Scheme 4 Different types of transformations in olefin metathesis (with selected examples) and the driving force(s) for each transformation (ROMP = Ring-opening metathesis polymerization; ADMET = Acyclic diene metathesis; RCM = Ring-closing metathesis; CM = Cross-metathesis).

Several metals catalyze the olefin metathesis reaction. In homogeneous catalysis, the most successful complexes are based on tungsten (W), molybdenum (Mo and ruthenium (Ru) (**Figure 3**). Amongst the diversified plethora of homogenous olefin metathesis (pre)-catalysts, the ruthenium-based complexes have received more attention due to their good activity and higher robustness to varying reaction conditions (**Figure 4**), allowing the transformation of molecules within a diverse range of complexity.[5,11,21,22]

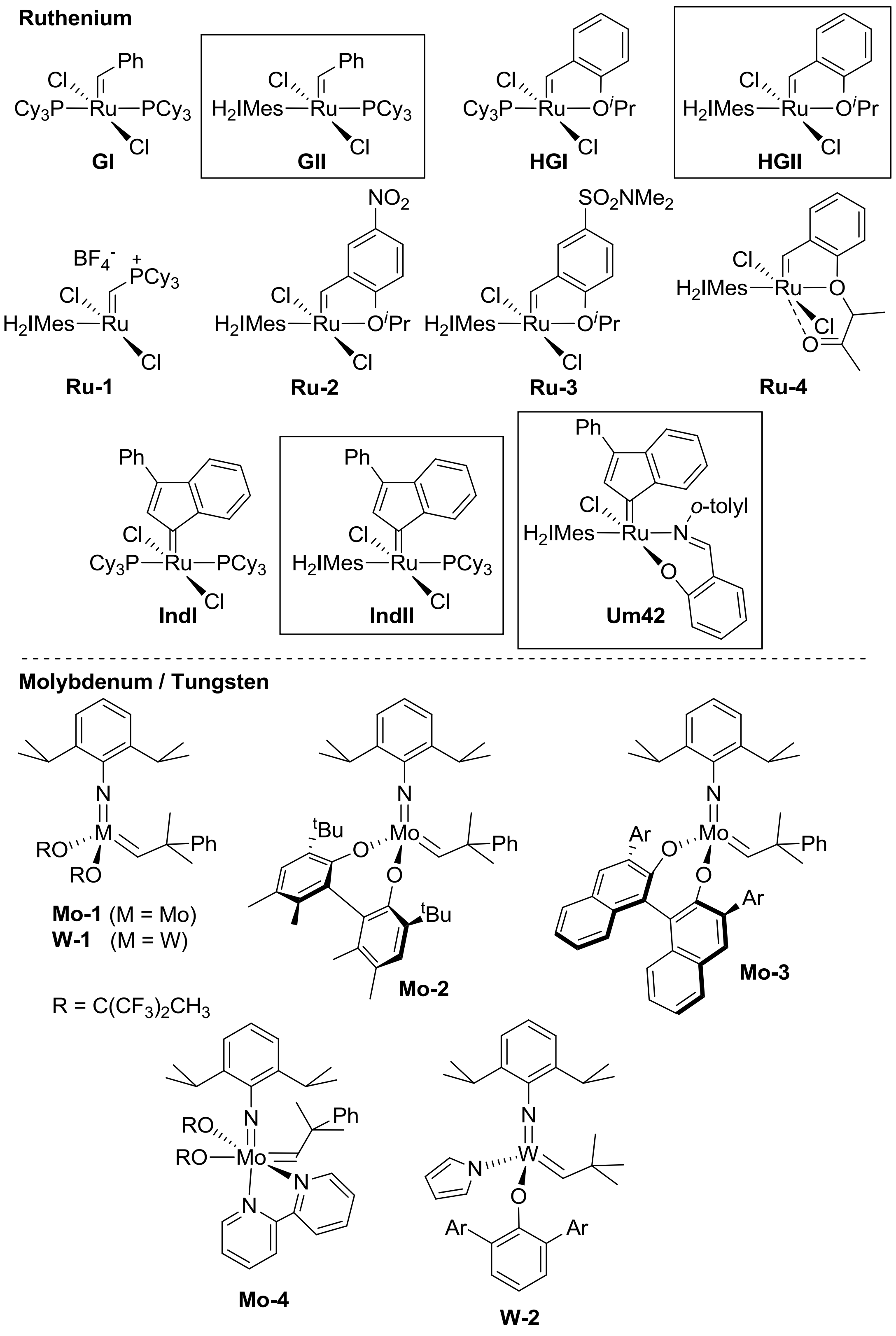
Ruthenium
GI
GII
HGI
HGII
Ru-1
Ru-2
Ru-3
Ru-4
IndI
IndII
Um42
Molybdenum / Tungsten
Mo-1 (M = Mo)
W-1 (M = W)
R = C(CF3)2CH3
Mo-2
Mo-3
Mo-4
W-2

Figure 3 Selected examples of olefin metathesis (pre)-catalysts. Inside the boxes, the (pre)-catalysts employed in this thesis.

Ruthenium-based olefin metathesis (pre)-catalysts are largely tolerant to functional groups (**Figure 4**). Except for nucleophilic functional groups, such as amines which can deactivate / decompose the active species, Ru-based complexes can be used in combination with a wide variety of functional groups, in the presence of water, and even in the presence of oxygen (only with very reactive substrates).[23]

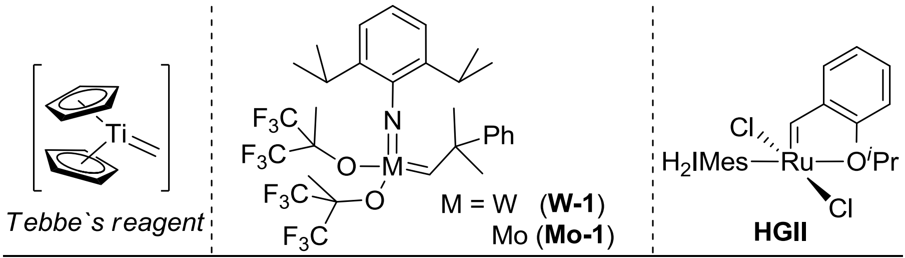

Tebbe`s reagent

M = W (**W-1**)
Mo (**Mo-1**)

HGII

Titanium	**Tungsten**	**Molybdenum**	**Ruthenium**
Acids	Acids	Acids	**Olefins**
Alcohols, water	Alcohols, water	Alcohols, water	Acids
Aldehydes	Aldehydes	Aldehydes	Alcohols, water
Ketones	Ketones	**Olefins**	Aldehydes
Esters, Amides	**Olefins**	Ketones	Ketones
Olefins	Esters, Amides	Esters, Amides	Esters, Amides

Reactivity increases

Figure 4 General trends in the functional group tolerance of titanium-, tungsten-, molybdenum- and ruthenium-based alkylidenes.

2.1.1 Olefin cross-metathesis

Compared to ROMP and RCM transformations, the olefin cross-metathesis (CM) is relatively less explored in this field. Nevertheless, in recent years CM has gained much more attention. CM affords convenient routes to functionalized olefins from simple alkene precursors. For instance, the installation of structural elements within complex natural products and the synthesis of reagents for further synthetic transformations can be accomplished by CM. If a strong enthalpic driving force or entropic advantages of intramolecular reactions immensely favour ROMP and RCM reactions, respectively, in CM such influences are absent, resulting generally in low product selectivity. Nevertheless, a few considerations on the reactivity of the olefins employed in the CM reaction can be taken into account to foresee the outcome of the reaction (**Figure 5**). Thus olefins are categorized in four types, based on the easiness of the homodimerization reaction (self-metathesis – SM) and the reactivity of the homodimers towards cross-metathesis.[24]

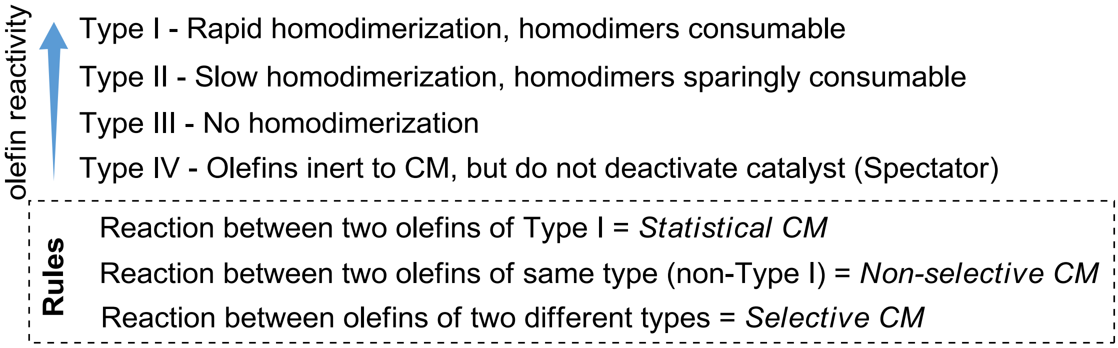
olefin reactivity
Type I - Rapid homodimerization, homodimers consumable
Type II - Slow homodimerization, homodimers sparingly consumable
Type III - No homodimerization
Type IV - Olefins inert to CM, but do not deactivate catalyst (Spectator)
Rules
Reaction between two olefins of Type I = *Statistical CM*
Reaction between two olefins of same type (non-Type I) = *Non-selective CM*
Reaction between olefins of two different types = *Selective CM*

Figure 5 Olefin categorization and rules for selectivity in cross-metathesis.

Therefore, to obtain selectivity in olefin CM, two olefins of different reactivity (different types) should be employed to achieve high yields, with the less reactive generally substrate used in excess. Examples of CM reactions are provided in **Sections 2.4** and **2.6**.

2.2 SYNTHESES OF COMPLEXES

A number of different strategies have been developed to prepare ruthenium alkylidene complexes active in olefin metathesis. The focus of the majority of such strategies consists in the preparation of analogues of the first-generation Grubbs metathesis (pre)-catalyst (**GI**) (**Scheme 5**). Further conversion of such complexes into second-generation Grubbs metathesis (pre)-catalyst analogues is then carried out treating the corresponding 1st generation complex with an *N*-heterocyclic carbene (NHC) ligand, via displacement of one phosphine ligand. Amongst the several synthetic routes developed so far for the synthesis of ruthenium alkylidene complexes, two are worth mentioning due to their versatility and broad applicability (routes **b** and **f** in **Scheme 5**).

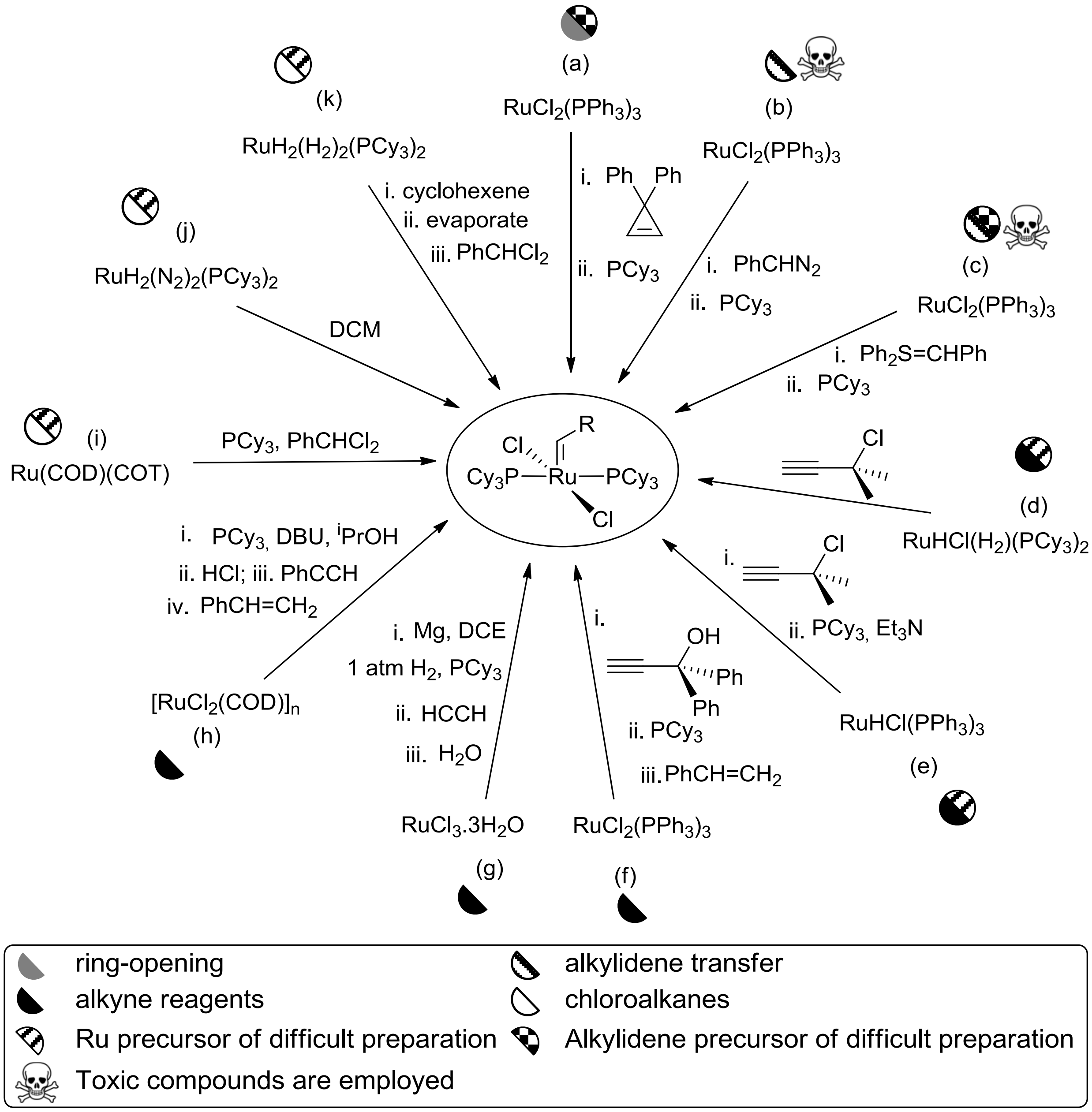
(a)
RuCl2(PPh3)3
i. Ph Ph
ii. PCy3
(b)
RuCl2(PPh3)3
i. PhCHN2
ii. PCy3
(c)
RuCl2(PPh3)3
i. Ph2S=CHPh
ii. PCy3
(d)
RuHCl(H2)(PCy3)2
Cl
(e)
RuHCl(PPh3)3
i.
Cl
ii. PCy3, Et3N
(f)
RuCl2(PPh3)3
i.
OH
Ph
Ph
ii. PCy3
iii. PhCH=CH2
(g)
RuCl3.3H2O
i. Mg, DCE
1 atm H2, PCy3
ii. HCCH
iii. H2O
(h)
[RuCl2(COD)]n
i. PCy3, DBU, iPrOH
ii. HCl; iii. PhCCH
iv. PhCH=CH2
(i)
Ru(COD)(COT)
PCy3, PhCHCl2
(j)
RuH2(N2)2(PCy3)2
DCM
(k)
RuH2(H2)2(PCy3)2
i. cyclohexene
ii. evaporate
iii. PhCHCl2
R
Cl
Cy3P
Ru
PCy3
Cl
ring-opening
alkyne reagents
Ru precursor of difficult preparation
Toxic compounds are employed
alkylidene transfer
chloroalkanes
Alkylidene precursor of difficult preparation

Scheme 5 Different synthetic routes to prepare ruthenium alkylidene complexes structurally similar to the first-generation Grubbs metathesis (pre)-catalyst (**GI**).[25]

2.2.1 Benzylidene-type (pre)-catalysts

The use of diazo reagents to install an alkylidene ligand into a ruthenium centre is the most common strategy in the metathesis field. This strategy, developed by the Grubbs group, employs the use of chemicals of easy preparation and results in the synthesis of the first-generation Grubbs metathesis (pre)-catalyst (**GI**) in good to excellent yields (**Scheme 6**).[26] The only drawback is the use of highly unstable and toxic phenyldiazomethane ($PhCHN_2$ - **11**).

The use of **11** to install an alkylidene to a ruthenium centre is still the dominant route, despite its toxicity and instability, and stoichiometric limitations caused by the low synthetic purity, facile decomposition, and consumption of free PPh_3 and PCy_3.[25] This route is, nevertheless, straightforward and reproducible. The easy preparation of the ruthenium precursor $RuCl_2(PPh_3)_{3-4}$ (**Ru-5**) (commercially available) is another positive point.

Briefly, $RuCl_2(PPh_3)_{3-4}$ (**Ru-5**) reacts with **11** liberating N_2 as co-product and generating the benzylidene complex $RuCl_3(=CHPh)(PPh_3)_2$. PCy_3 exchange (*in situ*) then affords the target **GI** complex. If the reaction with **11** and the PCy_3 exchange are monitored by ^{31}P NMR spectroscopy, the purification becomes much easier and yields are considerably improved. From **GI**, several other benzylidene-type complexes can be derived. Reacting **GI** with an *N*-heterocyclic carbene (NHC) (in its free or masked forms, or generated *in situ*) results in the displacement of one PCy_3 by the more σ-donating NHC ligand. One of the most common NHC ligands employed in the metathesis field is H_2IMes (1,3-bis(2,4,6-trimethylphenyl)-4,5-dihydroimidazol-2-ylidene). The reaction of H_2IMes with **GI** results in the formation of the second-generation Grubbs metathesis (pre)-catalyst (**GII**). Cross-metathesis of **GII** with 2-isopropoxystyrene (**^{i}PrOstyr**) results in the second-generation Hoveyda-Grubbs metathesis (pre)-catalyst (**HGII** - **Scheme 6**).

Amongst the most used ruthenium-based olefin metathesis catalysts developed so far, Hoveyda-type catalysts, specifically **HGII**, play an important role in the olefin metathesis field. Besides exhibiting higher turnover numbers (TON) than the analogous phosphine-containing catalysts in several transformations, **HGII** is used as precursor for the synthesis of complexes that display a regio- or enantiocontrol in olefin metathesis reactions (**Scheme 7** – bottom part).[27-33]

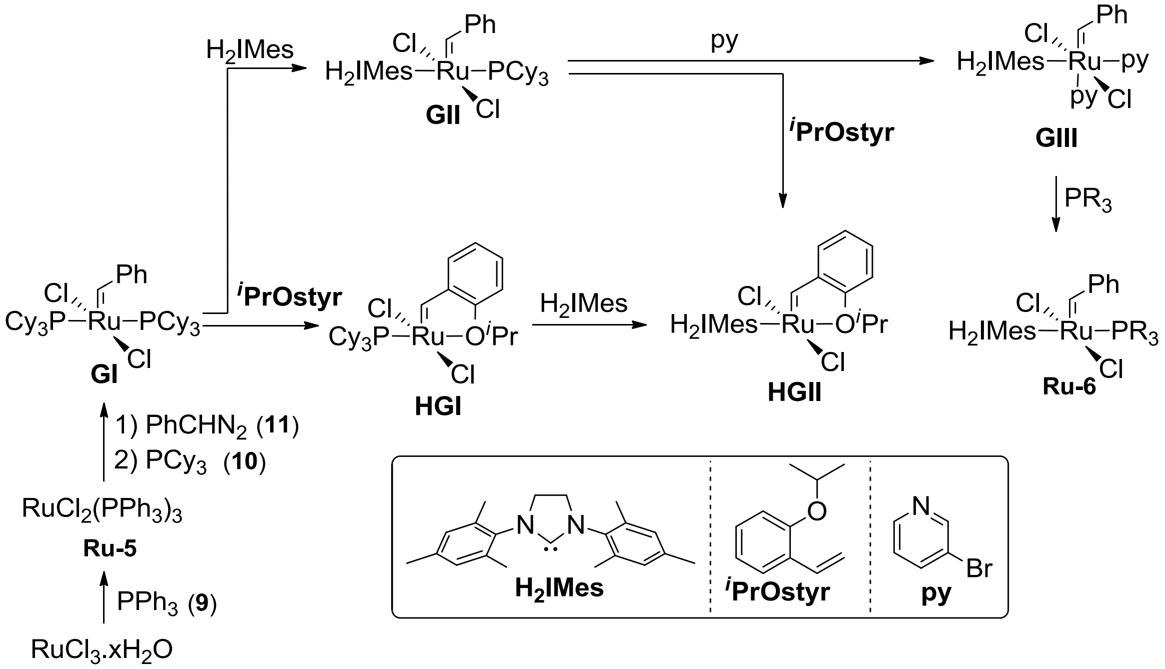

Scheme 6 General synthetic route used for the preparation of ruthenium-benzylidene complexes active in olefin metathesis.

Despite its importance in olefin metathesis, the synthesis of **HGII** lacks efficiency in terms of number of steps and the use of toxic, expensive and air/moisture sensitive chemicals. The most commonly applied synthetic route for the synthesis of **HGII** starts from $RuCl_2(PPh_3)_{3-4}$ via reaction with phenyldiazomethane ($PhCHN_2$ - **11**), followed by PPh_3 exchange with PCy_3 in a *one-pot* fashion, resulting in **GI**. Subsequent steps involve metathesis with 2-isopropoxystyrene (resulting in **HGI**) followed by PCy_3 exchange with H_2IMes (**Scheme 6**).[34] As a consequence of this synthetic strategy, the synthesis of **HGII** involves the use, and therefore the disposal, of two different phosphines and the use of toxic and unstable **11**. In general, the synthesis of each new ruthenium metathesis (pre)-catalyst starts from the previous generation (or from the same generation if a different type is the target - e.g. **HGI** from **GI**) by ligand exchange. This means that in each step sacrificial ligands are used to install the alkylidene, NHC, phosphine, among others. Overall, this multiple step approach has a detrimental influence on the atom economy of the synthesis and on the cost of these metathesis (pre)-catalysts.[35]

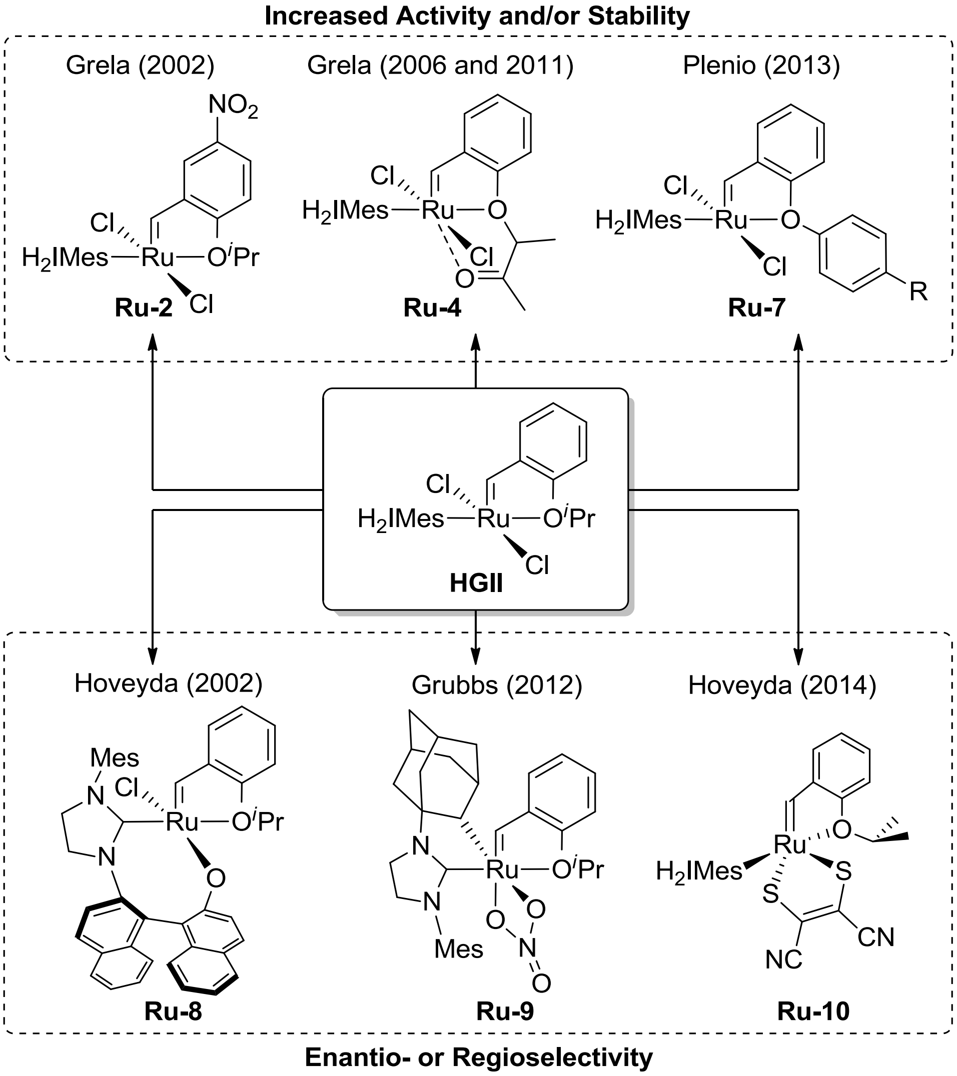
Increased Activity and/or Stability
Grela (2002)
Grela (2006 and 2011)
Plenio (2013)
Ru-2
Ru-4
Ru-7
HGII
Hoveyda (2002)
Grubbs (2012)
Hoveyda (2014)
Ru-8
Ru-9
Ru-10
Enantio- or Regioselectivity

Scheme 7 Selected examples of variations of the **HGII** complex resulting in improved activity/stability (top) or enantio- and regioselectivity (bottom).

2.2.2 Indenylidene-type (pre)-catalysts

1,1-Diphenylpropargyl alcohol provides an interesting alternative to install an alkylidene (see **Appendix I** for a summary of different classes of alkylidenes) in a Ru^{2+} centre.[36] This commercially available, stable, and non-toxic compound reacts with ruthenium(II) complexes, leading to the formation of an allenylidene, which, depending upon the conditions and the ligands around the metal centre, rearranges to form an indenylidene. Despite ruthenium-allenylidene complexes exhibit poor catalytic activity in olefin metathesis; the indenylidene isomers exhibit comparable activity as the analogous ruthenium-benzylidene (pre)-catalysts.[19]

Complexes containing an indenylidene ligand are synthesized similarly to the analogues Grubbs' (pre)-catalysts, except for the part of the installation of the alkylidene ligand (**Scheme 8**). The conversion of the 'first-generation' ruthenium-indenylidene complex **IndI** into **GI** is reported in the literature,[37] as well as the conversion of the 'second-generation' ruthenium-indenylidene complex **IndII** into **HGII**,[38] despite the low yield obtained (40 %) in the latter approach. The use of **IndII** or **IndIII** to prepare Hoveyda-Grubbs type complexes is well explored in the literature.[39- 47]

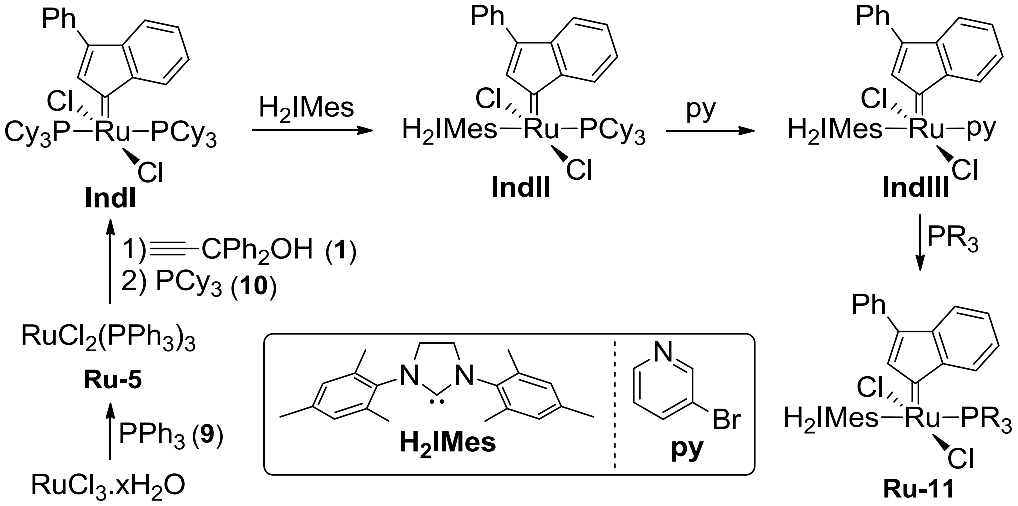
Ph
Cl
Cy_3P–Ru–PCy_3
Cl
IndI
H_2IMes
Ph
Cl
H_2IMes–Ru–PCy_3
Cl
IndII
py
Ph
Cl
H_2IMes–Ru–py
Cl
IndIII
1) ≡–CPh_2OH (1)
2) PCy_3 (10)
PR_3
$RuCl_2(PPh_3)_3$
Ru-5
PPh_3 (9)
$RuCl_3.xH_2O$
N
N
H_2IMes
N
Br
py
Ph
Cl
H_2IMes–Ru–PR_3
Cl
Ru-11

Scheme 8 General synthetic route employing 1,1-diphenylpropargyl alcohol as alkylidene source in the synthesis of ruthenium-indenylidene complexes active in olefin metathesis.

Ideally, the best approach to synthesize **HGII** would involve i) the use of a relatively inexpensive commercially available, or an easy-to-prepare, ruthenium precursor; ii) the use of non-toxic, inexpensive and relatively stable compounds, iii) an atom-economical process; and iv) few and high-yield steps.

One possibility for such approach would be the synthesis of 'third-generation' indenylidene complexes (**IndIII`**) (**Scheme 9**) via a straightforward procedure. **IndIII** could then be converted into **HGII** via metathesis with 2-isopropoxystyrene, 'second-generation' indenylidene complexes (compound **Ru-11** in **Scheme 9**), or complexes containing other types of ligands (compound **Ru-12** in **Scheme 9**; R = any neutral ligand able to coordinate to ruthenium).

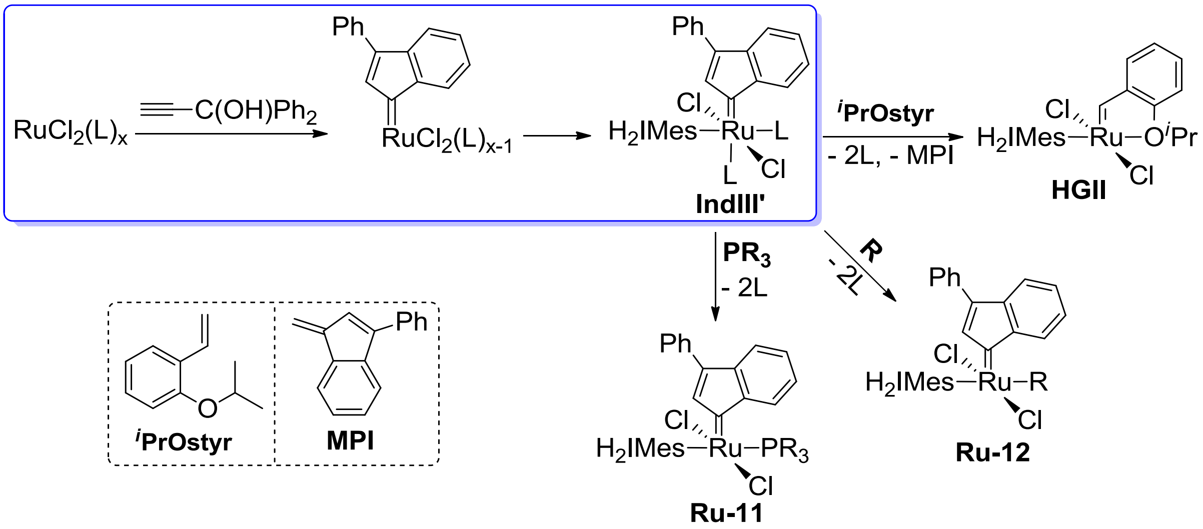

Scheme 9 Two-step synthesis and possible transformations of ‘third-generation’ indenylidene complexes (**IndIII`**).

The formation of an indenylidene from 1,1-diphenylpropargyl alcohol is outlined in **Scheme 10**. Upon η^2-coordination of the $C\equiv C$ of the alkyne to a coordinatively unsaturated ruthenium precursor (2.2.2-**A**), two alternative pathways are initially possible: oxidative addition followed by a 1,3-hydrogen shift (via formation of 2.2.2-**C**) or a 1,2-hydrogen shift. Both pathways result in the formation of a ruthenium-hydroxyvinylidene complex (2.2.2-**D**), and the preference for one or the other pathway relies on the electrophilicity of the metal centre. After spontaneous dehydration, a ruthenium-allenylidene complex is formed (2.2.2-**E**). The allenylidene moiety constitutes a linear σ-donor-π-acceptor double bond chain with C_α and C_γ carbons being electrophilic centers, while C_β carbon is nucleophilic. Protonation of the C_β of the allenylidene moiety results in the formation of an alkenylcarbyne complex (2.2.2-**F**) which, upon nucleophilic attack of one phenyl ring *orto*-carbon on the C_α, rearranges into an indenylidene complex (2.2.2-**G**).[48] Formation of the indenylidene moiety is not always straightforward and is very sensitive to the reaction conditions. For example, in the synthesis of the indenylidene **Ru-14** (**Scheme 10**), even when applying the same procedure, sometimes the target compound is obtained, but more often a μ_2-chloro-bridged bimetallic ruthenium allenylidene complex is observed. The presence of catalytic amounts of HCl favours the formation of the indenylidene moiety.[49-50]

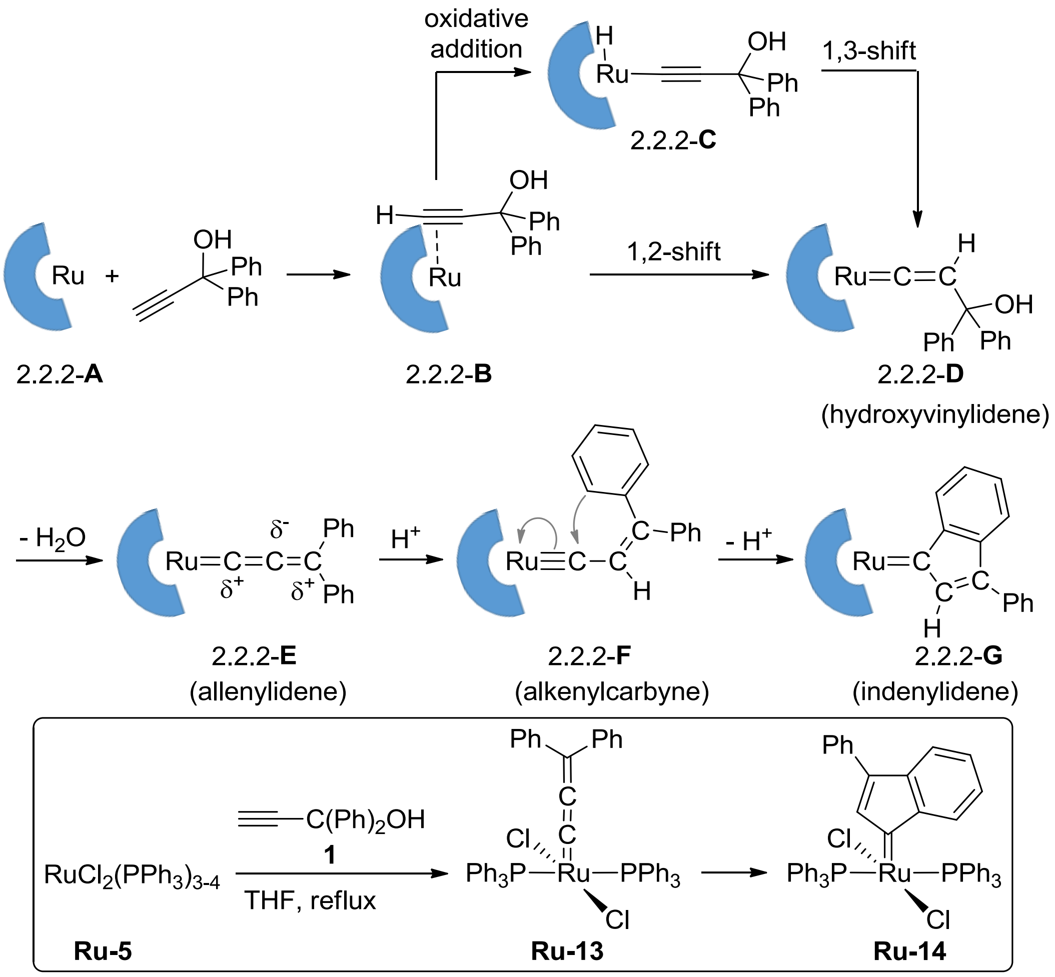
oxidative addition
1,3-shift
1,2-shift
2.2.2-A
2.2.2-B
2.2.2-C
2.2.2-D
(hydroxyvinylidene)
- H2O
H+
- H+
2.2.2-E
(allenylidene)
2.2.2-F
(alkenylcarbyne)
2.2.2-G
(indenylidene)
RuCl2(PPh3)3-4
C(Ph)2OH
1
THF, reflux
Ru-5
Ru-13
Ru-14

Scheme 10 Main steps involved in the formation of ruthenium-indenylidene complexes from 1,1-diphenylpropargyl alcohol.

2.3 OLEFIN METATHESIS MECHANISMS

Olefin metathesis is already a well-established reaction in academia and a growing strategy in the commodity and fine chemicals industries.[4,21,51] This is the result of years of research on the synthesis of a diversity of (pre)-catalysts, the understanding of the reaction mechanisms, stability of the (pre)-catalysts and their decomposition/deactivation pathways, allied with the understanding of substrate reactivity.[20,52-75]

The mechanisms of olefin metathesis have been studied in detail for a number of different complexes over the past decades. Important intermediates have been detected by spectroscopic techniques such as the key, propagating specie, ruthenacyclobutane proposed initially by Hérisson and Chauvin in 1971 and detected by low temperature

NMR by the Piers Group in 2005.[56] Especially for the ruthenium-based complexes, several studies delve on the initiation, propagation and deactivation/decomposition/ regeneration mechanisms (**Scheme 11**). For the sake of clarity, each of these steps will be discussed in separate in the subsections below, for the most common ruthenium complexes and using a model terminal olefin as substrate.

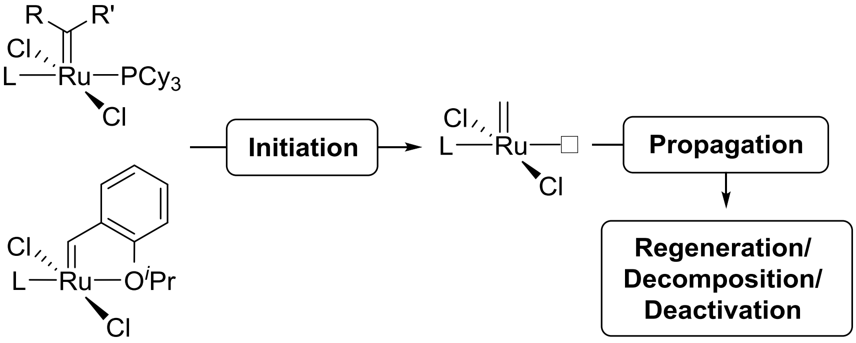

Scheme 11 Steps involved in the olefin metathesis reaction catalyzed by ruthenium complexes.

2.3.1 Initiation mechanism

A number of excellent papers delve into the issue of (pre)-catalyst initiation in olefin metathesis. This is the result of the very different activity exhibited by quite similar complexes. Although this activity difference cannot always be attributed solely to the initiation step, valuable insights are generally obtained.

Early reports dealing with the initiation mechanism appeared soon after the synthesis of the first active ruthenium-based metathesis (pre)-catalysts. Complexes of the Grubbs (e.g., **GI** and **GII**) and the indenylidene (e.g., **IndII**) types share a common initiation mechanism (**Scheme 12a**). The substitution of one phosphine ligand by one olefinic substrate occurs via a dissociative fashion to generate a 14e$^-$, four coordinate, intermediate (2.3.1-**A**). The 14e$^-$ intermediate can thus coordinate to an olefinic substrate (2.3.1-**B**) or reuptake the dissociated phosphine regenerating the 16e$^-$ (pre)-catalyst. The rate of the phosphine dissociation/re-coordination is crucial for the (pre)-catalyst activity. For instance, **GI** initiates approximately 70 times faster than **GII**, but is much less active than the later. This is the result of faster re-coordination of the dissociated PCy_3 to regenerate **GI** compared to the same process to regenerate **GII**. In other words, the 14e$^-$ intermediate specie generated upon PCy_3 dissociation in **GII** prefers to coordinate to an olefin rather than to the phosphine. It is therefore said that **GII** has a higher *olefin commitment* than **GI**.[57] Nolan's group reported that for indenylidene analogues of **GI/GII** the PCy_3 also dissociates via a dissociative fashion.[59]

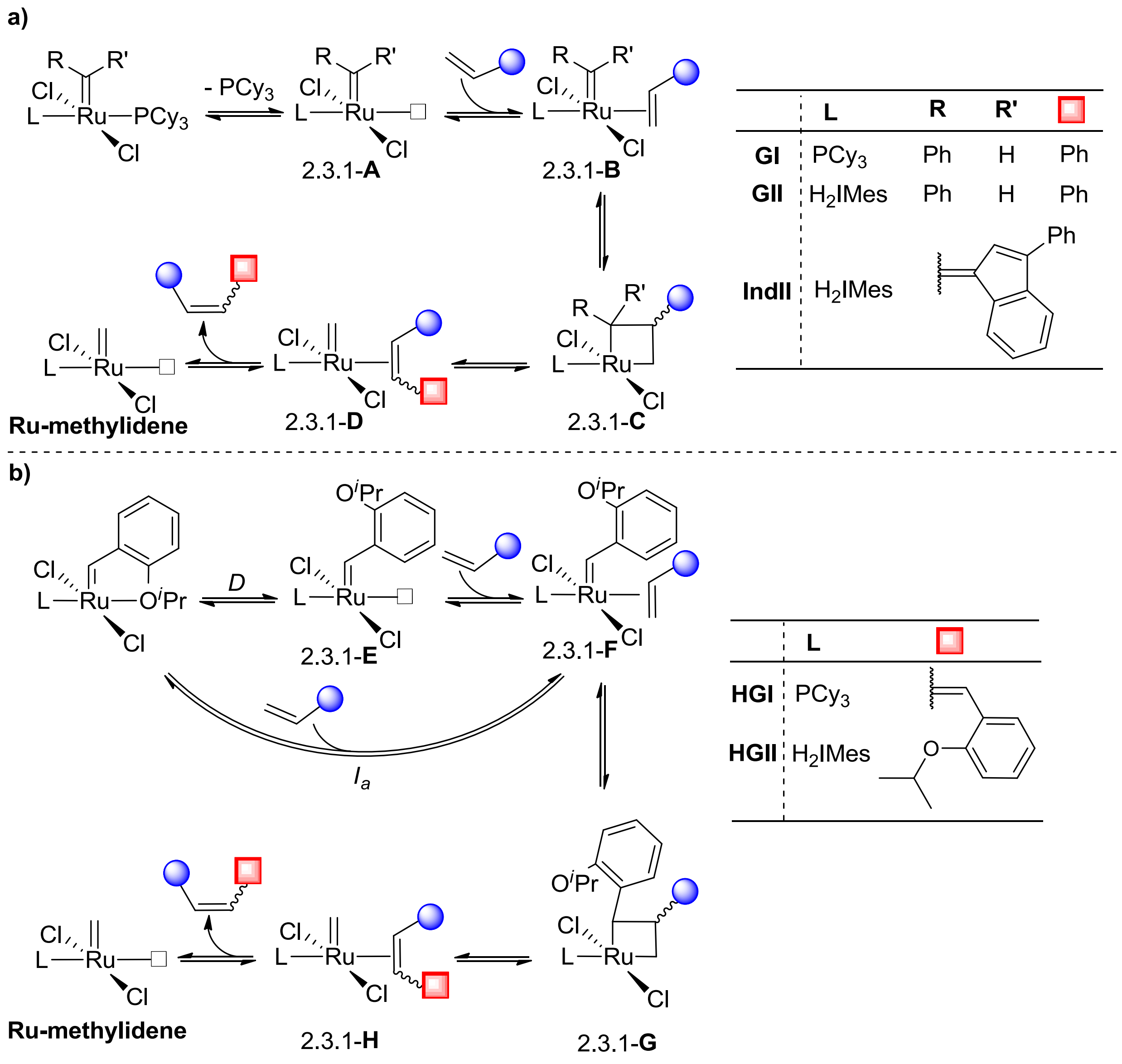
a)
- PCy3
2.3.1-A
2.3.1-B
2.3.1-C
2.3.1-D
Ru-methylidene
L
R
R'
GI
PCy3
Ph
H
Ph
GII
H2IMes
Ph
H
Ph
IndII
H2IMes
Ph
b)
D
2.3.1-E
2.3.1-F
2.3.1-G
2.3.1-H
Ia
Ru-methylidene
HGI
PCy3
HGII
H2IMes

Scheme 12 Initiation mechanism for the ruthenium-based metathesis catalysts of the a) Grubbs and b) Hoveyda-Grubbs types.

After olefin coordination to the metallic centre in the appropriate orientation, formation of the ruthenacyclobutane (2.3.1-**C**) followed by cycloreversion (2.3.1-**D**) with dissociation of the newly formed olefin, results in the exclusion of the phenyl (for **GI** and **GII** complexes) or phenylindenyl (for **IndII** complex) from the complex. The new $14e^-$ alkylidene (**Ru-methylidene**) formed is the propagating specie of the reaction.

Whether the initiation mechanism for phosphine-containing complexes is quite straightforward, the same does not hold true for the Hoveyda-Grubbs type (pre)-catalysts. Either dissociative (*D*) or interchange with associative mode of activation (I_a) mechanisms can occur depending on the substrate and the substituents in the isopropoxystyrene ligand (**Scheme 12b**). For **HGII**, electron-rich and sterically less demanding olefins (e.g, 1-hexene or butylvinyl ether, respectively) prefer the I_a activation mode, while for bulkier or less electron-rich olefins (e.g., diethyldiallyl malonate or styrene, respectively), the dissociative pathway is more important.[60,76] After the initiation step, formation of the ruthenacyclobuthane intermediate, cicloreversion and dissociation of the newly formed olefin generates the active, $14e^-$, propagating specie (**Ru-methylidene**).

2.3.2 Propagation

Once the active propagating specie is generated (**Ru-methylidene** shown in **Scheme 13**), productive cycles are able to occur. Steps involved during propagation are essentially the same as those of initiation, except for the phosphine/isopropoxystyrene dissociation step. Coordination of the olefinic substrate to the $14e^-$ complex **Ru-methylidene** results in the formation of the $16e^-$ intermediate 2.3.2-**A**, which leads to the formation of the ruthenacyclobutane 2.3.2-**B**. Cycloreversion of 2.3.2-**B** results in the, ethylene coordinated, intermediate complex 2.3.2-**C**. Ethylene dissociation results in the $14e^-$ intermediate 2.3.2-**D**. Coordination of another olefinic substrate leads to the subsequent formation of the intermediates 2.3.2-**E** and 2.3.2-**F**. Cycloreversion of ruthenacyclobutane 2.3.2-**F** and dissociation of the formed olefin regenerates the propagating **Ru-methylidene** specie. All steps in the catalytic cycle are reversible, accounting for the equilibrium nature of the olefin metathesis reaction.

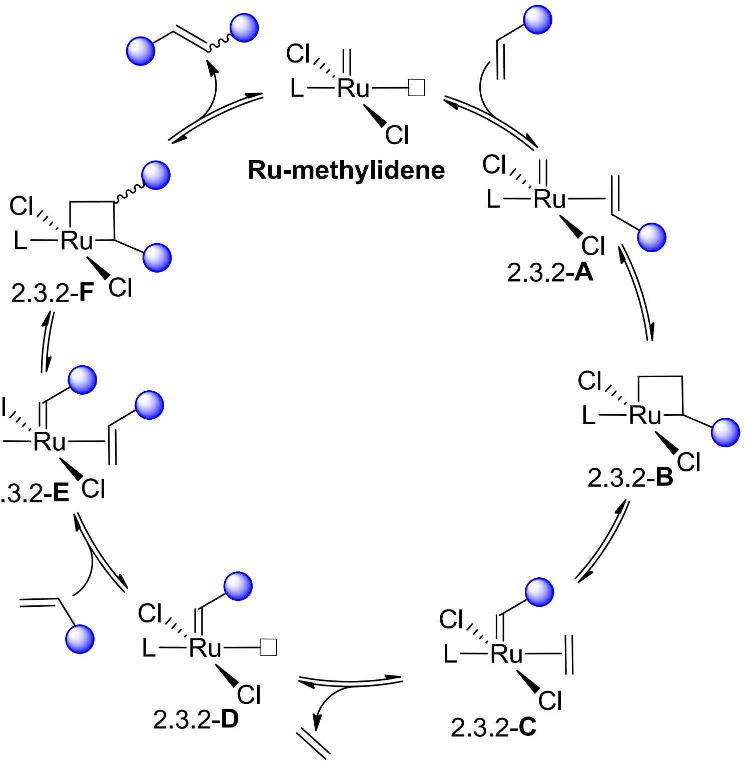

Scheme 13 Propagation mechanism of the ruthenium-based olefin metathesis catalysts.

2.3.3 Deactivation and decomposition

Undoubtedly, the knowledge of a reaction mechanism in as many details as possible allows the exploration of the full potential of the reaction by designing new catalysts or by the use of the reaction in innovative transformations. Nevertheless, the decomposition/deactivation pathways that a catalyst may encounter during the catalytic cycle provide valuable information to both extend the catalyst lifetime and to design more robust catalysts. The exploration of such pathways is sometimes an overlooked field in homogeneous catalysis. Fortunately, for olefin metathesis there is a considerable volume of literature that deals with this issue. (Pre)-catalyst decomposition/deactivation due to the presence of nucleophilic bases (e.g., alkoxides, amines, phosphines) or thermally induced are reported in the literature. Two of these pathways will be discussed in further detail due to the direct connection with the topic discussed in this thesis. The first pathway is the PCy_3-mediated decomposition of Ru-methylidene species, and the second pathway is the Michael addition of PCy_3 to acrylates, followed by attack on the ruthenacyclobutane intermediate.

A Ru-methylidene specie is propagating specie in any olefin metathesis transformation involving terminal olefins. In fact, the majority of the reactions explored in olefin metathesis involve at least one terminal C-C double bond. As a consequence, understanding the stability/reactivity of such propagating specie is of paramount importance.

The decomposition of the methylidene complex **GIIm** has been reported by the Grubbs group to produce a dinuclear ruthenium complex with a bridging carbide between the two ruthenium centers and a hydride ligand in one of the ruthenium (**Scheme 14**). Moreover, a η^6-binding of one of the ruthenium centers to one of the mesityl rings in the *N*-heterocyclic carbene is observed along with complete loss of phosphine ligands. This decomposition proceeds with first-order kinetics. The authors proposed that the decomposition of **GIIm** occurs mainly by the attack of the dissociated PCy_3 from **GIIm** on the methylidene carbon of the $14e^-$ propagating specie 2.3.3-**A** (**Scheme 14**). After a number of steps, 2.3.3-**A** losses the methylidene fragment via the formation of the phosphorus ylide **13**, and is converted into the $12e^-$ specie 2.3.3-**D**, which thus binds to one of the mesityl rings of the *N*-heterocyclic carbene of 2.3.3-**A**, forming a chloride-bridged dinuclear ruthenium complex 2.3.3-**E**. Abstraction of HCl from 2.3.3-**E** by the ylide **13** then generates the terminal alkylidyne 2.3.3-**F** and the phosphonium salt **12**. Oxidative addition of the terminal alkylidyne with migration of two chlorides results in the isolated complex **Ru-15**. None of the organometallic intermediates were observed by NMR spectroscopy.[67]

A particularly attractive transformation in olefin metathesis is the CM with acrylates, which has grown in importance in the recent years as a useful strategy in the preparation of a number of valuable products of commercial interest (see **sections 2.4** and **2.6**).[77-86] These include commodity products from vegetable oils (monomers, surfactants) and ingredients for cosmetic uses and compounds with biological applications.[15] For such transformations involving acrylates and other electron deficient olefins, the use of more expensive phosphine-free (pre)-catalysts (e.g., **HGII**) generally afford better results.[13,19,87-95] The mechanistic rationale behind such behavior was provided recently by the Fogg group, which demonstrated that the performance of **GII** in acrylate CM is undermined by Michael addition pathways enabled by free PCy_3.[63]

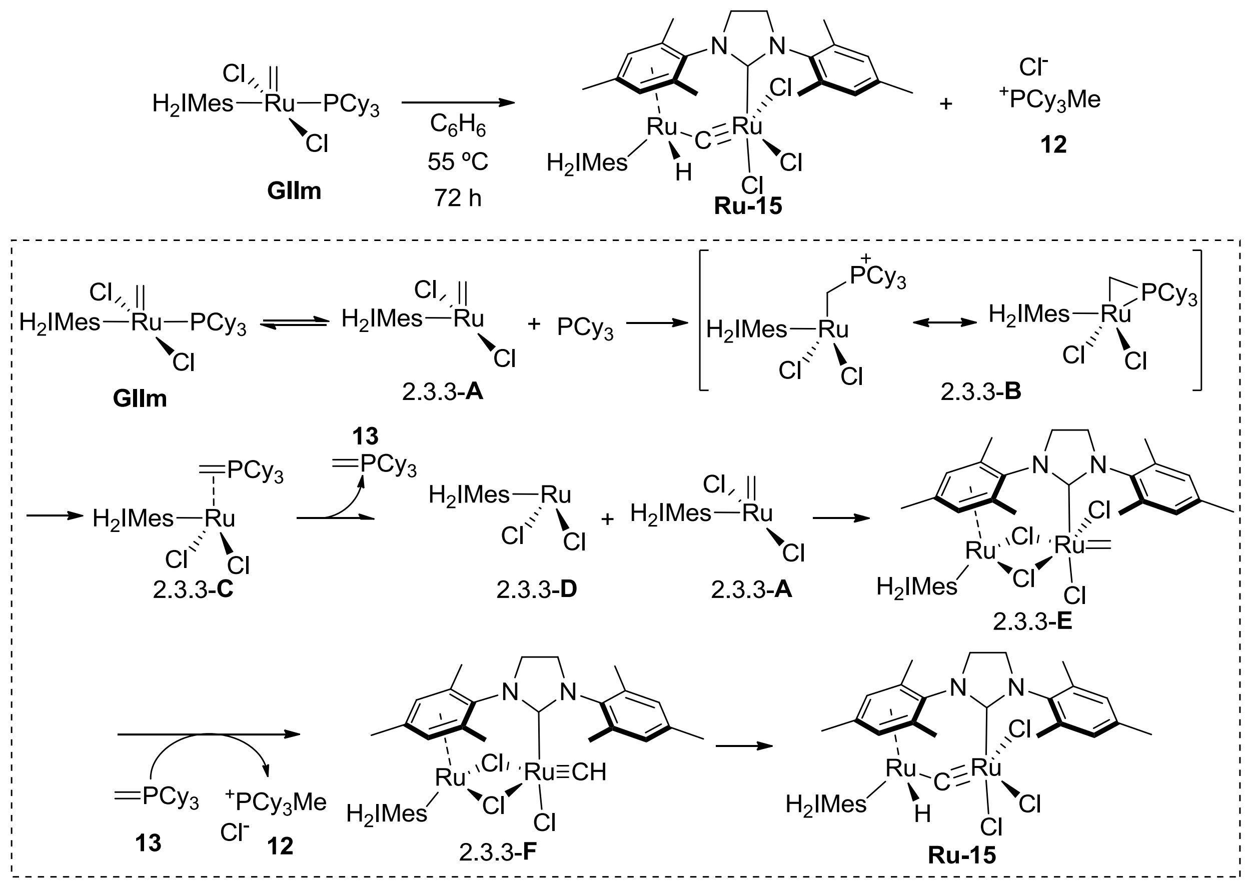

Scheme 14 Decomposition of **GIIm** into a dinuclear complex. Inside the dashed box, the proposed decomposition mechanism.

In a **HGII**-catalyzed control reaction with anethole and methyl acrylate (**7**), the authors observed that addition of 1 equivalent of PCy_3 added after 2 minutes of reaction completely knocked down the reaction. Comparatively, when the same procedure was employed in the self-metathesis (SM) of styrene, the addition of PCy_3 merely decrease the rate of the reaction, without affecting the final yield. These experiments clearly pinpointed the acrylate ester functionality as key to the deactivating effect of PCy_3 in acrylate metathesis catalyzed by phosphine-containing (pre)-catalysts.[63]

Upon monitoring the reaction of **HGII** and PCy_3 in excess **7** (**Scheme 15**) by NMR spectroscopy, the loss of the alkylidene signal of **HGII** (^1H NMR) and the parallel appearance of two singlet peaks in the ^{31}P NMR spectrum were observed. Compounds **14** and **15** were identified as the two major products, and were proposed to be generated by initial attack of PCy_3 on the acrylate, forming the corresponding zwitterion adduct **16**, which can participate in multiple subsequent pathways. The zwitterion **16** then attacks another molecule of acrylate forming the zwiterionic adduct **17**. Proton abstraction by **17** liberates the salt **15**. Because no reaction was observed in the absence of **HGII**, the authors speculated that the ruthenium species present in the reaction media supply the required proton and counter-anion. The ruthenacyclobutane intermediate was suggested as the likely target of attack, based on similar chemistry involving amines, reported by the same group.[69]

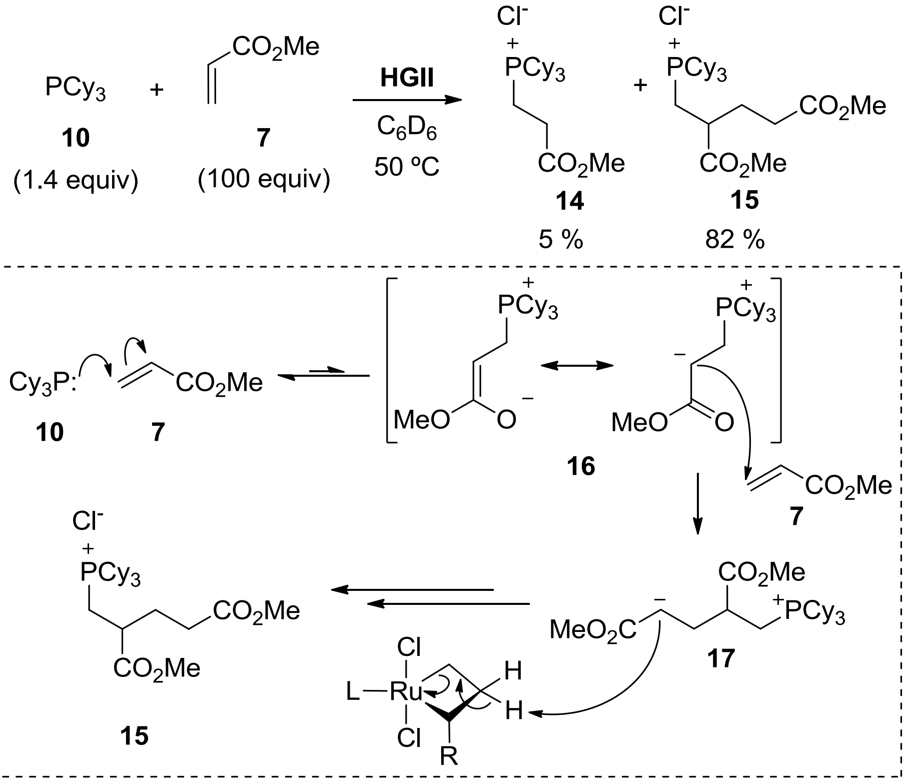
PCy3
+
CO2Me
10
7
(1.4 equiv)
(100 equiv)
HGII
C6D6
50 °C
Cl-
+PCy3
CO2Me
14
5 %
Cl-
+PCy3
CO2Me
CO2Me
15
82 %
Cy3P:
10
7
+PCy3
MeO
O
16
7
CO2Me
MeO2C
+PCy3
17
Cl
+PCy3
CO2Me
CO2Me
15
Cl
L—Ru
Cl
H
H
R

Scheme 15 Michael addition chemistry that results in the decomposition of **HGII** in the presence of added PCy_3.

2.3.4 Regeneration

In 1999, Amir Hoveyda reported the fortuitous isolation of a chelating etherbenzylidene complex derived from **GI**. The new complex was formed when **GI** was employed as (pre)-catalyst in the ring-opening/cross-metathesis (RO/CM) of 2-isopropoxystyrene with 3-phenoxy-*cis*-cyclooctene (**Scheme 16a**). Isolation and spectroscopic and crystallographic characterization of the new complex revealed the structure of **HGI** (**Scheme 16b**). (Pre)-Catalyst **HGI** proved to be quite remarkable. Besides exhibiting comparable activity to **GI**, **HGI** was more stable than **GI** and could also be recycled in high yield by silica gel chromatography at least three additional cycles. Based on the good activity and high recyclability of **HGI**, the authors proposed that the released 2-isopropoxystyrene in the initiation step (**Section 2.3.1**) captures back the propagating species regenerating the (pre)-catalyst (**Scheme 17**).[96]

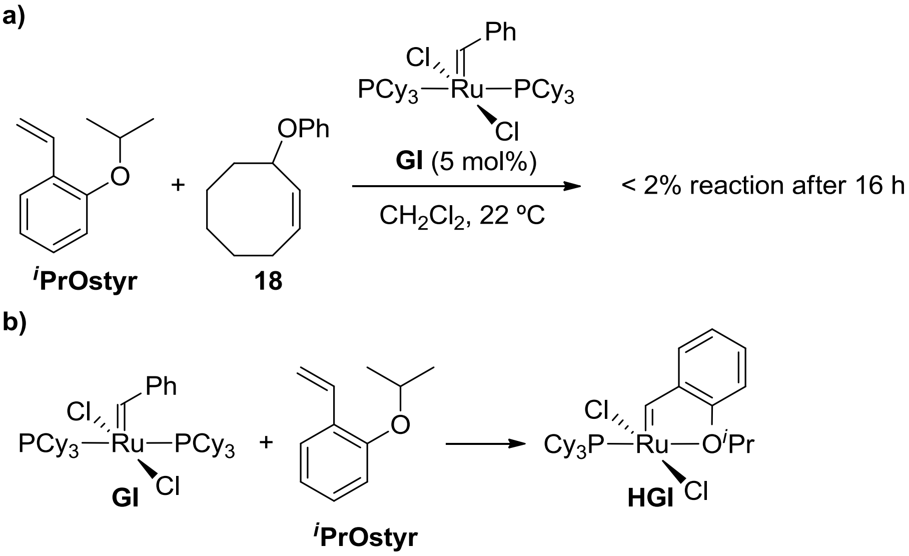
a)
GI (5 mol%)
CH2Cl2, 22 °C
< 2% reaction after 16 h
iPrOstyr
18
b)
GI
iPrOstyr
HGI

Scheme 16 Fortuitous discovery of chelating etherbenzylidene ruthenium metathesis (pre)-catalyst **HGI**. a) RO/CM of ***ⁱ*PrOstyr** with 3-phenoxy-*cis*-cyclooctene; b) synthesis of **HGI**.

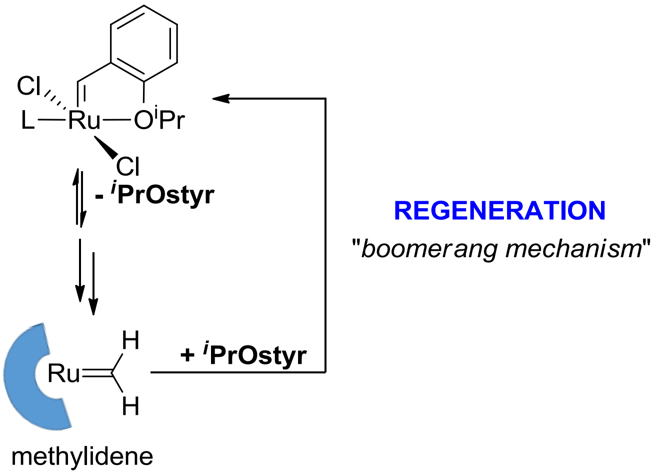
- iPrOstyr
REGENERATION
"boomerang mechanism"
+ iPrOstyr
methylidene

Scheme 17 The release-return (*boomerang*) mechanism for chelating ether-benzylidene ruthenium complexes.

This process of regeneration of the (pre)-catalyst was nicknamed of release-return mechanism (or *boomerang* mechanism) and was the reason for controversies in the metathesis community for several years.[19,20,54,97,98] Strong evidence supporting the *boomerang* mechanism was recently provided using ^{13}C-labeled 2-isopropoxystyrene (**^{i}PrOstyr*** - **Figure 6**). When 1 equivalent of **^{i}PrOstyr*** was added to the CM reaction of anethole with methyl acrylate catalysed by **HGII** (1 mol%), a 57:43 ratio of **HGII**:**HGII*** was obtained at 92 % conversion (ca. 1 h) (**Figure 6a**). Formation of **HGII*** in this system can only be explained by the uptake of **^{i}PrOstyr*** by the propagating species, thus providing strong evidence for the boomerang mechanism. In a control experiment without any substrate, uptake of **^{i}PrOstyr*** by **HGII** is very slow, reaching equilibrium after 50 h (**Figure 6b**).[20]

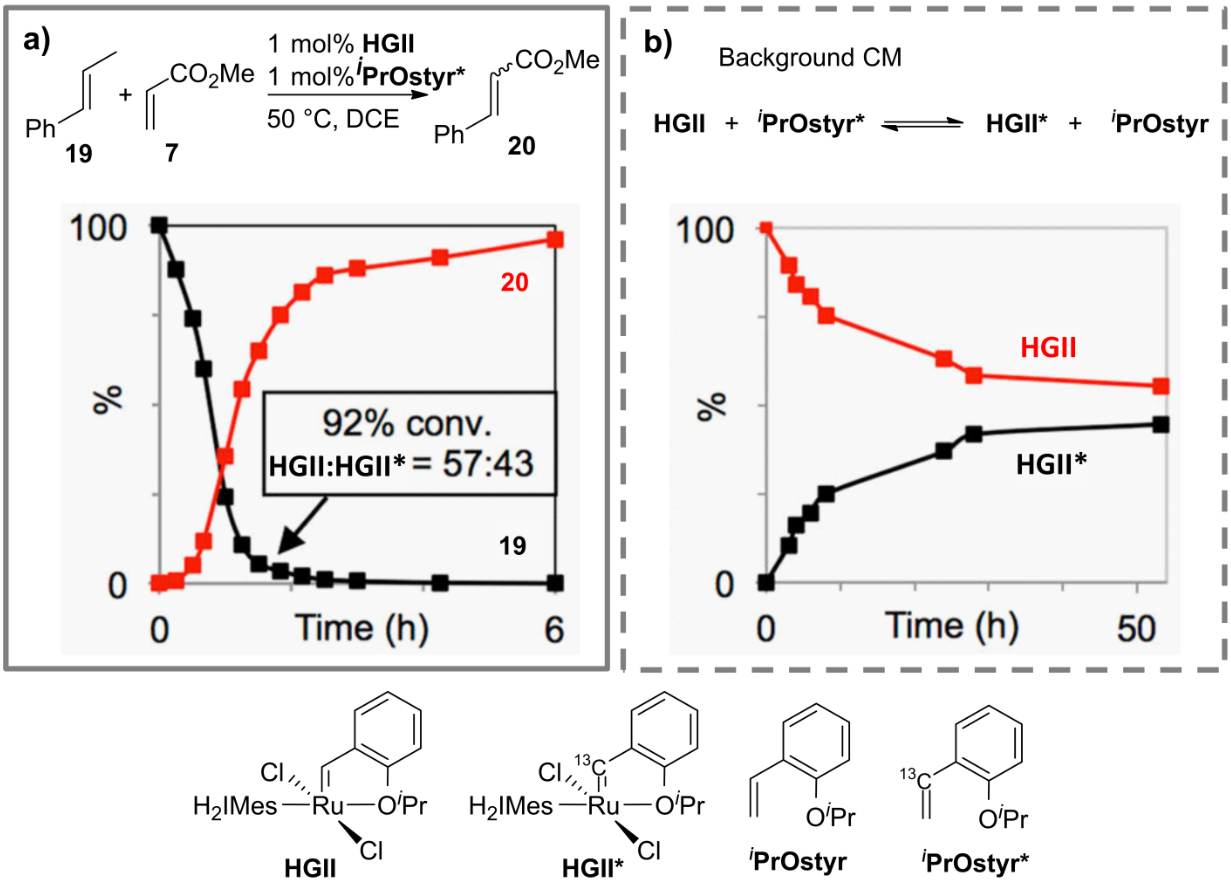

Figure 6 Experiment used to demonstrate the validity of the *boomerang* mechanism. a) CM of anethole with methyl acrylate catalysed by **HGII** in the presence of **^{i}PrOstyr***. b) Time scale equilibration of **^{i}PrOstyr*** in the absence of substrate. Ar = 4-methoxybenzene.

2.4 α,β-UNSATURATED CARBONYL COMPOUNDS

The preparation of α,β-unsaturated carbonyl compounds through olefin metathesis represents a valuable, yet challenging, transformation. α,β-Unsaturated carbonyl compounds are versatile compounds with potentially interesting applications as final products or as intermediates in the synthesis of more complex structures (**Figure 7**). Nevertheless, the preparation of such compounds via olefin metathesis involves the use of electron deficient, low reactive, unsaturated precursors, such as acrylic acid derivatives. As a general consequence, considerably high catalyst loadings and a large excess of the unsaturated carbonyl compound are required in order to achieve good conversion and selectivity.[15,77,78,80-82]

The CM with acrylates may involve the formation of two presumably very reactive and unstable species: the required formation of a Ru-methylidene and the not-required, yet plausible, Ru-enoic carbene intermediate. Formation of a Ru-methylidene is required, as the release of ethylene is necessary to drive the reaction to completion. Nevertheless, the formation of a Ru-enoic carbene is not a crucial requirement in this specific transformation, the only evidence for its formation being the observance of variable amounts of fumarate/maleate esters as by-products.

2.4.1 Enoic-carbene complexes relevant to olefin metathesis

Although the reactivity and stability of some Ru-methylidene complexes has been reported in the course of the last years,[67,99] reports on the chemistry of Ru-enoic carbenes in the vast field of olefin metathesis are surprisingly scarce. The few examples include the synthesis of complexes of the type $RuCl_2(=CHCOR)(PCy)_3$ via the innovative double oxidative addition of 2,2-dichloroacetate esters with the ruthenium(0) precursor $Ru(COD)_2$ (**Scheme 18**).[100]

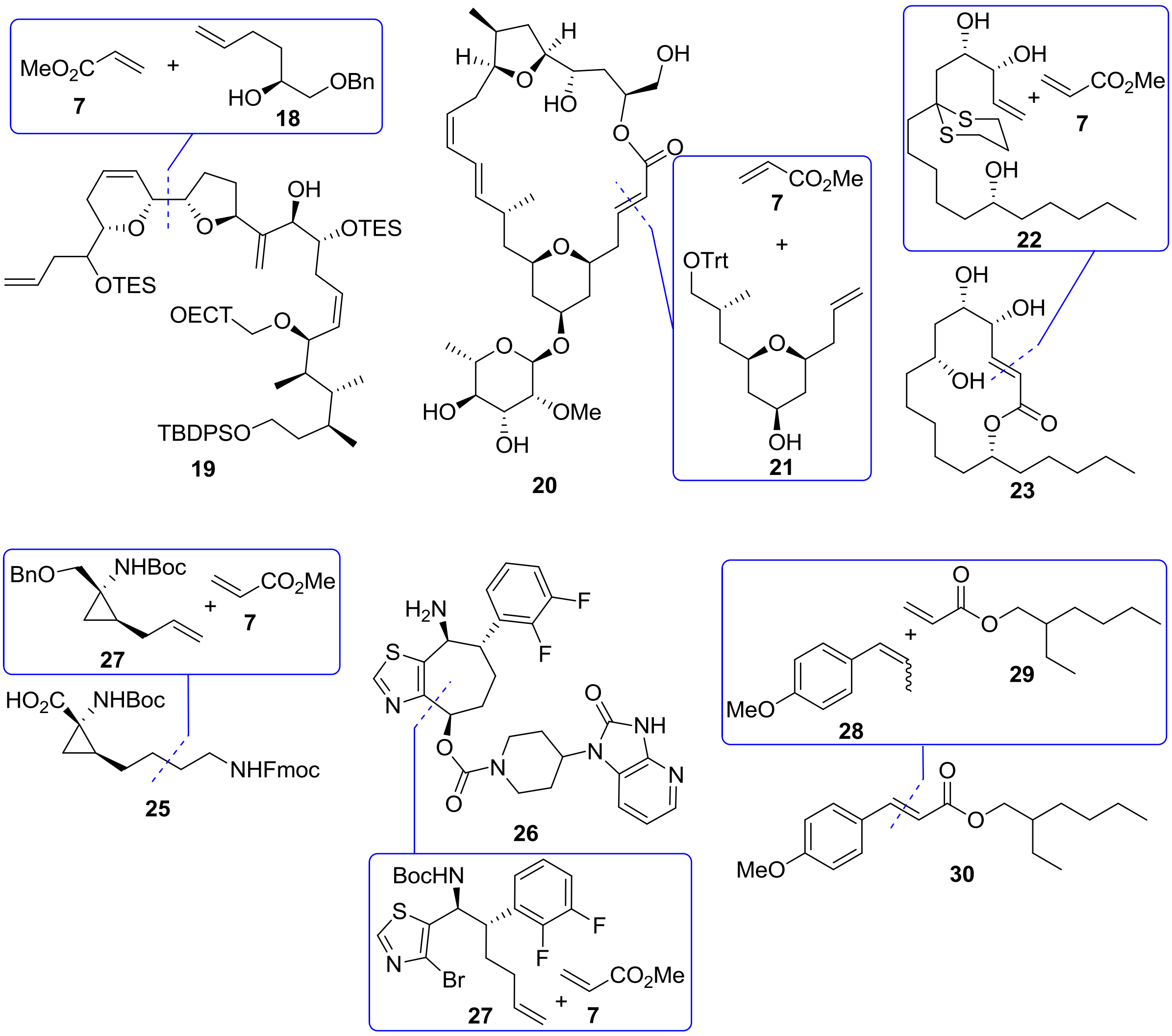
MeO2C
7
+
HO
OBn
18
OTES
OH
OTES
OECT
O
TBDPSO
19
H
H
O
HO
OH
O
O
20
HO
OMe
OH
CO2Me
7
+
OTrt
O
OH
21
OH
OH
S
S
+
CO2Me
7
OH
22
OH
OH
OH
O
O
23
BnO
NHBoc
+
CO2Me
7
27
HO2C
NHBoc
NHFmoc
25
H2N
S
N
F
F
O
N
O
NH
N
N
26
BocHN
S
N
Br
F
F
CO2Me
27
+
7
O
+
O
29
MeO
28
O
O
MeO
30

Figure 7 Selected examples of compounds prepared using olefin cross-metathesis with acrylates. Inside the boxes, the CM step.

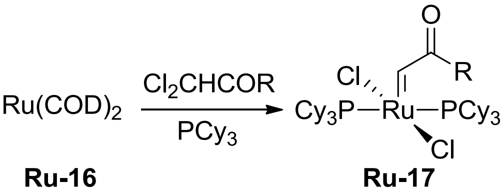
Ru(COD)2
Cl2CHCOR
PCy3
Cl
O
R
Cy3P—Ru—PCy3
Cl
Ru-16
Ru-17

R	k_{dec}* ($L.mol^{-1}.min^{-1}$)
-OMe	0.6
-O-*p*-tolyl	0.5
-O-^{t}Bu	0.4
-O-^{i}Pr	0.3
-O-cyclohexyl	0.2
-O-1-adamantyl	0.2
$-NH_2$	0

* at r.t. in C_6D_6.

Scheme 18 Synthesis of ruthenium enoic carbene complexes by double oxidative addition reported by Grubbs and the decomposition constants (k_{dec}) in C_6D_6 at room temperature.

The complexes were found to be very unstable in solution, decomposing via a bimolecular mechanism within a few hours at room temperature in benzene. Remarkable and unexplored is the stability of the NH_2-substituted enoic carbene complex. Because of the instability of the majority of the compounds, none of them was fully characterized or had its structure elucidated.[100] Consistent with the bimolecular decomposition kinetic data is the formation of dinuclear decomposition products from the $14e^-$ species generated upon dissociation of a PCy_3 ligand (**Scheme 19**).

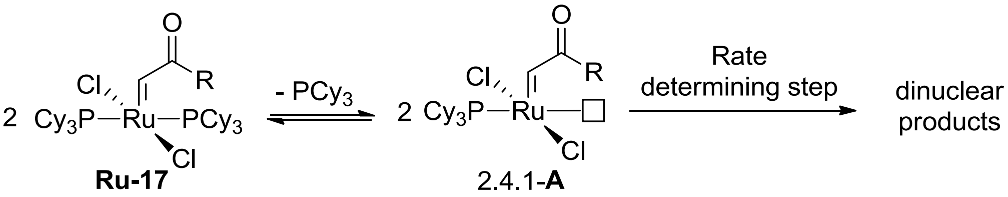

Scheme 19 Speculative initial step in the decomposition of the Ru-enoic carbene complexes reported by Grubbs.

The initial dissociation of one PCy_3 ligand is consistent with the general initiation mechanism for Grubbs-type olefin metathesis (pre)-catalysts (e.g., **GI** and **GII**)[57] and the rate of its dissociation should be faster for bulkier substituents (as observed for analogous **GI**-type complexes). Because the rate of a dinuclear decomposition mechanism is expected to decrease as the bulkiness around the metal centre is increased, it would explain the decomposition constants reported. The higher stability of the NH_2-substituted complex can be interpreted as the result of a, speculative, lower PCy_3 rate dissociation (similar to Ru-methylidene complexes).

The high reactivity of the Ru-enoic carbene complexes was proven from the reaction with cyclohexene (a generally unreactive substrate for olefin metathesis). Later, the scope of this chemistry was expanded to include the reaction of cyclohexene and other unstrained cycloalkanes with Ru-enoic carbenes generated *in situ* from the reaction of **GII** with acrylates.[101,102]

The striking increased reactivity of Ru-enoic carbene complexes as compared to the analogous benzylidene complexes were investigated computationally by the Fomine research group (**Figure 8**).[103] Apart from the lower PCy_3 dissociation energy for the Ru-enoic carbene complex as compared to **GII** (**Ru-18** versus **GII**), the formation of the key ruthenacyclobutane intermediate is less exergonic, starting from the Ru-enoic carbene complex, in 4.2 kcal.mol^{-1}. Moreover, stabilization of the 14e$^-$ intermediate complex **Ru-18-A** was observed to occur via *O*-chelation of the ester oxygen for the Ru-enoic carbene complex (**Ru-18-B**).

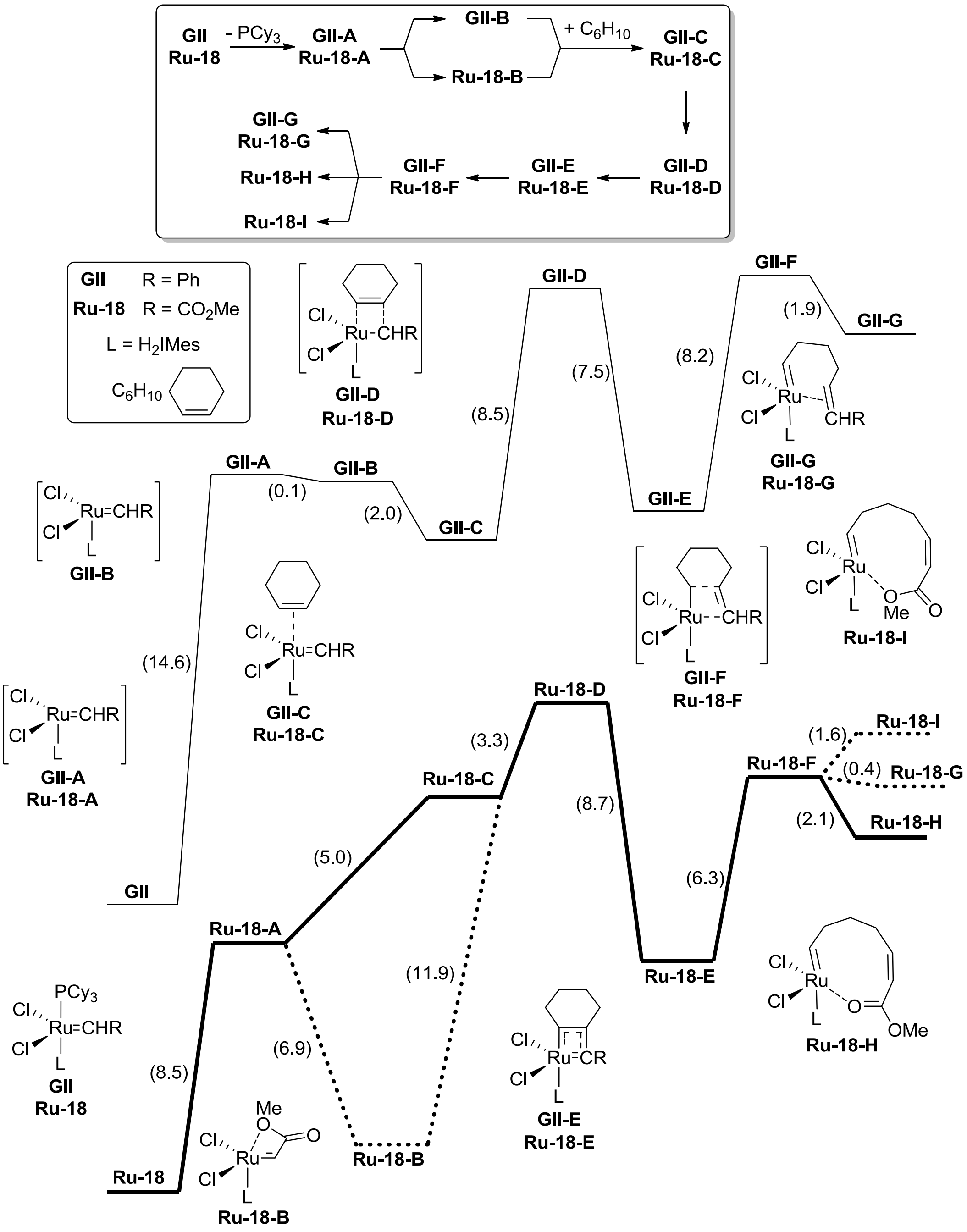
GII
Ru-18
- PCy3
GII-A
Ru-18-A
GII-B
Ru-18-B
+ C6H10
GII-C
Ru-18-C
GII-D
Ru-18-D
GII-E
Ru-18-E
GII-F
Ru-18-F
GII-G
Ru-18-G
Ru-18-H
Ru-18-I
GII R = Ph
Ru-18 R = CO2Me
L = H2IMes
C6H10
(0.1)
(2.0)
(8.5)
(7.5)
(8.2)
(1.9)
(14.6)
(3.3)
(5.0)
(8.7)
(6.3)
(1.6)
(0.4)
(2.1)
(11.9)
(6.9)
(8.5)
Cl
Ru=CHR
Ru-CHR
Ru=CR
Ru--CHR
L
PCy3
Me
O
OMe

Figure 8 Free Gibbs reaction energy profiles of the RCM of cyclohexene by complexes **GII** (top) and **Ru-18** (bottom, bold lines). The free Gibbs reaction energies for each step are given in parentheses (kcal.mol^{-1}).[ii]

[ii] Even though throughout the text similar complexes where drawn as square pyramids (distorted square pyramid geometries are observed in the single crystal structures of most of the five-coordinated, ruthenium-based alkylidene complexes), the structures in this figure were drawn differently, as reported in the paper, since these where the optimized calculated structures.

Hillmayer reported the use of **MA-H** as chain transfer agent to prepare telechelic polyolefins from cyclooctene (COE). With the objective to gain some insights in the stereochemical preference of the Ru-alkylidene species during each metathesis cycle, the CM of **MA-H** with *cis*-4-octene in THF-d_8 was also investigated (**Figure 9**).[104] A conversion higher than 90% and an *E*-selectivity were observed. It was suggested that the presence of a sterically unencumbered Ru-alkylidene (**GII-B** - **Figure 9b**) is crucial for efficient metathesis with **MA-H**. It is important to consider that **MA-H** is an electron deficient olefin (a type II-III olefin),[24] and therefore should be less reactive than *cis*-4-octene (type I olefin). The presence of small amounts of *trans*-cinnamic acid indicates that the formation of **GII-B** is not a strict requisite for the reaction to occur. The authors, nevertheless, also observed that self-metathesis of **MA-H** under identical conditions converted only 2.5 mol% of the double bonds to the *E* configuration (maleic to fumaric acid isomerization) (**Figure 9c**). This result is more likely due to the instability of the generated enoic carbene (**GII-A**) than the lack of reactivity of **MA-H** with the more encumbered Ru-benzylidene in **GII**. The fate of the ruthenium-alkylidene(s) in the reaction was not pursued. Interestingly is the fact that no excess of one of the reactants was necessary to achieve high conversion (despite the rather high catalyst loading - 3.12 mol% per double bond), opposed to the required excess when acrylic acid or acrylates are used as metathesis partner.[20]

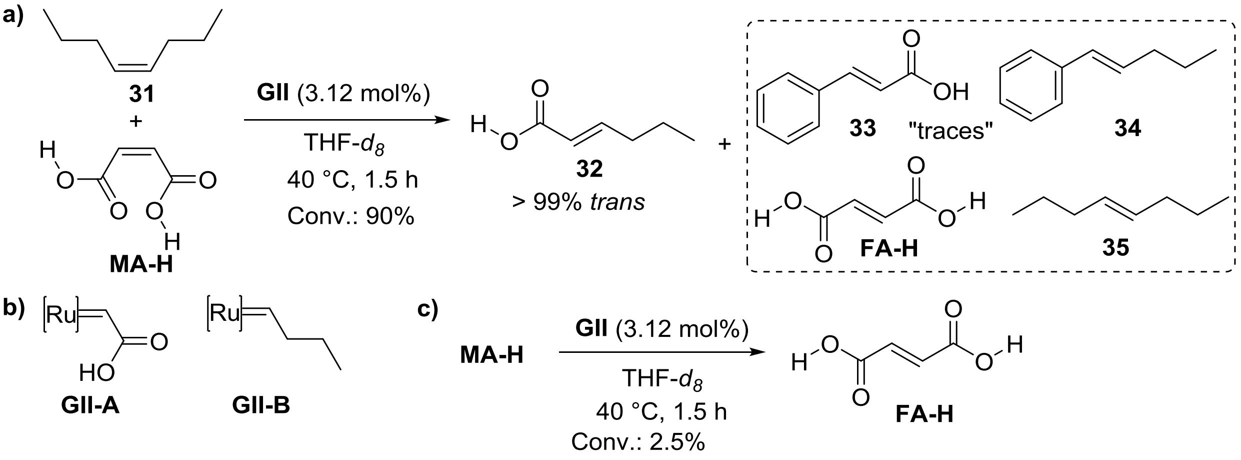

Figure 9 a) CM of *cis*-4-octene with **MA-H** promoted by **GII**; b) the two possible alkylidene intermediates generated in the reaction. c) SM of **MA-H**.

2.4.2 Other Metal-enoic carbene complexes

A metal-enoic carbene is also an important intermediate in transformations beyond olefin metathesis with acrylates. Cyclopropanation of olefins and metal-catalysed olefination of carbonyl compounds are commonly studied using ethyl diazoacetate as the carbene transfer reagent. Examples of transition metal complexes employed in such transformations are based on rhodium, ruthenium and copper. Within the context of cyclopropanation and olefination reactions, a larger number of papers appears in the literature, including successful examples of isolation and spectroscopic / crystallographic characterization of enoic carbene complexes (**Figure 10**).[105-108]

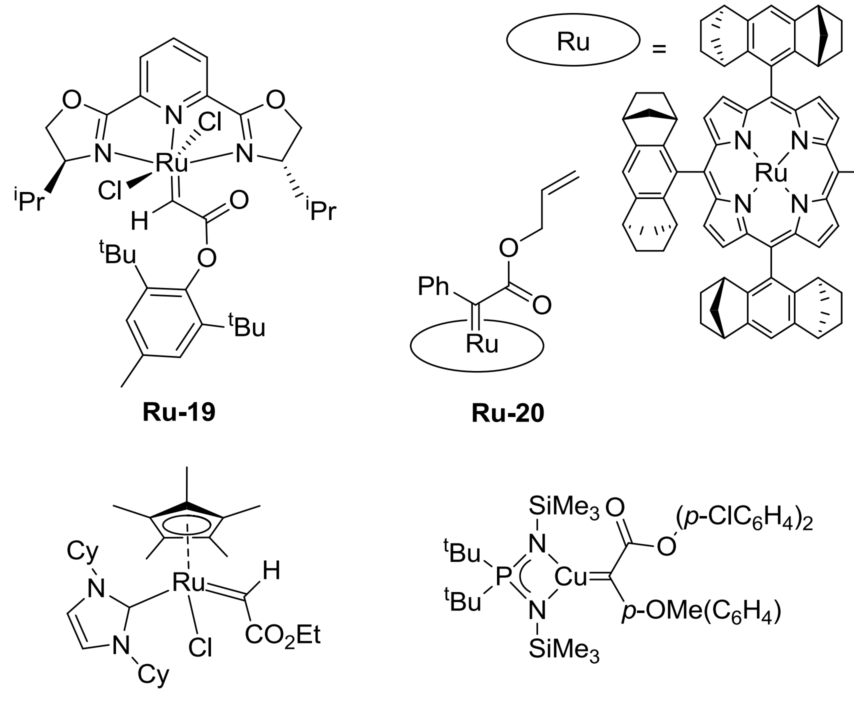

Ru-19 **Ru-20**

Ru-21 **Cu-1**

Figure 10 Examples of some isolated enoic carbene complexes.

A common characteristic of these complexes is their preparation via decomposition of diazo compounds via elimination of nitrogen gas (**Scheme 20**). This strategy is commonly employed in the activation of olefin metathesis, olefin cyclopropanation and/or carbonyl olefination pre-catalysts. For the latter reactions, the diazo compound is also one of the reactants.

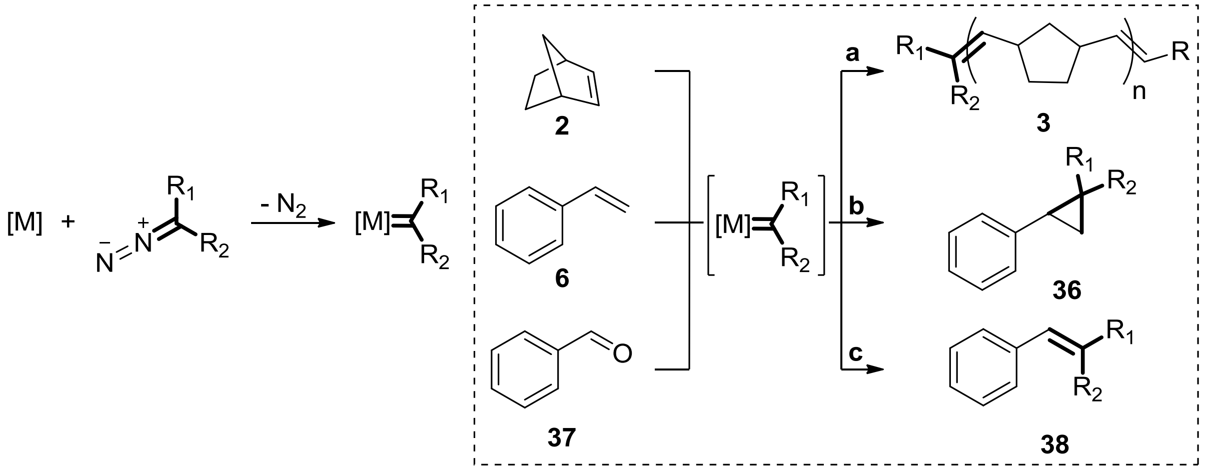

Scheme 20 Decomposition of diazocompounds in the preparation of enoic carbene complexes and the use of *in situ* generated complexes for ROMP (**a**); olefin cyclopropanation (**b**) and carbonyl olefination (**c**).

2.5 INDUSTRIAL OLEFIN METATHESIS

The potential of the olefin metathesis reaction expands the horizons dreamt by academia. Since its early days, the industry has recognized the olefin metathesis as a profitable transformation and has enormously contributed to the maturity of this field. Selected examples of industrial applications of the olefin metathesis reaction are summarized in **Table 1**. The olefin metathesis presence in industry is diversified, ranging from the use of ill-defined catalytic systems in the SHOP process to the use of well-defined catalysts in the synthesis of complex structures by pharmaceutical companies.

One of the earliest successful applications of olefin metathesis in industry is the SHOP process for the production of blends of olefins, which are used in the preparation of surfactants. Briefly, ethylene is oligomerized by a nickel pre-catalyst resulting in a mixture of linear C_4-C_{40} terminal olefins in an Anderson-Shulz-Flowry distribution. Distillation separates the C_6-C_{18} fraction and the remaining fractions (< C_6 and > C_{18}) are isomerized to internal olefins. The isomerized olefins are then passed through a alumina-supported molybdenum catalyst (metathesis step), resulting in the formation of a new blend of internal olefins of different sizes. The C_{10}-C_{14} fraction is separated by distillation and the remaining fractions re-enter in the isomerization / metathesis steps.

Table 1 Selected examples of industrially relevant applications of olefin metathesis.

Company	Segment	Metathesis product
SHELL	Oil and Gas	SHOP - Shell higher olefin process
Elevance renewable Sciences, Inc	Specialty chemicals	Bio-derived compounds
Johnson & Johnson	Pharmaceutical	HCV drug Simeprevir (Olysio^{TM})
Materia Inc.	Catalysts and advanced polymers	Ruthenium-based Catalysts
Umicore	Materials technology	Ruthenium-based Catalysts

Another more recent process is employed by Elevance Renewable Sciences using bio-derived oils as the core feedstock. In the process, bio-derived oils are dimerized via self-metathesis and the products are converted into cleaning / personal care ingredients (**Scheme 21**).

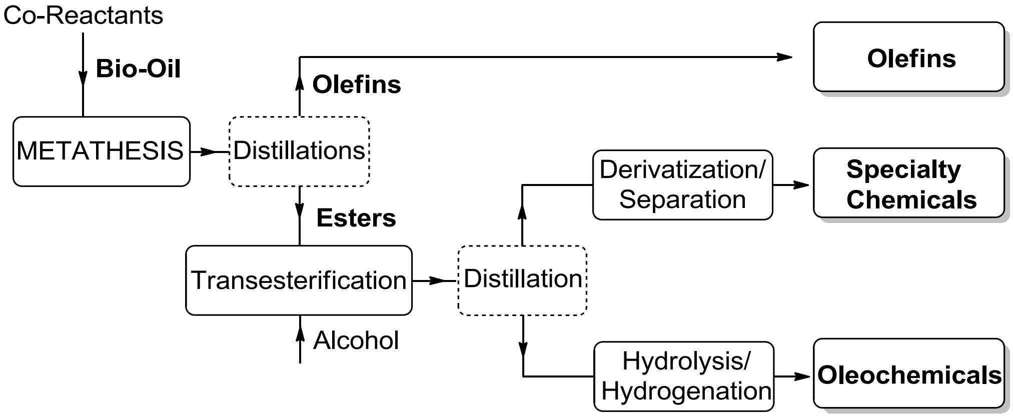
Co-Reactants
Bio-Oil
METATHESIS
Distillations
Olefins
Olefins
Esters
Derivatization/ Separation
Specialty Chemicals
Transesterification
Distillation
Alcohol
Hydrolysis/ Hydrogenation
Oleochemicals

Scheme 21 Biorefinery process developed by Elevance Renewable Sciences® using olefin metathesis as key step in the valorization of bio-oils.

The potential of olefin metathesis in the synthesis of active pharmaceutical ingredients has for long been acknowledged. The most relevant olefin metathesis transformation in this field is the olefin RCM reaction to prepare cyclic molecules of variable ring sizes. Johnson & Johnson launched the Hepatitis C virus (HCV) protease inhibitor Simeprevir (**Figure 11**) on market in December 2013. The RCM step involves the slow addition of both diene and pre-catalyst (**IndII**) under “infinite dilution” conditions, to limit intermolecular reaction of the diene (formation of oligomers) and to retard catalyst deactivation.[21]

Another relevant industrial application of olefin metathesis is the commercialization of (pre)-catalysts. In this area, two companies are worth mentioning: Materia® and Umicore. Materia® is the provider of a series of ruthenium-based metathesis (pre)-catalysts (including several of those developed by Robert Grubbs), while the Umicore portfolio of Ru-metathesis (pre)-catalysts is mostly restricted to indenylidene type complexes.[109-110]

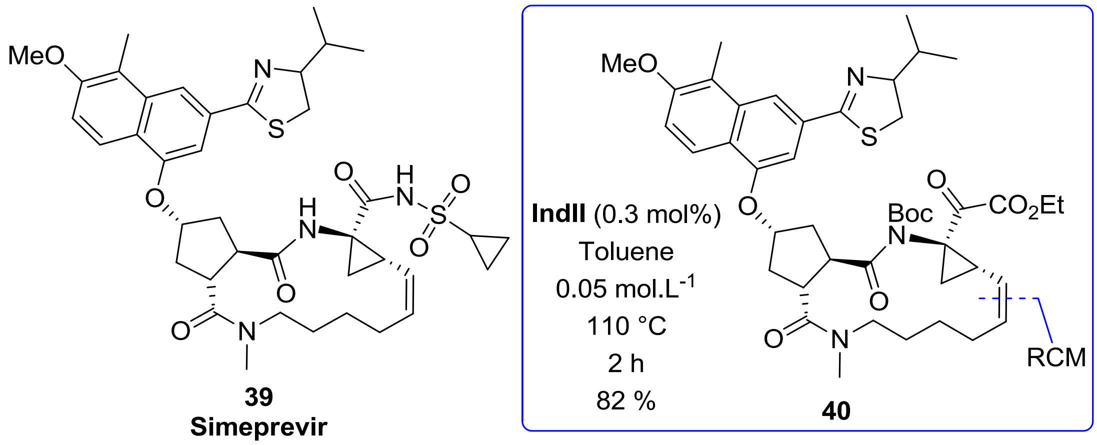

39
Simeprevir
Johnson & Johnson; Olysio™

40

Figure 11 Structure of the Hepatitis C Virus (HCV) drug Simeprevir developed by Medivir and Johnson & Johnson and sold under the name of Olysio™. Inside the box, the conditions used in the metathesis step.

2.6 RENEWABLE OLEFIN METATHESIS

Olefin metathesis has also been explored in the recent quest for sustainable transformations in Chemistry. Although the use of renewable substrates does not necessarily characterize sustainability, the use of such substrates has to some extent being associated with sustainable processes.[111] Whichever the point is, the use of substrates from renewable sources brings new challenges to the field of olefin metathesis, especially regarding purification issues.

The number of naturally occurring olefins is considerably small. Even so, good examples of metathesis transformations involving renewable olefins can be found in the recent literature. The Mecking group has reported the ROMP of the cyclic sesquiterpenes caryophyllene (**41**) and humulene (**42**), components of glove and hop oils (**Scheme 22**). Polymers with M_n in the range of 2-3 x 10^4 g.mol^{-1} with M_w/M_n of ca. 2 were obtained. The unsaturated polymers were then hydrogenated to produce polyethylene-like polymers. Interestingly, the authors observed that for both monomers, only one of the C-C double bonds reacts in the metathesis step. For caryophyllene, the exocyclic double bond remains intact during the reaction, while for humulene, only one of the trisubstituted double bonds reacts.[16]

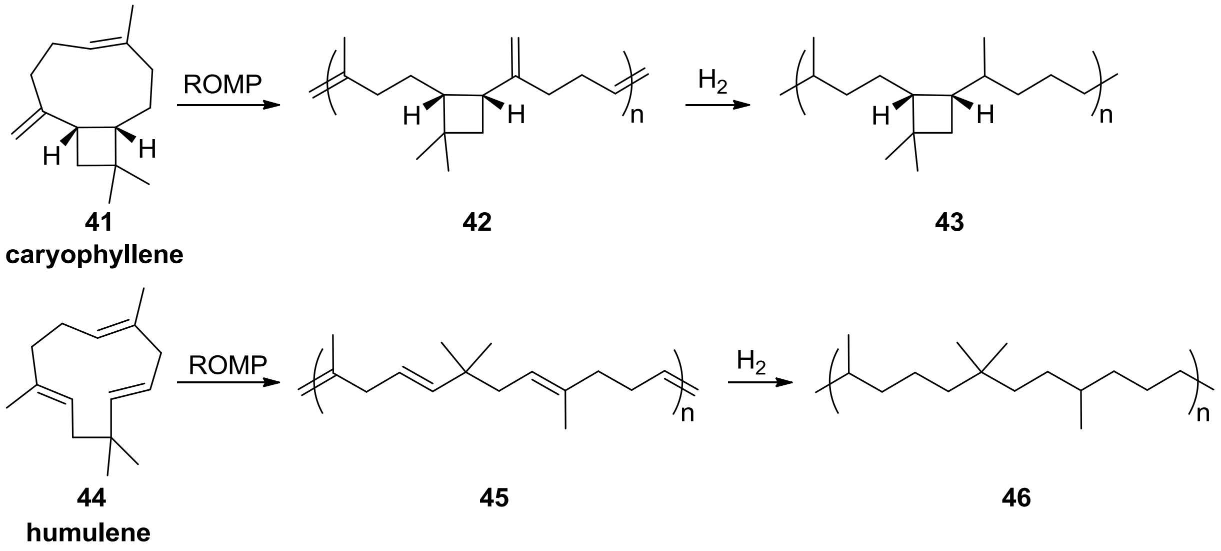

Scheme 22 ROMP of the sesquiterpenes caryophyllene and humulene.

The Meier group has reported the CM with acrylates and the ROMP of lactonic sophorolipid, the major fermentation product derived from the yeast *Candida bombicola*.[112,113] CM of lactonic sophorolipid (**47**) with acrylates was found to occur with nearly quantitative yields but only when high catalyst loadings (5 mol% of **IndII**) were employed. Further alcoholysis of the CM product results in a carbohydrate based surfactant (**49** - **Scheme 23**). ROMP of lactonic sophorolipid resulted in polymers with M_n of ca. 1-2 x 10^5 g.mol^{-1} and M_w/M_n of 1.7.

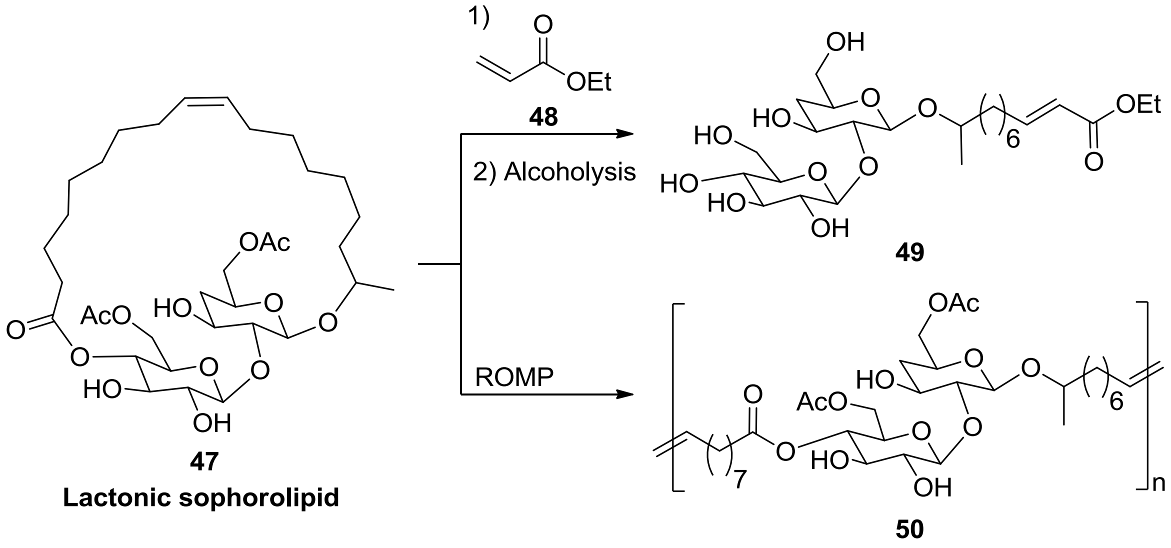

Scheme 23 Metathesis transformations of lactonic sophorolipid.

Itaconic acid (51) is currently produced in an industrial scale of about 80,000 tons per year by fermentation of carbohydrate biomass using strains of filamentous fungus *Aspergillus* (e.g., *Aspergillus terreus* and *Aspergillus itaconicus*). The Meier group also explored the use of itaconic acid in olefin metathesis. Esterification of the acid and subsequent Diels-Alder reaction resulted in the synthesis of the corresponding 2,2-disubstituted norbenene in a diastereomeric mixture (endo – 75 %; exo – 25 %). The ROMP of norbornenes is generally straightforward, due to the ring-strain release occurred in the process. The ROMP of the itaconic acid derived norbonene **52** resulted in high molecular weight polymers (8.7 x 10^4 g.mol^{-1}) with good control in the molecular weight distribution (M_w/M_n = 1.26) (**Scheme 24**).[114]

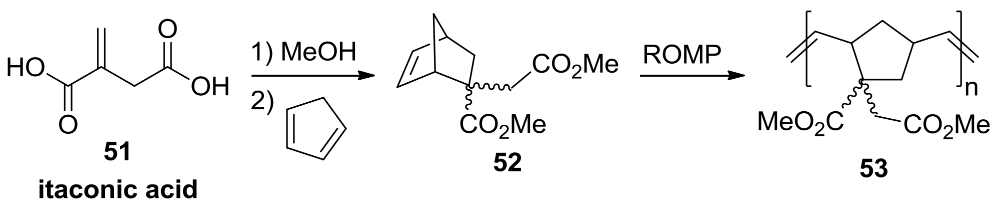

Scheme 24 ROMP of an itaconic acid derived norbornene.

Plant oils have been explored in a diversity of olefin metathesis transformations. CM with either acrylates or ethylene (ethenolysis) are the two most explored transformations. An interesting strategy involving plant oils and olefin metathesis was reported by Mathers (**Scheme 25**).[115] Metathesis of polyunsaturated oils rich in linoleic (C18:2) and linolenic (C18:3) fatty acids and distillation produce the cyclic diene 1,4-cyclohexadiene (**54**), which was isomerized to the conjugated diene with an appropriate isomerization catalyst ($RuClH(CO)(PPh_3)_3$) and polymerized with $Ni(acac)_2/MAO$. Alternatively, the last two steps were also performed in a tandem fashion.

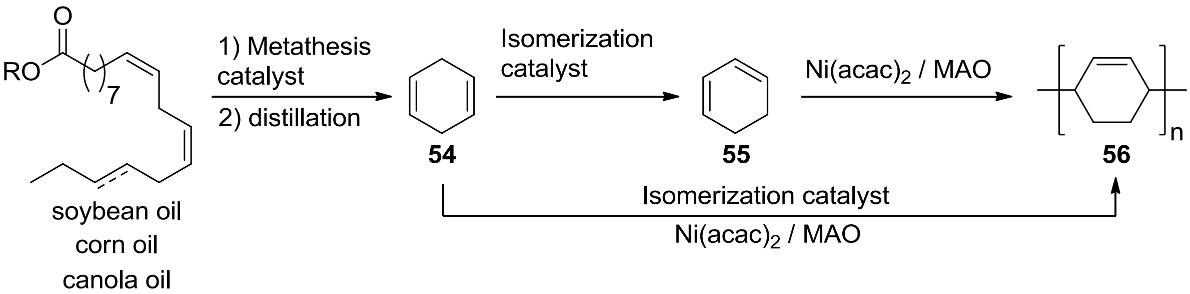

Scheme 25 Synthesis of the monomer 1,3-hexadiene from plant oils.

Another interesting transformation with potential for applications in industry is the CM of vegetable oil components (e.g., methyl oleate) with functionalized terminal olefins (e.g., acrylates, acrylonitrile, acrolein). Such transformations afford useful components with applications in polymer and surfactant synthesis (**Scheme 26**). CM of methyl oleate or methyl 9-decenoate with acrylonitrile, followed by hydrogenation and hydrolysis result in the formation of a linear α,ω-aminoacid useful for the preparation of Nylon 11.[88,90,93] If the same reactions are performed with methyl acrylate as metathesis partner, a α,ω-dicarboxylic acid and a monocarboxylic acid are obtained, which can be used as monomer for the preparation of polyesters or as surfactant ingredient, respectively.[94] The CM of oleyl alcohol[95] and *N*-acetylated oleylamine[116] with acrylates has also been explored. CM of methyl oleate with acrolein was recently reported in the literature.[87]

CM of essential oils derivatives with acrylates represents an interesting transformation for the preparation of valuable products with applications in the perfumery and cosmetics industries. Estragole, eugenol and safrole are phenylpropenoids found as the major constituents of essential oils. The isomerized version of estragole, anethole, is produced on a scale of 750,000 tons/year from star anise, anise and fennel as well as from turpentine oils from wood processing. Eugenol is the major component of clove oil. Estragole is the primary constituent of essential oil of basil oil, tarragon, pine oil, turpentine, fennel and anise. Safrole can be extracted from the root-bark or fruit of sassafras plants or from ‘pimenta-longa’ (*Piper hispidinervium*). CM of anethole, isoeugenol and isosafrole with acrylate esters produces cinnamates and ferulates (**Scheme 27**), substances with antioxidant properties. For instance, the compound octyl methoxycinnamate (R_1 = Me; R_2 = H, R_3 = isooctyl) is an important sunscreen agent.[15]

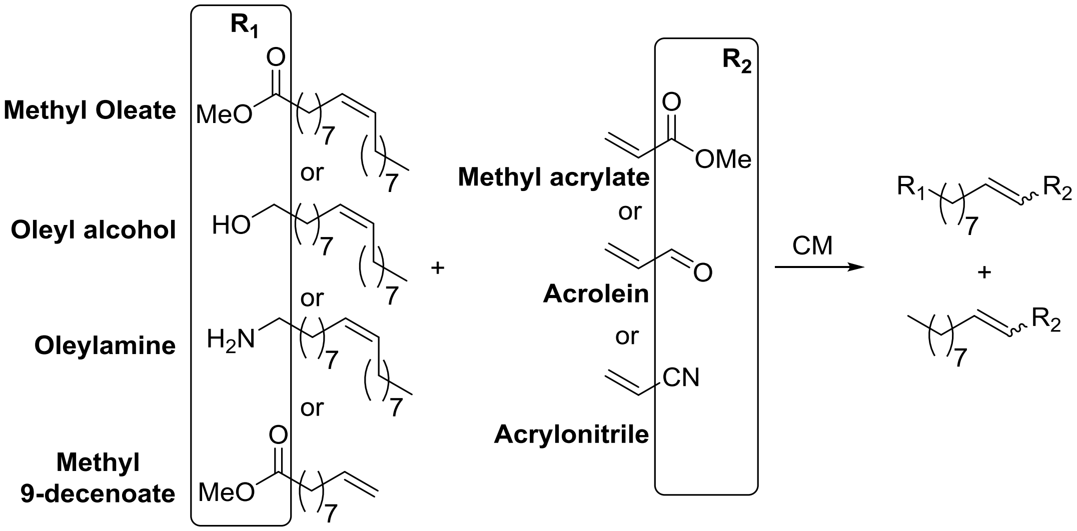
R1
Methyl Oleate
MeO
or
Oleyl alcohol
HO
Oleylamine
H2N
Methyl 9-decenoate
7
+
R2
OMe
Methyl acrylate
Acrolein
Acrylonitrile
CN
CM
R1
R2

Scheme 26 Cross metathesis of fatty acid derivatives with acrylates, acrolein and acrylonitrile.

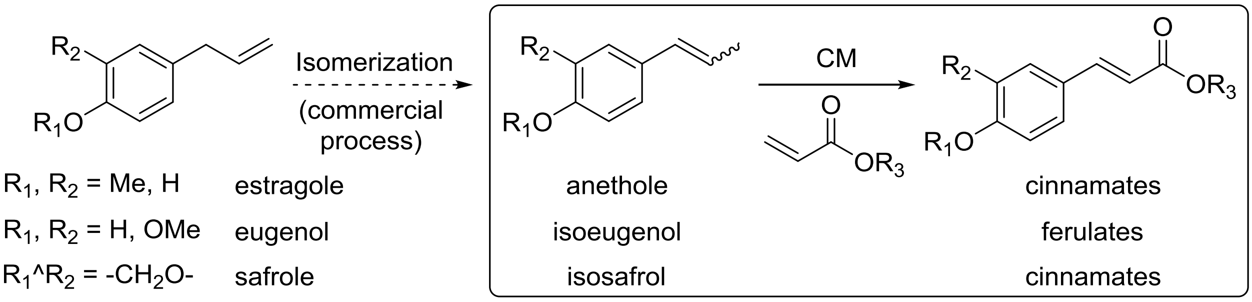
R2
R1O
Isomerization
(commercial process)
R1, R2 = Me, H
R1, R2 = H, OMe
R1^R2 = -CH2O-
estragole
eugenol
safrole
anethole
isoeugenol
isosafrol
CM
OR3
cinnamates
ferulates
cinnamates

Scheme 27 CM of essential oils with acrylate esters.

2.7 GENERAL CONSIDERATIONS ON CARBENES AND ALKYLIDENES[iii]

Neutral species containing divalent carbons (and therefore only six valence electrons) are defined as carbenes (or alkylidenes), which may react either as an electrophile or as a nucleophile depending on whether the two unshared electrons on the carbon are unpaired (a triplet carbene) or paired (a singlet carbene). Metal-alkylidene complexes can be classified in a similar way based on their reactivity toward electrophiles and nucleophiles. Complexes containing a M=C bond that are nucleophilic at the carbon are called Schrock-type complexes while complexes containing an M=C bond that are electrophilic at the carbon are called Fischer-type complexes (**Figure 12**).[117]

Alkylidenes are usually prepared by the loss of small and stable molecules (e.g., N_2) from alkylidene precursors. Alkylidenes can therefore be prepared by the thermal or photolytic decomposition of diazocompounds (normally tosylhydrazone derivatives), elimination mediated by bases or decomposition of diazocarbonyl compounds catalyzed by metals. Metal-alkylidene complexes are useful catalysts in olefin metathesis, olefin cyclopropanation and carbonyl olefination reactions.

An extreme case of Fischer-alkylidenes is the NHC (*N-heterocyclic carbene* – Wanzlick-Lappert-Arduengo carbenes) carbenes. These ligands are an extreme case of the traditional Fischer-type complexes because the π-donation from the two nitrogen lone pairs into the carbon *p* orbital is so extensive that several free NHCs are stable without metal coordination.[117]

Typically, NHCs coordinate to metals predominantly by strong σ-donation through the carbon lone pair, and they generally behave as unreactive ancillary $2e^-$ donor ligands similar to phosphines. In general, NHCs behave as better donors than the best phosphine donor ligands with the exception of the sterically demanding *N,N*`-adamantyl carbene.[118] NHCs have been extensively used in recent years as ancillary ligands in organometallic chemistry.[119,120]

[iii] In the GOLD BOOK of IUPAC there is no distinction between the terms carbene and alkylidene. For clarity, in this thesis only the *N*-heterocyclic carbenes (NHC) will be referred to as "Carbenes", all other species will be referred to as "Alkylidenes". In the literature, some distinction is generally (but not always) made: complexes of the Fischer-type are referred to as "Carbenes" while complexes of the Schrock type are referred to as "Alkylidenes".

	Schrock	Fischer	Wanzlick-Lappert-Arduengo
Example	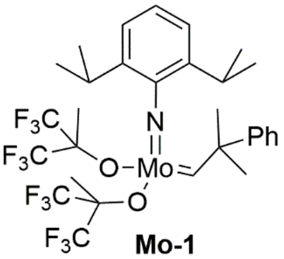 F3C F3C O N Mo Ph F3C O F3C **Mo-1**	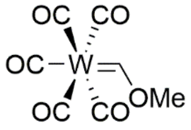 OC CO OC W OMe OC CO **W-3**	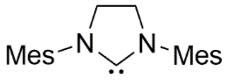 **H_2IMes**
Ground state of free carbene	triplet	singlet	singlet
Typical metal centers	higher oxidation state earlier transition metals	lower oxidation state later transition metals	variable
Character of metal-bound carbene carbon	nucleophilic 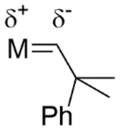	electrophiic 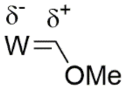	variable
Illustration of bonding interactions	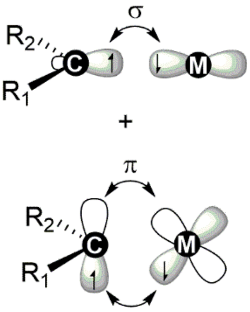 σ R2 C M R1 + π R2 C M R1	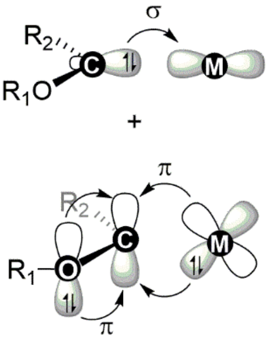 σ R2 C M R1O + π R2 C M R1 O π	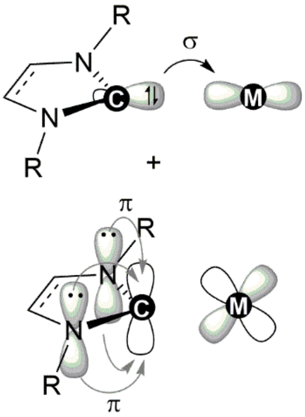 R σ N C M N R + π R N C M N R π

Figure 12 General properties of Schrock and Fischer alkylidenes and NHC carbenes.

3.1 CROSS-METATHESIS WITH MALEIC ACID

3.1.1 System optimization

The purification of the substrates (especially those from natural sources) is sometimes an overlooked parameter that is rarely investigated during the optimization of catalytic reactions. Therefore, the purification of the methyl oleate (**MO**) was the first parameter to be investigated in this study of the cross-metathesis (CM) of **MO** with maleic acid (**MA-H**) (**Scheme 28**). Based on the literature, four purification methods were investigated. All methods have in common the use of Magnesol/Celite as purifying agents. The use of Magnesol/Celite has been reported to dramatically improve the propenolysis of soybean oil FAME (Fatty acid methyl ester).[121-125] The initial experiments were performed at 50 °C using a 1:1 molar ratio of **MO**:**MA-H** in THF. **GII** was used as (pre)-catalyst because it was shown to exhibit good activity in the synthesis of carboxy-telechelic polymers via the ROMP of cyclooctene with **MA-H** as chain-transfer agent.[104]

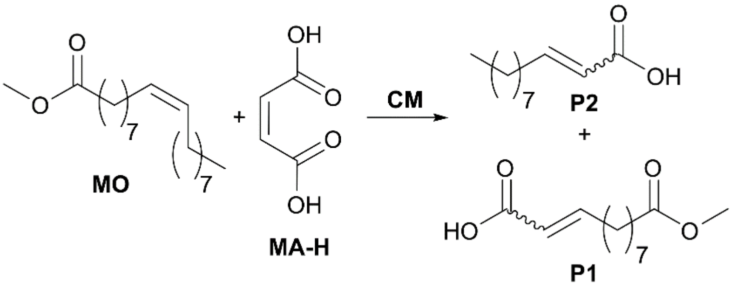

Scheme 28 CM of methyl oleate (**MO**) with maleic acid (**MA-H**).

Purification of **MO** over Magnesol (2.5 wt %) and Celite (1.5 wt %) at 40 °C for 12 h (purification method A) prior to use afforded almost a quantitative yield and an excellent selectivity towards the CM products in the reaction with **MA-H**, when applying either 0.4 or 0.2 mol% of **GII** (**Table 2** – entries 1-2, respectively). Decreasing the catalyst loading to 0.1 and 0.05 mol% resulted in steadily reducing conversions of 73 and 4 %, respectively (**Table 2** – entries 3-4). In both experiments, the reaction occurred only in the initial 10 min (**Figure 13**), suggesting catalyst decomposition by remaining impurities.

Purification method B involves treating **MO** with Magnesol (2.5 wt%) and Celite (1.5 wt%) at 80 °C for 1 h. With this procedure, a **MO** conversion of 81 % and yield of CM products of 66 % were obtained with a catalyst loading of 0.1 mol% (**Table 2** – entry 5), being a slight improvement in comparison to the purification method A.

With the observed positive temperature effect on the treatment of **MO**, the next step was to determine if pre-drying the Magnesol and Celite could result in further improvement. Nevertheless, when **MO** was treated with the dried Magnesol (2.5 wt%) and Celite (1.5 wt%) and subjected to the cross-metathesis reaction, a decrease in both conversion (70 %) and yield of CM products (55 %) was observed (**Table 2** – entry 6).

Titanium alkoxides have been used as additives or as co-catalysts in some metathesis transformations of oxygen- and nitrogen-containing substrates.[126-129] Recently, the treatment of natural oils with $Ti(O^iPr)_4$ has been disclosed for use as olefin metathesis substrates.[130] Although the role of $Ti(O^iPr)_4$ in the treatment of **MO** is merely speculative, it may trap nitrogen-containing impurities via coordination. Aiming the further improvement in the **MO** conversion, the treatment of **MO** with titanium(IV) isopropoxide was explored. The treatment of **MO** with $Ti(O^iPr)_4$ (2 mol%), Magnesol (2.5 wt%) and Celite (1.5 wt%) resulted in a conversion of 81 % and yield of CM of 69 % with 0.1 mol% of **GII** as (pre)-catalyst (**Table 2** – entry 7). Altogether, purification method D is better than the methods A and C, and slightly better than method B, showing a slight improvement in the selectivity.

Table 2 Influence of the **MO** purification method on the **GII**-catalyzed CM of **MO** with **MA-H**.

Entry	GII (mol%)	Purification method	Conversion (%)	Yield (%)	
				CM	SM
1	0.4	A	98	96	1
2	0.2	A	97	94	2
3	0.1	A	73	48	20
4	0.05	A	4	<2	2
5	0.1	B	81	66	14
6	0.1	C	70	55	18
7	0.1	D	81	69	10

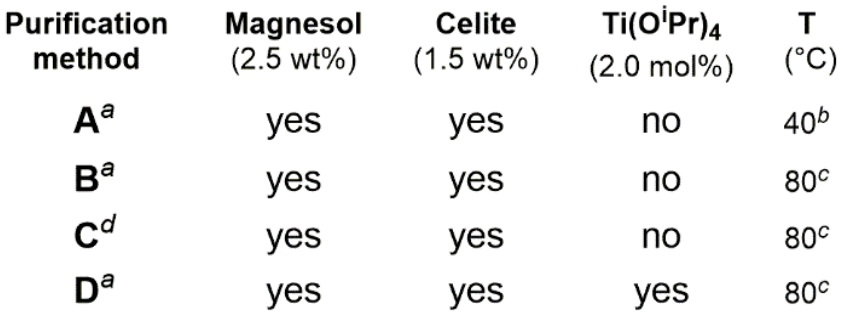

Purification method	Magnesol (2.5 wt%)	Celite (1.5 wt%)	$Ti(O^iPr)_4$ (2.0 mol%)	T (°C)
A[a]	yes	yes	no	40[b]
B[a]	yes	yes	no	80[c]
C[d]	yes	yes	no	80[c]
D[a]	yes	yes	yes	80[c]

Conditions: **MO**:**MA-H** molar ratio = 1:1 (**MO** = 1.77 mmol); THF = 7.0 mL; reactions performed at T = 50 °C. Isomerization products complete the mass balance. [a] Magnesol and Celite were used as received; [b] heated for 12 h; [c] heated for 1 h; [d] Magnesol and Celite dried at 160 °C for 48 h prior to use.

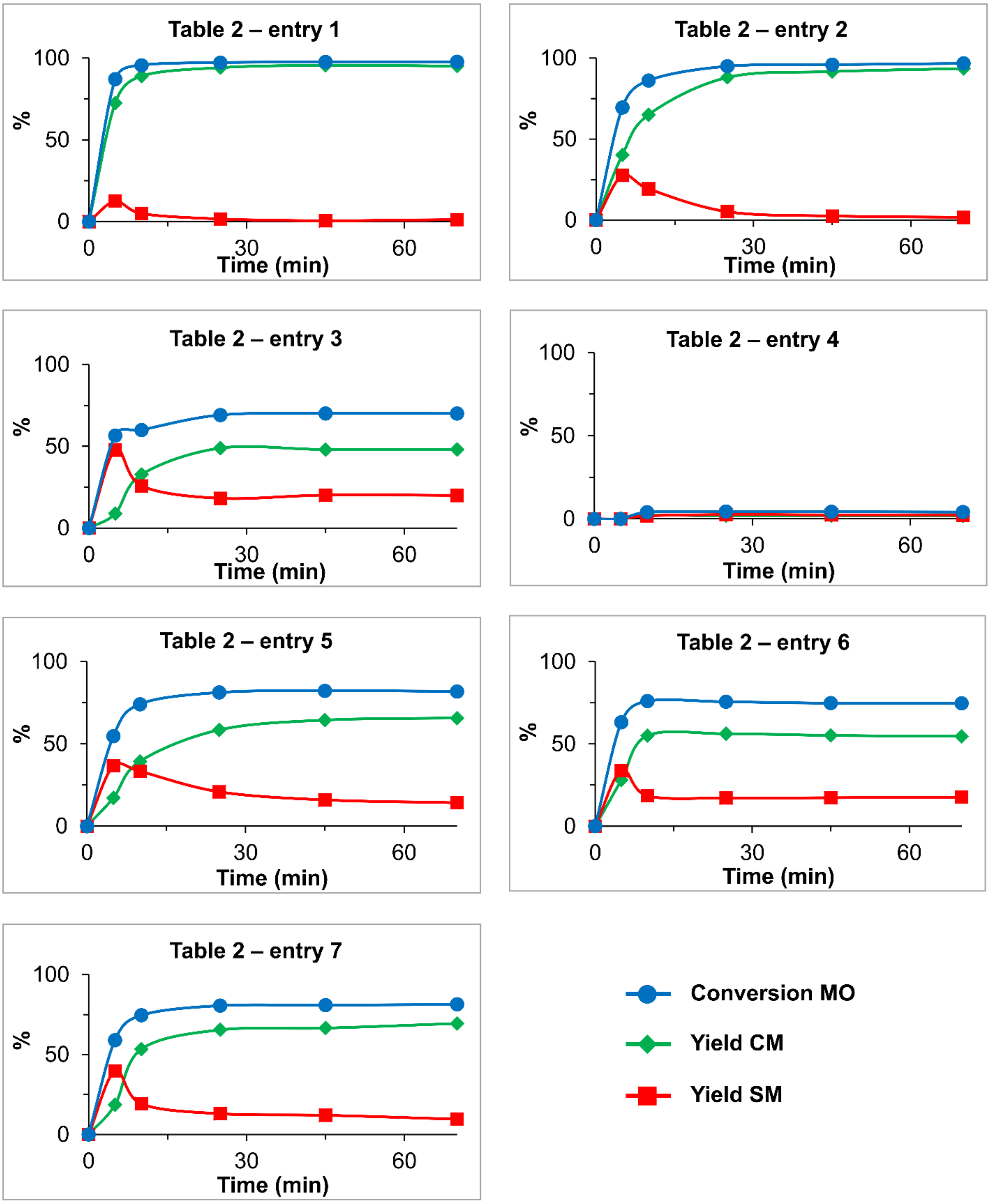

Figure 13 Time-dependent plots of the effect of the **MO** purification procedure on the product distribution in the CM of **MO** with **MA-H** catalyzed by **GII** (data are summarized in **Table 2**). The lines were added with the only purpose to aid visualization.

Interestingly, regardless the purification method employed and the catalyst loading, all the reactions occurred within the first 25 minutes (**Figure 13**), which indicates that despite **MA-H** being electronically deficient; its reactivity is comparable to that of **MO**. Moreover, high selectivity towards the CM products was only obtained with high conversion. This finding is not surprising when the reactivity of the SM and CM products are taken into consideration. The SM products, *E/Z* dimethyl 9-octadecenedioate (**P3**) and *E/Z* 9-octadecene (**P4**), are type I olefins (i.e., homodimerize quickly and are promptly consumed)[24] and have similar reactivity as **MO**. As a consequence, the SM is an equilibrium reaction. On the other hand, the CM products, 11-methoxy-11-oxoundec-(2*E/Z*)-2-enoic acid (**P1**) and (2*E/Z*)-2-undecenoic acid (**P2**), are type IV olefins (i.e., are not reactive towards olefin metathesis) and, as a consequence, CM with **MA-H** is an irreversible reaction (**Scheme 29**).

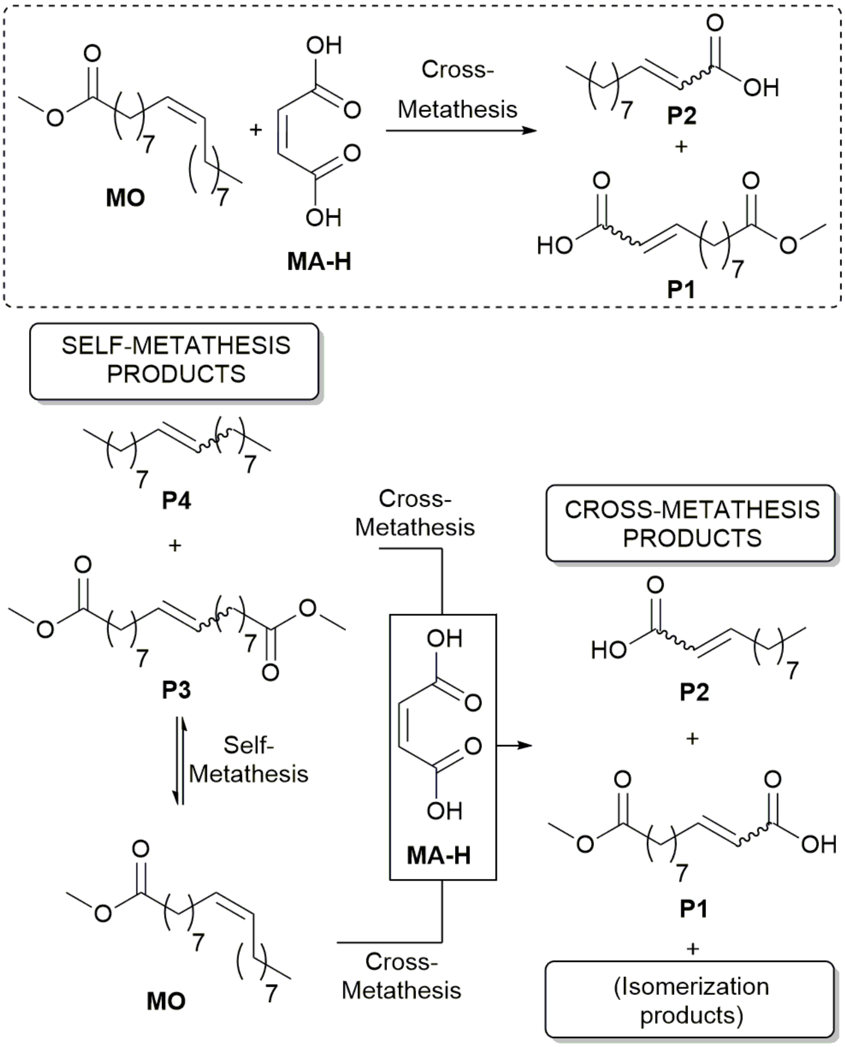

MO
MA-H
Cross-
Metathesis
P2
P1
SELF-METATHESIS PRODUCTS
P4
P3
Self-
Metathesis
MO
Cross-
Metathesis
MA-H
Cross-
Metathesis
CROSS-METATHESIS PRODUCTS
P2
P1
(Isomerization products)

Scheme 29 CM of **MO** with **MA-H**.

The purification method D ($Ti(O^iPr)_4$ - 2 mol%, Magnesol - 2.5 wt%, and Celite - 1.5 wt%) was used to further optimize the reaction conditions. In the next step, the influence of the **MO**:**MA-H** ratio on both the conversion and selectivity was investigated. Increasing the **MO**:**MA-H** molar ratio from 1:1 to 1:5 resulted in an initial increase in both conversion and yield of CM products, which remained more or less steadily for the ratios studied (**Table 3** – entries 7-11). Only a minor decrease in the conversion was observed when a ratio of 1:5 (**MO**:**MA-H**) was used (**Table 3** – entry 11). Additionally, the effect on the selectivity (yield of CM vs yield of SM) was only evident at the higher ratio of **MO**:**MA-H**. The decrease in both conversion and selectivity by increasing the amount of **MA-H** could be attributed to the decomposition of enoic-carbene species, as the increase in the concentration of **MA-H** would favour the formation of such intermediates. The **MO**:**MA-H** ratio of 1:2 was chosen for further optimization and a decrease in the catalyst loading to 0.05 mol% resulted in a conversion of 83 % and a 63 % yield of the CM products (**Table 3** – entry 12). Further decrease in the catalyst loading was not pursued as in this scenario it would not be possible to obtain high selectivity[131] and therefore the reaction would be better described as the inhibition of the **MO** SM by the cross-metathesis partner.[132]

Table 3 Effect of the **MO**:**MA-H** molar ratio on the **GII**-catalyzed CM of **MO** with **MA-H**.

Entry	**MO:MA-H**	**Conversion (%)**	**Yield (%)**	
			CM	**SM**
7	1:1	81	69	10
8	1:2	96	89	4
9	1:3	96	90	2
10	1:4	95	88	3
11	1:5	90	80	7
12*	1:2	83	63	17

Conditions**:** THF = 7 mL; **GII** = 0.1 mol% (vs **MO**; **MO** = 1.77 mmol); T = 50 °C; purification method D. Isomerization products complete the mass balance. * **GII** = 0.05 mol% (vs **MO**).

The decrease in the solvent amount in a reaction is an advantageous parameter for more sustainable processes. Moreover, the amount of the solvent (i.e., the concentration of the reactants) does sometimes influence the outcome of metathesis reactions (specifically in ring-closing metathesis reactions). Although the studied reaction cannot be performed under neat conditions due to solubility restrictions inherited by the use of **MA-H**, the amount of solvent was changed in order to observe its influence on the reaction. As summarized in **Figure 14**, the concentration of the reactants had just a minor effect on the conversion of **MO**. The increase of the concentration up to 1.2 mol.L^{-1} (1.5 mL of THF) resulted in an increase of 10 % in the conversion and an increase in the yield of the CM products from 63 to 84 %. The increase to higher concentrations was not feasible due to the limited solubility of **MA-H** in THF. At the optimum concentration, high **MO** conversion with good selectivity towards the CM products (84 % yield of CM products) was achieved (**Figure 14**).

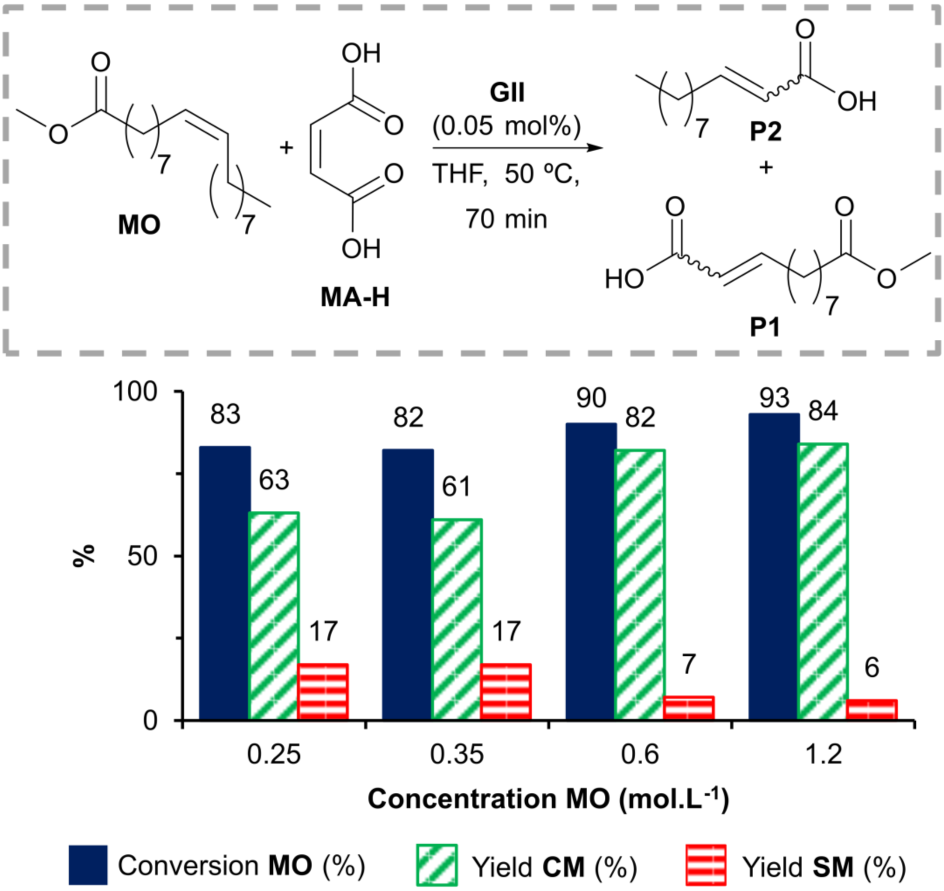

Figure 14 Effect of the substrates concentration on the cross-metathesis of **MO** with **MA-H** using (pre)-catalyst **GII**. Conditions: **MO**:**MA-H** molar ratio = 1:2 (**MO** = 1.77 mmol); **GII** = 0.05 mol%; T = 50 °C; purification method D. Isomerization products complete the mass balance.

Surprisingly, the temperature has just a minor influence on the conversion of the explored reaction using **GII** as (pre)-catalyst. Only a small variation (4 %) was observed in the temperature range of 40 °C to reflux (b.p. THF = 65 °C) (**Figure 15**). Under refluxing conditions, however, an indication of a detrimental effect on the yield of the CM products was observed, consistent with the thermal decomposition of the catalytic species.

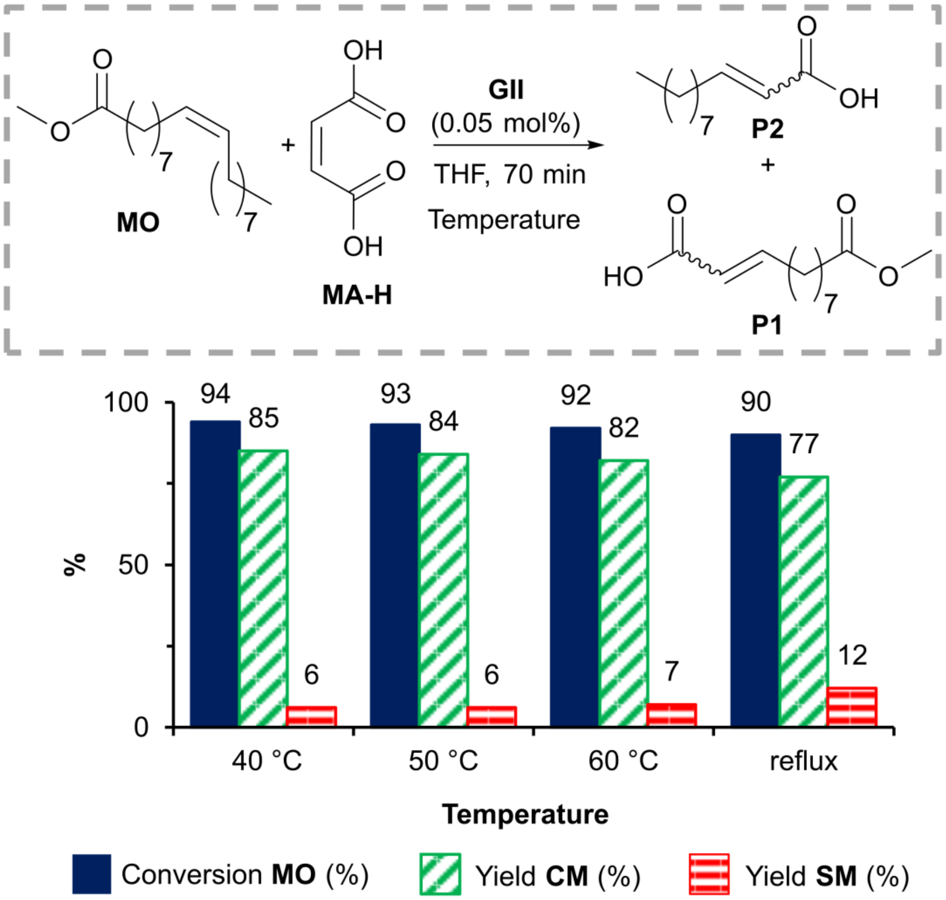

Figure 15 Effect of the temperature on the CM of **MO** with **MA-H**. Conditions: **MO**:**MA-H** molar ratio = 1:2 (**MO** = 1.77 mmol, [**MO**] = 1.2 mol.L^{-1}); **GII** = 0.05 mol%; THF = 1.5 mL; purification method D. Isomerization products complete the mass balance.

After establishing the optimal purification method, catalyst loading, **MO**:**MA-H** molar ratio, concentration of substrates and temperature, the performance of some (pre)-catalyst was then investigated. Three additional ruthenium-based metathesis (pre)-catalysts were selected. The selection of the complexes was based on the nature (phosphine containing versus phosphine-free complexes) and the type (PCy$_3$, chelating 2-isopropoxybenzylidene and chelating phenoxy-imine) of the departing ligand in the dissociation step and the type of alkylidene (benzylidene, indenylidene or 2-isopropoxybenzylidene) (**Figure 16**).

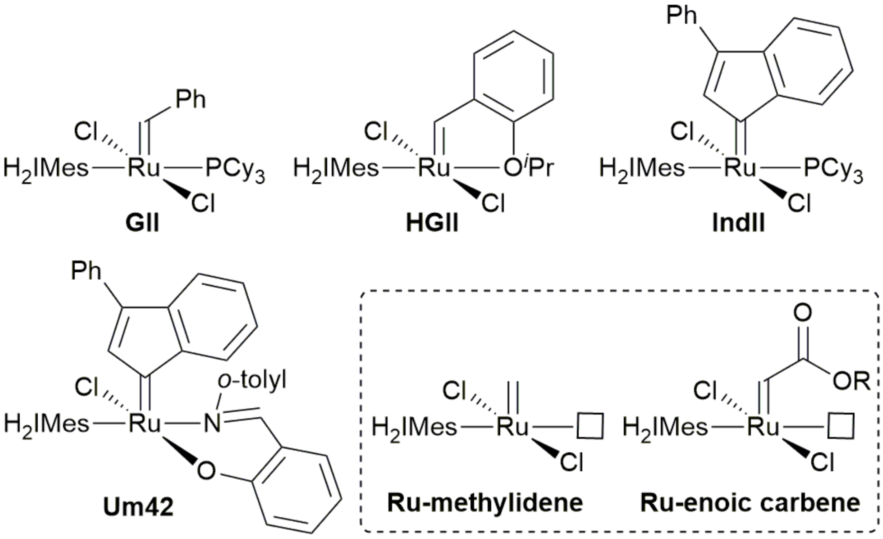
Ph
Cl
H2IMes—Ru—PCy3
Cl
GII
Cl
H2IMes—Ru—O^{i}Pr
Cl
HGII
Ph
Cl
H2IMes—Ru—PCy3
Cl
IndII
Ph
Cl
o-tolyl
H2IMes—Ru—N
O
Um42
Cl
H2IMes—Ru
Cl
Ru-methylidene
O
OR
Cl
H2IMes—Ru
Cl
Ru-enoic carbene

Figure 16 (Pre)-Catalysts employed in the CM of **MO** with maleic and acrylic acid derivatives. Inside the dashed box, the propagating species formed during the metathesis of terminal and/or α,β-unsaturated carboxylic acid derivatives.

The second-generation Hoveyda-Grubbs metathesis catalyst - **HGII** - is considered the (pre)-catalyst of choice in the cross-metathesis with electron deficient substrates (e.g., acrylates). Interestingly, in comparison to **GII**, **HGII** provided a similar conversion under the same conditions, although the CM yield was somewhat lower (**Figure 17**). Regarding the temperature, both complexes operate better at 60 °C (**Table 4**), showing signs of catalyst decomposition at reflux.

The complex **IndII**, an indenylidene analogue of **GII**,[36,133,134] performed similarly to both **GII** and **HGII**, but as depicted in the time-dependent plots (**Figure 17b,c**), the conversion of **MO** was slower in the case of both **HGII** and **IndII**. As seen in **Figure 17b,c**, the **GII**-catalyzed reaction occurred within approximately 10 minutes as opposed to the reactions catalyzed by **HGII** and **IndII**. For the latter systems, a plateau was reached after approximately 35 minutes.

Table 4 Effect of the catalyst on the CM of **MO** with **MA-H**.

Entry	Cat.	Temp. (°C)	Conv. (%)	Yield (%)	
				CM	SM
13[a]	**GII**	40	94	85	6
14[a]	**GII**	50	93	84	6
15[a,b]	**GII**	60	92	82	7
16[a]	**GII**	reflux	90	77	12
17	**HGII**	50	82	57	21
17[b]	**HGII**	60	88	69	15
19	**HGII**	reflux	82	60	20
20[b]	**IndII**	60	90	73	13
21[b]	**Um42**	60	56	14	41
22	**Um42**	reflux	60	17	42

Conditions: **MO**:**MA-H** molar ratio = 1:2 (**MO** = 1.77 mmol); **Cat.** = 0.05 mol%; THF = 1.5 mL; purification method D. Isomerization products complete the mass balance. [a] values plotted in **Figure 15**. [b] Values plotted in **Figure 17**.

The fourth complex explored was the phosphine-free, indenylidene-type, **Um42** complex. **Um42** is a “latent” catalyst due to the presence of the non-labile phenoxy-imine chelating ligand. It has been reported that this complex is activated thermally or chemically by the use of Brönsted acids or silanes.[135-138] It was therefore envisaged that such complex could perform well in our system, as **MA-H** could serve as both activating agent and substrate. Nevertheless, the **CM** reaction catalyzed by **Um42** under refluxing conditions was less productive and resulted in only 60 % conversion with 17 % of CM products (**Figure 4a-c**).

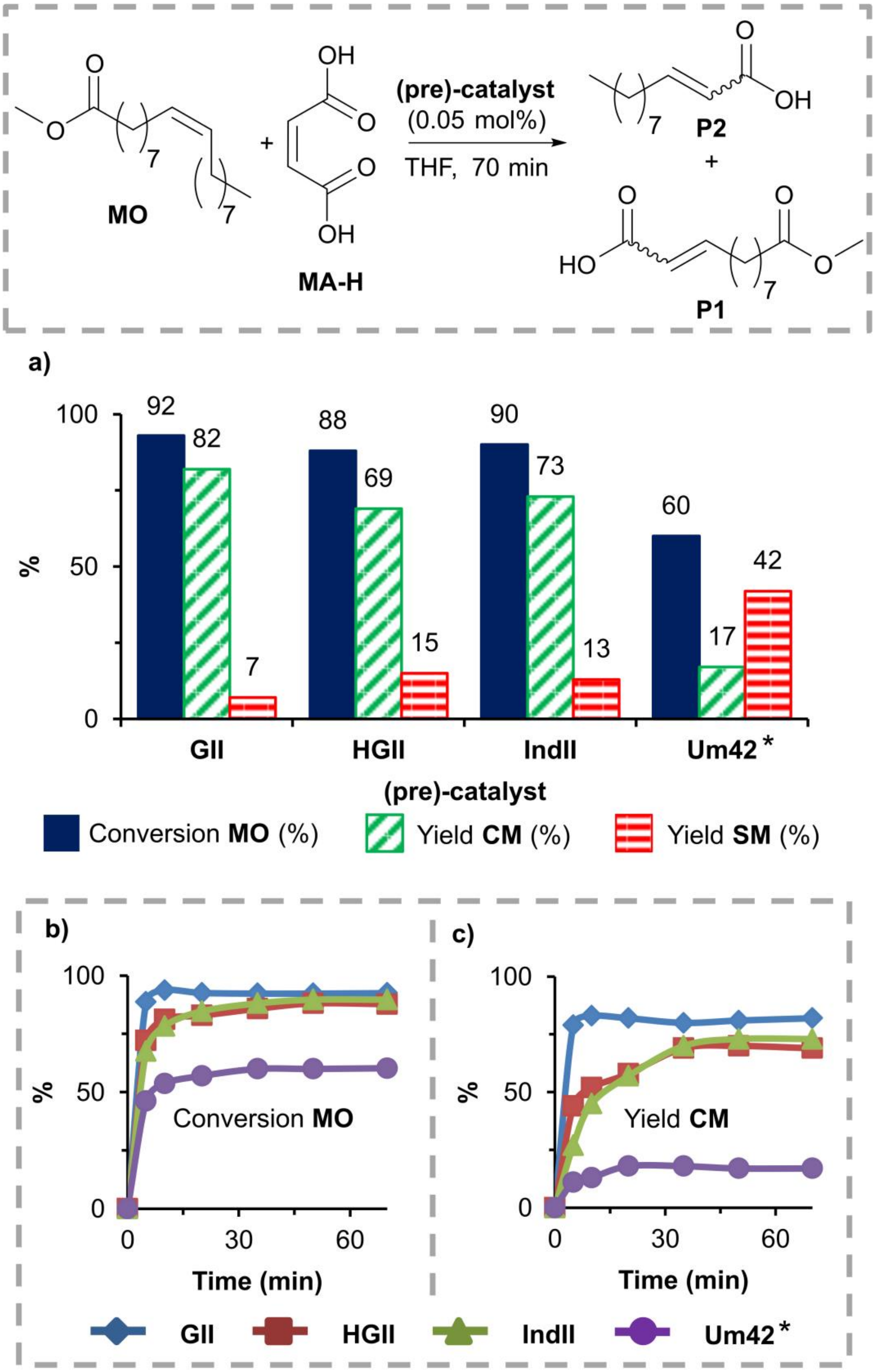

Figure 17 Influence of the (pre)-catalyst on the CM of **MO** with **MA-H** a); and time-dependent plots of: b) the conversion of **MO** and c) the yield of the CM products. Lines were added in the time-dependant plots with the only purpose to aid visualization. Conditions: **MO**:**MA-H** molar ratio = 1:2 (**MO** = 1.77 mmol); THF = 1.5 mL; purification method D; T = 60 °C; 0.05 mol% of (pre)-catalyst. Isomerization products complete the mass balance. * Reaction performed at reflux.

3.1.2 Maleic acid vs maleates

In an attempt to establish the effect of the structure of the CM partner on the conversion and selectivity, a series of reactions of **MO** with two selected maleate esters were performed. Reactions were performed with both **GII** and **HGII** under the optimized reaction conditions established (i.e., purification method D, 0.05 mol% of (pre)-catalyst, 1.2 mol.L^{-1} of **MO** and 60 °C) (**Figure 18**). The (pre)-catalysts **GII** and **HGII** were chosen for the continuity of this study due to a number of reasons: a) superior performance in the optimization reactions; b) **HGII** is generally the best (pre)-catalyst when employing electron-deficient olefins; c) **GII** and **HGII** are standard (pre)-catalysts in olefin metathesis; and d) a direct influence of the presence of PCy_3 in the reaction media is possible to obtain with this combination, considering that the same propagating species are formed with both (pre)-catalysts.

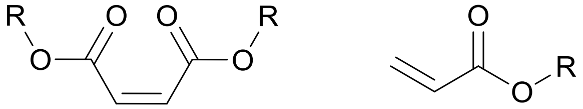

MA-H R = H
MA-Me R = Me
MA-^{i}Pent R = *i*-Pentyl

AA-H R = H
AA-Me R = Me

Figure 18 Cross-metathesis partner scope.

The use of dimethyl maleate (**MA-Me**) resulted in a decrease in the conversion to about half the conversion obtained with **MA-H** for both **GII** and **HGII** (**Figure 19**).[139-141] The effect on the yield of CM products (i.e., on the selectivity) of this substrate is even more pronounced, resulting in less than 15 % of the CM products. This decrease in both conversion and selectivity is likely due to the presence of the bulkier methyl group of **MA-Me**. In previous literature reports of the CM reaction with acrylates no considerable influence of the alkoxy substituent bulkiness was observed. Nevertheless, significantly higher catalyst loadings (0.5 or 5 mol% of **HGII**) were employed.[15,142] A comparative reaction was performed to check this assumption, using the bulkier di-isopentylmaleate (**MA-^{i}Pent**) as the CM partner. Conversions were similar as those obtained with **MA-Me**, but only traces (> 6 %) of the target CM products were obtained.

The carboxylate salt formed in the reaction of **MA-H** + PCy_3 could play a role in catalyst decomposition. A control reaction was conducted to test this hypothesis: 20 equivalents (versus **GII**) of disodium maleate were added to the reaction of **MO** with **MA-H** and keeping the **MO**:(**MA-H** + disodium maleate) ratio equal to 1:2 (**GII** = 0.05 mol%, 60 °C, 70 min., 1.5 mL of THF). An expressive decrease in both conversion and selectivity was observed (**MO** conversion = 61 %; CM yield = 24 % and SM yield = 36 %). Nevertheless, although the addition of 20 equivalents of the disodium maleate salt represents a maximum 40-fold increase in the concentration of the carboxylate anion, the results obtained under this condition are still superior to those obtained using **GII** and **MA-Me**, confirming the overall positive effect of **MA-H**. Altogether, the outcome of these reactions was mainly governed by the steric bulkiness of the metathesis substrate, regardless of the (pre)-catalyst used. This influence might be associated to the coordination step and/or to the (de)stabilization of intermediate species. Interestingly, the similar (pre)-catalysts performances indicate that the dissociated PCy_3 from **GII** had no major influence on the reaction.

The difference in reactivity of maleic acid/maleates can be attributed to steric effects only. As indicated by the chemical shifts in **Table 5**, **MA-Me** and **MA-*ⁱ*Pent** are slightly less electron poor than **MA-H** and therefore would be more reactive if the influence of the steric effects was negligible.

Table 5 ^{13}C NMR chemical shifts of the olefinic ($\delta_{\underline{C}=\underline{C}}$) and carbonylic ($\delta_{\underline{C}=O}$) carbons of **MA-H**, **MA-Me** and **MA-^{i}Pent**.

Compound	**^{13}C NMR chemical shift (ppm)**			
	$\delta_{\underline{C}=\underline{C}}$	Δ*	$\delta_{\underline{C}=O}$	Δ*
MA-H	131.84	0	167.03	0
MA-Me	130.68	1.16	166.25	0.78
MA-^{i}Pent	130.67	1.17	165.74	1.29

Conditions: 101 MHz; $CD_3(CO)CD_3$; 0.1 mol.L^{-1}; 2000 scans. * versus **MA-H**.

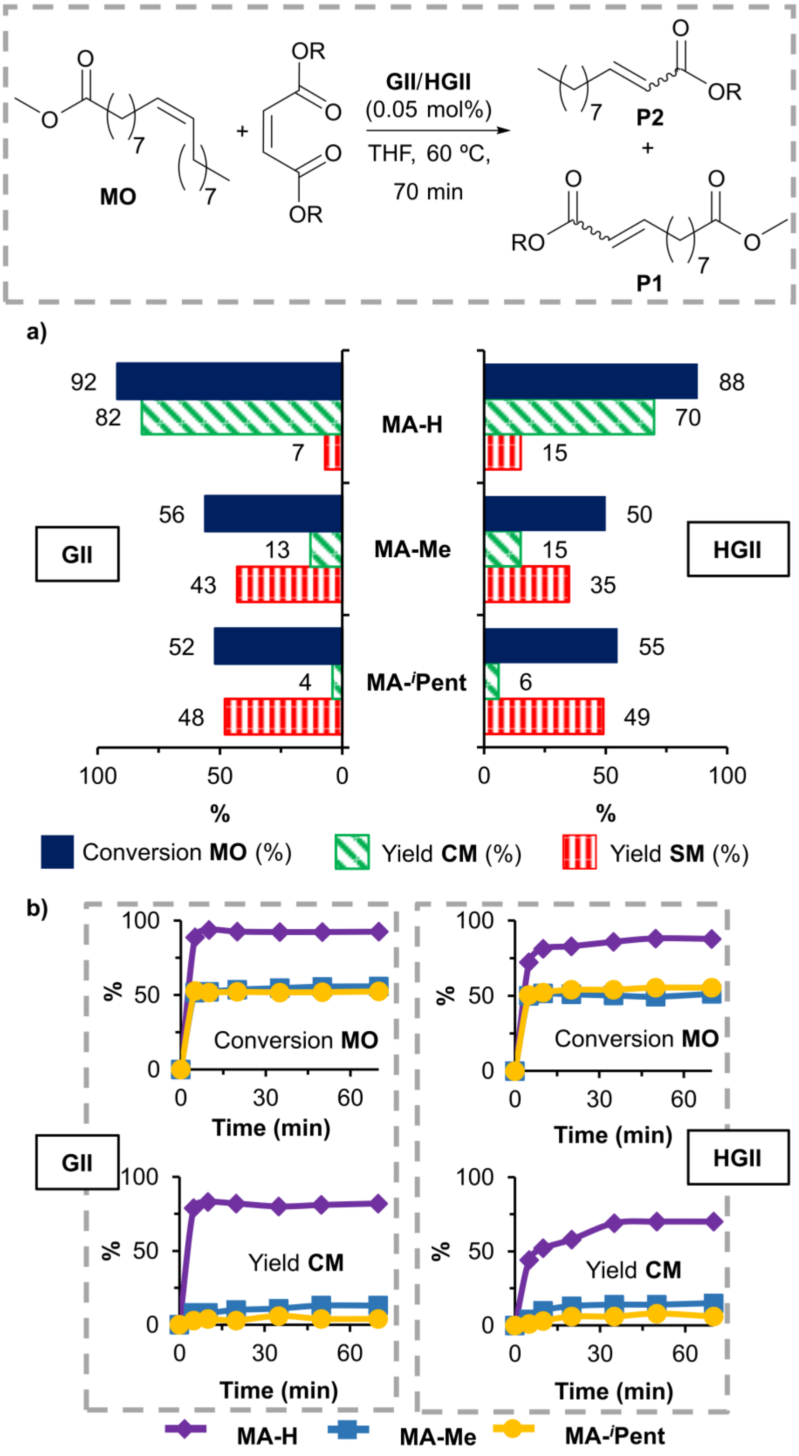

Figure 19 a) Influence of the CM partner on the conversion (blue bars) and yields of CM (dashed green bars) and SM (dashed red bars) of the reaction with **MO** – **MA-H** vs **MA-Me** and **MA-^{i}Pent**. b) Time-dependent plots using **GII** and **HGII**, respectively. Lines were added in the time-dependant plots with the only purpose to aid visualization. **MO**:CM partner molar ratio= 1:2 (**MO** = 1.77 mmol); THF = 1.5 mL; catalyst: 0.05 mol% (vs **MO**); T = 60 °C; purification method D. Isomerization products complete the mass balance.

3.1.3 Maleic acid versus acrylic acid

In order to investigate the effect of a terminal monosubstituted olefin versus a disubstituted olefin on the catalytic activity, reactions with acrylic acid (**AA-H**) and methyl acrylate (**AA-Me**) were also investigated. To allow an efficient removal of the co-product ethylene, these reactions were performed under a continuous flow of argon. In contrast to the use of **MA-H** and maleates, CM of **MO** with **AA-H** and **AA-Me** affords highly distinct results when **GII** and **HGII** are employed (**Figure 20**). In the case of **GII**, the conversion and CM yield steadily decreased when changing the CM partner **MA-H** for **AA-H** and **AA-Me**, respectively. The use of **HGII** instead of **GII** resulted in a different profile. Initially, a slightly higher selectivity was obtained for the CM products changing from **MA-H** to **AA-H**, while maintaining a similar **MO** conversion. Next, a decrease in both yield of CM products and **MO** conversion was observed when **AA-Me** was used as cross-metathesis partner. Comparatively, the use of **AA-Me** as CM partner resulted in lower conversion and selectivity for both catalysts, but **HGII** outperformed **GII**. Although the steric bulkiness of **AA-H** and **AA-Me** also played an important role on the catalytic performance of both **GII** and **HGII**, the catalytic performance was affected by another feature. **HGII** was not negatively affected by the formation of propagating Ru-methylidene species. The detrimental effect on the **GII**-catalyzed reaction could be ascribed to PCy_3-mediated decomposition/deactivation of propagating Ru-methylidene species. This also signifies that the use of carboxylic acid substrates does not successfully trap the free PCy_3 to inhibit the Ru-methylidene decomposition pathway.

Altogether, the lower bulkiness of the carboxylic acid substrates accounts predominantly for the higher catalytic productivity when compared to the corresponding esters. For the phosphine-containing (pre)-catalyst **GII**, the avoidance of the formation of Ru-methylidene propagating species is crucial. So when applying **MA-H** as substrate, the more expensive **HGII** can be substituted by **GII**. If terminal olefins should be applied as substrate, **HGII** remains the (pre)-catalyst of choice.

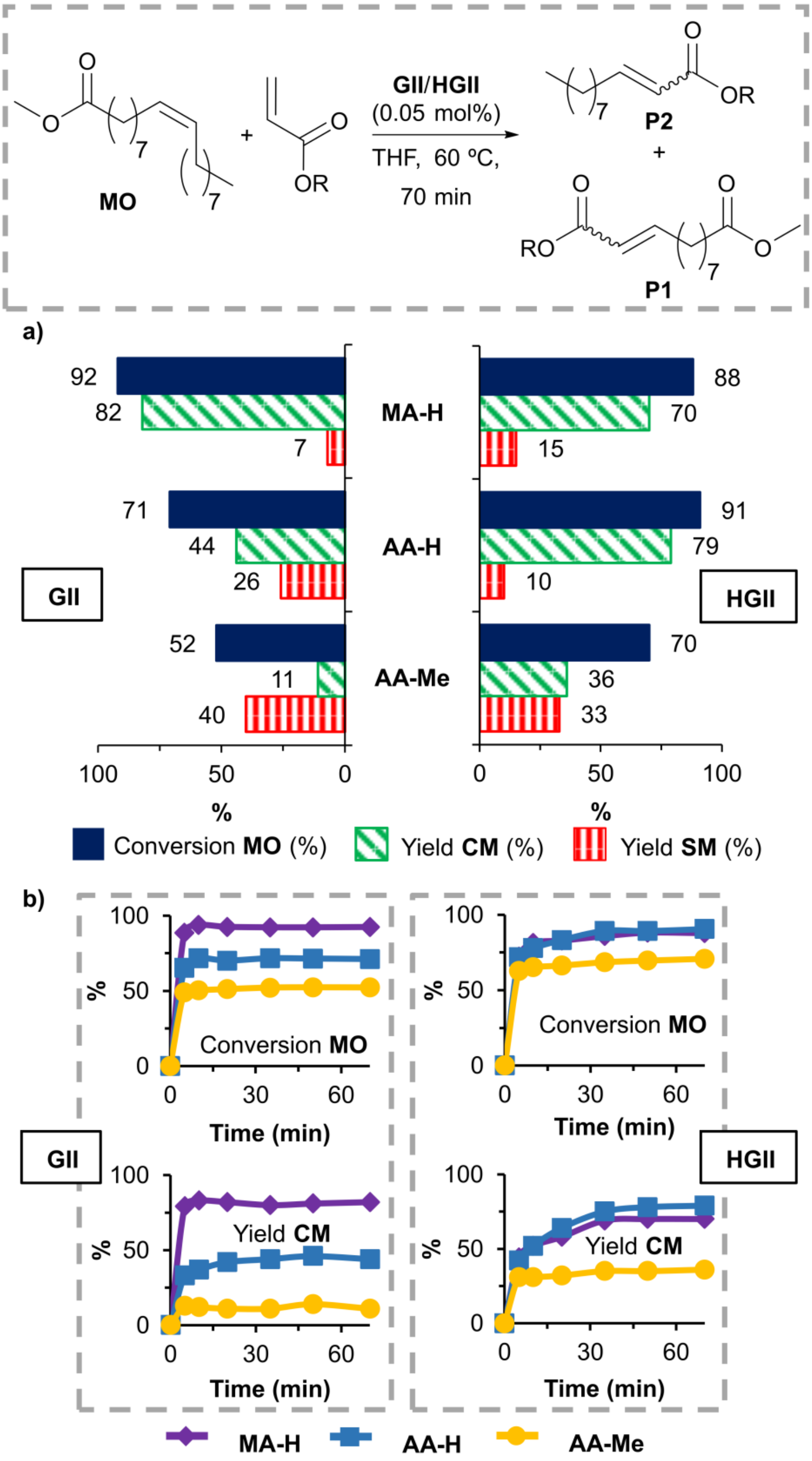

Figure 20 a) Influence of the CM partner on the conversion (blue bars) and yields of CM (dashed green bars) and SM (dashed red bars) of the reaction with **MO** – **MA-H** vs **AA-H** and **AA-Me**. b) Time-dependent plots using **GII** and **HGII**, respectively. Lines were added in the time-dependent plots with the only purpose to aid visualization. Conditions: **MO**:**MA-H** molar ratio = 1:2 (**MO** = 1.77 mmol); **MO**:**AA-H**/**AA-Me** molar ratio = 1:4; THF = 1.5 mL; catalyst: 0.05 mol% (vs **MO**); T = 60 °C; purification method D. Isomerization products complete the mass balance.

3.1.4 Vegetable oils as substrate

To increase the scope of the **MA-H**-based CM, the reaction was also explored using various vegetable oils. Naturally occurring oils and fats (from vegetable and animal origin) are renewable feedstocks of most importance in the chemical industry.[12] For the majority of vegetable oils, most of the side chains in the triglycerides are saturated (C16:0 and C18:0), monounsaturated (C16:1 and C18:1) or polyunsaturated (C18:2 and C18:3) fatty acids (**Figure 21**). The content of each of these fatty acid chains depends on a number of factors, including the type of the oil (**Table 6**). The use of vegetable oils offers direct advantages compared to the use of **MO**, such as atom and time economy by avoiding one initial step of transesterification. This also broadens the number of products obtained by enabling the use of vegetable oils with different compositions, and may facilitate in the separation of the final product mixture.[143]

Table 6 Composition of the vegetable oils used.

Oil	**%***						
	C18:1	**C18:2**	**C18:3**	**C16:1**	**C18:0**	**C16:0**	**Others**
Canola	62.5	21.5	8.7	0.2	2.4	4.7	7.1
Linseed	22.3	15.0	52.8	0.1	4.1	5.7	9.8
Sunflower	40.1	47.7	1.5	0.1	3.1	7.6	10.6
Grapeseed	20.5	68.2	0.3	0.1	3.7	7.2	10.9
Corn	34.2	51.3	0.8	0.1	0.9	12.7	13.6
Soybeam	23.2	55.9	6.4	0	3.0	11.5	14.5
Olive	78.3	6.2	0	0.7	3.0	11.7	14.8
Peanut	52.3	31.9	0	0.2	3.0	12.5	15.6
Rice	41.6	35.5	1.8	0.1	1.6	19.4	21
Cottonseed	15.3	59.0	0.1	0.4	2.0	23.2	25.2
Palm	55.4	12.7	0	0.2	3.0	28.7	31.7

* Calculated by GC.

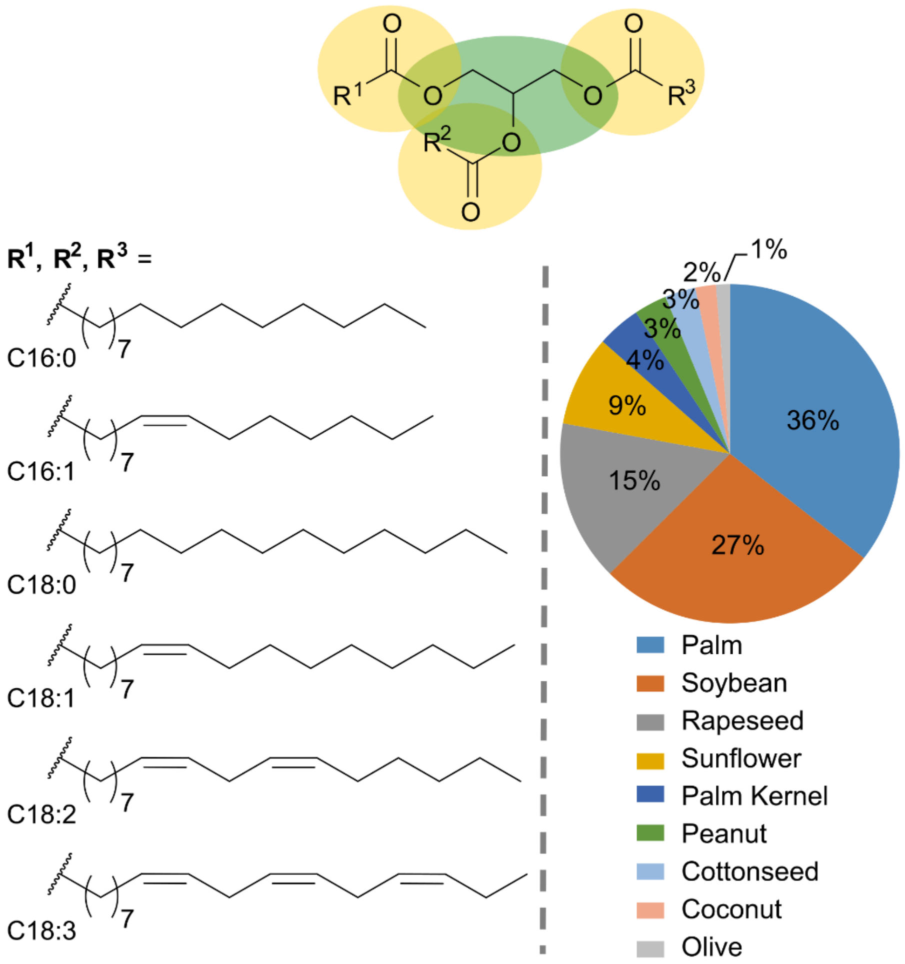

Figure 21 General structure of a triglyceride with the most common fatty acid side chains and the global market consumption of vegetable oils in 2014/15 (100 % = 175.65 million metric tons).[144]

CM of several different vegetable oils with **MA-H** under the optimized reaction conditions afforded the results shown in **Figure 22**. **GII** was used with a catalyst loading of 0.05 mol% (versus C-C double bond in the oil). Yields of the CM products were roughly within the observed value for **MO** (82 %). A trend in the yield of the CM products versus the composition of the oil was not observed, suggesting that none of the major components influence the catalyst productivity. Yields of the CM products were calculated by ^{1}H NMR (see **Appendix IV** for the formulae used) because the GC traces became too complex for appropriate determination and quantification. The decrease in the conversion for some of the oils (e.g., cottonseed and peanut oils) was more likely due to the presence of residual contaminants not removed during the purification step.

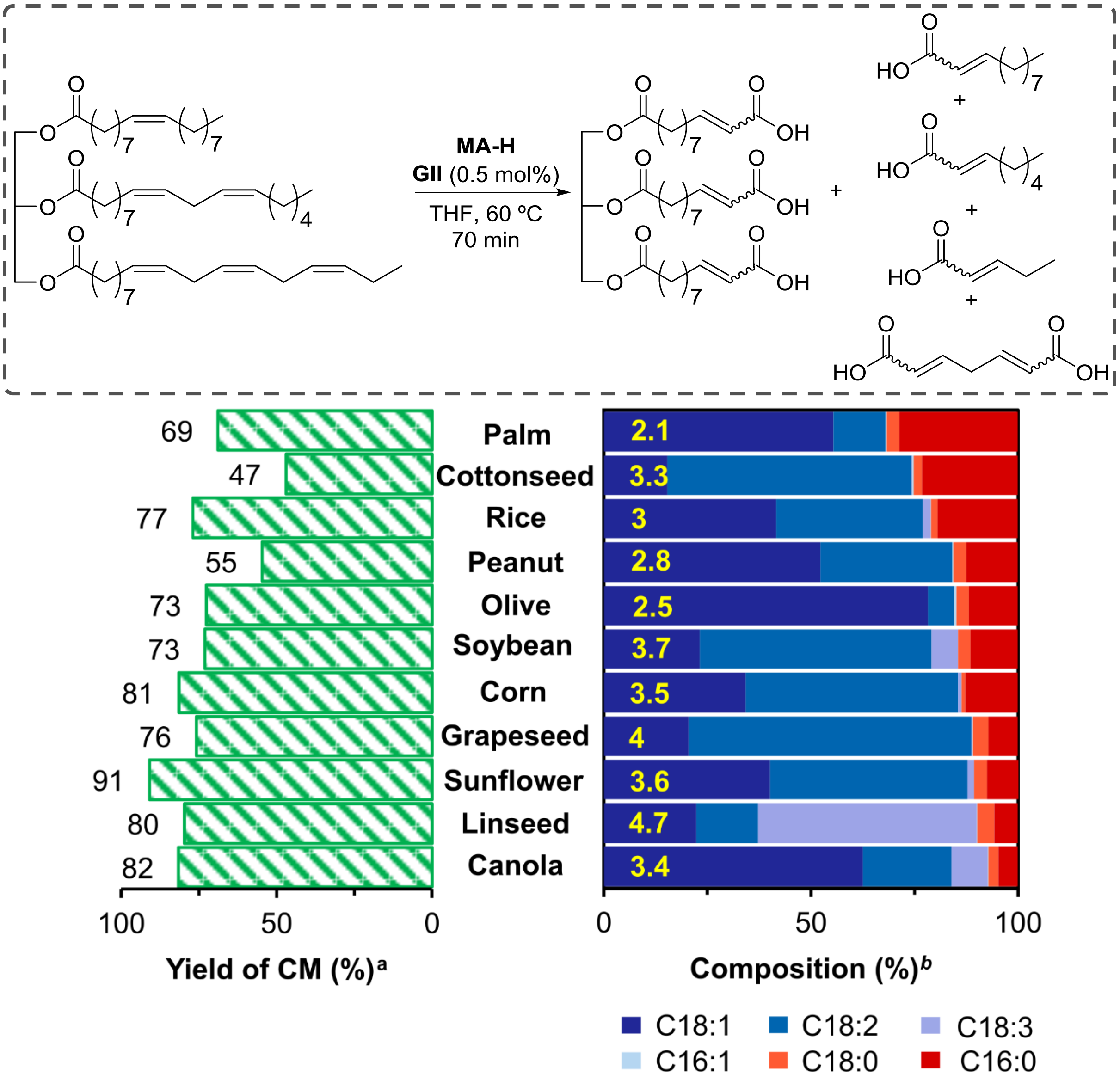

Figure 22 Effect of the vegetable oil composition on the yield of the CM products. Conditions: Oil(C=C):**MA-H** molar ratio = 1:2; THF = 1.5 mL; **GII** = 0.05 mol% (vs C=C); T = 60 °C; purification method D; reaction time = 70 min. [a] Yield of CM calculated by ^{1}H NMR. [b] Composition determined by GC. Yellow numbers shown in the blue bars are the number of C=C bonds (calculated by ^{1}H NMR – see **Appendix IV**) per triglyceride.

3.1.5 Monitoring the formation of a Ru-enoic carbene from the reaction of GII with MA-H

Inspired by the positive influence that **MA-H** displayed in the reactions aforementioned, the reaction of **MA-H** with **GII** was investigated in an attempt to detect the intermediate ruthenium-enoic specie. **MA-H** is the ideal substrate for checking the formation of a Ru-enoic carbene complex in CM with **GII** due to two main reasons: a) a sole intermediate specie is to be formed and b) the co-product formed from the reaction of **MA-H** with **GII** (*trans*-cinnamic acid) does not react back to regenerate the initial complex (*trans*-cinnamic acid is a type IV olefin).

The reaction of **GII** (1 equivalent) with **MA-H** (6 equivalents) in an NMR tube proceeded smoothly at 20 °C. A sole alkylidenic hydrogen resonance (18.61 ppm) was formed at a lower frequency to that from **GII** (19.25 ppm) in the ^{1}H NMR spectrum (**Figure 23**). Integration of both alkylidene resonances (versus 1,3,5-trimethoxybenzene as internal standard) reveals > 90% conversion over the course of 7 hours, and the plot of ln %**GII** versus time indicates that this reaction is of observed first order kinetic (**Figure 24**). No signals develop in frequencies lower than 0 ppm (spectra acquired until -50 ppm), a strong indication that no hydride species formed during the reaction. Additionally, no other signals, besides those above mentioned, appear in the range of 13 – 30 ppm, which indicates that a sole alkylidene product was formed in the reaction.

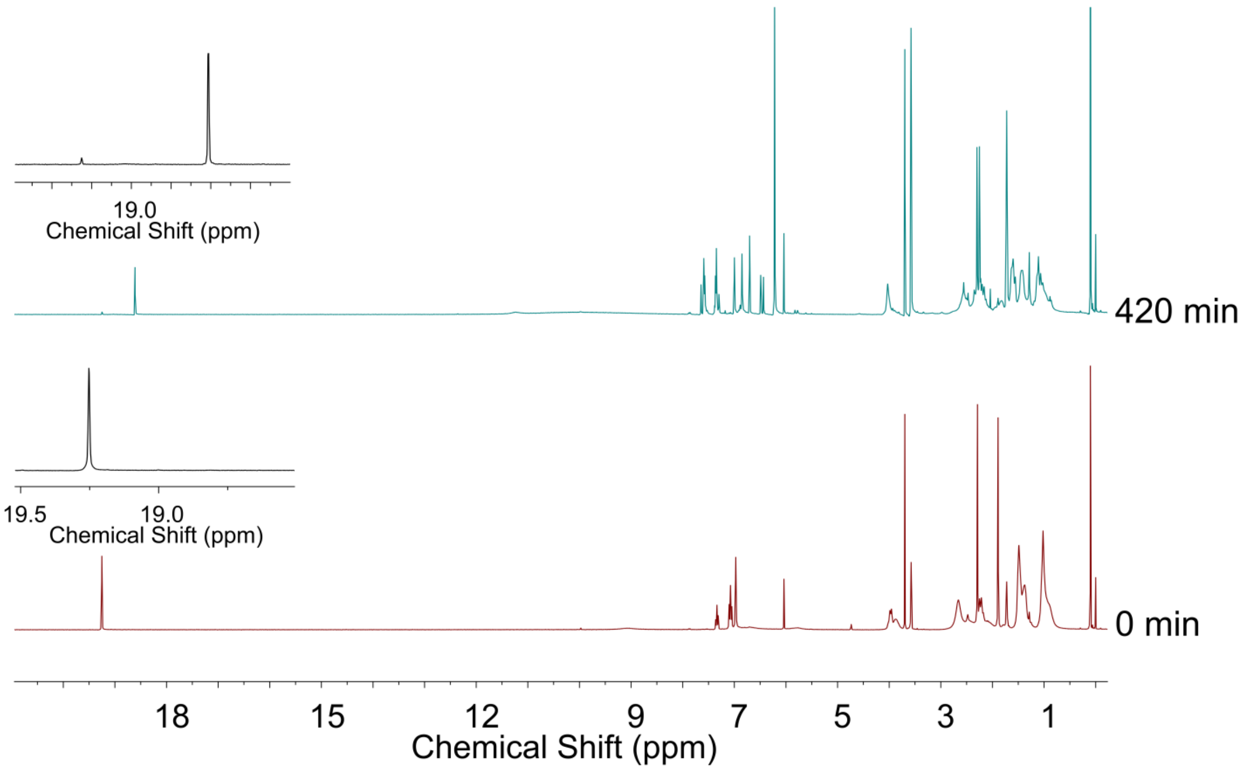

Figure 23 ^{1}H NMR spectra (300 MHz, THF-d_8, 20 °C) of the reaction of **GII** (10 mg, 0.0118 mmol) and **MA-H** (0.07 mmol).

Interestingly, the new alkylidene signal that appears in the ^{1}H NMR spectra splits into a doublet with a coupling constant of 1.3 Hz. This is likely due to the coupling with the phosphorous atom in the PCy_3 ligand. Similar coupling constants have also been observed for $^3J_{P,H}$ couplings in sterically unencumbered ruthenium-alkylidene complexes (**Figure 25**).[145] Alkylidenes with sterically unhindered substituents can adopt a conformation with a P-Ru-C dihedral angle slightly different than that adopted by the benzylidene in **GII** (~ 90 º - differently from $^3J_{H,H}$ coupling constants that obey the relationship established in the Karplus diagram, a direct relationship is not observed for $^3J_{P,H}$ couplings[146]).

Further insights in the nature of the newly formed complex can be extracted from the aromatic region of the ^{1}H NMR spectra (**Figure 26**). Phenyl resonances from the benzylidene moiety of **GII** slowly decreased over the course of the reaction, while several new sets of resonances had their intensities slowly increased at a similar rate. The singlet at 6.71 ppm comes from the olefinic hydrogens of fumaric acid (confirmed by spiking the reaction with an authentic sample) and is another strong indication that the reaction of **GII** with **MA-H** was taking place. The doublet at 6.46 ppm ($^3J_{H,H}$ = 16.0 Hz) can be assigned to the olefinic *alpha*-hydrogen (to the carboxyl group) of *trans*-cinnamic acid, the co-product of the reaction. The formation of *trans*-cinnamic acid provides strong evidence that the resonance in 18.61 ppm is the result of a different alkylidene and not from a rearranged and/or six coordinate complex analogue of **GII**. The assignment of the doublet at 6.46 ppm was confirmed by spiking the system with an authentic sample of *trans*-cinnamic acid.

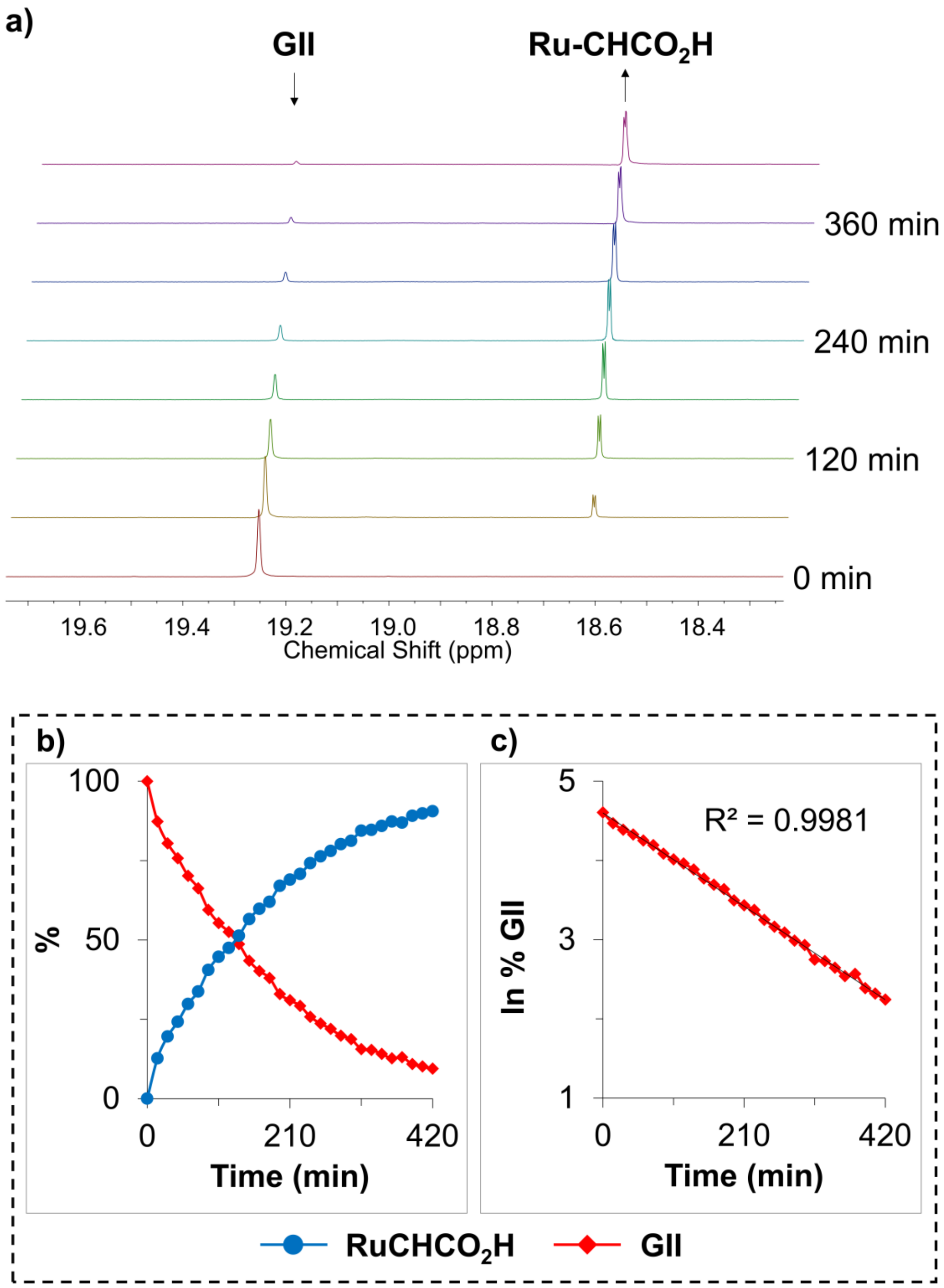

Figure 24 a) Staggered ^{1}H NMR spectra (300 MHz, THF-d_8, 20 ºC) of the alkylidene region in the reaction of **GII** with **MA-H**; **b)** time-dependant plot of the variation of the alkylidenic signals in the ^{1}H spectra; **c)** plot of the ln of %**GII** versus time.

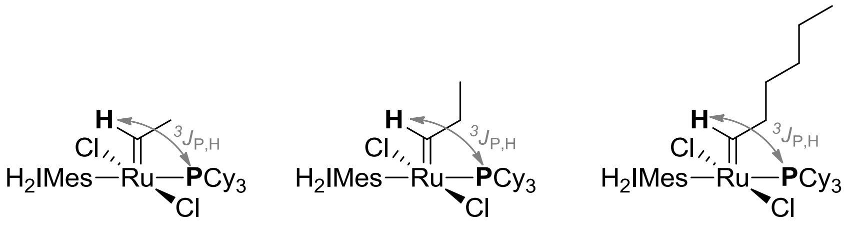

$^3J_{P,H}$ = 0.7 Hz　　$^3J_{P,H}$ = 1.1 Hz　　$^3J_{P,H}$ = 1.2 Hz

Ru-22　　**Ru-23**　　**Ru-24**

Figure 25 Examples of second-generation ruthenium alkylidene complexes exhibiting a small coupling $^3J_{P,H}$.

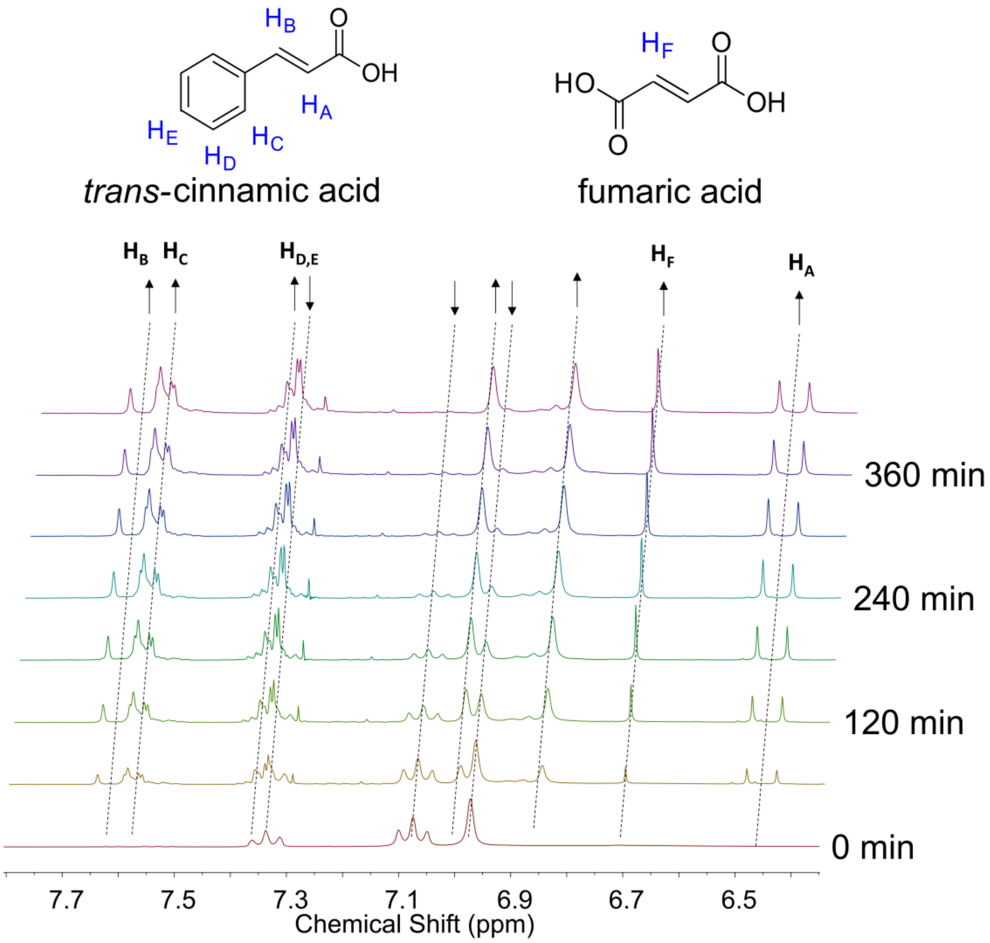

Figure 26 Staggered ^1H NMR spectra (300 MHz, THF-d_8, 20 ºC) of the aromatic and olefinic regions in the reaction of **GII** and **MA-H**.

The $^{31}P\{^{1}H\}$ NMR spectra exhibit only the presence of three resonances over the entire course of the reaction (**Figure 27**). Two new resonances with higher frequencies than that from **GII** (δ = 31.49 ppm) develop during the reaction. The singlet at 35.81 ppm increased in a similar rate as the decrease of the phosphorous resonance from **GII** (31.49 ppm). The singlet at 33.76 ppm experienced only small variations during the reaction with < 3% intensity after 7 h.[iv] At the end of the reaction the conversion of **GII** was > 90%. A resembling profile was determined from the time-dependent plot obtained from the integration of the phosphorous resonances. Based on the time-dependent plots derived from the ^{1}H and $^{31}P\{^{1}H\}$ NMR spectra, it is safe to attribute the resonance at 18.61 ppm in the ^{1}H NMR spectrum to the same compound that origins the resonance at 35.81 ppm in the $^{31}P\{^{1}H\}$ NMR spectrum. The small singlet at 33.76 ppm likely arises from the attack of the dissociated PCy_3 on **MA-H** (Michael addition).

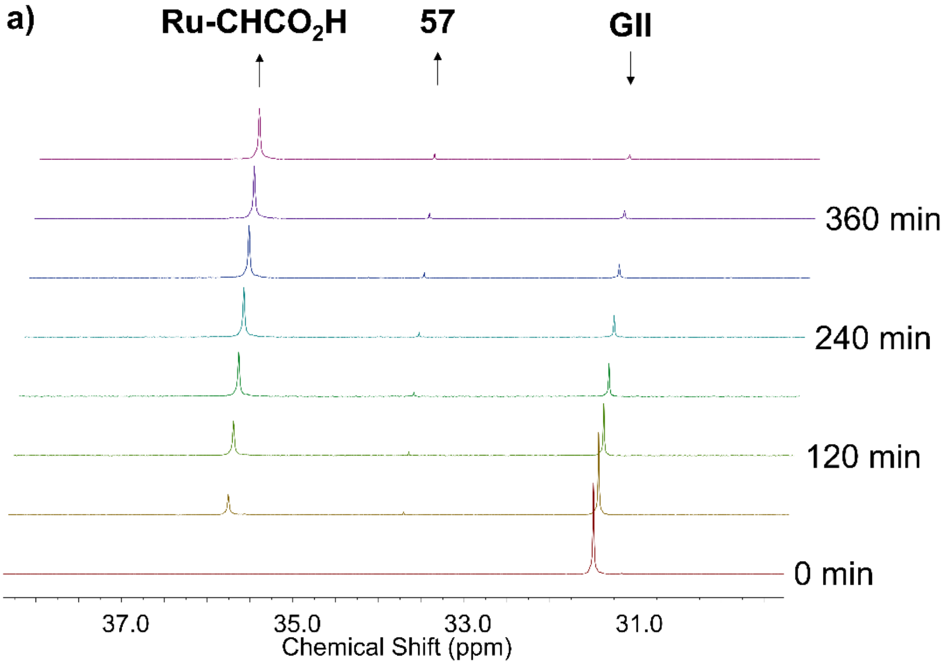

[iv] The reaction proceeded faster at 25 °C, and a similar conversion obtained after 4 h. Nevertheless, the ^{31}P resonance at 33.76 ppm was more intense (ca. 6 %) at 4 h of reaction.

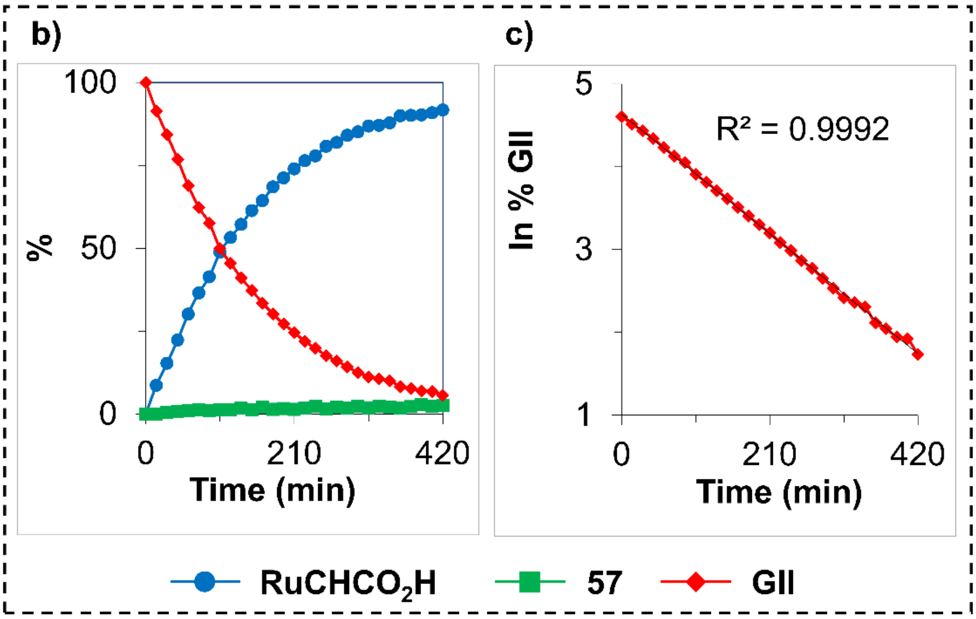

Figure 27 **a)** Staggered $^{31}P\{^1H\}$ NMR spectra (121.5 MHz, THF-d_8, 20 °C) in the reaction of **GII** with **MA-H**; **b)** time-dependant plot of the variation of intensity of the signals in the $^{31}P\{^1H\}$ spectra; and **c)** plot of the ln of %**GII** versus time.

A control reaction of **MA-H** with free PCy_3 was performed to obtain any insight in the nature of the product corresponding to the small signal (< 3 %) at 33.76 ppm in the $^{31}P\{^1H\}$ spectra. Addition of 2.5 equivalents of **MA-H** to a solution of PCy_3 in THF-*d8* resulted in the formation of a sole major product as observed by $^{31}P\{^1H\}$ NMR spectroscopy (**Figure 28**) (PCy_3 = 10.5 ppm).

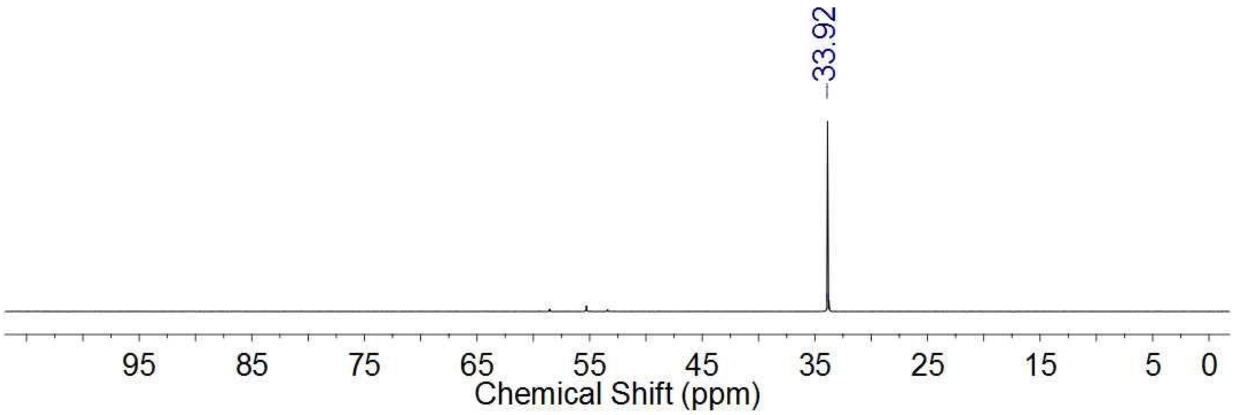

Figure 28 $^{31}P\{^1H\}$ NMR spectrum (101 MHz, THF-d_8) of the reaction between **MA-H** and PCy_3.

Similarly, the ^{1}H NMR spectrum (**Figure 29**) shows that PCy_3 reacted with **MA-H**, as evidenced by the three sets of signals that appeared in the 2.5 – 4 ppm region of the spectrum. Even though only the two analysis do not suffice for the proper identification of the compound formed in the reaction of **MA-H** with PCy_3, it is suggested that the compound might originate from the Michael addition of PCy_3 to **MA-H**, followed by further attack of the resulting adduct in another molecule of **MA-H** (**Scheme 30**). Similar chemistry was reported recently, but for methyl acrylate instead of **MA-H**.[63]

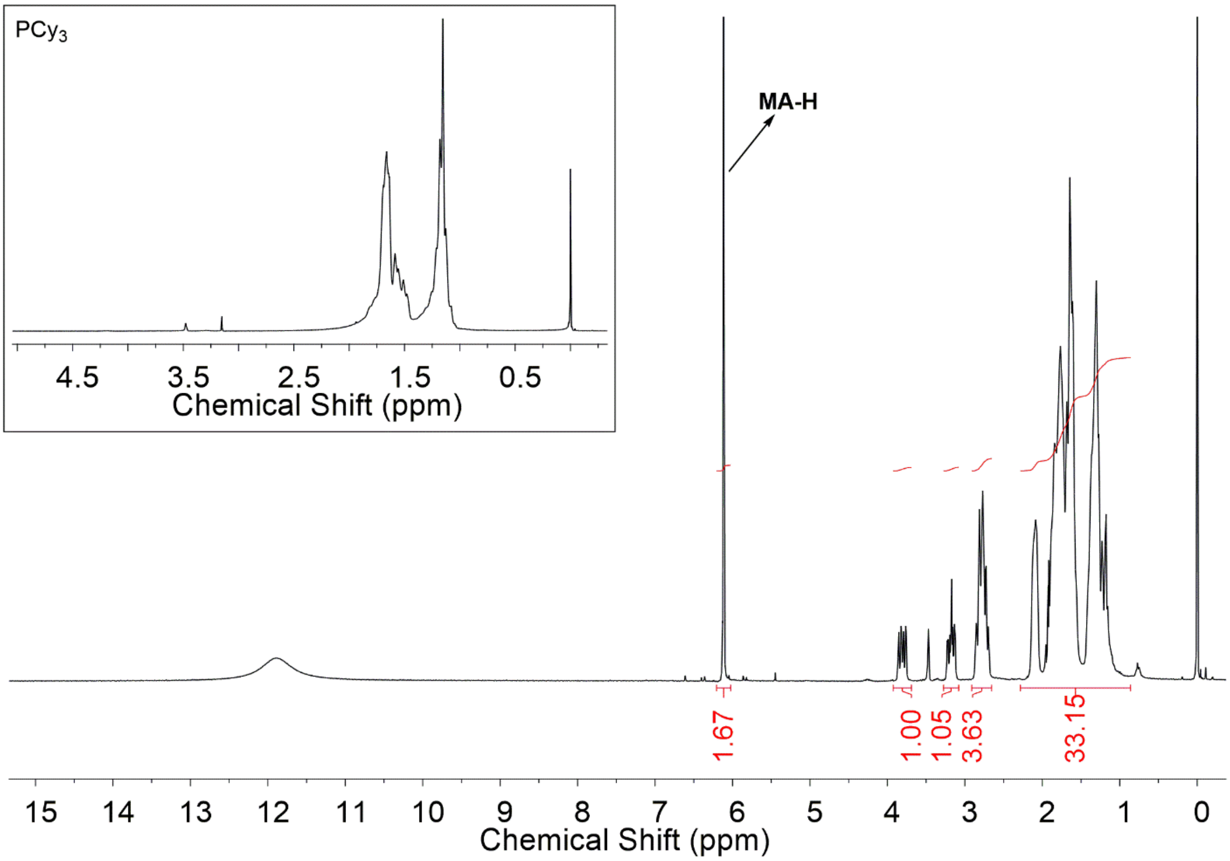

Figure 29 ^{1}H NMR spectrum (300 MHz, THF-d_8) of the reaction between **MA-H** and PCy_3. The ^{1}H NMR spectrum of PCy_3 is shown in the inset at the top.

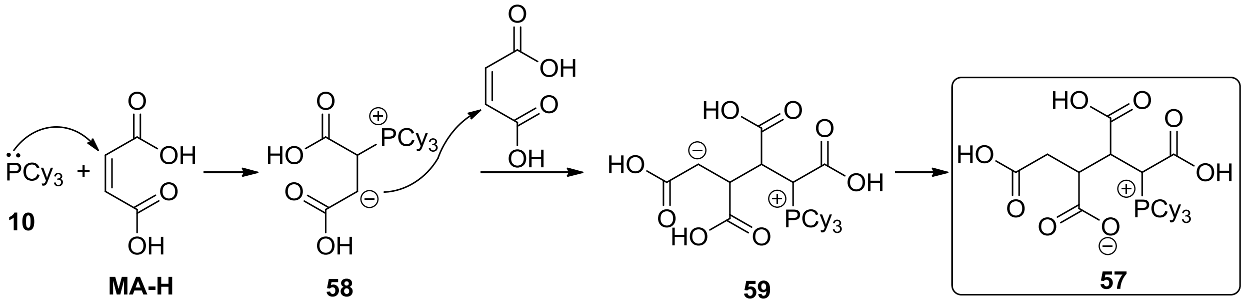

Scheme 30 Proposed reaction that occurred between **MA-H** and PCy$_3$.

It is therefore very likely that the small resonance that developed in the $^{31}P\{^1H\}$ NMR spectra is the result of the reaction between the dissociated PCy$_3$ from **GII** and **MA-H**. The small variation in the chemical shift (0.16 ppm) can be attributed to the different chemical environment of the samples.

Recently, Hillmayer reported the use of **MA-H** as chain transfer agent in the ROMP of cyclooctene to prepare telechelic polyolefins. In the same work, the authors studied the reaction of **MA-H** (32 equiv) with **GII** (1 equiv) in THF-d_8 at 40 ºC for 1.5 h, observing only 2.5 % conversion of **MA-H** into fumaric acid (*cis-trans* isomerization) together with the complete loss of alkylidenic signals in the spectrum.[104] Based on the experiments performed in the present work, this can be attributed to the negative influence that a higher temperature has on the reaction. In the present work, it was observed that the small increase in the temperature to 25 ºC resulted in faster conversion of **GII** (4 h) at the cost of the formation of increased amounts of the decomposition product observed in the $^{31}P\{^1H\}$ spectra. Since the presence of free PCy$_3$ is apparently necessary to trap the propagating specie into a speculative, inactive 16e$^-$ complex, decomposition of the propagating 14e$^-$ Ru-enoic carbene specie takes place, resulting in the loss of the alkylidenic signals and low conversion of **MA-H**.

Altogether, the data aforementioned provides fundamental information that hints the formation of a ruthenium-enoic carbene complex (**RuCHCO$_2$H** – **Scheme 31**). As already known from the literature, **GII** initiates by PCy$_3$ dissociation (rate limiting step – **section 2.3.1**),[57] consistent with the observed first order kinetic. The 14e$^-$ benzylidene thus reacts with **MA-H** liberating one molecule of *trans*-cinnamic acid and one ruthenium-enoic propagating specie, which can either react with another molecule of

MA-H or be trapped as a metathesis inactive 16e$^-$ complex **Ru-CHCO$_2$H** by the dissociated PCy$_3$.

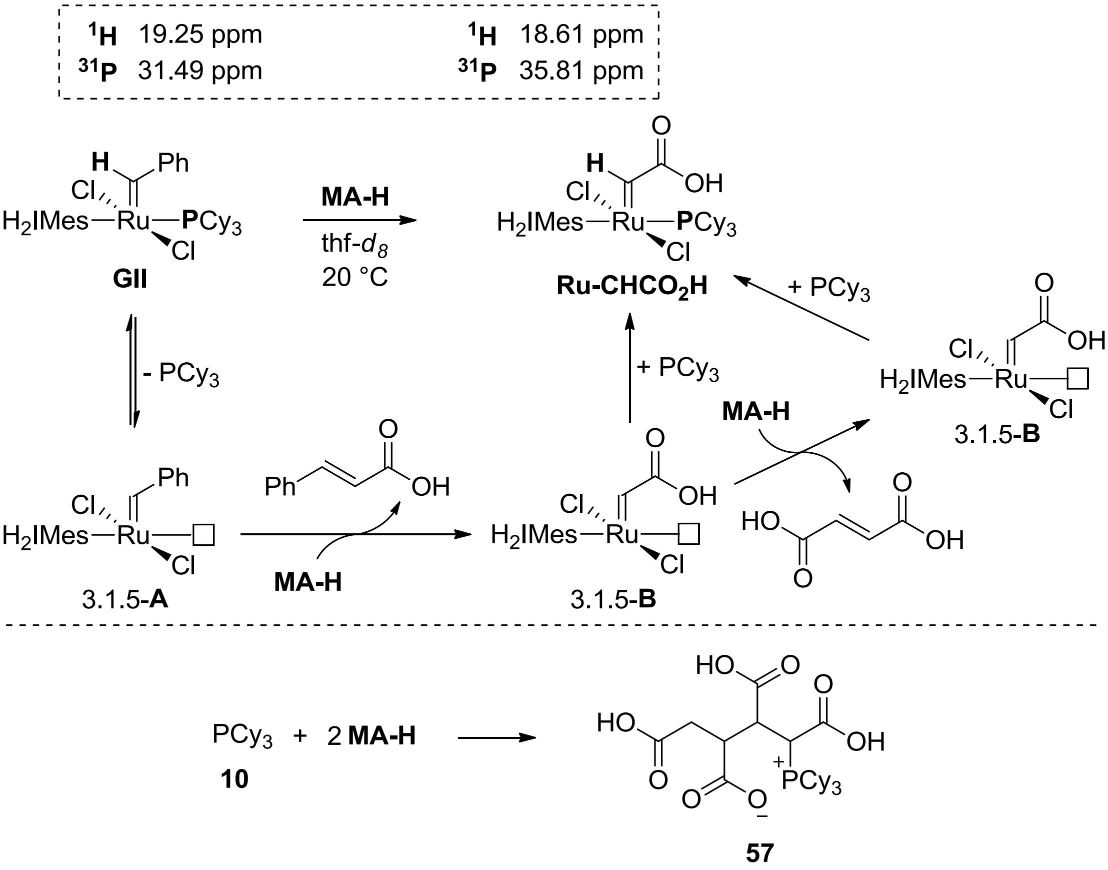

Scheme 31 Schematic representation of the reaction between **GII** and **MA-H** resulting in the formation of the Ru-enoic carbene complex. Values correspond to the ^{1}H and ^{31}P resonances observed for the atoms selected in bold in the structures.

In an attempt to obtain more detailed information about the structure of the complex formed, the reaction was repeated on a larger scale in a Schlenk flask. Reaction of the brick red **GII** (85 mg, 0.1 mmol) with **MA-H** (70.7 mg, 0.6 mmol) in THF resulted in the formation of an ochre solution after 12 h at 14-17 °C. The formed complex was then purified by removing the THF under reduced pressure, dissolving the dark ochre residue in minimum amounts (3 x 3 mL) of cold toluene (ca. 0 ºC) and cannula-filtering of the suspension. After removal of the toluene, the yellow ochre solid was crushed with pentane (4 x 5 mL) and the remaining solid dried for 36 h. A yellow ochre solid was obtained in 91 % yield based on **GII**. ^{1}H and ^{31}P{^{1}H} NMR spectra of the material reveal the presence of ca. 1% of unreacted **GII** and ca. 1.5 % of **57**. The ^{1}H

NMR spectrum also shows remaining *trans*-cinnamic acid. Further attempts to completely purify the compound proved to be unsuccessful (although the same purification procedure was successfully used to purify a previous reaction that started with 15 mg of **GII**). The $^{13}C\{^{1}H\}$ spectrum of the compound (**Figure 30**) exhibits a characteristic resonance of alkylidenes at 290.11 ppm (d, $^{2}J_{P,C}$ = 4.8 Hz), together with a doublet centered at 217.77 ppm (d, $^{3}J_{P,C}$ = 69.0 Hz) characteristic of the C1 carbon of the H_2IMes carbene *trans* to the PCy_3 ligand (**Figure 31**).[147-153]

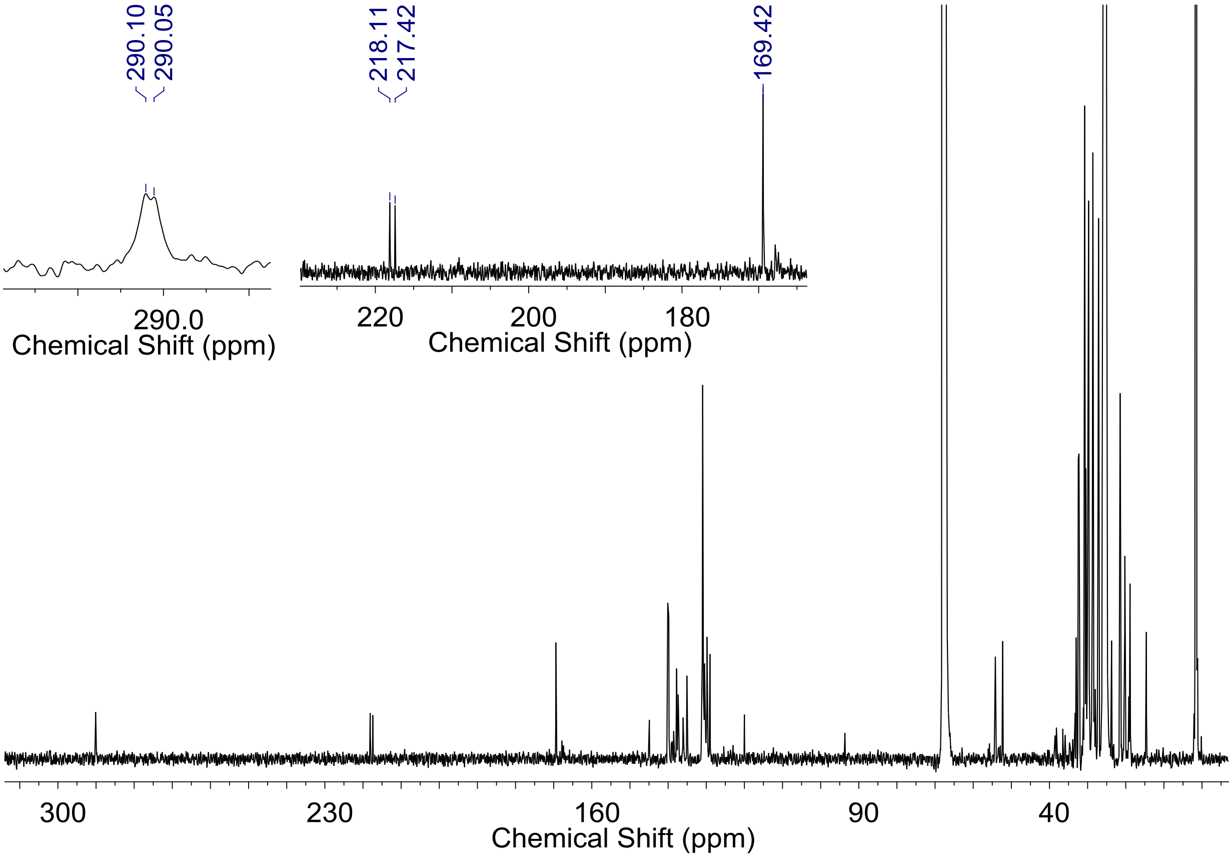

Figure 30 $^{13}C\{^{1}H\}$ NMR spectrum (100 MHz, THF-d_8) of the compound **Ru-CHCO$_2$H**.

The ^{13}C chemical shifts used for proving the formation of the **Ru-CHCO$_2$H** complex are similar to those reported for other ruthenium complexes. Nishiyama reported the synthesis of hexacoordinated ruthenium(II) complexes containing a tridentate NNN ligand and an enoic carbene ligand (**Figure 31**). ^{13}C resonances at 305.7 and 183.2 ppm were observed for the alkylidenic (C_α) and carbonyl (C_β) carbons, respectively.[105] Basi *et al*. reported the immobilization of second-generation Grubbs metathesis (pre)-catalyst onto polyisobutylene. ^{13}C chemical shifts of 305.90 and 210.22 ppm were found for the C_α-benzylidene and NHC-C1 carbons, respectively.[154]

Additionally, the $^{2}J_{P,C}$ coupling constants observed in the $^{13}C\{^{1}H\}$ spectrum offer a strong indication that the H_2IMes and PCy_3 ligands are *trans* to each other, and that the $=CHCO_2H$ ligand is located *cis* to the phosphine ligand. These observations are not surprising, given the steric bulkiness of both H_2IMes and PCy_3 ligands.

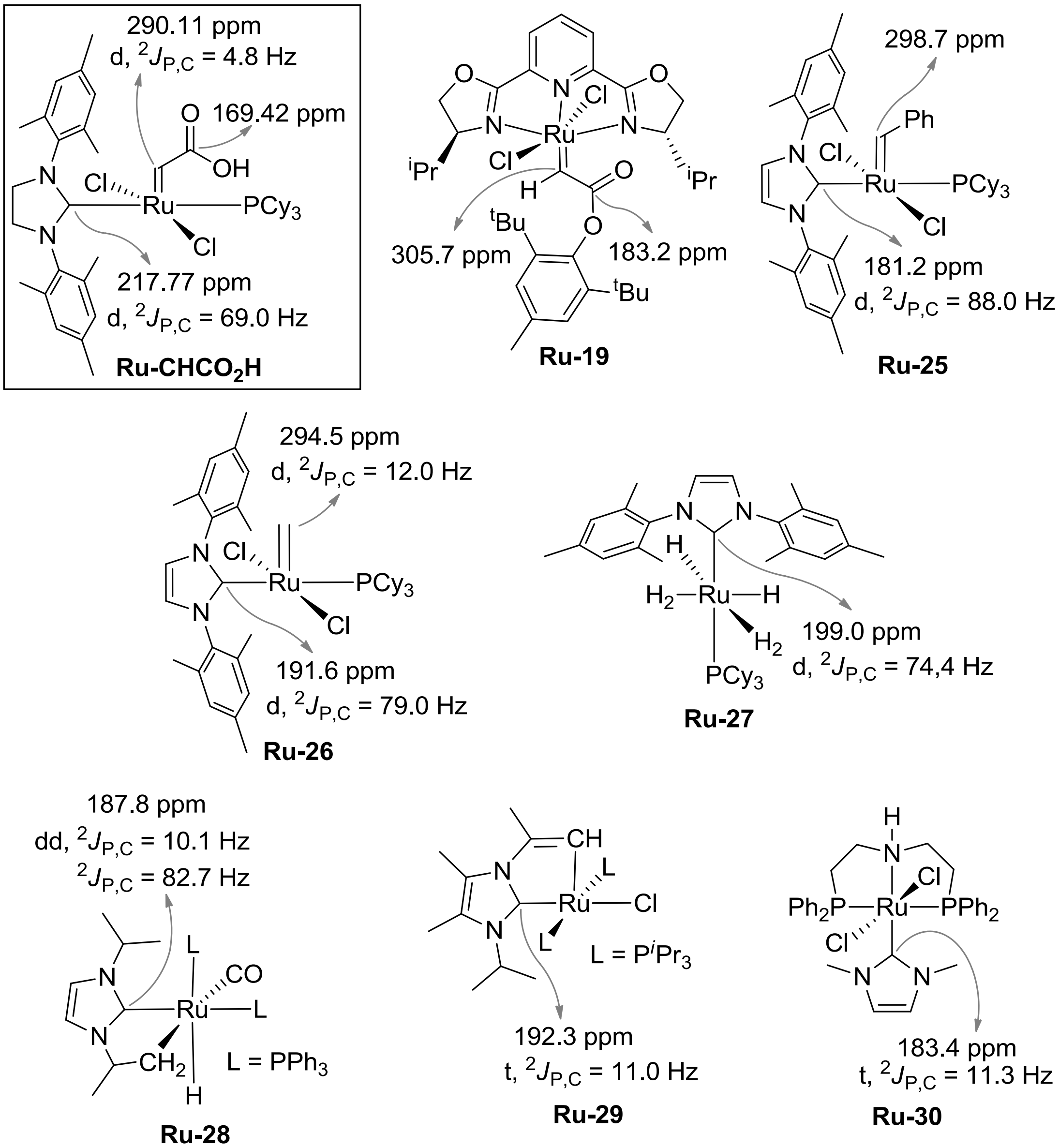

290.11 ppm
d, $^{2}J_{P,C}$ = 4.8 Hz
169.42 ppm
217.77 ppm
d, $^{2}J_{P,C}$ = 69.0 Hz
Ru-CHCO2H
305.7 ppm
183.2 ppm
Ru-19
298.7 ppm
181.2 ppm
d, $^{2}J_{P,C}$ = 88.0 Hz
Ru-25
294.5 ppm
d, $^{2}J_{P,C}$ = 12.0 Hz
191.6 ppm
d, $^{2}J_{P,C}$ = 79.0 Hz
Ru-26
199.0 ppm
d, $^{2}J_{P,C}$ = 74,4 Hz
Ru-27
187.8 ppm
dd, $^{2}J_{P,C}$ = 10.1 Hz
$^{2}J_{P,C}$ = 82.7 Hz
L = PPh3
Ru-28
L = P^{i}Pr3
192.3 ppm
t, $^{2}J_{P,C}$ = 11.0 Hz
Ru-29
183.4 ppm
t, $^{2}J_{P,C}$ = 11.3 Hz
Ru-30

Figure 31 Characteristic ^{13}C resonances observed for the compound **Ru-CHCO$_2$H** and examples of other complexes with similar ligands.

The hydrogen resonance at 18.61 ppm correlates through one chemical bond with the carbon resonance at 290.11 ppm (^{1}H-^{13}C HSQC - **Figure 32**) and through two chemical bonds with the carbon resonance at 169.42 ppm (^{1}H-^{13}C HMBC - **Figure 33**), confirming the formation of a ruthenium-enoic carbene complex. Resonances arising from the H_2IMes ligand are found in both ^{1}H and ^{13}C{^{1}H} spectra, confirming that such ligand remained unaltered during the reaction.

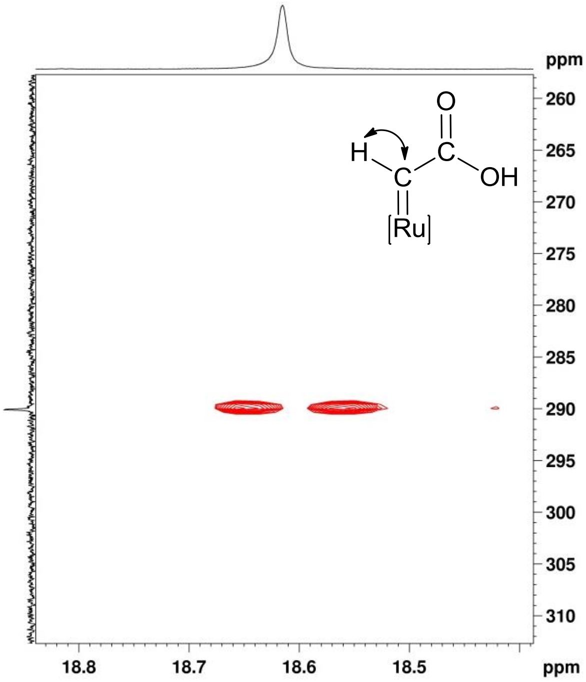

Figure 32 Expansion of the ^{1}H-^{13}C HSQC spectrum showing the correlation of the alkylidenic hydrogen signal at 18.61 ppm with the carbon resonance at 290.11 ppm.

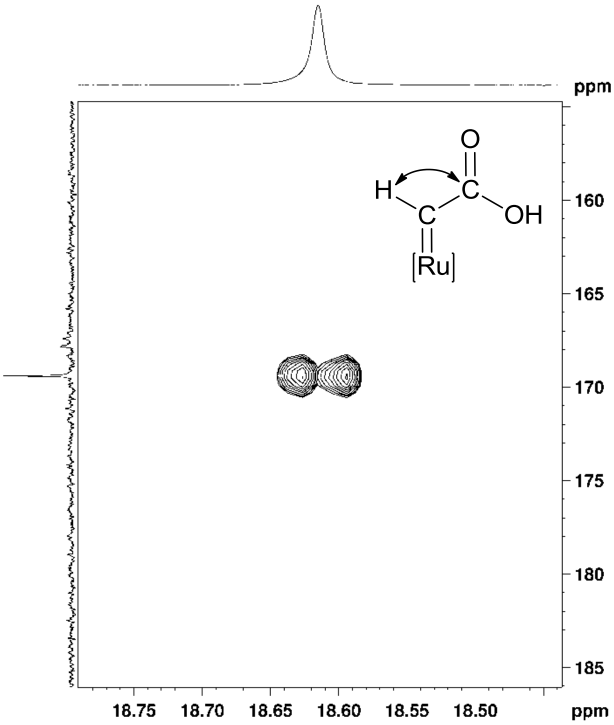

Figure 33 Expansion of the ^{1}H-^{13}C HMBC spectrum showing the correlation of the alkylidenic hydrogen signal at 18.61 ppm with the carbon resonance at 169.42 ppm.

Altogether, the NMR experiments support the formation of a new Ru-enoic carbene complex, which structure in solution displays the ligands H_2IMes and PCy_3 *trans* to each other. The 2D ^{1}H-^{13}C techniques corroborate with the installation of the $=CHCO_2H$ enoic carbene in the complex and this ligand is located *cis* to the phosphine. Based on other similar complexes containing both bulky NHC and PCy_3 ligands, and two chloride ligands (e.g., **GII**, **Ru-25** and **Ru-26** - **Figure 31**), the complex **Ru-CHCO$_2$H** corresponds to the structure as drawn in **Figure 31**.

3.2 DEVELOPMENT OF A PHOSPHINE-FREE STRATEGY FOR THE SYNTHESIS OF RU-ALKYLIDENE COMPLEXES[v]

3.2.1 *trans*-Dichlorotetrakis(pyridine)ruthenium(II) (*trans*-$RuCl_2(py)_4$)

Among the possible ruthenium(II) precursors, *trans*-$RuCl_2(py)_4$ seemed to be the likely choice in the development of a synthetic strategy for the preparation of **HGII** that does not involve the use of phosphines. Within the considered strategies, this approach would be the most atom-economical possible (without considering the precursor synthesis) and the product that would be obtained in the second step ($RuCl_2(Ind)(NHC)(py)_2$ – **IndIII'**; L = py - **Scheme 32**) is already known and well characterized in the literature. However, *trans*-$RuCl_2(py)_4$ is not commercially available and is obtained by ligand exchange from either $RuCl_2(PPh_3)_3$ or $RuCl_2(DMSO)_4$.

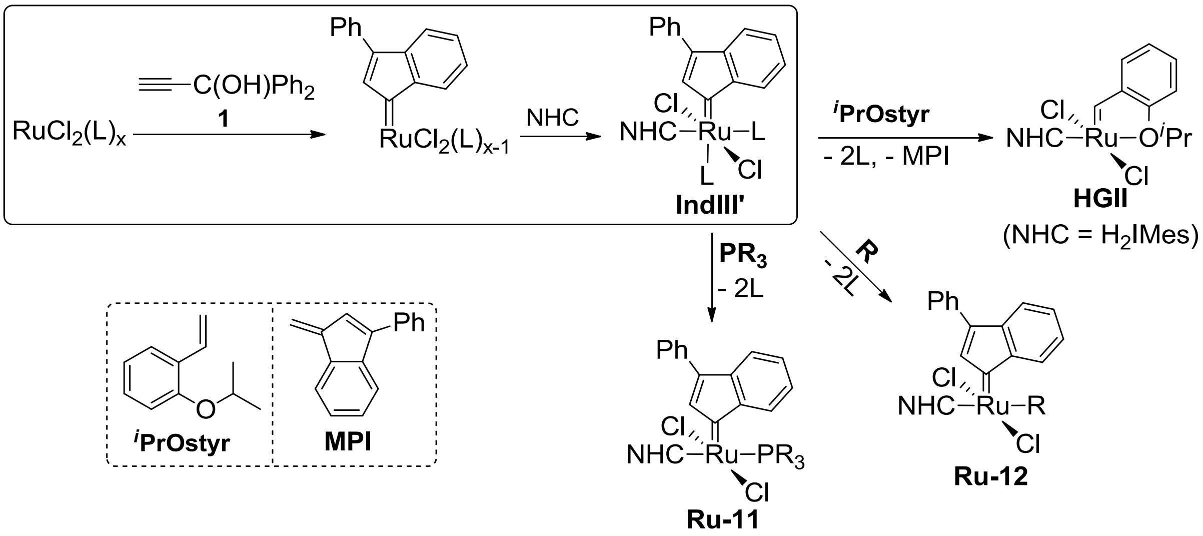

Ph
C(OH)Ph2
1
RuCl2(L)x
RuCl2(L)x-1
NHC
Cl
NHC–Ru–L
L
Cl
IndIII'
iPrOstyr
- 2L, - MPI
NHC–Ru–OiPr
HGII
(NHC = H2IMes)
PR3
- 2L
R
- 2L
NHC–Ru–PR3
Ru-11
NHC–Ru–R
Ru-12
O
iPrOstyr
MPI

Scheme 32 Two-step synthesis and possible transformations of 'third-generation' indenylidene complexes (**IndIII'**).

Attempts to install an indenylidene ligand in *trans*-$RuCl_2(py)_4$ are summarized in **Table 7**. In all cases, no changes were observed in the ^1H NMR spectrum of the solid obtained after drying the reaction mixture (**Figure 34**), even though in some cases a colour change from light yellow to light brown was observed. *trans*-$RuCl_2(py)_4$ is insoluble in all solvent combinations tested (slightly soluble in chloroform). Even the use of harsher conditions did not result in the formation of any compound observable by ^1H NMR spectroscopy. Acetyl chloride (**Table 7** - entry 4) was added as a source of HCl. The liberated HCl would protonate any free pyridine dissociated from the $18e^-$ precursor and, as consequence, lower the rate of its re-coordination to the metal. Moreover, Brønsted acids promote the rearrangement of ruthenium-allenylidenes into ruthenium-indenylidenes.[49,155] Also no reaction was observed under this condition. Altogether, these results suggest that the pyridine ligands are not labile in this precursor, and therefore the required $16e^-$ complex does not form, even for short periods.

---

[v] Most of the work presented and discussed in this section was performed at the University of Ottawa, in the laboratory of Professor Deryn E. Fogg, during the period of January-June, 2014.

Table 7 Conditions tested to prepare a Ru-indenylidene complex from *trans*-$RuCl_2(py)_4$.

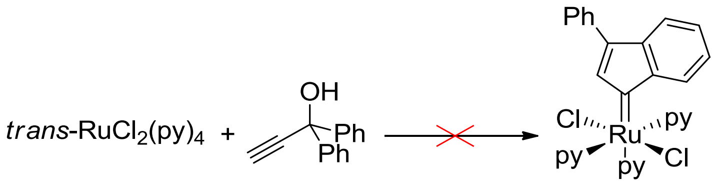

Ru-31 **1** **Ru-32**

Entry	**Solvent**	**Temp. (°C)**	**Time**	**Comments**
1	$CDCl_3$	55	Overnight	No changes in ^1H NMR
2	THF	Reflux	2 h	No changes in ^1H NMR
3	MeOH/Toluene	Reflux	18 h	No changes in ^1H NMR
4	DCM/EtOH	Reflux	17 h	2 drops of acetyl chloride added; no changes in ^1H NMR

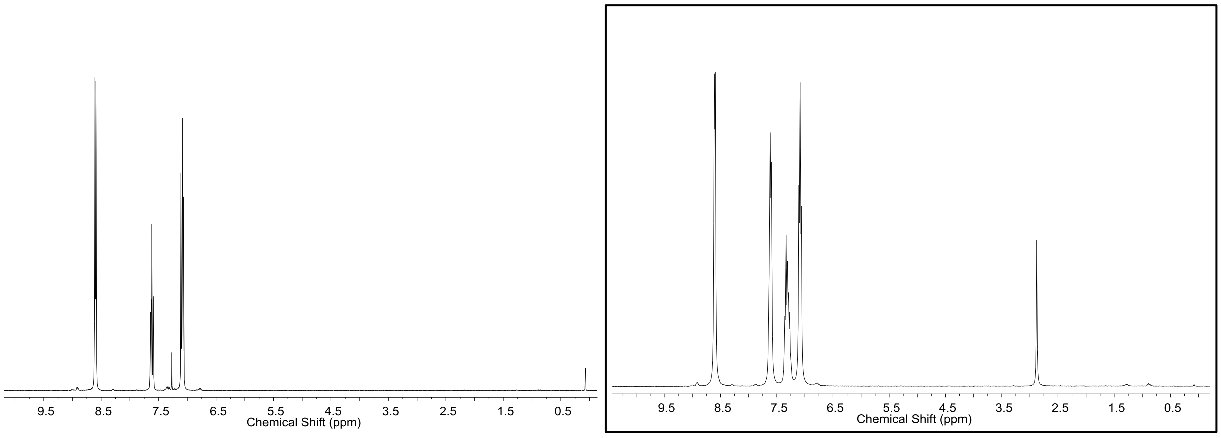

Figure 34 ^{1}H NMR spectra ($CDCl_3$, 300 MHz) of *trans*-$RuCl_2(py)_4$ (left) and after heating overnight at 55 °C with 1,1-diphenylpropargyl alcohol (right) (the resonances at 2.88 and 7.33 ppm are from the alkyne).

3.2.2 Dichloro(*p*-cymene)ruthenium(II) dimer ([$RuCl_2$(*p*-cymene)]$_2$)

Due to the lack of reactivity of *trans*-$RuCl_2(py)_4$ (attributed to lability reasons), the use of the dimeric ruthenium(II) precursor [$RuCl_2$(*p*-cymene)]$_2$ was then investigated. The use of [$RuCl_2$(*p*-cymene)]$_2$ is reported in some papers related to olefin metathesis, either in the synthesis of well-defined complexes or in the *in situ* formation of catalytically active species.[156-158] For instance, Dixneuf`s and Fürstner`s groups reported that the formation of ruthenium-allenylidene complexes from $RuCl_2$(*p*-cymene)(phosphine) occurs in very mild conditions and the conversion to the corresponding indenylidenes can be catalysed by the addition of Brønsted acids. This isomerization proceeds via the formation of a carbyne intermediate and was monitored by nuclear magnetic resonance spectroscopy.[155,159] The compound $RuCl_2$(*p*-cymene)(IMes) and its allenylidene derivative are also reported. Interestingly, the successful synthesis of the H_2IMes analogue, $RuCl_2$(*p*-cymene)(H_2IMes), is yet not reported and Ledoux reports that attempts in the preparation of such complex by different approaches failed in all cases.[160] Isomerization of [RuCl(*p*-cymene)(diphenylallenylidene)(IMes)]$^+$ into the corresponding ruthenium-indenylidene is reported to not proceed, likely because of electronic reasons, even though the complex efficiently catalyses the ROMP (ring-opening metathesis polymerization) of strained olefins. The likely mechanism involves the *in situ* rearrangement to indenylidene complexes, which are considered the active species.[155]

Reaction of the dark red $[RuCl_2(p\text{-cymene})]_2$[161] (**Figure 35**) with IMes in C_6D_6 in an NMR tube resulted in an instantaneous colour change to dark brown. The reaction is depicted in **Scheme 33**. ^1H NMR analysis after 10 minutes revealed the complete conversion of the dimeric precursor to the corresponding monomeric product. The two set of doublets from the aromatic *p*-cymene protons shifted to lower frequencies by 0.55 and 0.81 ppm (**Figure 36a**) because of the decrease in the Lewis acidity of the metallic centre caused by the coordination of the strong σ-donor NHC ligand.[119]

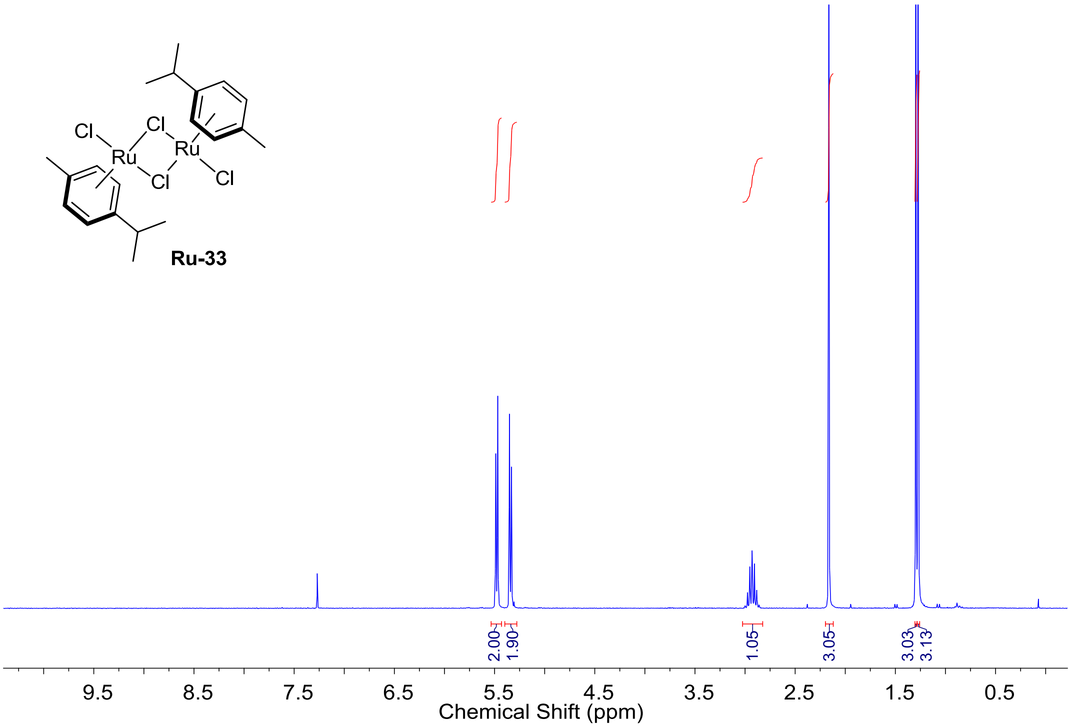

Figure 35 ^1H NMR spectrum ($CDCl_3$, 300 MHz) of the dimer $[RuCl_2(p\text{-cymene})]_2$.

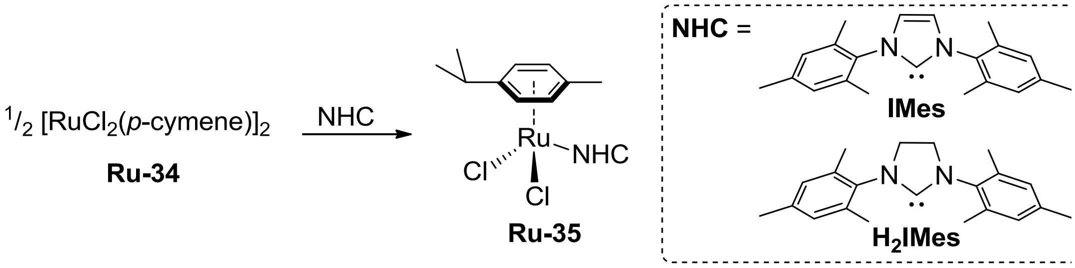

Scheme 33 Synthesis of half-sandwich $RuCl_2(p\text{-cymene})(NHC)$ complexes.

When the same procedure was performed using H_2IMes instead of IMes, the formation of the target compound, $RuCl_2(p\text{-cymene})(H_2IMes)$, could also be observed.

The presence of unidentified by-products was also detected. Nevertheless, compound $RuCl_2$(*p*-cymene)(H_2IMes) could be successfully synthesized with good conversion and very small amounts of by-products by the slow addition of an H_2IMes solution (in C_6D_6) to a vigorously stirred suspension of the Ru-dimer (also in C_6D_6 - [$RuCl_2$(*p*-cymene)]$_2$ is sparingly soluble in C_6D_6).

Both $RuCl_2$(*p*-cymene)(IMes) and $RuCl_2$(*p*-cymene)(H_2IMes) were then prepared in a larger scale by slow addition of a solution of the corresponding NHC ligand in dry benzene into a suspension of [$RuCl_2$(*p*-cymene)]$_2$ (in dry benzene), over a period of 15-30 minutes. After that, the solvent was stripped off and the brown solid analysed by ^{1}H NMR spectroscopy (**Figure 36**). Both $RuCl_2$(*p*-cymene)(IMes) and $RuCl_2$(*p*-cymene)(H_2IMes) slowly decompose in C_6D_6 resulting in the loss of the *p*-cymene ligand (Figure **37**). It is possible that *p*-cymene is being replaced by the less congested C_6D_6. The same behaviour was observed in $CDCl_3$, THF-d_8 or CD_3OD solutions, although with a much slower rate. The decomposition seems to decrease as the polarity of the solvent increases. At first, it was thought that the decomposition was due to the exposition of the sample to light. A test was conducted maintaining the J Young tube wrapped in aluminium foil and monitoring the decomposition of $RuCl_2$(*p*-cymene)(H_2IMes) in C_6D_6 by ^{1}H NMR spectroscopy. The loss of *p*-cymene was slower, though an appreciable amount of free *p*-cymene was observed (**Figure 38**). The identity of free *p*-cymene was confirmed by spiking the mixture with an authentic sample.

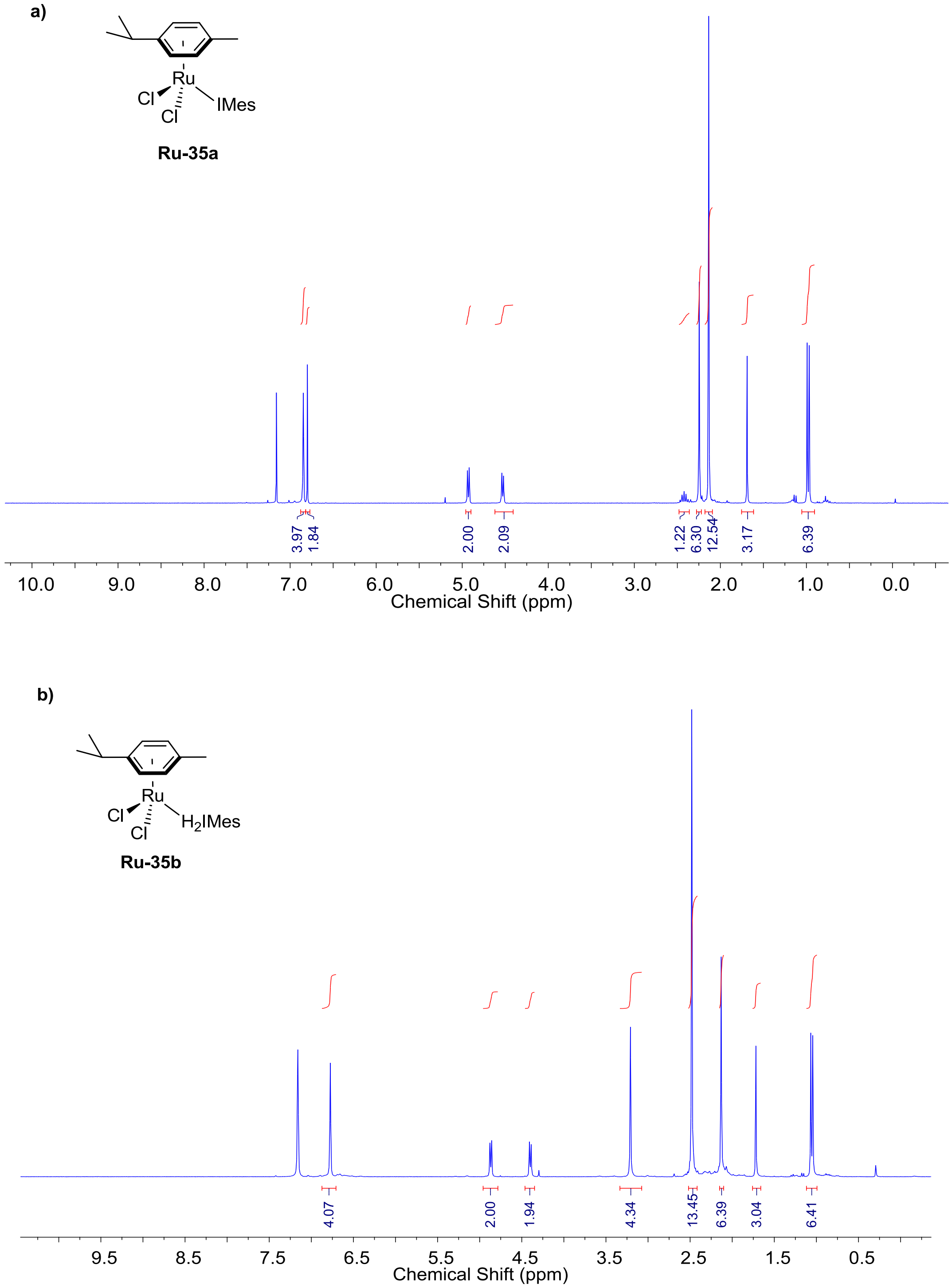

Figure 36 ^{1}H NMR spectra ($CDCl_3$, 300 MHz) of $RuCl_2$(*p*-cymene)(IMes) (a) and $RuCl_2$(*p*-cymene)(H_2IMes) (b).

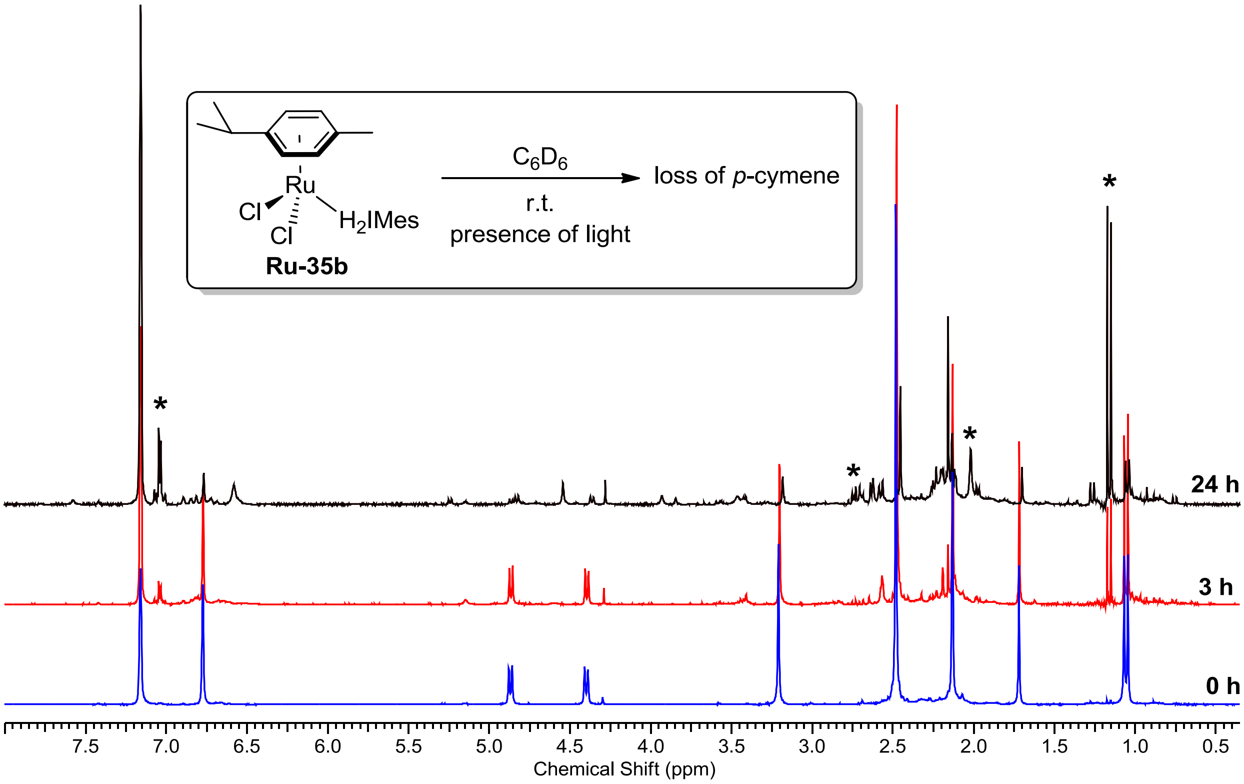

Figure 37 Loss of *p*-cymene in the complex RuCl$_2$(*p*-cymene)(H$_2$IMes) in the presence of light. Asterisks (*) indicate the signals from free *p*-cymene.

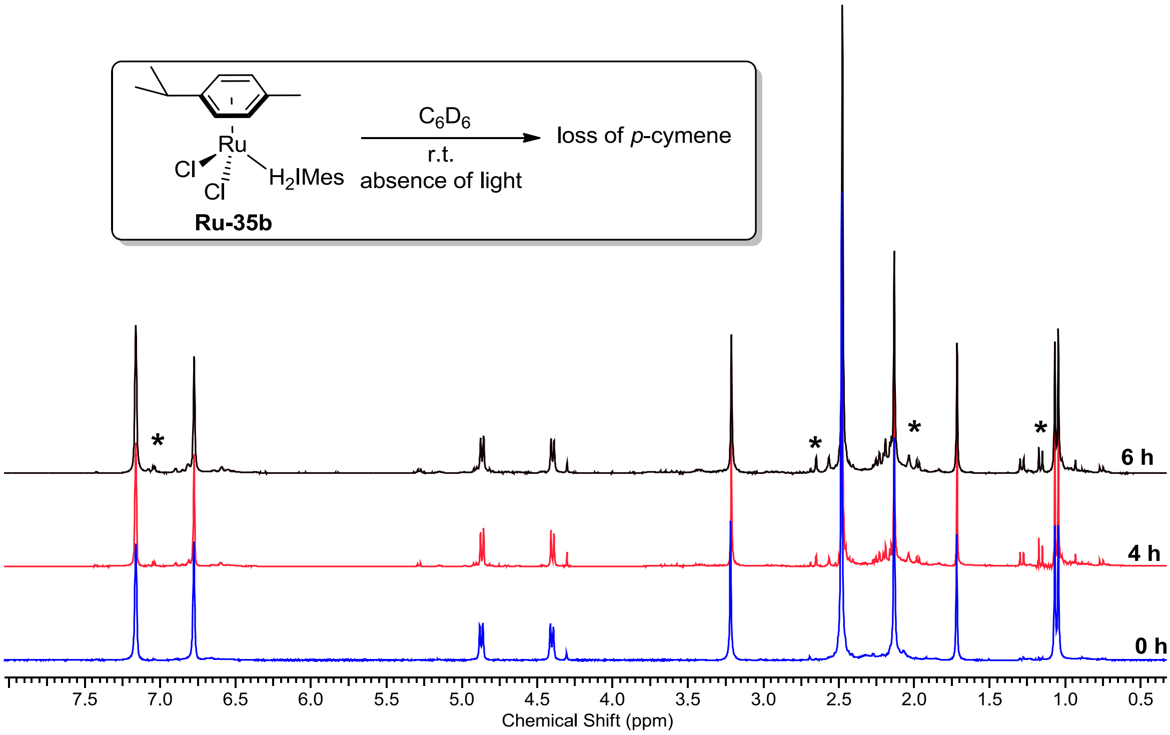

Figure 38 Loss of *p*-cymene in the complex RuCl$_2$(*p*-cymene)(H$_2$IMes) in the absence of light. Asterisks (*) indicate the signals from free *p*-cymene.

Both $RuCl_2$(*p*-cymene)(IMes) and $RuCl_2$(*p*-cymene)(H_2IMes) react with 1,1-diphenylpropargyl alcohol in CD_3OD (**Scheme 34**) as evidenced by the split of the two sets of doublets from the aromatic *p*-cymene proton resonances into four signals (highlighted regions of **Figure 39**). This split is expected due to the loss of the σ plane of symmetry in $RuCl_2$(*p*-cymene)(NHC). CD_3OD was used as solvent because polar protic solvents favour the dissociation of halides and the formation of cationic ruthenium-(*p*-cymene) complexes.

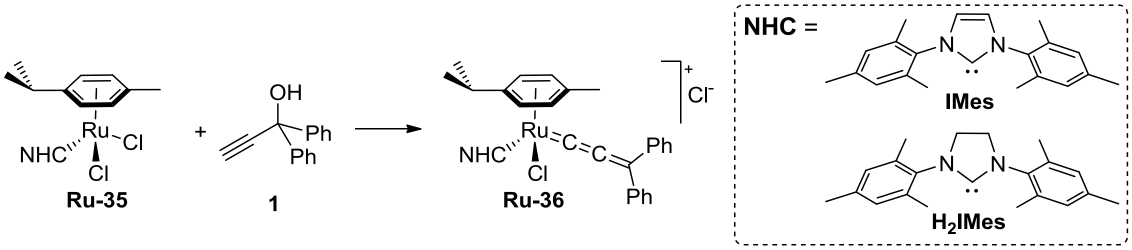

Scheme 34 Cationic RuCl(*p*-cymene)(diphenylallenylidene)(NHC) complexes.

In **Figure 39** the reaction of 1,1-diphenylpropargyl alcohol is clearly confirmed by the decrease in the methynic proton signal at ~ 3.25 ppm and the split of the two sets of doublets corresponding to the aromatic *p*-cymene protons into four sets of doublets. The reaction is complete after 9 hours at room temperature, as evidenced by the complete disappearance of the characteristic resonances discussed above. Moreover, the two equivalent CH_3 groups of the *p*-cymene also split into two doublets, suggesting that the rotation of the $CH(CH_3)_2$ group is restricted under the conditions the spectra were acquired (**Figure 40**).

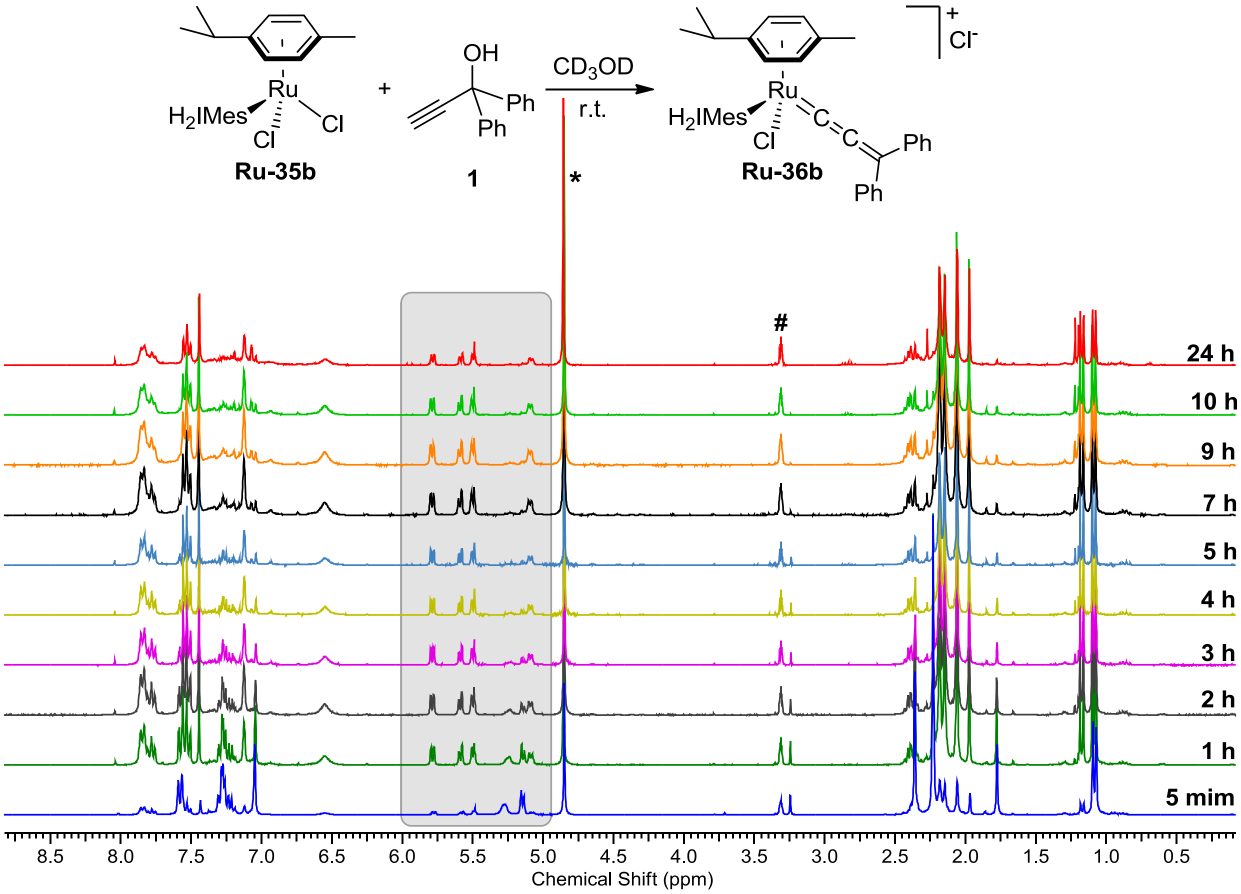

Figure 39 ^{1}H NMR spectra of the reaction between RuCl$_2$(*p*-cymene)(IMes) and 1,1-diphenylpropargyl alcohol in CD$_3$OD at room temperature (* = residual water present in the solvent; # = residual solvent peak).

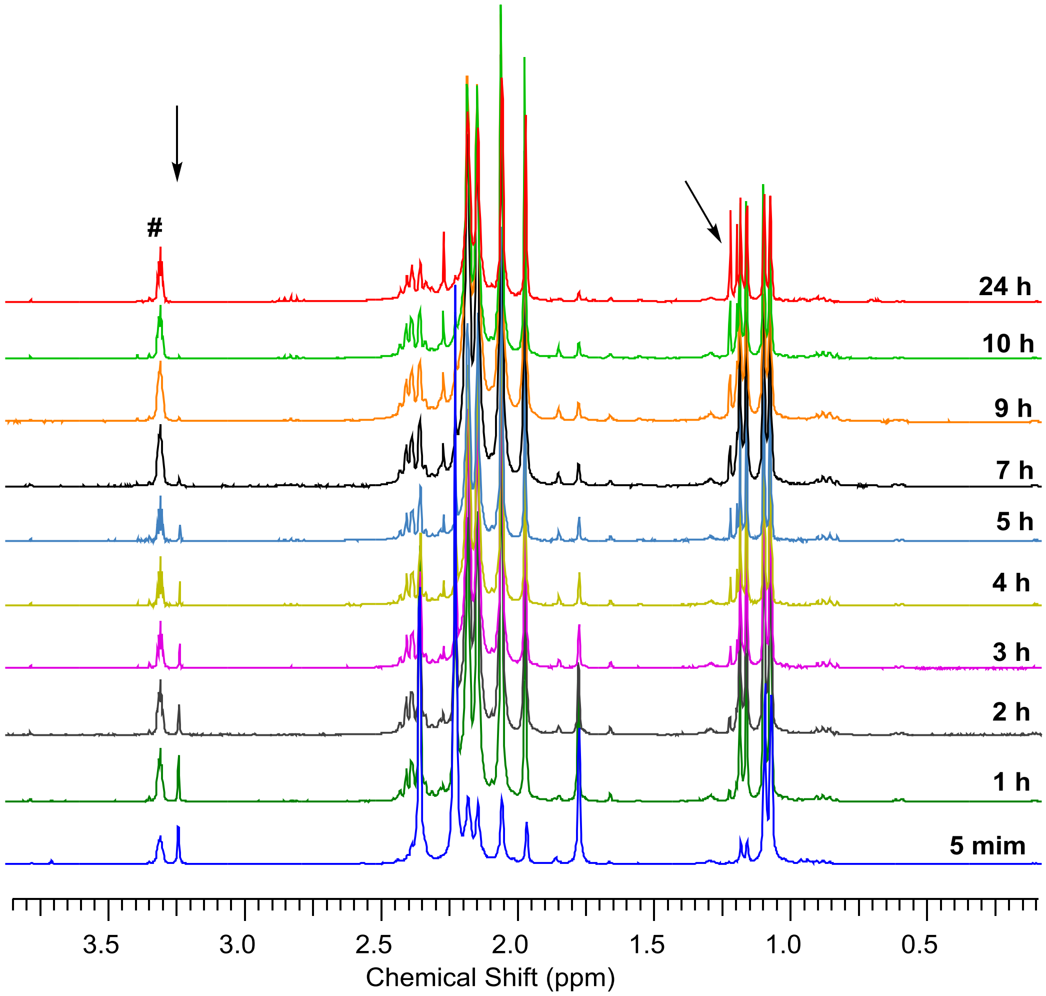

Figure 40 Inset of the ^{1}H NMR spectra of the reaction between $RuCl_2$(*p*-cymene)(IMes) and 1,1-diphenylpropargyl alcohol in CD_3OD at room temperature showing the aliphatic region. (# = solvent residual peak).

The CH($\underline{CH_3}$)$_2$ resonance (doublet at ~ 1,07 ppm in $RuCl_2$(*p*-cymene)(IMes)), is a good probe to monitor the loss of *p*-cymene. The resonances due to the methyl protons of the isopropyl group appear in higher frequencies in free *p*-cymene as compared to the same resonances in the coordinated *p*-cymene. In **Figure 40**, it is possible to observe that the loss of *p*-cymene occured concomitantly with the formation of the allenylidene complex, at a lower rate though. This behaviour could have been very useful in the current strategy, as it would facilitate the displacement of the allenylidene (after rearrangement to the corresponding indenylidene) by 2-isopropoxystyrene. All attempts to prepare **HGII** from the one-pot reaction of $RuCl_2$(*p*-cymene)(IMes), 1,1-diphenylpropargyl alcohol and 2-isopropoxystyrene in CD_3OD did not result in the formation of **HGII** (**Scheme 35**).

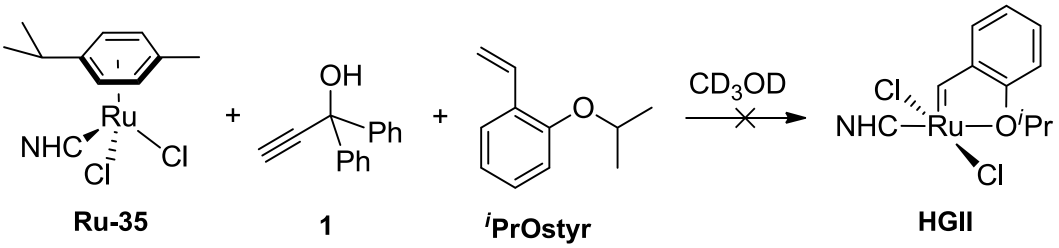

Scheme 35 Attempted one pot synthesis of **HGII** from $RuCl_2$(*p*-cymene)(NHC).

3.2.3 *cis*-Dichloro*tetrakis*(dimethylsulfoxide)ruthenium(II) (*cis*-$RuCl_2(DMSO)_4$)

cis-$RuCl_2(DMSO)_4$ can be easily prepared by refluxing $RuCl_3.xH_2O$ in DMSO, followed by the partial removal of DMSO and precipitation with cold acetone.[162] The light yellow solid, slightly soluble in chloroform, is formulated as *fac*-$RuCl_2(DM\underline{S}O)_3(DMS\underline{O})$.[vi] Three of the DMSO ligands are *S*-coordinated (in a *fac* mode) while the fourth DMSO ligand is coordinated through the oxygen. The *O*-coordinated ligand is more labile than the S-coordinated ones (**Figure 41**).[163]

Despite the quite complicate ^1H NMR spectrum, only the *fac* isomer has been isolated and crystallographically characterized. The complex crystalizes in different forms depending upon the crystallization conditions. No solvent of crystallization has been observed, regardless the crystallization conditions. In solution a variable number of peaks with variable intensities are observed in the ^1H NMR spectrum, including one signal corresponding to free DMSO. These observations suggest that in solution one DMSO reversible dissociates from the metal centre (*O*-coordinated DMSO) resulting in a five coordinated structure, which can adopt a square pyramidal or trigonal bypyramidal geometry. Therefore, it is likely that a mixture of the six coordinated and one of the (or both) five coordinated species are the responsible for the variable number of signals in the ^1H NMR spectrum.[164]

The compound *cis*-$RuCl_2(DMSO)_4$ reacts with monodentate ligands to form only one product (without isomers). Reaction of *cis*-$RuCl_2(DMSO)_4$ with CO results in three equally intense peaks in the ^1H NMR spectrum, which corresponds to two *S*-

---

[vi] The underlined letter indicates the atom coordinated to the metal ($\underline{S}$ = sulfur; $\underline{O}$ = oxygen). The same notation is used for other similar complexes. For clarity, the complex is referred as *cis*-$RuCl_2(DMSO)_4$ throughout the text.

coordinated DMSO and one *O*-coordinated DMSO ligands, yielding *cis*,*trans*,*cis*-$RuCl_2(CO)(DMS\underline{O})(DM\underline{S}O)_2$ (spectroscopically and crystallographically characterized).[165] Similarly, the allenylidene complex $RuCl_2(=C=C=C(Ph)_2)(DM\underline{S}O)_2(PCy_3)$ was prepared in a two-step synthesis from the precursor *cis*-$RuCl_2(DMSO)_4$. It is not possible to infer the configuration around the metal of the complex formed with the limited spectroscopic information provided by the authors.[166]

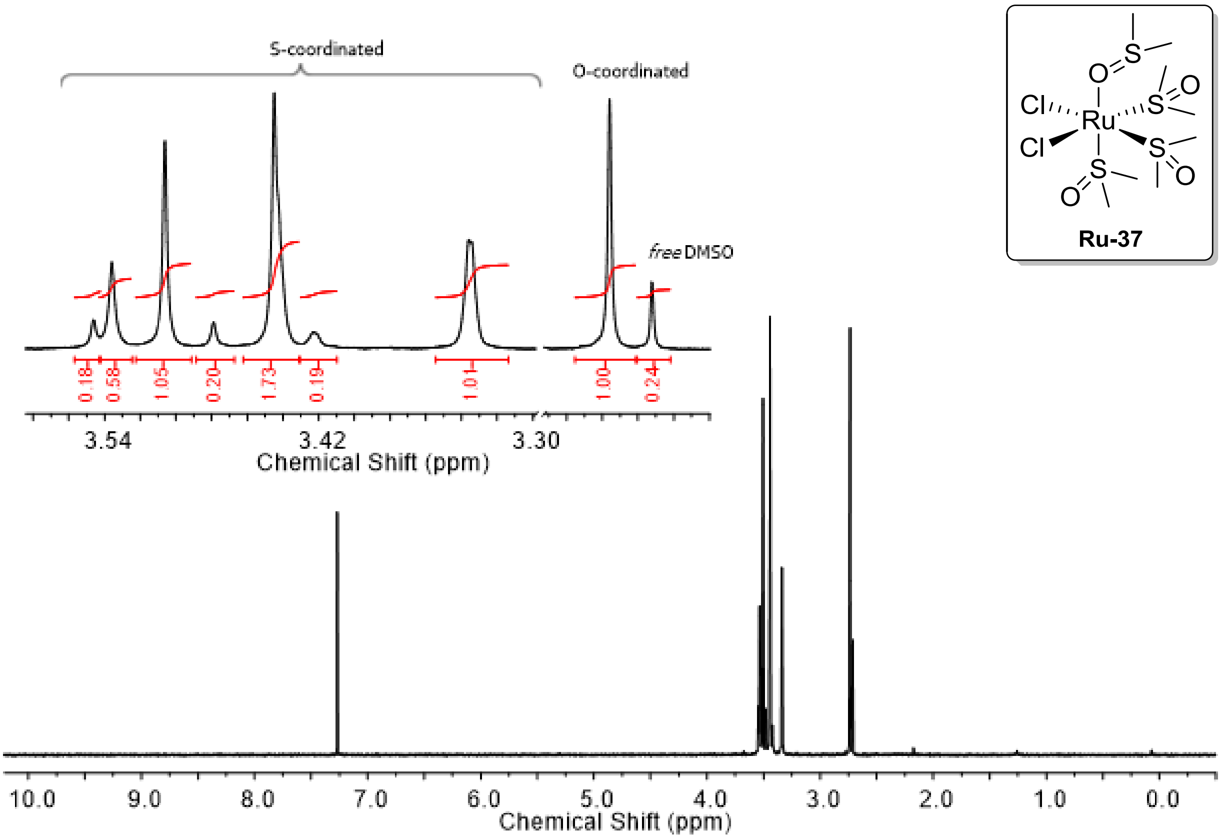

Ru-37

Figure 41 ^1H NMR spectrum ($CDCl_3$, 300 MHz) of *cis*-$RuCl_2(DMSO)_4$ showing the signals of *S*-coordinated, *O*-coordinated and free DMSO.

The combination of the aforementioned properties and the selected examples from literature was a stimulus to attempt the reaction of this precursor with 1,1-diphenylpropargyl alcohol to synthesize our target complex (**Scheme 36**).

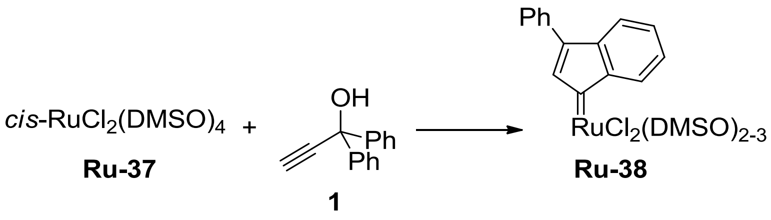

Scheme 36 Attempted synthesis of an indenylidene complex from *cis*-$RuCl_2(DMSO)_4$.

Monitoring a mixture of *cis*-$RuCl_2(DMSO)_4$ and 1,1-diphenylpropargyl alcohol in $CDCl_3$ at 50 °C showed a decrease of the methynic proton resonance of the propargyl alcohol at 2.88 ppm, and the increase of the free DMSO methyl resonance at 2.61 ppm (**Figure 42**) was observed. This suggests that at least one DMSO ligand has been replaced, even though, it was not possible to determine which specie(s) was (were) formed. Moreover, the spectrum became considerably complex due to the possible formation of several isomers. Although the isolation and characterization of the products were not possible, these results show that the reaction of 1,1-diphenylpropargyl alcohol with a ruthenium centre is facile, once a coordination site for reaction is provided. This corroborates with the idea that the lack of reactivity of *trans*-$RuCl_2(py)_4$ is due to lability reasons.

With the objective to obtain a sole product, harsher conditions were then employed. Reaction of the ruthenium precursor *cis*-$RuCl_2(DMSO)_4$ with a 3-fold excess of 1,1-diphenylpropargyl alcohol in boiling dichloromethane resulted in a complex mixture of products as judged by the ^1H and ^{13}C spectra of the crude mixture (**Figure 43** - only two insets of selected regions are shown for clarity).

Although in the ^1H NMR spectrum it is very difficult to obtain any insight about the identity of the possible products formed, the ^{13}C NMR spectrum allows some considerations. Ruthenium-alkylidene complexes (specifically those prepared from propargylic alcohols - see **Appendix II**) exhibit some characteristic signals in their ^{13}C NMR spectrum that can be used as characteristic resonances to help assigning the corresponding structure (see **Appendix II**).

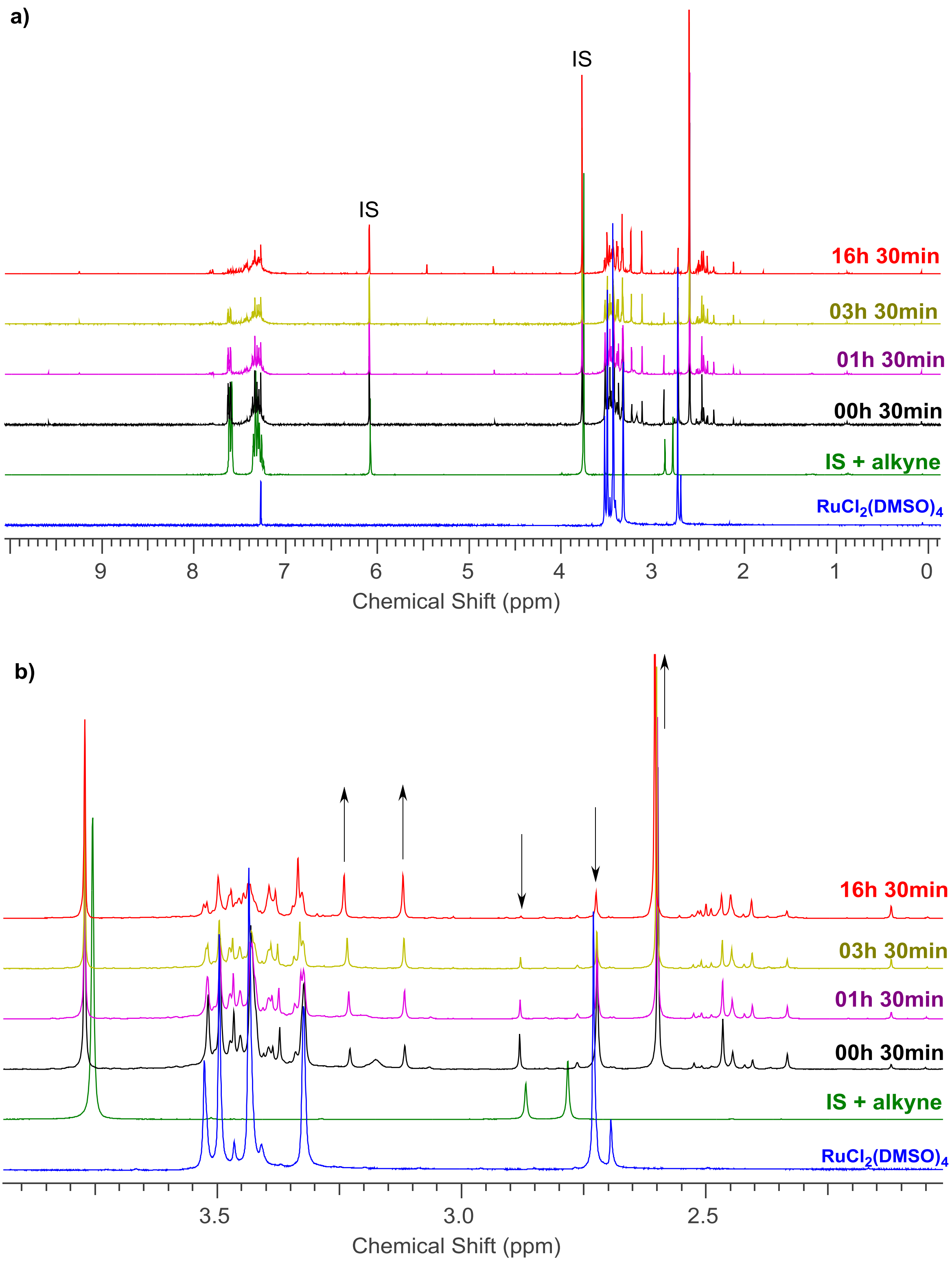

Figure 42 ^{1}H NMR spectra ($CDCl_3$; 300 MHz) of the reaction between *cis*-$RuCl_2(DMSO)_4$ and 1,1-diphenylpropargyl alcohol. Full spectra (a) and inset of the region containing the signals from DMSO and propargyl alcohol methynic (2.88 ppm) protons (b). IS (Internal standard) = 1,3,5-trimethoxybenzene.

Except for ruthenium-alkynyl complexes (Ru–≡–R), all other ruthenium complexes prepared from 1,1-diphenylpropargyl alcohol exhibit a signal at ~ 300 ppm (C_α) in the ^{13}C NMR spectrum. Although this is a characteristic signal that can be used to confirm the formation of ruthenium-alkylidene (or -carbyne) species, the nature of the C_α carbon (quaternary carbon bonded to a metallic center) may preclude its visualization in the spectrum due to the corresponding low intensity. Based on the aforementioned, it was not possible to confirm or rule out the formation of none of the possible complexes.

Evidences towards the formation of either allenylidene complexes (C_β at δ ~190 ppm - see **Appendix II**) or alkenylcarbyne complexes (Cγ at δ ~ 190 ppm - see **Appendix II**) can be encountered based on the $^{13}C\{^1H\}$ NMR spectrum of the crude mixture (**Figure 43**). The singlets in the region ranging from ~4.5 to ~6.0 ppm in the ^{1}H NMR spectrum may also be due to an alkenylcarbyne (H_β vs Ru). The formation of an allenylidene cannot be either confirmed or ruled out by the ^{1}H NMR spectroscopic data.

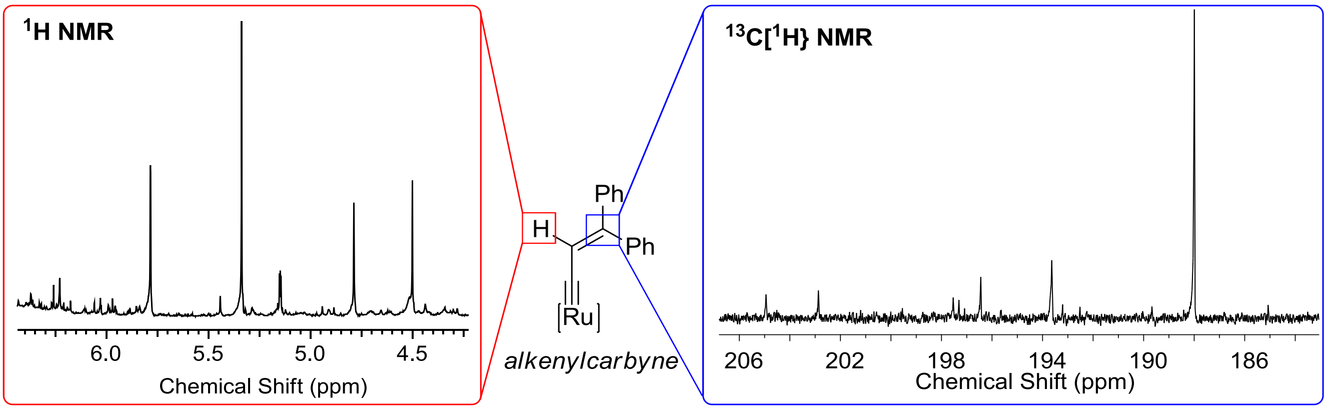

Figure 43 Insets of the ^{1}H (300 MHz, $CDCl_3$ - left) and $^{13}C\{^1H\}$ (75.5 MHz, $CDCl_3$ - right) NMR spectra showing resonances that are likely from a mixture of alkenylcarbyne complexes.

The formation of alkenylcarbyne complexes was observed by the Dixneuf group during a study on the allenylidene-to-indenylidene rearrangement in ruthenium(*p*-cymene)(allenylidene) complexes (**Scheme 37**).[155] In their study it was observed that allenyllidene-ruthenium complexes of the type $[RuCl(=C=C=CR_2)(\eta^6\text{-}p\text{-cymene})(PR'_3)]OTf$ (R = Ph, fluorene, Me; R' = Cy, ^{i}Pr, Ph), when treated with triflic acid (HOTf) at -40 °C are completely transformed into the corresponding alkenylcarbyne complexes. The alkenylcarbyne complexes then, upon heating to -20 °C, undergo an intramolecular rearrangement resulting in the corresponding indenylidene complexes (**Scheme 37**).

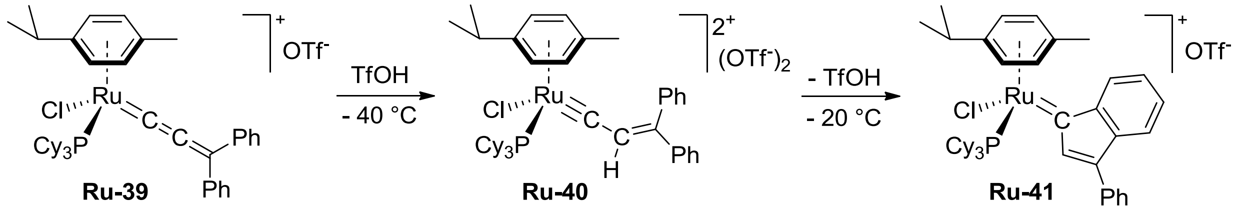

Scheme 37 Ruthenium allenylidene-to-indenylidene rearrangement via the formation of an alkenylcarbyne intermediate.

The sole formation of the neutral Ru(IV) alkenylcarbyne $RuCl_3(\equiv C-CH=C(Ph)_2)(PPh_3)_2$ has been observed upon refluxing the ruthenium(II) precursor $RuCl_2(PPh_3)_{3-4}$ with 1,1-diphenylpropargyl alcohol and excess of HCl in DCM for 90 min.[49] Interestingly, the isolated alkenylcarbyne does not react further when reflux ed in DCM, but it rearranges to the corresponding Ru(II) indenylidene complex ($RuCl_2$(phenylindenylidene)$(PPh_3)_2$) in refluxing THF. Therefore, the allenylidene-to-indenylidene rearrangement is postulated to occur via an alkenylcarbyne intermediate.[155]

Attempts to promote the further conversion of the formed species into the target indenylidene complex using harsher conditions (use of a higher boiling point solvent - THF) did not result in the formation of indenylidene species (as judged by comparing both ^1H and $^{13}C\{^1H\}$ spectra of the crude mixtures in each reaction). However, when catalytic amounts of HCl (20 mol% vs [Ru]) were used in boiling THF, one specie seemed to be favoured (δ = 5.36 ppm in the ^1H NMR spectrum inset) (**Figure 44** vs **Figure 43**).

Further evidences that help in the assignment of an alkenylcarbyne complex from the data obtained are found in the 2D ^1H-^{13}C HMQC and HMBC spectra. The ^1H-^{13}C HMQC spectrum shows a correlation of the resonance corresponding to the singlet at δ = 5.36 ppm in the ^1H spectrum with a carbon resonance at δ = 113.2 ppm (**Figure 45a**). Correlation of the same singlet with a carbon resonance at δ = 186.9 ppm is also observed in the ^1H-^{13}C HMBC spectrum (**Figure 45b**). These data support the proposed assignment to an alkenylcarbyne complex (in the presence of other unidentified compounds, possibly allenylidenes). An attempted crystallization by layering a DCM solution of the mixture with hexane was unsuccessful.

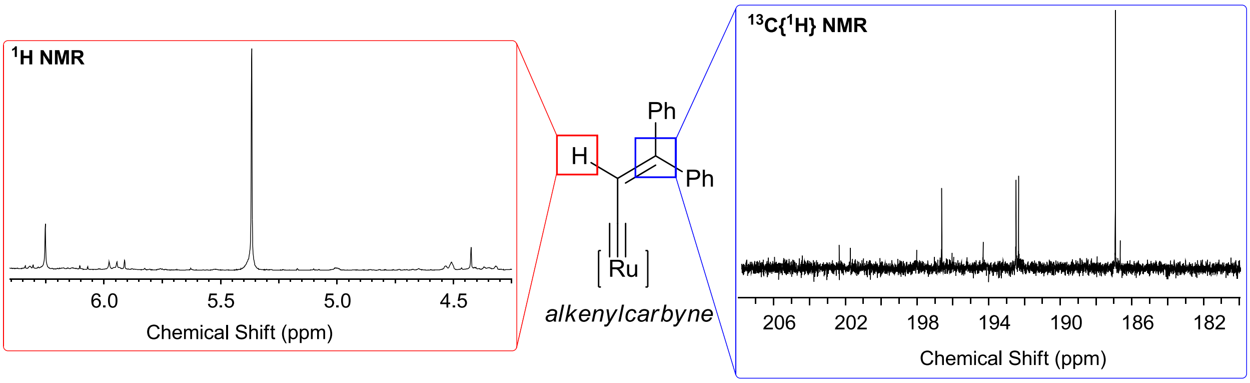

Figure 44 Insets of the ^{1}H (left) and ^{13}C{^{1}H} (right) NMR spectra of the crude mixture obtained in the reaction of *cis*-$RuCl_2(DMSO)_4$ and 1,1-diphenylpropargyl alcohol in boiling THF in the presence of 20 mol% (vs [Ru]) of HCl.

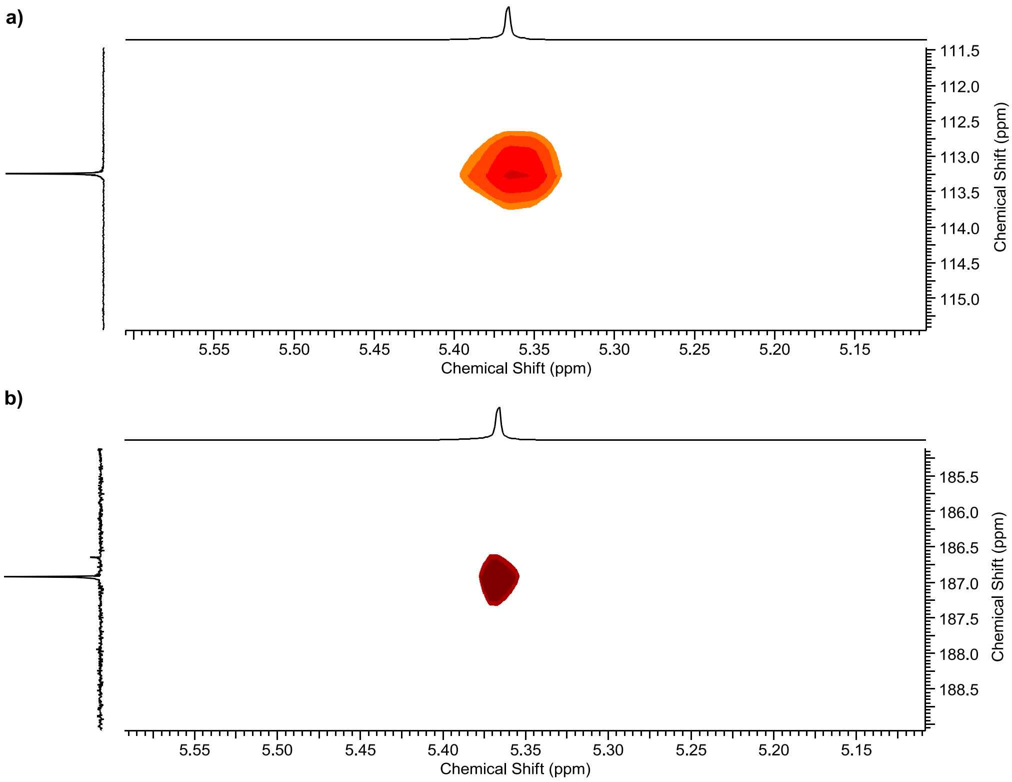

Figure 45 Insets from the ^{1}H-^{13}C HMQC (a) and ^{1}H-^{13}C HMBC (b) spectra of the crude mixture obtained in the reaction of *cis*-$RuCl_2(DMSO)_4$ and 1,1-diphenylpropargyl alcohol with 20 mol% of HCl (vs [Ru]), showing the correlations of the singlet at δ = 5.36 ppm with the carbon resonances at 113.4 and 186.8 ppm, respectively.

4

CONCLUSIONS

4.1 CROSS-METATHESIS WITH MALEIC ACID

Cross-metathesis (CM) of methyl oleate (**MO**) with maleic acid (**MA-H**) was investigated using four commercially available ruthenium metathesis (pre)-catalysts. The parameters method of **MO** purification, **MO**:**MA-H** ratio, **MO** concentration, temperature, time, and type and concentration of (pre)-catalyst were investigated. Purification method D, which consists in treating **MO** with Magnesol (2.5 wt%), Celite (1.5 wt%) and $Ti(O^iPr)_4$ (2 mol%) for 1 h at 80 ºC before use, resulted in the best **MO** conversions and yields of the CM products. Only a small excess of **MA**:**H** was required to obtain the best results (**MO**:**MA-H** ratio of 1:2). Surprisingly, the temperature and the **MO** concentration had only small influences on the outcome of the studied reaction. Amongst the four (pre)-catalysts investigated, only the complex containing a phenoxy-imina ligand (**Um42**) displayed a significantly inferior performance in the cross-metathesis of **MO** with **MA-H**.

All reactions were complete within ~ 35 minutes. Self-metathesis of **MO** occurs in the first minutes of the reaction and then the SM products react with **MA-H** to form the respective CM products, 11-methoxy-11-oxoundec-2-enoic acid (**P1**) and 2-undecenoic acid (**P2**). The CM products are also formed via the direct reaction of **MO** and **MA-H**, as determined by the time dependant reaction profiles.

Selectivity towards the CM products was observed in the reactions with complete conversion. Besides, remaining SM products were also observed in the cases with incomplete conversions. Only traces (< 2%) of the products from the regioisomerization of **MO** (or SM/CM products) were observed.

Second-generation Grubbs (**GII**) and Hoveyda-Grubbs (**HGII**) metathesis (pre)-catalysts were further employed in the CM of **MO** with maleate esters and acrylic acid (**AA-H**)/methyl acrylate (**AA-Me**). It was observed that when using maleic acid/maleates, both **GII** and **HGII** displayed the same performance and the bulkiness of the alkoxy-substituent of the CM-partner (H, Me or ^{i}Pent) controled the **MO** conversion and the yield of CM products. The increase in the alkoxy group bulkiness had a detrimental effect on the outcome of the reaction. Conversely, the use of **AA-H** and **AA-**

Me culminated in very different performances for **GII** and **HGII**. **HGII** outperformed **GII** in the reactions were **AA-H** and **AA-Me** were used as CM-partners, being a consequence of the formation of ruthenium-methylidene propagating species and their decomposition mediated by the dissociated PCy_3 (in the case of **GII**).

Reactions were also performed using eleven different vegetable oils as substrate, **MA-H** as CM-partner and **GII** as (pre)-catalyst, using the conditions optimized for **MO**. The use of vegetable oils as CM-partners resulted in similar performance as compared to the use of **MO**. The majority of the oils resulted in yields of the CM products higher than 73%. Only cottonseed (47%) and peanut (55%) oils exhibited poor CM yields. The oils tested have very different compositions, but no trend correlating the composition with the yield of the CM products was observed, an indication that none of the components of the oils affects the reaction explored.

Overall, in comparison to the "protected" ester equivalents, the direct use of the carboxylic acid substrates **MA-H** and **AA-H** in the Ru-catalyzed cross-metathesis with **MO** afforded superior conversions and CM yields. This turns these substrates attractive for the direct synthesis of α,β-unsaturated carboxylic acids, which can be ascribed to the lower steric bulkiness of the $–CO_2H$ group. In the case of a phosphine-containing (pre)-catalyst like **GII**, the avoidance of the formation of Ru-methylidene species is crucial for obtaining good catalytic productivities. This was effectively suppressed by using **MA-H** as internal olefin, which only leads to the formation of Ru-enoic carbene species. Under this condition, **GII** can be used as a cheaper alternative for **HGII** in the reaction with **MO** and a variety of vegetable oils. When applying **AA-H** as substrate, which leads to the formation of Ru-methylidene species, **HGII** remains the (pre)-catalyst of choice. Altogether, these findings have the potential to serve as a rational guideline for determining the reaction conditions in the preparation of α,β-unsaturated carboxylic acid derivatives.

Reaction of **GII** with **MA-H** was also investigated by means of ^1H and $^{31}P\{^1H\}$ NMR spectroscopy in THF-d_8. **GII** slowly reacts with **MA-H** resulting in the formation of a new specie containing a different alkylidenic fragment. The reaction proceeds with an observed first order kinetics, consistent with the dissociation of the PCy_3 ligand being the rate-limiting step of the reaction. Analysis of the new specie by $^{13}C\{^1H\}$, ^1H-^{13}C HSQC and ^1H-^{13}C HMBC indicated that the ruthenium-enoic carbene complex **Ru-CHCO$_2$H** was formed.

4.2 DEVELOPMENT OF A PHOSPHINE-FREE STRATEGY FOR THE SYNTHESIS OF RU-ALKYLIDENE COMPLEXES

Synthesis of the target ruthenium indenylidene complex $RuCl_2(Ind)L_2$ (Ind = 3-phenylindenylidene) via a phosphine-free strategy was investigated using *trans*-$RuCl_2(py)_4$, $[RuCl_2(p\text{-cymene})]_2$ and *cis*-$RuCl_2(DMSO)_4$ precursors. The 18e$^-$ pyridine precursor did not react with 1,1-diphenylpropargyl alcohol under the conditions studied, likely because the low lability of pyridine in this complex.

Reaction of the dimeric $[RuCl_2(p\text{-cymene})]_2$ with IMes (1,3-bis(2,4,6-trimethylphenyl)-imidazol-2-ylidene) and H_2IMes (1,3-bis(2,4,6-trimethylphenyl)-4,5-dihydroimidazol-2-ylidene) resulted in the formation of the monomeric compounds $RuCl_2(p\text{-cymene})(IMes)$ and $RuCl_2(p\text{-cymene})(H_2IMes)$, respectively. Both complexes decompose in solution, in the presence and absence of light, via loss of the *p*-cymene ligand. In CD_3OD, the complexes slowly react at room temperature with 1,1-diphenylpropargyl alcohol to afford complexes proposed as cationic allenylidenes of the type $[RuCl(=C=C=CPh_2)(p\text{-cymene})(NHC)]^+$ based on their ^1H NMR spectra. The loss of *p*-cymene occurs concomitantly with the formation of the allenylidene complexes. The one pot reaction of $RuCl_2(p\text{-cymene})(NHC)$, 1,1-diphenylpropargyl alcohol and 2-*iso*propoxystyrene did not result in the formation of the second-generation Hoveyda-Grubbs metathesis catalyst (**HGII**).

The DMSO precursor *cis*-$RuCl_2(DMSO)_4$ reacts with 1,1-diphenylpropargyl alcohol resulting in the formation of several species. In the presence of 20 mol% HCl, one of the species was predominant and evidences that support its identification as a ruthenium alkenylcarbyne were encountered spectroscopically (^1H, ^{13}C, ^1H-^{13}C HMQC and ^1H-^{13}C HMBC NMR spectroscopy). Ruthenium-alkenylcarbynes are intermediates in the formation of ruthenium-indenylidene complexes. Despite some attempts, the isolation and complete characterization of the alkenylcarbyne complex was not possible.

5

EXPERIMENTAL

5.1 CROSS-METATHESIS WITH MALEIC ACID

General considerations

MA-H, **AA-H** (ultrapure), 1,3,5-trimethoxybenzene, **GII**, **HGII**, **IndII** and **Um42** were used as received. THF was distilled over Na/benzophenone and stored over activated molecular sieves under an argon atmosphere. **MA-Me** and **AA-Me** were distilled prior to use. **MO** (> 99% purity) was purchased from TRC Inc. Magnesol was purchased from Magnesol® XL Oil Solutions. The vegetable oils were purchased from the local commerce. Gas chromatogram traces were acquired on a DANI gas chromatograph equipped with a DN-WAX (30 m, 0.32 mm I.D., 0.25 µm film thickness) column and a FID detector. 1,3,5-Trimethoxybenzene was used as internal standard. NMR spectra were recorded on a Bruker (400 MHz) or a Varian Inova 300 (300 MHz) equipment at ambient temperature. The chemical shifts are given in parts per million (ppm) and referenced to the residual solvent signal ($CDCl_3$ = 7.26 (^1H), 77.16 (^{13}C); CD_3OD = 3.31 (^1H), 49.00 (^{13}C)). Infrared spectra were recorded on a Bruker ALPHA FT-IR ATR spectrometer. High-resolution mass spectrometry spectra were recorded on an electrospray ionization (ESI) Micromass Q-Tof Micro™ equipment in the positive mode.

*General procedure for the cross-metathesis of **MO** with **MA-H***

MO, Magnesol (2.5 wt% vs **MO**), Celite (1.5 wt% vs **MO**) and $Ti(O^iPr)_4$ (0 or 2.0 mol% vs **MO**) were transferred to a Schlenk tube and the system evacuated for 10 minutes before backfilling with argon and stirring for 1 or 12 h at 80 or 50 °C, respectively. The mixture was then passed through a PTFE membrane filter (0.45 µm pore diameter). The vegetable oils were purified using the same approach.

Freshly purified **MO** (0.523 g; 1.77 mmol; 1.0 equiv), **MA-H** (0.206 g; 1.77 mmol; 1.0 equiv) and 1,3,5-trimethoxybenzene (0.304 g; 1.80 mmol; internal standard for GC) were transferred to a Schlenk tube, degassed by five consecutive *freeze-pump-thaw* cycles and dissolved in an appropriate amount of dry THF. Then a freshly prepared solution of the (pre)-catalyst of known concentration (in dry THF) was added to the substrates solution and the Schlenk tube was immersed in a pre-heated oil bath at the reaction temperature. A “time zero” (t_0) aliquot (~ 250 µL) was taken before the addition of the catalyst solution. Aliquots were taken after determined time intervals and added to test tubes containing 3 drops of a 6.0 mmol.L^{-1} KTp methanolic solution (KTp = potassium trispyrazolylborate) to guarantee the quenching of the reaction.[167]

Aliquots derivatization: To each test tube 1.0 mL of a 2.52 mol.L^{-1} methanolic H_2SO_4 solution was added. The tubes were closed with rubber septa and stirred at 63 °C for 2 h. After cooling to 0 °C, hexane (4.0 mL) and deionized water (1.0 mL) were added; and the mixture was centrifuged at 2000 rpm for 8 min. The upper layer was collected and analyzed by GC-FID. Reactions were performed in duplicate and variations in the results are within 1-4% of the average reported values.

Synthesis of MA-^{i}Pent

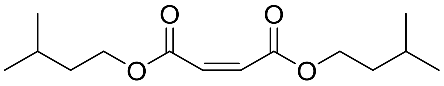

MA-H (12.37 g; 106.6 mmol; 1.0 equiv), *p*-toluenesulfonic acid (1.07 g; 6.2 mmol; 0.06 equiv) and isopentyl alcohol (28.19 g; 334.3 mmol; 3.1 equiv) were refluxed in toluene (100 mL) in a Dean-Stark apparatus for 18 h. The mixture was then cooled to room temperature, washed with deionized water (3 x 80 mL) and dried over anhydrous magnesium sulfate. After solvent removal, distillation of the crude mixture under reduced pressure afforded the target compound as a colourless liquid. Yield: 61% (16.62 g; 64.8 mmol). ^1H NMR (400 MHz, $CDCl_3$) δ 6.18 (s, 2H, $-C\underline{H}=C\underline{H}-$), 4.17 (t, *J* = 6.9 Hz, 4H, $-C\underline{H_2}O-$), 1.73-1.57 (m, 2H, $-C\underline{H}(CH_3)_2$), 1.52 (q, *J* = 6.9 Hz, 4H, $-C\underline{H_2}-$), 0.88 (d, *J* = 6.7 Hz, 12H, $–CH(C\underline{H_3})_2$). ^{13}C NMR (101 MHz, $CDCl_3$) δ 165.3 ($\underline{C}=O$), 129.8 ($-\underline{C}H=\underline{C}H-$), 63.9 ($-\underline{C}H_2O-$), 37.1 ($-\underline{C}H_2-$), 24.9 ($-\underline{C}H(CH_3)_2$), 22.4 ($-CH(\underline{C}H_3)_2$). Integration revealed the presence of < 2% of the fumarate isomer (olefinic singlet at 6.79 ppm). FT-IR (ATR, cm^{-1}) 1728, 1646, 1158. ESI(+)-MS: $C_{14}H_{25}O_4^+$ - calculated: 257.1751, obtained: 257.1753; $C_{14}H_{24}NaO_4^+$ (sodium adduct) - calculated: 279.1567, obtained: 279.1534.

5.2 MONITORING THE FORMATION OF A RU-ENOIC CARBENE FROM THE REACTION OF GII WITH MA-H

General considerations

THF, toluene, diethyl ether and pentane were distilled with Na/Benzophenone under an argon atmosphere and stored over activated molecular sieves under argon. NMR solvents were degassed by 5 consecutive freeze-pump-thaw cycles and stored over molecular sieves under an argon atmosphere. **GII** was used as received. Maleic acid was recrystallized from acetone. Dimethyl maleate was distilled prior to use. NMR spectra were acquired on a Varian Inova equipment (^{1}H – 300 MHz, ^{13}C – 75 MHz, ^{31}P 101.6 MHz). Spectra were referenced against the residual solvent peak of THF-d_8 for ^{1}H (3.58 ppm) and the signal centered at 67.57 ppm for ^{13}C. H_3PO_4 85 wt% was used as external standard for ^{31}P NMR experiments (0.00 ppm). All spectra were acquired at 20 °C. All the manipulations were carried out using standard Schlenk tube techniques under argon atmosphere.

General procedure for the NMR tube scale reactions

2 mL of a 35.4 mmol.L^{-1} solution of **MA-H** (0.071 mmol, 6 equiv) in acetone was dried for 12 h and then dissolved in 0.15 mL of THF-$_{d8}$. Then **GII** (10 mg, 0.0118 mmol, 1 equiv) was loaded into an NMR tube and dissolved in 0.4 mL of THF-$_{d8}$. The “time zero” spectrum was acquired and the maleic acid added. Spectra were acquired at 15 minutes intervals (^{1}H NMR = 64 scans; ^{31}P NMR = 200 scans) during 7 hours (420 minutes).

Synthesis of RuCHCO$_2$H

To a Schlenk tube loaded with **GII** (85.5 mg, 0.1 mmol, 1 equiv) was added a solution of **MA-H** (70.9 mg, 0.61 mmol, 6.1 equiv) in 5 mL of THF and the Schlenk tube immersed in a water bath cooled at 14-17 °C and stirred for 12 h. Then the solvent was removed under reduced pressure for 8 hours and the resulting solid suspended in 3 mL of cold toluene (0 °C). The mixture was filtered through a PTFE membrane (0.45 µm pore diameter) via cannula and the remaining solid extracted with additional amounts of cold toluene (2 x 3 mL) and filtered. The combined toluene fractions were dried under reduced pressure for 20 h. The ochre solid was then crushed with pentane (4 x 5 mL) and the finely divided powder dried under reduced pressure for 30 h. A yellow ochre solid was obtained in 91% yield (75.4 mg, 0.092 mmol).

5.3 DEVELOPMENT OF A PHOSPHINE-FREE STRATEGY FOR THE SYNTHESIS OF RU-ALKYLIDENE COMPLEXES

General considerations

All organic reagents and solvents were purchased from commercial suppliers (Sigma-Aldrich, Alfa Aesar or Merck) and, unless otherwise stated, used without further purification. $RuCl_3.xH_2O$ (41-43 % in Ru) was purchased from Alfa Aesar. Dried solvents were either obtained from an MBraun solvent purification system or distilled according to literature procedures and stored over molecular sieves under an inert atmosphere (N_2 or Ar). Spectra were acquired on Varian (300 MHz for ^1H or 75 MHz for ^{13}C) or Bruker (400 MHz for ^1H or 100 MHz for ^{13}C) equipments. Air and/or moisture sensitive compounds were analysed using dry (molecular sieves) and oxygen-free (*freeze-pump-thaw* cycles) deuterated solvents. For other compounds, the deuterated solvents were used as received. Chemical shifts (δ) are given in parts per million (ppm) and are referenced against the residual signal of the deuterated solvent (relative to TMS; $\delta = 0.00$ ppm). For ^1H NMR: $CHCl_3$ = 7.27 ppm; C_6D_5H = 7.16 ppm; CD_2HOD = 3.31 ppm, $(CD_3)SO(CD_2H)$ = 2.50 ppm and HDO = 4.79 ppm. For ^{13}C NMR: $CDCl_3$ = 77.16 ppm.[48] Multiplicities are described as follows: s = singlet; d = doublet; t = triplet; dd = doublet of doublet; sept = septet; m = multiplet.

Ru precursor syntheses

trans-$RuCl_2(py)_4$ was kindly donated by Dr. Bianca van Lierop from the Deryn E. Fogg group (prepared from $RuCl_2(PPh_3)_3$).

[$RuCl_2$(*p*-cymene)]$_2$

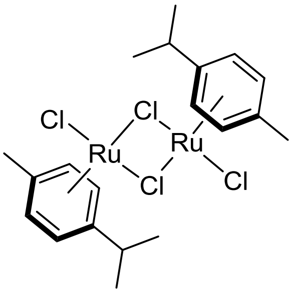

Reaction carried out under N_2 atmosphere and work up performed under atmospheric condition.[161] Ethanol (95%) was refluxed for 1 h under N_2 atmosphere and cooled to room temperature prior to use. $RuCl_3.xH_2O$ (2.04 g; 8.49 mmol) was transferred to a 2-neck round-bottom flask equipped with a condenser and the system was 5 times evacuated and backfilled with N_2. Ethanol (100 mL) and α-phellandrene (10 mL) were cannula-transferred, and the mixture refluxed for 4 h. The initially dark brown solution turned brick red after approximately 30 min. The solution was then cooled to room temperature and then to 0 °C. A crystalline brick red solid precipitated that was collected by filtration, washed with cold ethanol and dried under reduced pressure. The filtrate was concentrated to approximately 25 mL and kept in the fridge for a few days, resulting in an additional batch of the product, which was treated as described above. Combined yield: 90% (4.67 g; 7.63 mmol). ^1H NMR (300 MHz, $CDCl_3$) δ 5.48 (d, J = 6.0 Hz, 2H, 2 x C$\underline{H}$), 5.34 (d, J = 6.0 Hz, 2H, 2 x C$\underline{H}$), 2.93 (sept, J = 7.0 Hz, 1H, C$\underline{H}(CH_3)_2$), 2.16 (s, 3H, C$\underline{H_3}$), 1.28 (d, J = 7.0 Hz, 6H, CH(C$\underline{H_3}$)$_2$).

cis-$RuCl_2(DMSO)_4$

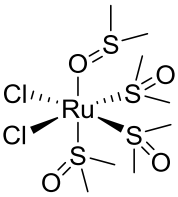

Reaction carried out under argon using untreated solvents and work up performed under atmospheric conditions. The Reaction was performed using a slight modification of the procedure reported by Wilkinson.[162] $RuCl_3.xH_2O$ (0.52 g; 2.14 mmol) was transferred to a two-neck round-bottom flask and a condenser fitted to the flask. The system was 5 times evacuated and backfilled with N_2. Then DMSO (12 mL) was added and the flask immersed in a silicon oil bath pre-heated at 200 °C. The initially dark brown solution turned to bright yellow within 5 minutes, passing by dark red and orange. After 6 min, the flask was removed from the oil bath and the solvent reduced to approximately 4 mL, resulting in the precipitation of a yellow solid. Acetone (2 x 12 mL) was added and the mixture cooled to 0 °C and then the acetone was removed with a pipette. The same procedure was repeated with Et_2O (2 x 10 mL). After removing the remaining solvent under reduced pressure, the solid was dissolved in 5 mL of hot DMSO (150 °C) and the solvent was allowed to slowly evaporate at this temperature (~ 2 h). After complete evaporation of the solvent, the yellow crystalline solid was cooled to 0 °C and washed with acetone (2 x 5 mL), Et_2O (2 x 5 mL) and dried under reduced pressure. Yield: 63% (0.65 g; 1.35 mmol). ^1H NMR spectroscopic data are in good agreement with reported values.[43] ^1H NMR (300 MHz, $CDCl_3$) δ 3.55 (s), 3.54 (s), 3.51 (s), 3.48 (s), 3.44 (s), 3.42 (s), 3.34 (s), 2.74 (s), 2.71 (s) (before crystallization). ^1H NMR (300 MHz, $CDCl_3$) δ 3.52 (s), 3.49 (s), 3.43 (s), 3.32 (s), 2.73 (s), 2.61 (s) (after crystallization).

NHC syntheses

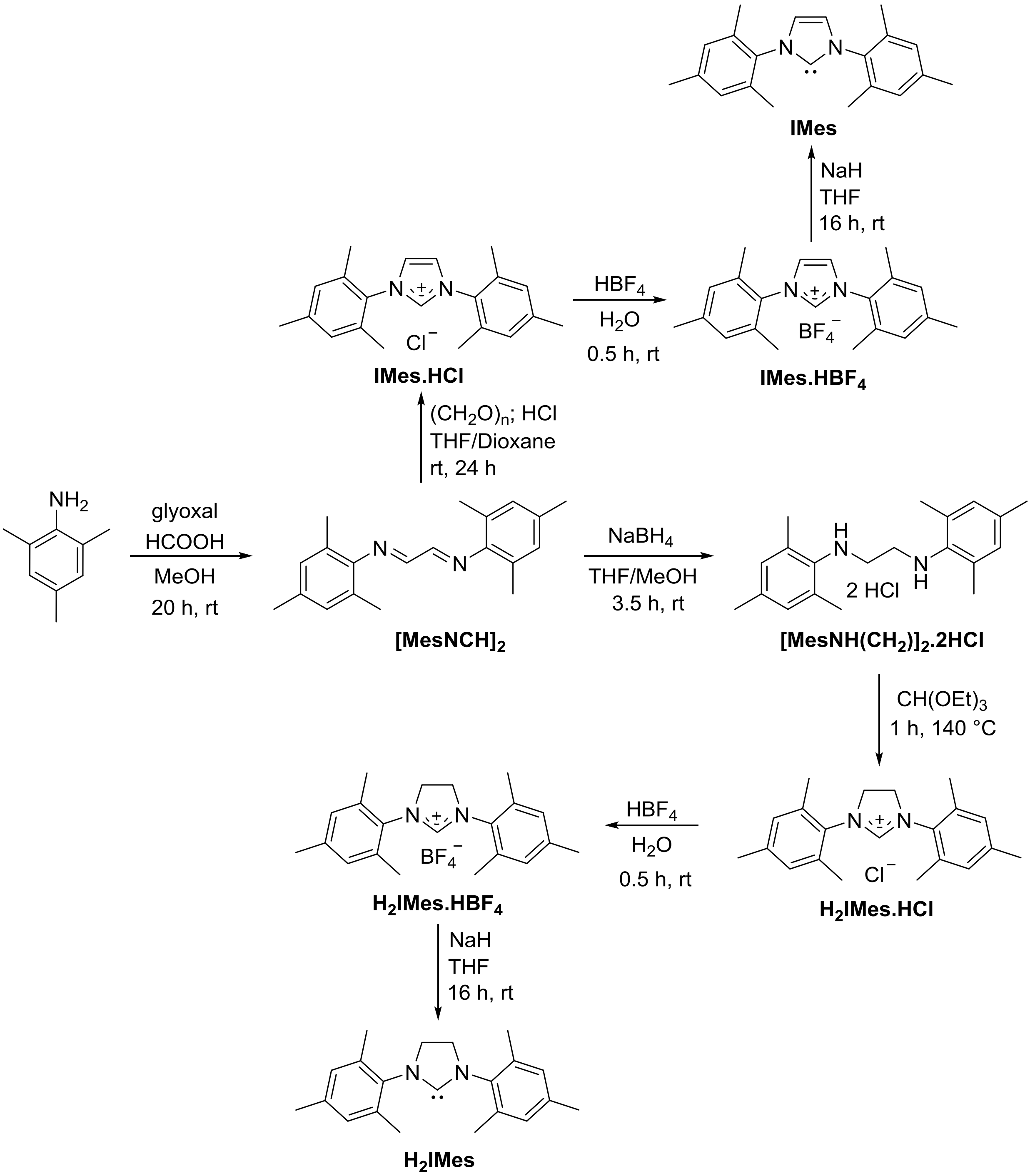
IMes
NaH
THF
16 h, rt
Cl⁻
IMes.HCl
HBF4
H2O
0.5 h, rt
BF4⁻
IMes.HBF4
(CH2O)n; HCl
THF/Dioxane
rt, 24 h
NH2
glyoxal
HCOOH
MeOH
20 h, rt
[MesNCH]2
NaBH4
THF/MeOH
3.5 h, rt
2 HCl
[MesNH(CH2)]2.2HCl
CH(OEt)3
1 h, 140 °C
HBF4
H2O
0.5 h, rt
BF4⁻
H2IMes.HBF4
Cl⁻
H2IMes.HCl
NaH
THF
16 h, rt
H2IMes

***N,N'*-Dimesitylethane-1,2-diimine ([MesNCH]$_2$)**

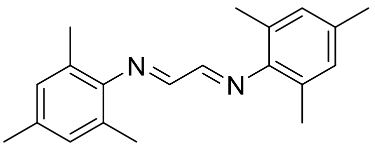

Reaction carried out under atmospheric conditions. This known compound was prepared using a slight modification of the procedure described by Arduengo.[168] 2,4,6-Trimethylaniline (21.32 g; 158 mmol) was dissolved in MeOH (80 mL) and 10 drops of formic acid were added. Then, under vigorous stirring, a glyoxal solution (9.40 g; 75 mmol; 40 wt% in H_2O) was slowly added. A yellow solid started to precipitate within a few minutes. The mixture was stirred for 20 h at rt, the yellow solid was filtered, washed with MeOH (3 x 50 mL) and dried under reduced pressure. The ^1H NMR spectroscopy data are consistent with the literature reported values.[168] Yield: 62% (13.66 g; 46.7 mmol). ^1H NMR (300 MHz, $CDCl_3$) δ 8.12 (s, 2H, 2 x NC$\underline{H}$), 6.93 (s, 4H, 4 x C$\underline{H}_{\text{(Mes)}}$), 2.31 (s, 6H, 2 x *p*-C${\underline{H_3}}_{\text{(Mes)}}$), 2.18 (s, 12H, 4 x *o*-C${\underline{H_3}}_{\text{(Mes)}}$).

***N,N'*-Dimesitylethane-1,2-diamine dihydrochloride ([MesNH(CH$_2$)]$_2$.2HCl)**

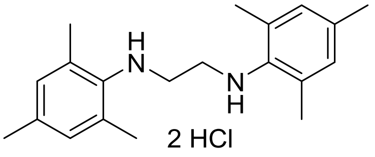

Reaction carried out under atmospheric conditions. The known compound was prepared using a slight modification of the literature procedure described by Nolan.[169] **[MesNCH]$_2$** (12.16 g; 41.6 mmol) was partially dissolved in THF/MeOH (120 mL; 10/2) and then $NaBH_4$ (6.08 g; 161 mmol) was added in 4 portions in 30 min intervals. The mixture was stirred at rt for 3.5 h when the solution turned white, which was then cooled to 0 °C and quenched with 0.1 mol.L^{-1} HCl until pH ~ 1.0. The white precipitate was collected, washed with deionized water and dried under reduced pressure. The ^1H NMR spectroscopic data are in good agreement with those reported in the literature.[169] Yield: 88% (13.55 g; 36.7 mmol). ^1H NMR (400 MHz, DMSO-*d*$_6$) δ 6.88 (s, 4H, 4 x C$\underline{H}_{\text{(Mes)}}$), 3.34 (d, J = 20.5 Hz, 4H, 2 x N$\underline{H_2}$), 3.32 (s, 4H, 2 x NC$\underline{H_2}$), 2.32 (s, 12H, 4 x *o*-C${\underline{H_3}}_{\text{(Mes)}}$), 2.19 (s, 6H, 2 x *p*-C${\underline{H_3}}_{\text{(Mes)}}$).

1,3-Dimesitylimidazolinium chloride (H$_2$IMes.HCl)

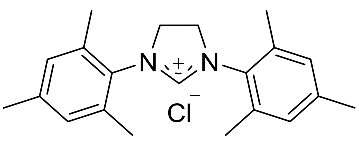

Reaction carried out under atmospheric conditions. The known compound **H$_2$IMes.HCl** was prepared using a slight modification of the literature procedure described by

Arduengo.[168] To a round bottom flask containing **[MesNH(CH$_2$)]$_2$.2HCl** (13.23 g; 35.8 mmol), triethylorthoformate (106.92 g; 721 mmol) and formic acid (10 drops) was connected a microdestillation setup and the system heated at 140 °C for 50 min. Then reduced pressure was applied to the system and the heating was continued for 10 min. After cooling to °C, the white solid was filtered, washed with cold Et$_2$O (4 x 50 mL) and dried under reduced pressure. The ^{1}H NMR spectroscopic data are consistent with those reported in the literature.[168] Yield: 98% (12.0 g; 35 mmol). ^{1}H NMR (400 MHz, CDCl$_3$) δ 9.43 (s, 1H, NC$\underline{H}$N), 6.92 (s, 4H, 4 x C$\underline{H}_{(Mes)}$), 4.55 (s, 4H, 2 x NC$\underline{H_2}$), 2.36 (s, 12H, 4 x *o*-C$\underline{H_3}_{(Mes)}$), 2.26 (s, 6H, 2 x *p*-C$\underline{H_3}_{(Mes)}$).

1,3-Dimesitylimidazolinium tetrafluoroborate (H$_2$IMes.HBF$_4$)

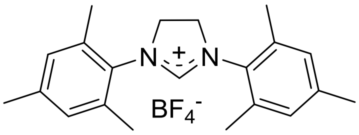

Reaction carried out under atmospheric conditions. **H$_2$IMes.HCl** (9.63 g; 28.09 mmol) was dissolved in deionized water (550 mL) and the solution filtered to remove small amounts of an insoluble material. 5 mL of HBF$_4$ (48 wt% in water) was slowly added under vigorous stirring. The white precipitate formed was stirred for an additional 20 min and then collected on a Büchner funnel, washed with hexanes (3 x 50 mL), Et$_2$O (1 x 50 mL) and then dried under reduced pressure to afford H$_2$IMes.HBF$_4$ as a white fluffy solid. Yield: 90% (9.92 g; 25.17 mmol). ^{1}H NMR (300 MHz, dmso-*d$_6$*) δ 8.98 (s, 1H, NC$\underline{H}$N), 7.09 (s, 4H, 4 x C$\underline{H}_{(Mes)}$), 4.44 (s, 4H, 2 x NC$\underline{H_2}$), 2.35 (s, 12H, 4 x *o*-C$\underline{H_3}_{(Mes)}$), 2.29 (s, 6H, 2 x *p*-C$\underline{H_3}_{(Mes)}$).

1,3-Bis(2,4,6-trimethylphenyl)-4,5-dihydroimidazol-2-ylidene (H$_2$IMes)

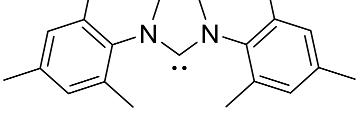

Reaction performed in a dry box under N$_2$ atmosphere using dry solvents. The synthesis of the known compound **H$_2$IMes** was performed according to the procedure described by Arduengo,[168] with a slight modification. To a suspension of **H$_2$IMes.HBF$_4$** (2.51 g; 6.34 mmol) in THF was added NaH (0.40 g; 16.63 mmol) and the mixture was stirred for 17 h. The flask was kept open in the first hour and then closed for the remaining time. After the allotted time, the suspension was filtered through a small pad of Celite® and the solvent stripped off. The pinkish solid was then dissolved in benzene (~ 7 mL), and filtered through a sintered funnel. The solvent was stripped off and the solid washed with hexanes (3 x 5 mL). After removal of the solvent, the target compound was obtained as a white solid. The filtrate was kept at -30 °C, resulting in an additional batch of the product as a crystalline colourless material. Combined yield: 47% (0.915 g; 2.98 mmol). The ^{1}H NMR spectroscopy data are in good agreement with the reported values.[168] ^{1}H NMR (300 MHz, C_6D_6) δ 6.84 (s, 4H, 4 x C$\underline{H}_{(Mes)}$), 3.27 (s, 4H, 2 x NC$\underline{H_2}$), 2.30 (s, 12H, 4 x *o*-C$\underline{H_3}_{(Mes)}$), 2.17 (s, 6H, 2 x *p*-C$\underline{H_3}_{(Mes)}$).

1,3-Dimesitylimidazolium chloride (IMes.HCl)

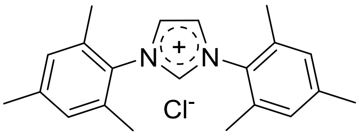

Reaction carried out under atmospheric conditions. To a suspension of **[MesNCH$_2$]$_2$** (4.64 g; 15.85 mmol) and paraformaldehyde (0.62 g; 20.72 mmol) in THF (100 mL) was added 4.3 mL of a 4.0 mol.L^{-1} HCl solution in dioxane over a period of 10 min and the mixture was stirred at rt for 24 h. The precipitate that was formed was collected in a Büchner funnel and the solid washed with THF until the washings were colourless. The remaining white solid was dried under reduced pressure. Yield: 36% (2.54 g; 7.45 mmol). ^{1}H NMR (300 MHz, $CDCl_3$) δ 10.79 (t, *J* = 1.5 Hz, 1H, HC$\underline{H}$N), 7.66 (d, *J* = 1.5 Hz, 2H, 2 x NC$\underline{H}$), 6.99 (s, 4H, 4 x C$\underline{H}_{(Mes)}$), 2.31 (s, 6H, 2 x *p*-C$\underline{H_3}_{(Mes)}$), 2.14 (s, 12H, 4 x *o*-C$\underline{H_3}_{(Mes)}$).

1,3-Dimesitylimidazolium tetrafluoroborate (IMes.HBF$_4$)

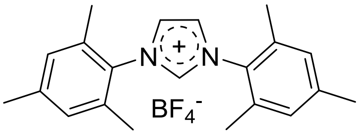

Reaction carried out under under atmospheric conditions. **IMes.HCl** (2.0 g; 5.87 mmol) was dissolved in deionized water (60 mL) and the HBF$_4$ solution (1.1 mL; 48 wt% in water) was slowly added under vigorous stirring. The white precipitate formed was collected on a Büchner funnel, washed with deionized water (40 mL), dissolved in DCM (10 mL) and dried over anhydrous MgSO$_4$. After stripping off the solvent, the target compound was obtained as a white solid. Yield: 90% (2.07 g; 5.28 mmol). ^{1}H NMR (300 MHz, $CDCl_3$) δ 8.85 (t, *J* = 1.6 Hz, 1H, NC$\underline{H}$N), 7.56 (d, *J* = 1.6 Hz, 2H, 2 x NC$\underline{H}$), 7.02 (s, 4H, 4 x C$\underline{H}_{(Mes)}$), 2.34 (s, 6H, 2 x *p*-C$\underline{H_3}_{(Mes)}$), 2.10 (s, 12H, 4 x *o*-C$\underline{H_3}_{(Mes)}$).

1,3-Bis(2,4,6-trimethylphenyl)imidazol-2-ylidene (IMes)

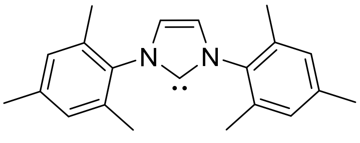

Reaction performed in a dry box under N_2 atmosphere using dry solvents. The procedure was identical to that described for the synthesis of **H_2IMes**. **IMes.HBF$_4$** (1.0 g; 2.55 mmol), NaH (0.08 g; 3.1 mmol). Yield: 40% (0.31 g; 1.02 mmol). ^{1}H NMR (300 MHz, C_6D_6) δ 6.81 (s, 4H, 4 x C$\underline{H}_{(Mes)}$), 6.50 (s, 2H, 2 x NC$\underline{H}$), 2.16 (s, 18H, 2 x *p*-C$\underline{H}_{3(Mes)}$ + 4 x *o*-C$\underline{H}_{3(Mes)}$).

2-Isopropoxystyrene synthesis

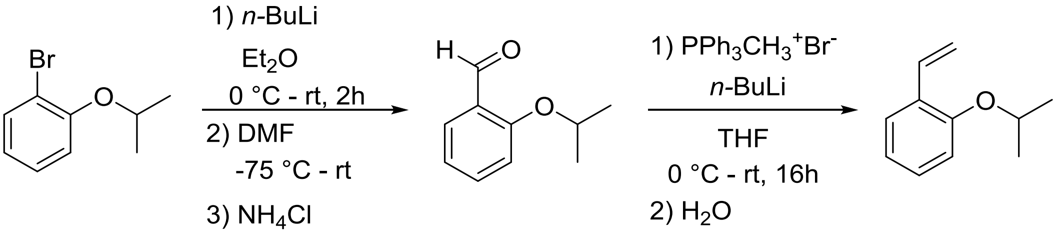

2-Isopropoxybenzaldehyde

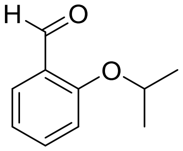

Experiment carried under a nitrogen atmosphere using dry solvents. Synthesis of the known compound 2-*iso*propoxybenzaldehyde was performed according to procedure described by Marciniec,[170] with slight modification. A three-neck round-bottom flask containing Et_2O (130 mL) was cooled to 0 °C and *n*BuLi 2.5 mol.L^{-1} (11 mL, in hexanes) was added. Then 2-*iso*propoxybromobenzene (5.86 g; 27.2 mmol) was added and the mixture kept stirring for 30 min at 0 °C and then at room temperature for 1.5 h. A white solid precipitated. The system was then cooled to -78 °C (dry ice/acetone bath) and anhydrous DMF (2.2 mL; 28.4 mmol, dissolved in 20 mL of dry Et_2O) was added drop-by-drop over a period of 30 min. The system was then allowed to warm to room temperature before quenching. *From this point forward, manipulations were performed under atmospheric conditions, using untreated solvents*. Saturated NH_4Cl solution (60 mL) was added to the reaction mixture resulting in the formation of two phases. The aqueous phase was extracted with Et_2O (3 x 60 mL), the organic phases combined, washed with brine (1 x 60 mL), dried over anhydrous $MgSO_4$ and the solvent stripped off. The yellow liquid obtained was used without further purification. ^{1}H NMR (300 MHz, $CDCl_3$) δ 10.50 (s, 1H, C$\underline{H}$O), 7.83 (dd, *J* = 7.8, 1.8 Hz, 1H, C$\underline{H}_{(Ph)}$), 7.61-7.46 (m, 1H, C$\underline{H}_{(Ph)}$), 7.06-6.93

(m, 2H, 2 x C*H*$_{(Ph)}$), 4.69 (sept, *J* = 6.1 Hz, 1H, C*H*(CH$_3$)$_2$), 1.41 (d, *J* = 6.1 Hz, 6H, CH(C*H*$_3$)$_2$).

2-*iso*propoxystyrene

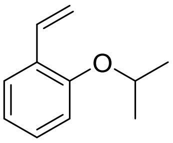

Experiment performed under a nitrogen atmosphere using dry solvents. The synthesis of the known compound 2-isopropoxystyrene was performed according to the procedure described by Marciniec,[170] with a slight modification. Methyltriphenylphosphonium bromide (13.78 g; 38.57 mmol) was transferred to a three-neck round-bottom flask and dried under reduced pressure for 20 h. The phosphonium salt was then suspended in THF (200 mL), cooled to 0 °C, and 2.5 mol.L^{-1} *n*-BuLi (15.4 mL; 38.5 mmol) added. The mixture was stirred for 1.5 h. 2-Isopropoxybenzaldehyde was added and the mixture stirred at rt for 16 h. *From this point forward, manipulations were performed under atmospheric conditions, using untreated solvents*. Deionized water (80 mL) was added to quench the reaction and the solvents were stripped off. The residue obtained was extracted with Et_2O (4 x 80 mL) and the combined organic phases were dried over anhydrous $MgSO_4$. Solvent removal afforded a yellow oil that was purified by column chromatography (SiO_2; hexanes/Et_2O = 95/5, R_f = 0.79). A light yellow liquid was obtained. Yield: 74% (2.93 g; 18.05 mmol). ^{1}H NMR (300 MHz, $CDCl_3$) δ 7.50 (dd, *J* = 7.6, 1.7 Hz, 1H, C*H*$_{(Ph)}$), 7.25-7.17 (m, 1H, C*H*$_{(Ph)}$), 7.08 (dd, *J* = 17.8, 11.2 Hz, 1H, C*H*=CH$_2$), 6.98-6.85 (m, 2H, 2 x C*H*$_{(Ph)}$), 5.75 (dd, *J* = 17.8, 1.6 Hz, 1H, CH=C*H*$_{2(trans)}$), 5.25 (dd, *J* = 11.2, 1.6 Hz, 1H, CH=C*H*$_{2(cis)}$), 4.56 (sept, *J* = 6.1 Hz, 1H, C*H*(CH$_3$)$_2$), 1.37 (d, *J* = 6.1 Hz, 6H, CH(C*H*$_3$)$_2$).

General procedure for the attempted reaction of *trans*-$RuCl_2(py)_4$ with 1,1-diphenylpropargyl alcohol

Inside a dry box a suspension of *trans*-$RuCl_2(py)_4$ (~ 20 mg), 1,1-diphenylpropargyl alcohol (~ 10 mg) and the solvent (typically 5 mL) were transferred to a 2-neck round-bottom flask. Outside the dry box the flask was fitted to a condenser and the suspension stirred under N_2 atmosphere for the appropriate time under reflux or 55 °C (solvent = $CDCl_3$). After stripping off the solvent, the remaining solids were analyzed by ^{1}H NMR spectroscopy. Only starting materials were observed in all cases.

$RuCl_2$(*p*-cymene)IMes

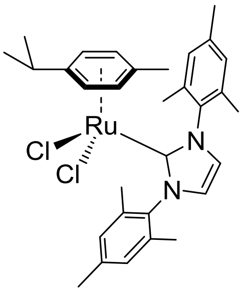

Reaction performed inside a dry box under N_2 atmosphere using dry solvents. To a vigorously stirred suspension of $[RuCl_2(p\text{-cymene})]_2$ (0.25 g; 0.404 mmol) in benzene (20 mL) was added a solution of IMes (0.26 g; 0.848 mmol) in benzene (10 mL) over a period of 15 min. Then the dropping funnel was rinsed with 5 mL of benzene and the brown solution was stirred for an additional 5 min. After stripping off the solvent, a brown solid was obtained, which was used without further purification. ^{1}H NMR (300 MHz, $CDCl_3$) δ 6.96 (s, 4H, 4 x C*H*$_{(Mes)}$), 6.91 (s, 2H, 2 x NC*H*), 5.04 (d, *J* = 6.1 Hz, 2H, 2 x C*H*$_{(p\text{-cymene})}$), 4.64 (d, *J* = 6.1 Hz, 2H, 2 x C*H*$_{(p\text{-cymene})}$), 2.60-2.48 (m, 1H, C*H*$(CH_3)_2$), 2.36 (s, 6H, 2 x *p*-C*H*$_{3(Mes)}$), 2.25 (s, 12H, 4 x *o*-C*H*$_{3(Mes)}$), 1.80 (s, 3H, C*H*$_{3(p\text{-cymene})}$), 1.09 (d, *J* = 6.9 Hz, 6H, CH(C*H*$_3$)$_2$).

$RuCl_2$(*p*-cymene)H_2Imes

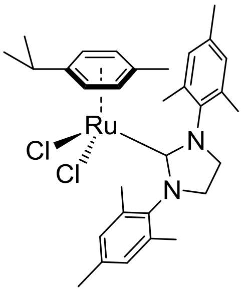

Reaction performed inside a dry box under N_2 atmosphere using dry solvents. To a vigorously stirred suspension of $[RuCl_2(p\text{-cymene})]_2$ (0.25 g; 0.40 mmol) in benzene (20 mL) was added a solution of H_2IMes (0.26 g; 0.86 mmol) in benzene (30 mL) over a period of 30 min. Then the dropping funnel was rinsed with 10 mL of benzene and the brown solution stirred for additional 5 min. After stripping off the solvent, a brown solid was obtained, which was used without further purification. ^{1}H NMR (300 MHz, C_6D_6) δ 6.77 (s, 4H, 4 x C*H*$_{(Mes)}$), 4.87 (d, *J* = 6.0 Hz, 2H, 2 x C*H*$_{(p\text{-cymene})}$), 4.40 (d, *J* = 6.0 Hz, 2H, 2 x C*H*$_{(p\text{-cymene})}$), 3.22 (s, 4H, 2 x NC*H*$_2$), 2.48 (s, 13H, 4 x *o*-C*H*$_{3(Mes)}$ + C*H*$(CH_3)_2$), 2.13 (s, 6H, 2 x *p*-C*H*$_{3(Mes)}$), 1.72 (s, 3H, C*H*$_{3(p\text{-cymene})}$), 1.06 (d, *J* = 6.9 Hz, 6H, CH(C*H*$_3$)$_2$).

General procedure for the decomposition studies of $RuCl_2$(*p*-cymene)(NHC)

Inside the dry box a J Young NMR tube was loaded with $RuCl_2$(*p*-cymene(NHC) (~ 20 mg) and ~ 0.5 mL of the deuterated solvent, and ^{1}H NMR spectra were acquired at predetermined time intervals.

General procedure for the reaction of $RuCl_2$(*p*-cymene)(NHC) with 1,1-diphenylpropargyl alcohol

Inside a dry box a J Young NMR tube was loaded with $RuCl_2$(*p*-cymene)(NHC) (~27 mg), 1,1-diphenylpropargyl alcohol (~ 10 mg) and 0.5 mL of CD_3OD to form a dark brown solution. ^1H NMR spectra were acquired at predetermined time intervals. Formation of the allenylidene complex could be observed by comparing the ^1H NMR spectroscopic data with those reported in the literature for the complex [$RuCl_2$(=C=C=CPh_2)(*p*-cymene)(IMes)]OTf.[155]

NMR scale reaction of *cis*-$RuCl_2(DMSO)_4$ with 1,1-diphenylpropargyl alcohol

Inside a dry box a J Young NMR tube was loaded with *cis*-$RuCl_2(DMSO)_4$ (14 mg; 0.029 mmol), 1,1-diphenylpropargyl alcohol (6.5 mg; 0.032 mmol) and 0.5 mL of $CDCl_3$. The tube was shaken manually for 30 seconds and then ^1H NMR spectra were acquired at predetermined time intervals.

General procedure for the reactions of *cis*-$RuCl_2(DMSO)_4$ with 1,1-diphenylpropargyl alcohol

Reactions performed under argon using Schlenk techniques. *cis*-$RuCl_2(DMSO)_4$ (0.039 g; 0.008 mmol) and 1,1-diphenylpropargyl alcohol (0.052 g; 0.025 mmol) were transferred to a Schlenk tube and 5 times evacuated/backfilled with argon. Dry THF (5 mL) was added and the suspension sonicated for 5 min before the addition of 80 µL of a 0.24 mol.L^{-1} HCl solution in THF (prepared by the addition of 0.2 mL of conc. HCl to a suspension of 2.0 g of $CaCl_2$ in 10 mL of dry THF). The Schlenk tube was connected to a condenser and heated to reflux under an argon flow for 18 h. The solvent was stripped off and the remaining sticky orange-brown solid was analyzed by ^1H, ^{13}C, ^1H-^{13}C HMQC and ^1H-^{13}C HMBC spectroscopy. The reactions performed without addition of HCl were prepared similarly.

Appendix I Summary of different classes of alkylidenes

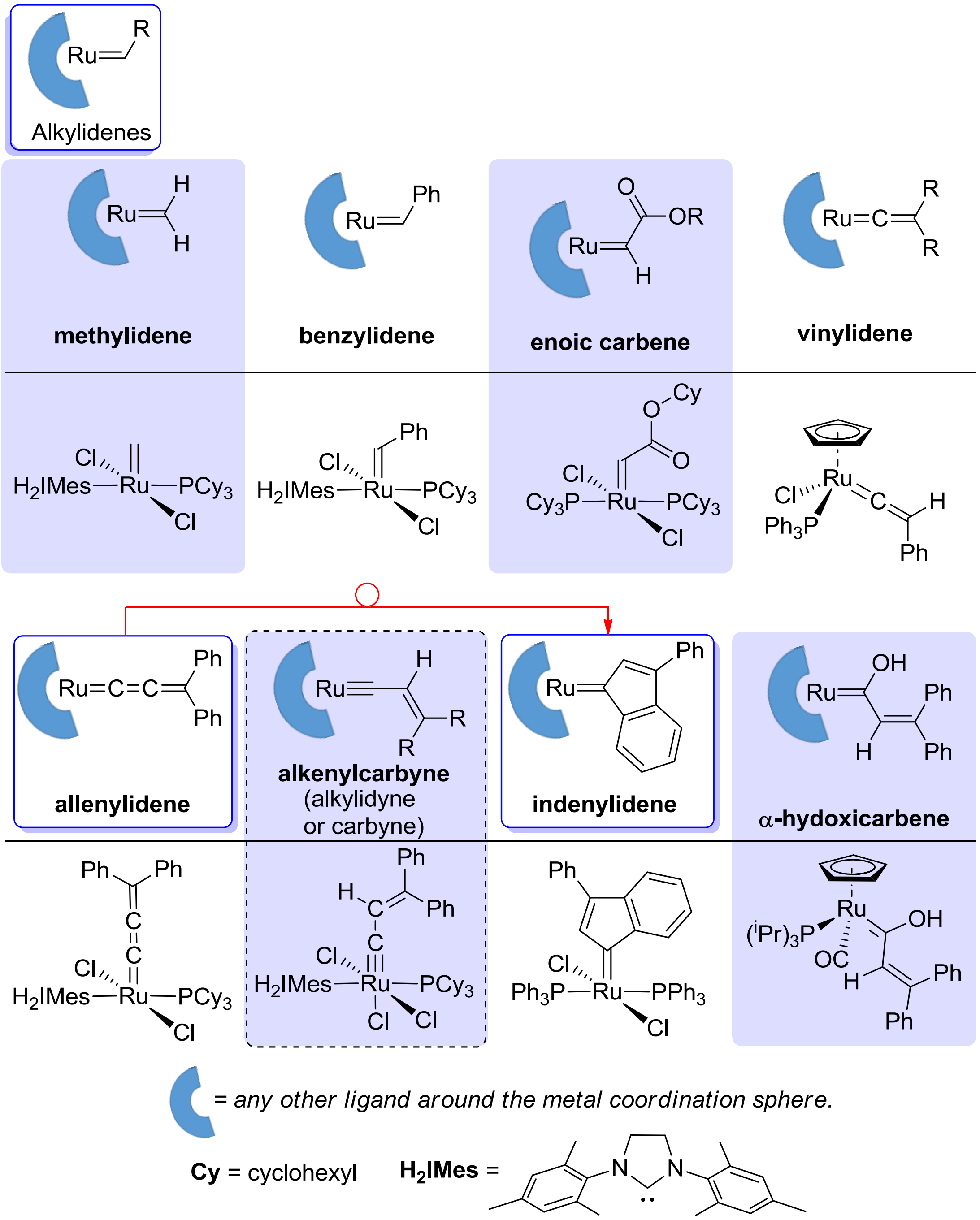
Ru
R
Alkylidenes
methylidene
benzylidene
enoic carbene
vinylidene
Cl
H_2IMes
PCy_3
Cy_3P
Ph_3P
allenylidene
alkenylcarbyne
(alkylidyne
or carbyne)
indenylidene
α-hydoxicarbene
PPh_3
$(^iPr)_3P$
OC
OH
Ph
= any other ligand around the metal coordination sphere.
Cy = cyclohexyl
$\mathbf{H_2IMes}$ =

Appendix II Characteristic chemical shifts (^{13}C, ^{1}H and ^{31}P NMR) of selected 1,1-diphenylpropargyl alcohol derived ruthenium complexes.

Complex	L_1	L_2	C_α	C_β	C_γ	H_β	^{31}P	Comments	Ref.
			(ppm)						
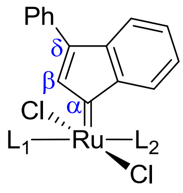	PPh_3	PPh_3	301.0	139.4	145.4	6.38	28.7		171
	PCy_3	PCy_3	293.9	139.1	139.8	7.39	32.6		
	H_2IMes	PPh_3	300.9	139.1	141.2	7.10	27.3		134
	H_2IMes	PCy_3	292.2	137.8	138.0	7.84	27.0		
	H_2IMes	py	300.4	139.3	139.2	7.22	---		
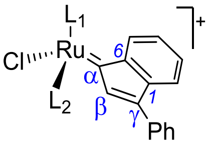	*p*-cymene	PCy_3	334.1	143.1	154.6	6.88	48.3		155
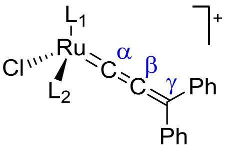	*p*-cymene	PCy_3	282.0	187.6	166.2		59.2		159
	p-cymene	IMes	284.1	188.7	160.5	---	---		
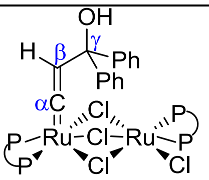	---	---	308.7	243.4	150.4	4.38	51.5 50.1 44.7 40.9	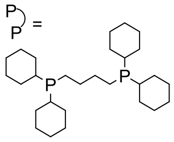	172
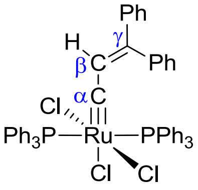	---	---	δ not provided			5.67	13.6	---	49
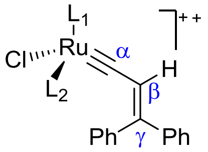	*p*-cymene	PCy_3	328.1	130.5	193.2	7.05	78.6	C_β (HMQC) and C_γ (HMBC) correlate with H_β	155
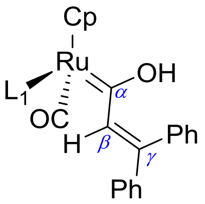	P^iPr_3	---	298.7	140.0	145.3	7.09	66.5	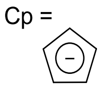	173
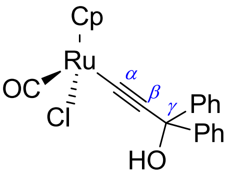	---	---	95.3	112.1	75.8	---	---	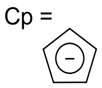	174

Appendix II Continuation.

Complex	L_1	L_2	C_α (ppm)	C_β (ppm)	C_γ (ppm)	H_β (ppm)	^{31}P (ppm)	Comments	Ref.
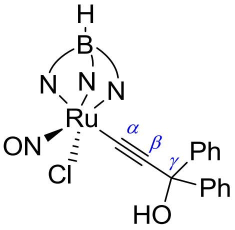	---	---	94.8	112.1	74.9	---	---	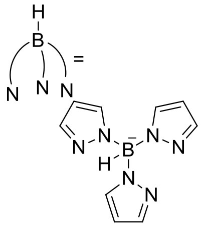	175

Appendix III Selected Chromatograms

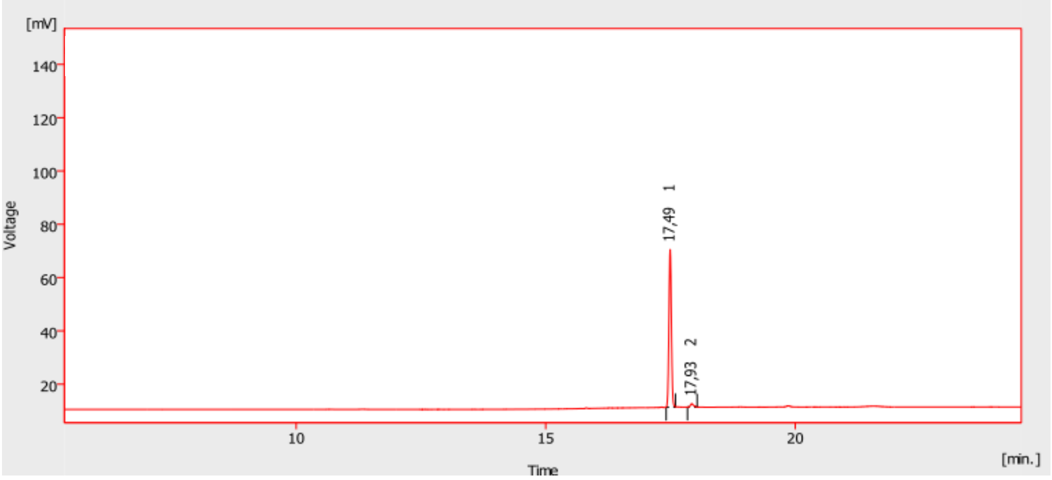

Figure 46 Chromatogram of methyl oleate.

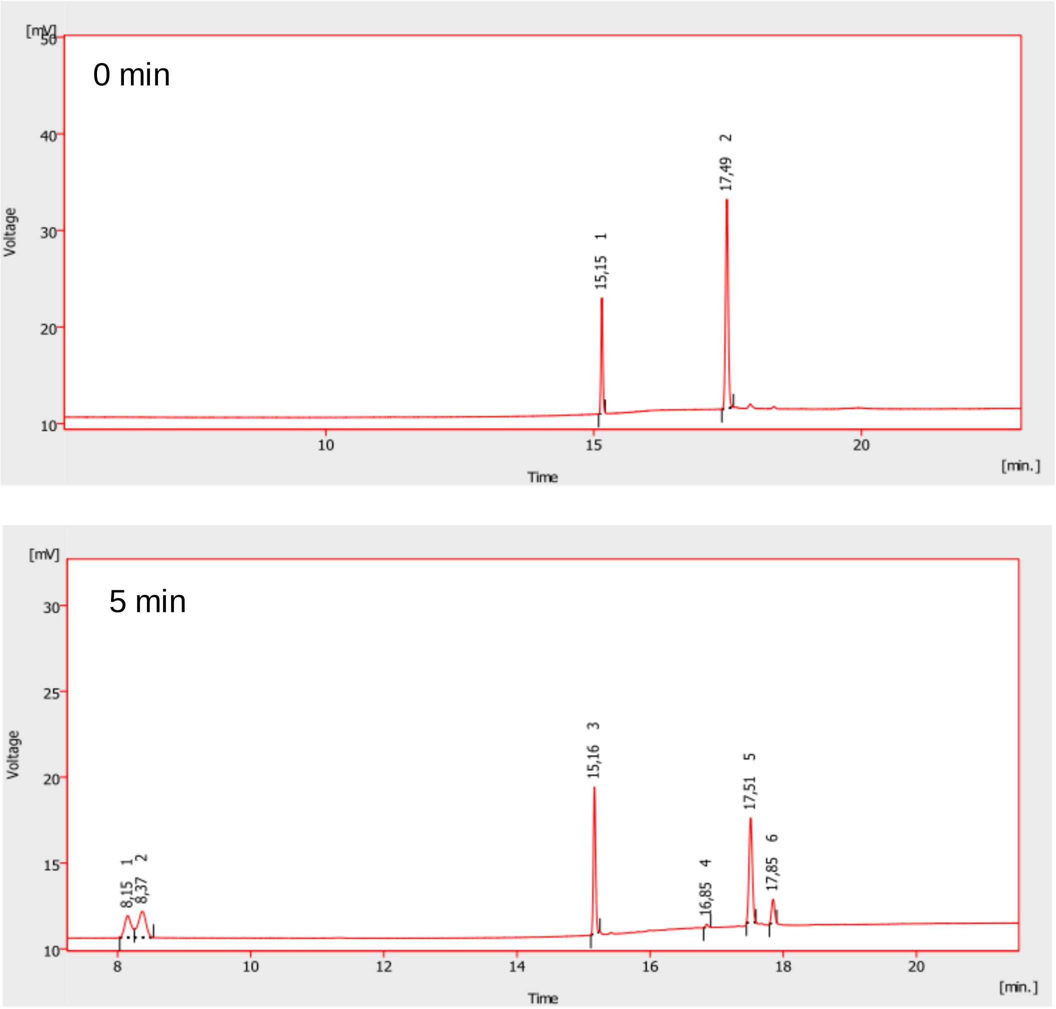

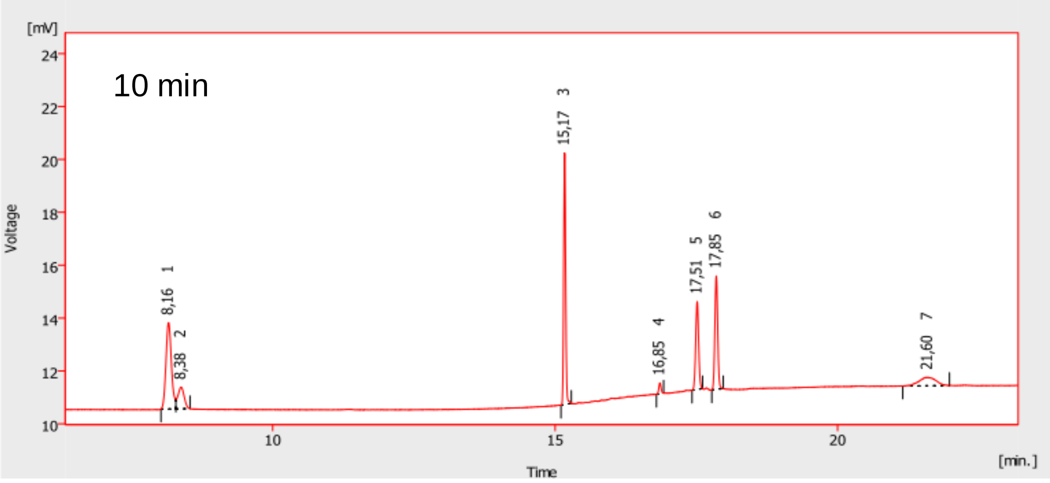
10 min
[mV]
24
22
20
18
16
14
12
10
Voltage
8,16 1
8,38 2
15,17 3
16,85 4
17,51 5
17,85 6
21,60 7
10
15
20
Time
[min.]

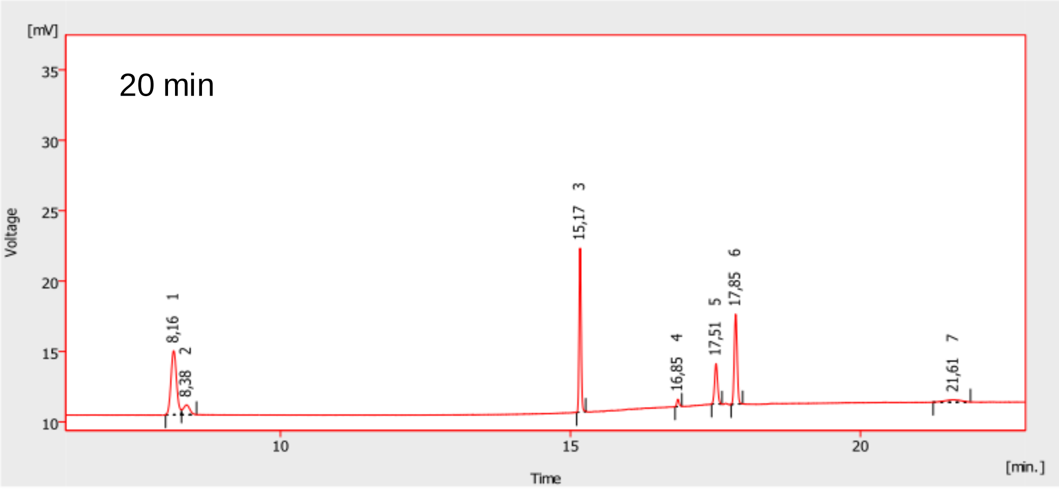
20 min
[mV]
35
30
25
20
15
10
Voltage
8,16 1
8,38 2
15,17 3
16,85 4
17,51 5
17,85 6
21,61 7
10
15
20
Time
[min.]

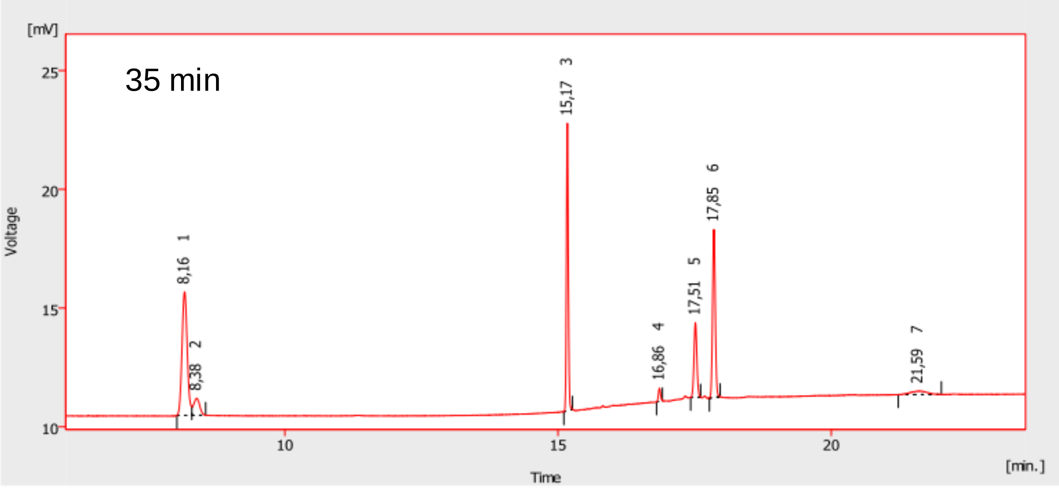
35 min
[mV]
25
20
15
10
Voltage
8,16 1
8,38 2
15,17 3
16,86 4
17,51 5
17,85 6
21,59 7
10
15
20
Time
[min.]

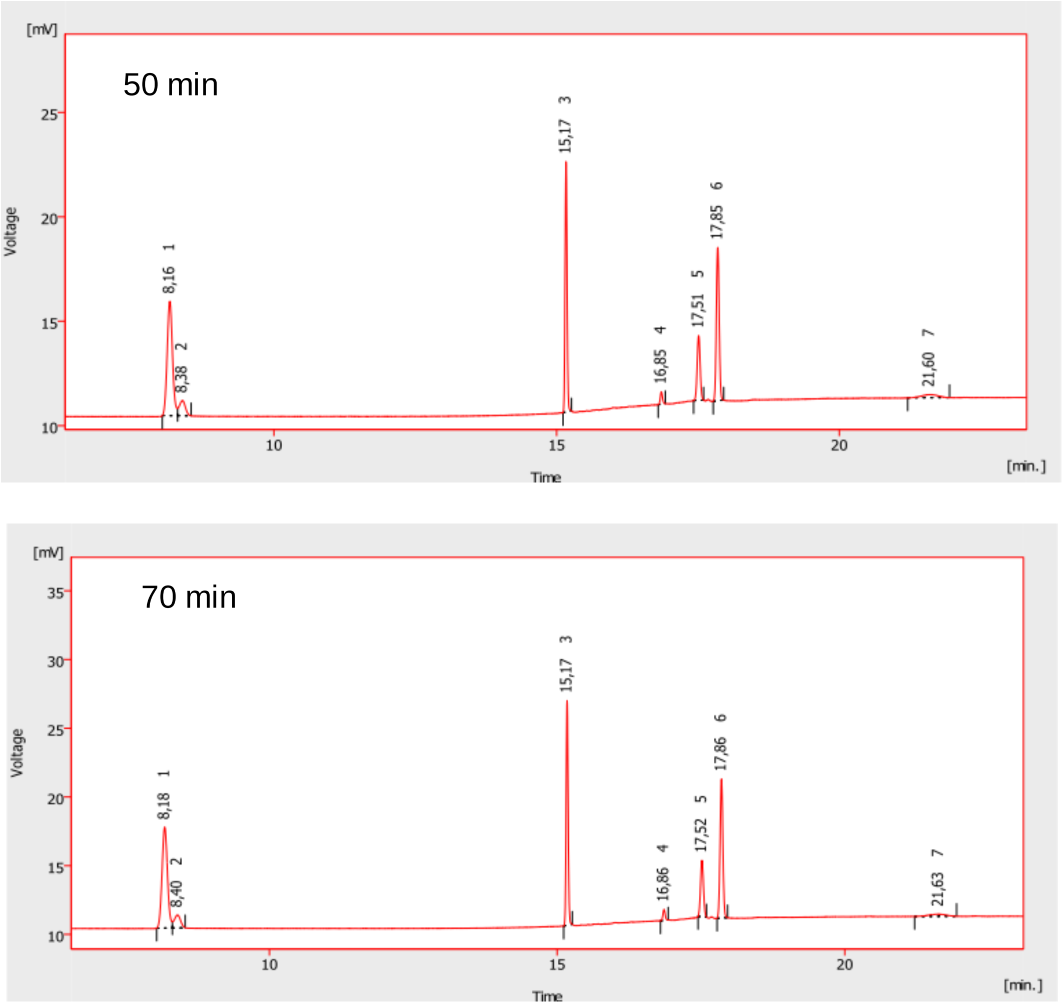

Figure 47 Typical chromatograms obtained in the cross-metathesis of **MO** with **MA-H** (after derivatization). From top to bottom: after 0, 5, 10, 20, 35, 50 and 70 min, respectively. Methyl 2-undecenoate (8.18 min); 9-octadecene (8.40 min); internal standard (1,3,5-trimethoxybenzene; 15.17 min); unknown compound (16.86 min); methyl oleate (17.52 min); dimethyl 2-undecenedioate (17.86 min); dimethyl 9-octadecenedioate (21.63 min).

Conditions: **MO**: 0.5236 g (1.7660 mmol); **MA-H**: 0.2086 g (1.7972 mmol); 1,3,5-trimethoxybenzene: 0.3056 g (1.817 mmol); **GII**: 3 mL of a 0.5889 mol.L^{-1} THF solution (0.00176 mmol); THF: 7 mL in total; reaction time: 70 min; temperature: 50 °C.

GC method: Column: DN-WAX (polyethyleneglycol, diameter: 0.32 mm; length: 30.0 m; film thickness: 0.25 µm); injector temperature: 230 °C; carrier gas: N_2 (3.6 mL/min); detector temperature: 230 °C; split flow: 180 mL/min; split rate: 1:50; oven temperature:

	Temp. (°C)	**Time (min)**	**Rate (°C/min)**
1	120.0	1.00	1.0
2	130.0	1.00	20.0
3	210.0	9.00	0.00

Appendix IV Formulae used to calculate the yield of CM products in reactions with vegetable oils

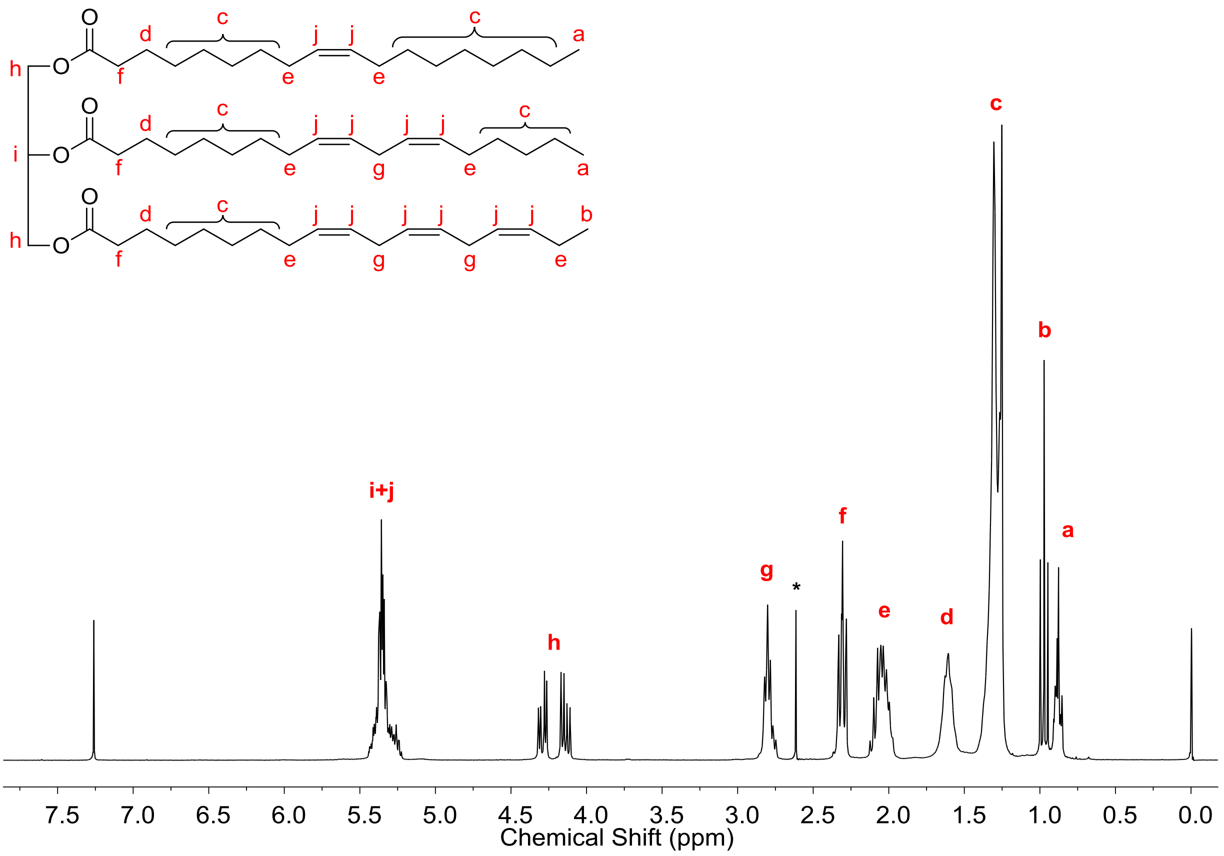

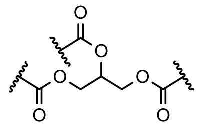

$$\mathbf{MW:}\ \overset{-CH_3}{15.03((\Sigma_{a,b})/3Ap)} + \overset{-CH_2-}{14.03((\Sigma_{c\text{-}g})/2Ap)} + \overset{-CH=CH-}{26.02((i+j - Ap)/2Ap)} \quad + \quad 173.1$$

Ap: h/4

Number of C=C: (i+j)/(2*Ap)

Figure 48 Typical ^{1}H NMR spectrum of a vegetable oil with the signal attributions and the formulae used to calculate the molecular weight and number of C=C double bonds per triglyceride. * Residual water.

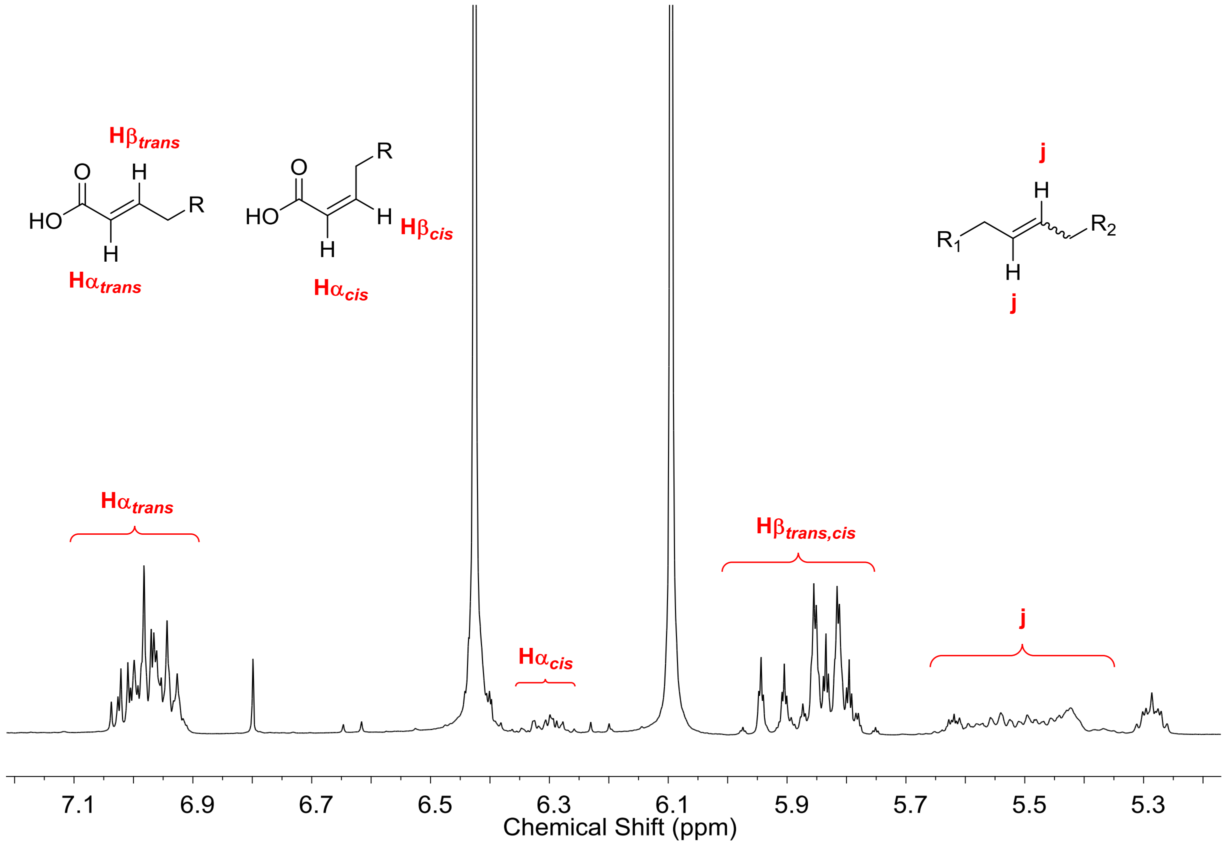

Yield CM: $(H\alpha_{trans}+H\alpha_{cis}+H\beta_{trans,cis})/(H\alpha_{trans}+H\alpha_{cis}+H\beta_{trans,cis} + j)$

Figure 49 Inset of the olefinic region of a typical ^{1}H NMR spectrum of the CM of vegetable oils with **MA-H** with the signal attributions and the formula used to calculate the yield of cross-metathesis products.

Appendix V Spectra

MA-^{i}Pent

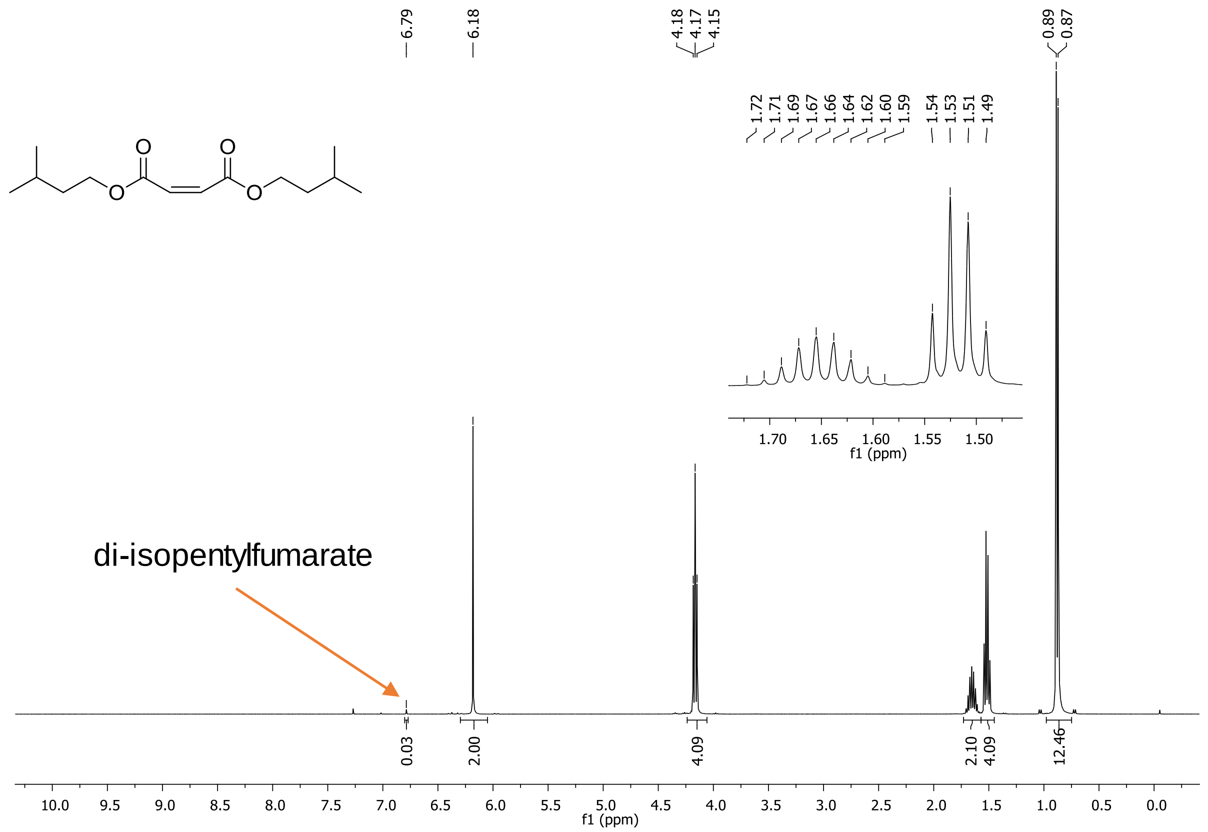

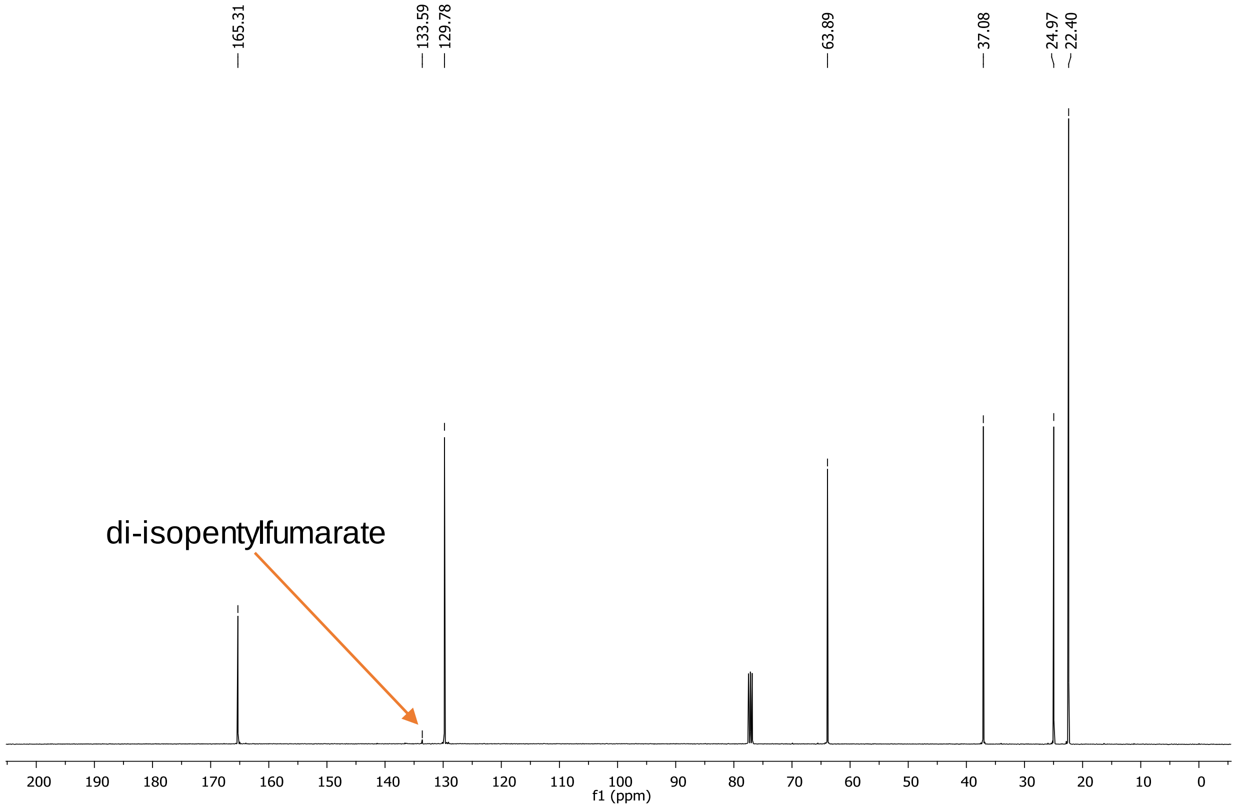

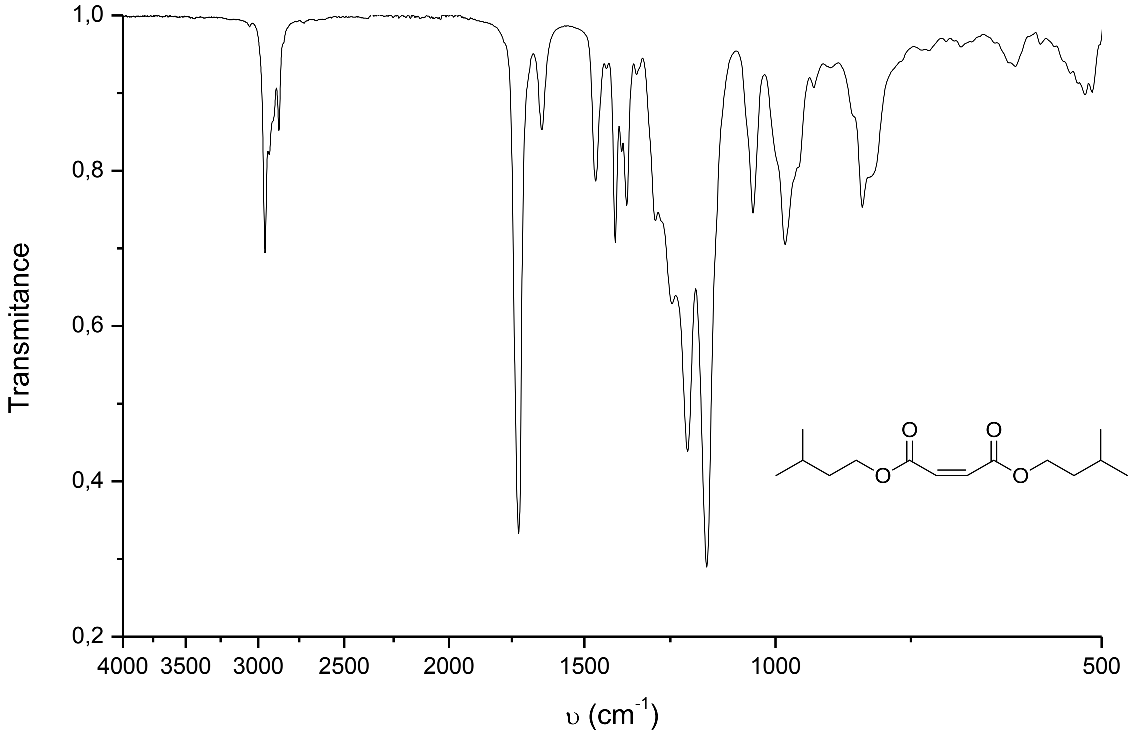
1,0
0,8
0,6
0,4
0,2
Transmitance
4000
3500
3000
2500
2000
1500
1000
500
υ (cm^{-1})
O
O
O
O

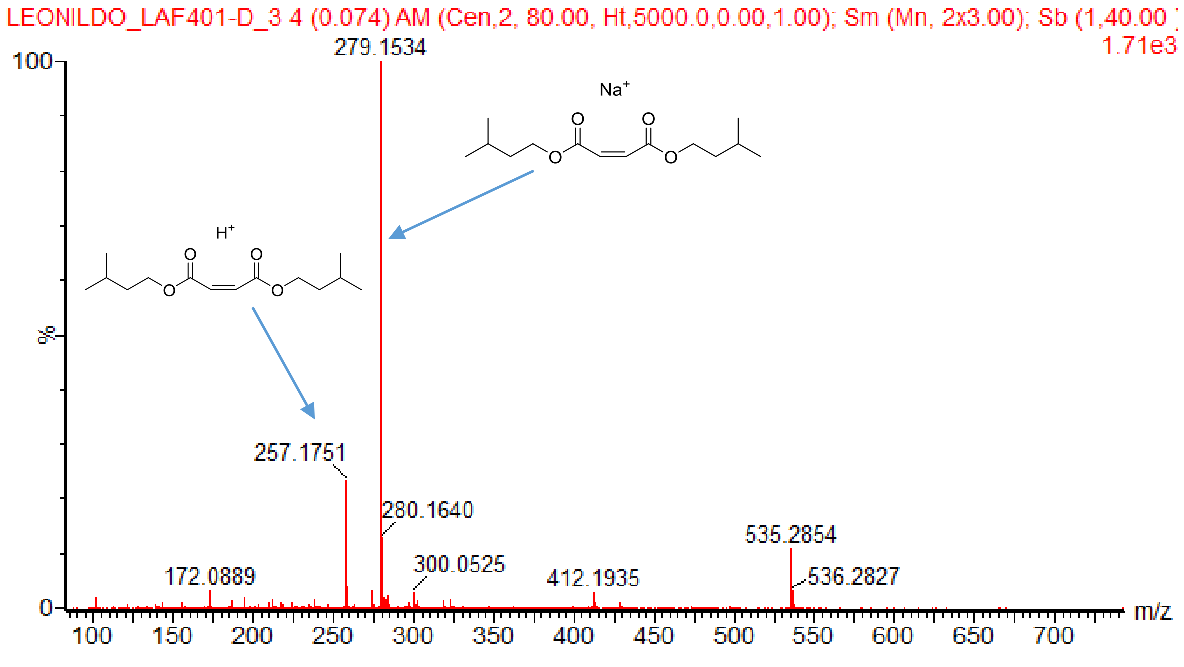
LEONILDO_LAF401-D_3 4 (0.074) AM (Cen,2, 80.00, Ht,5000.0,0.00,1.00); Sm (Mn, 2x3.00); Sb (1,40.00)
1.71e3
100
%
0
279.1534
Na$^+$
H$^+$
257.1751
280.1640
172.0889
300.0525
412.1935
535.2854
536.2827
100
150
200
250
300
350
400
450
500
550
600
650
700
m/z

Methyl (*E*)-undec-2-enoate

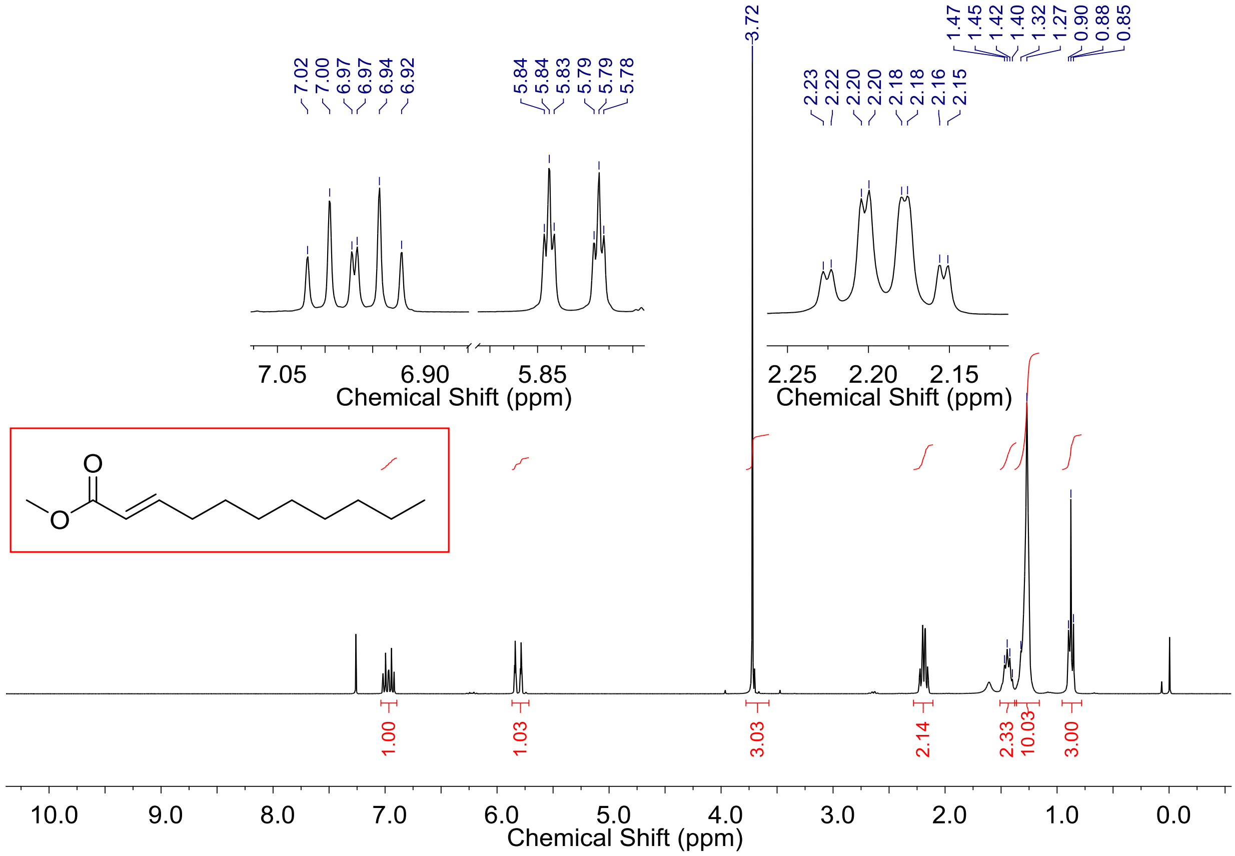

^{1}H NMR (300 MHz, CDCl$_3$) δ 6.97 (dt, *J* = 15.6, 7.0 Hz, 1H), 5.81 (dt, *J* = 15.6, 1.5 Hz, 1H), 3.72 (s, 3H), 2.19 (qd, *J* = 7.0, 1.5 Hz, 2H), 1.51 – 1.36 (m, 2H), 1.38 – 1.16 (m, 10H), 0.88 (t, *J* = 6.7 Hz, 3H).

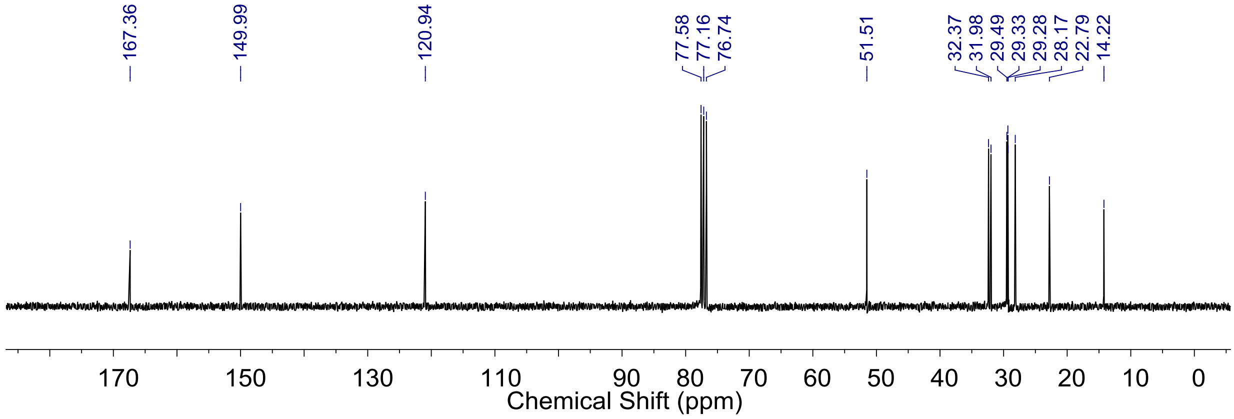

^{13}C NMR (75 MHz, CDCl$_3$) δ 167.36, 149.99, 120.94, 51.51, 32.37, 31.98, 29.49, 29.33, 29.28, 28.17, 22.79, 14.22.

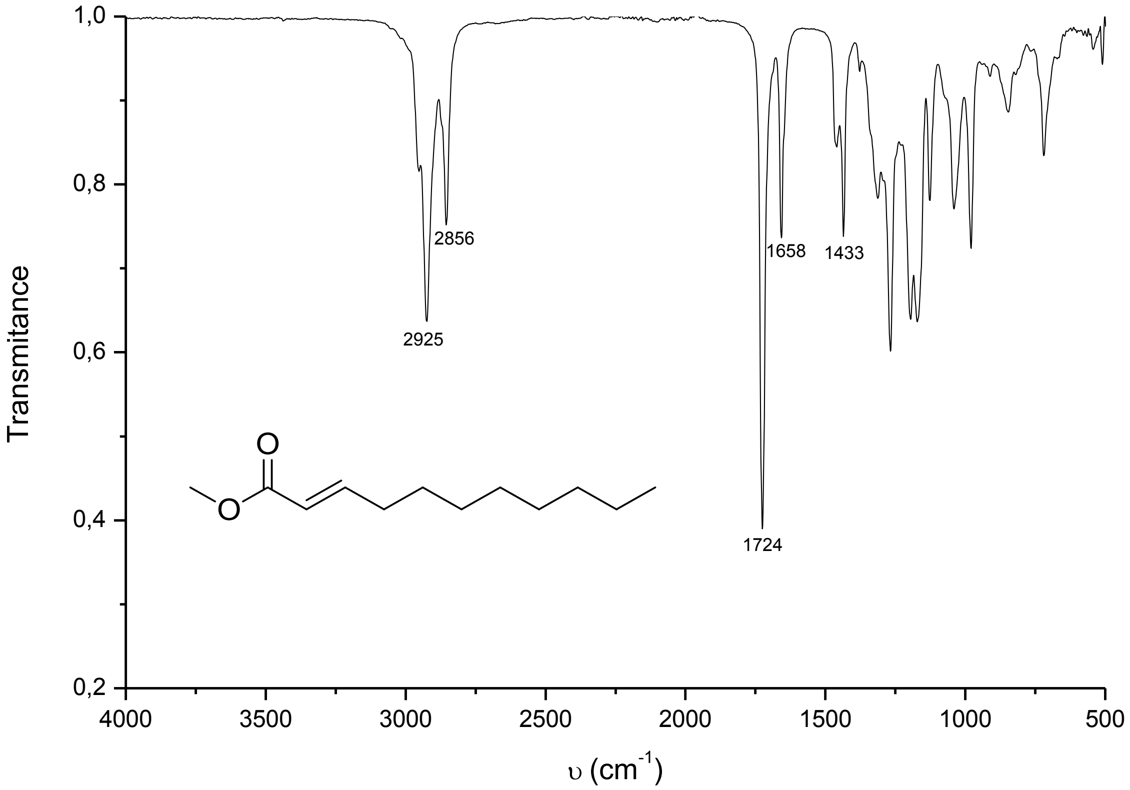
1,0
0,8
0,6
0,4
0,2
Transmitance
4000
3500
3000
2500
2000
1500
1000
500
υ (cm-1)
2925
2856
1724
1658
1433
O
O

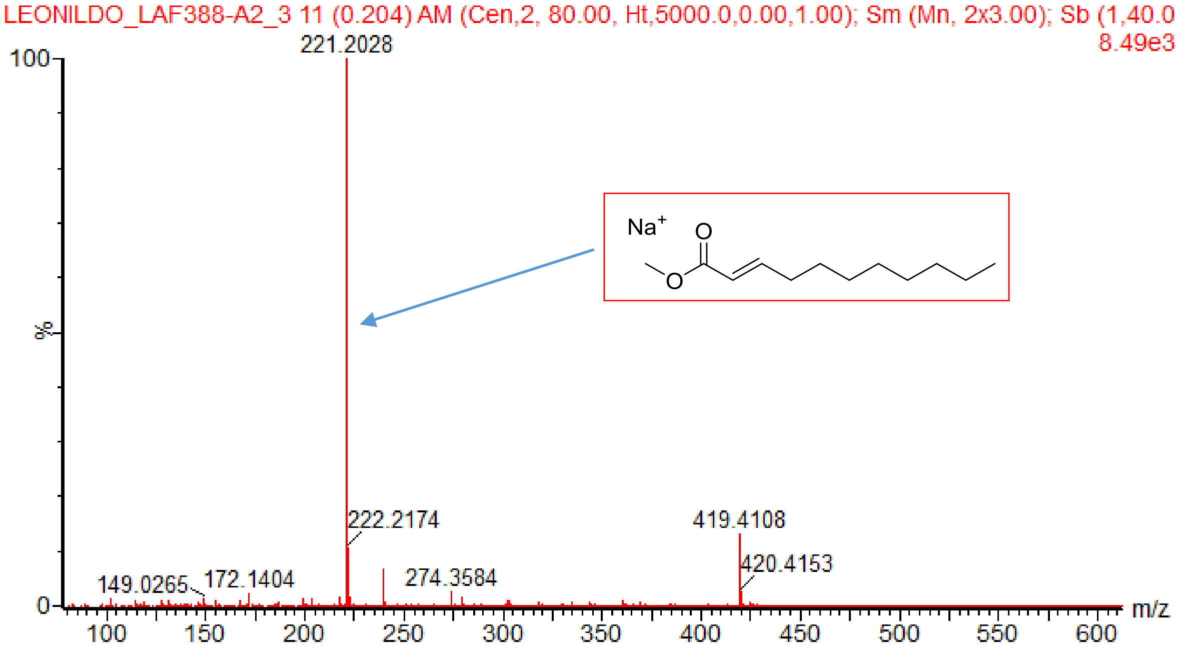
LEONILDO_LAF388-A2_3 11 (0.204) AM (Cen,2, 80.00, Ht,5000.0,0.00,1.00); Sm (Mn, 2x3.00); Sb (1,40.0
8.49e3
100
%
0
221.2028
222.2174
149.0265
172.1404
274.3584
419.4108
420.4153
Na+
O
O
m/z
100
150
200
250
300
350
400
450
500
550
600

Dimethyl (*E*)-undec-2-enedioate

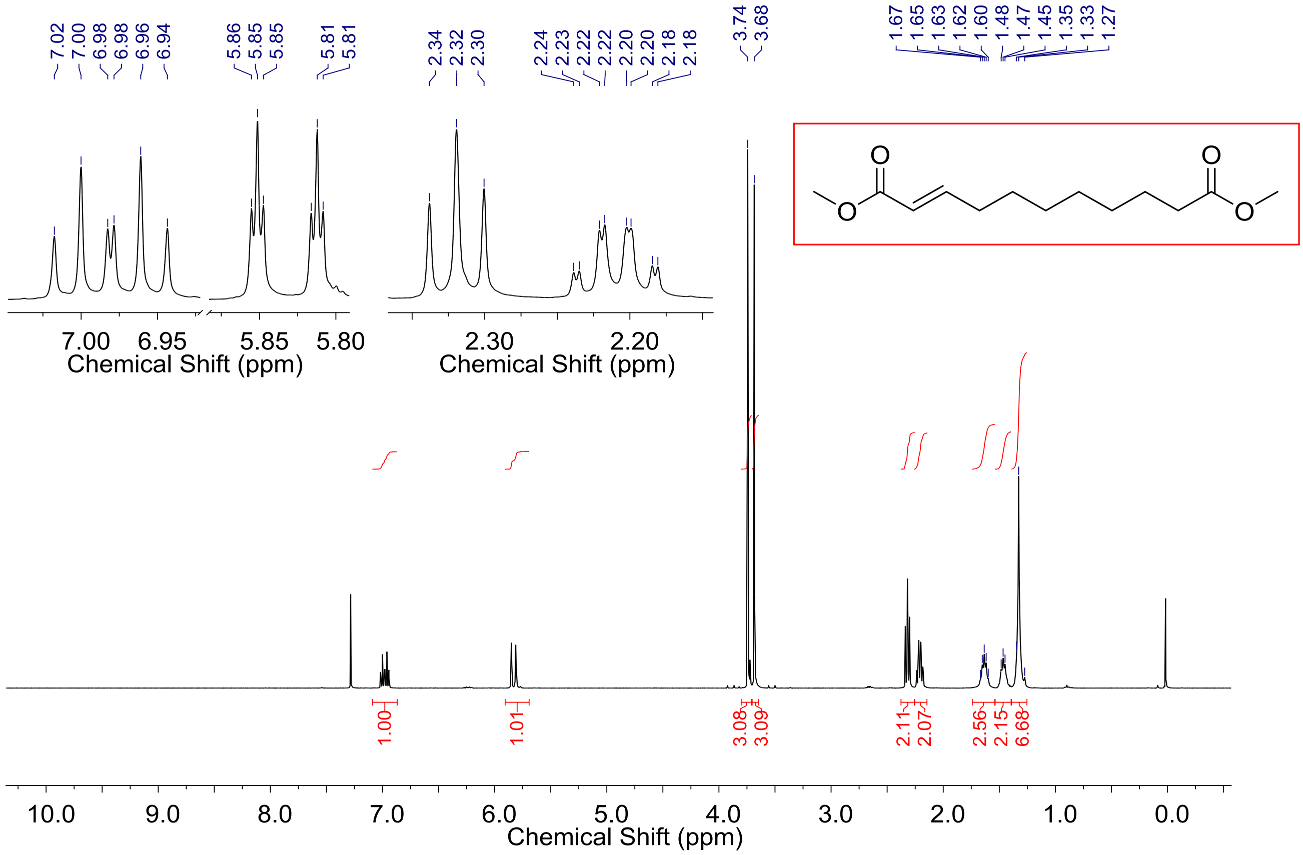

^{1}H NMR (400 MHz, $CDCl_3$) δ 6.98 (dt, *J* = 15.6, 7.0 Hz, 1H), 5.83 (dt, *J* = 15.6, 1.6 Hz, 1H), 3.74 (s, 3H), 3.68 (s, 3H), 2.32 (t, *J* = 7.5 Hz, 2H), 2.21 (qd, *J* = 7.0, 1.6 Hz, 2H), 1.74 – 1.54 (m, 2H), 1.54 – 1.39 (m, 2H), 1.39 – 1.25 (m, 6H).

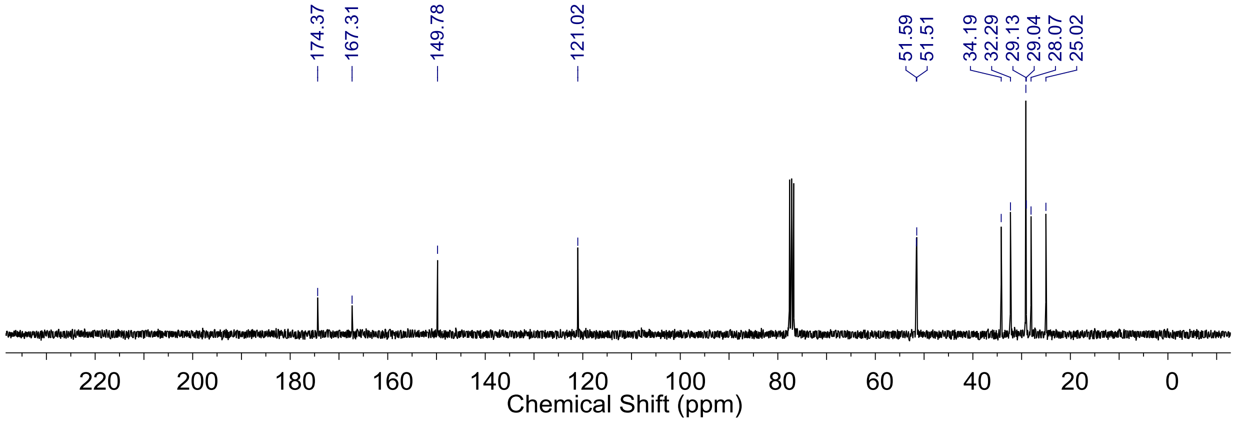

^{13}C NMR (75 MHz, $CDCl_3$) δ 174.37, 167.31, 149.78, 121.02, 51.59, 51.51, 34.19, 32.29, 29.13, 29.04, 28.07, 25.02.

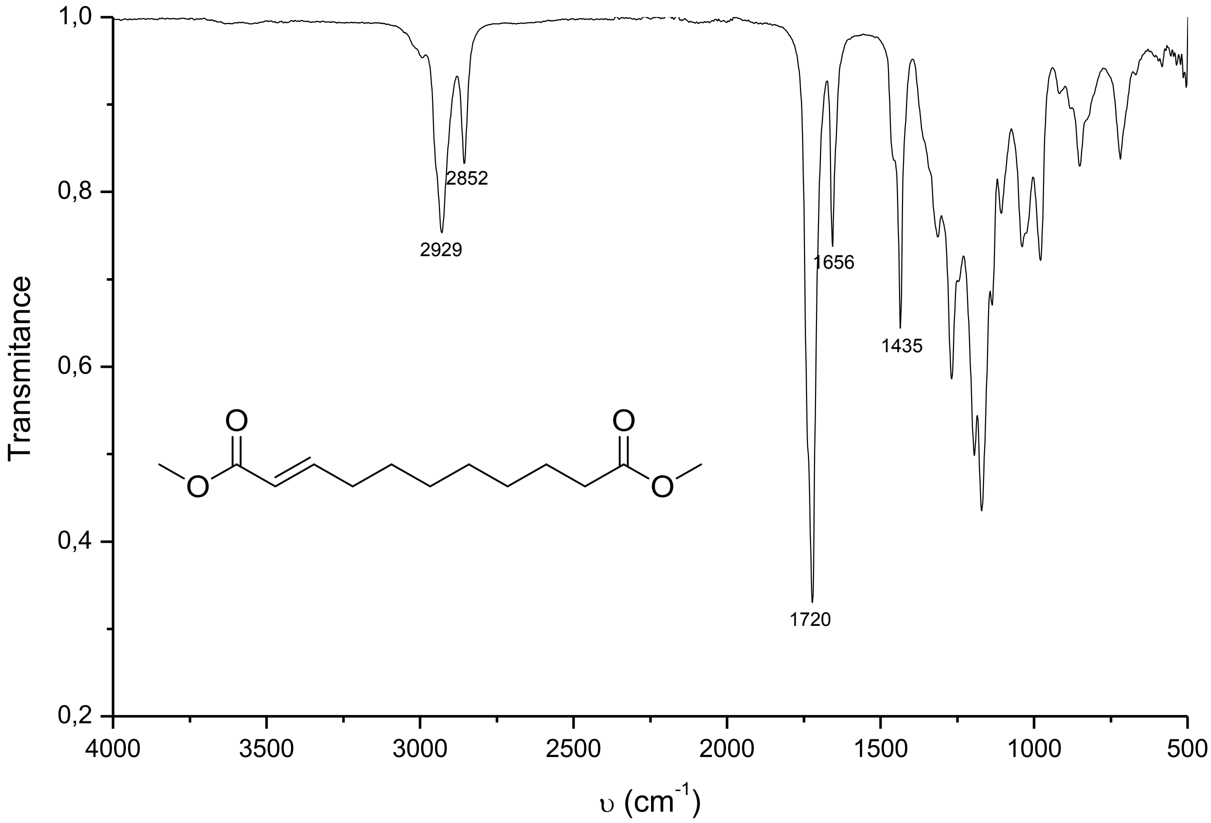
1,0
0,8
0,6
0,4
0,2
Transmitance
2852
2929
1656
1435
1720
4000
3500
3000
2500
2000
1500
1000
500
υ (cm-1)
O
O
O
O

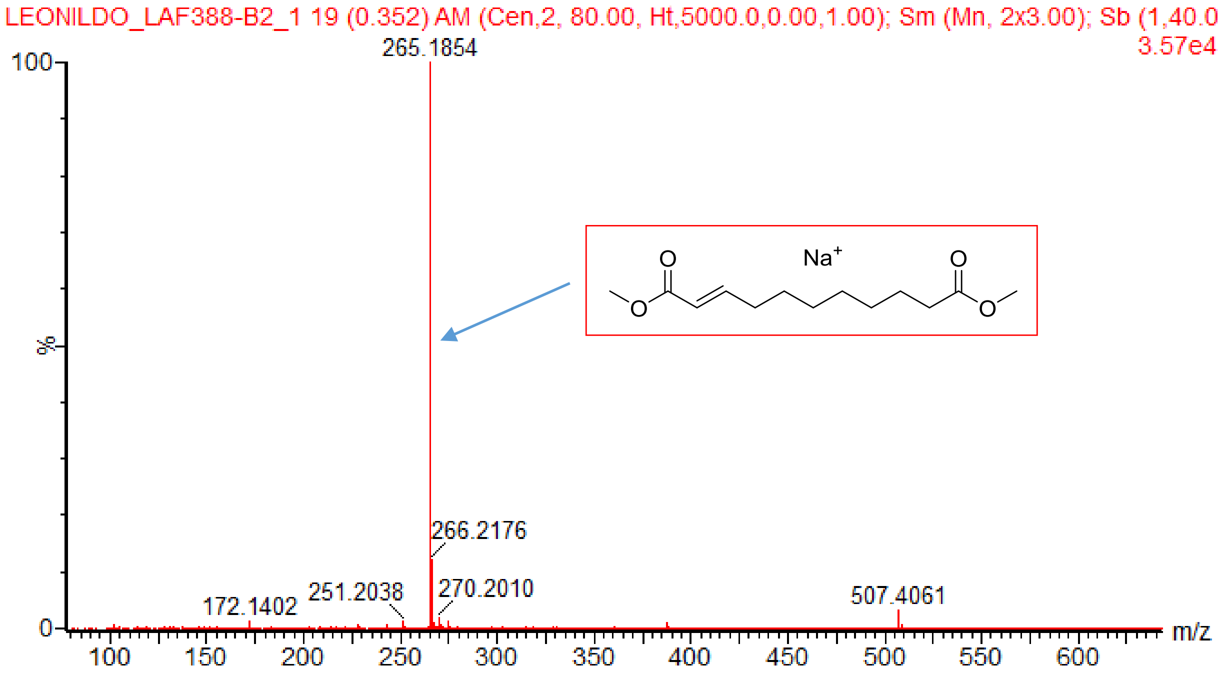
LEONILDO_LAF388-B2_1 19 (0.352) AM (Cen,2, 80.00, Ht,5000.0,0.00,1.00); Sm (Mn, 2x3.00); Sb (1,40.0
3.57e4
265.1854
100
%
0
266.2176
172.1402
251.2038
270.2010
507.4061
100
150
200
250
300
350
400
450
500
550
600
m/z
Na+
O
O
O
O

Full ^{1}H-^{13}C HSQC spectrum of **Ru-CHCO$_2$H**

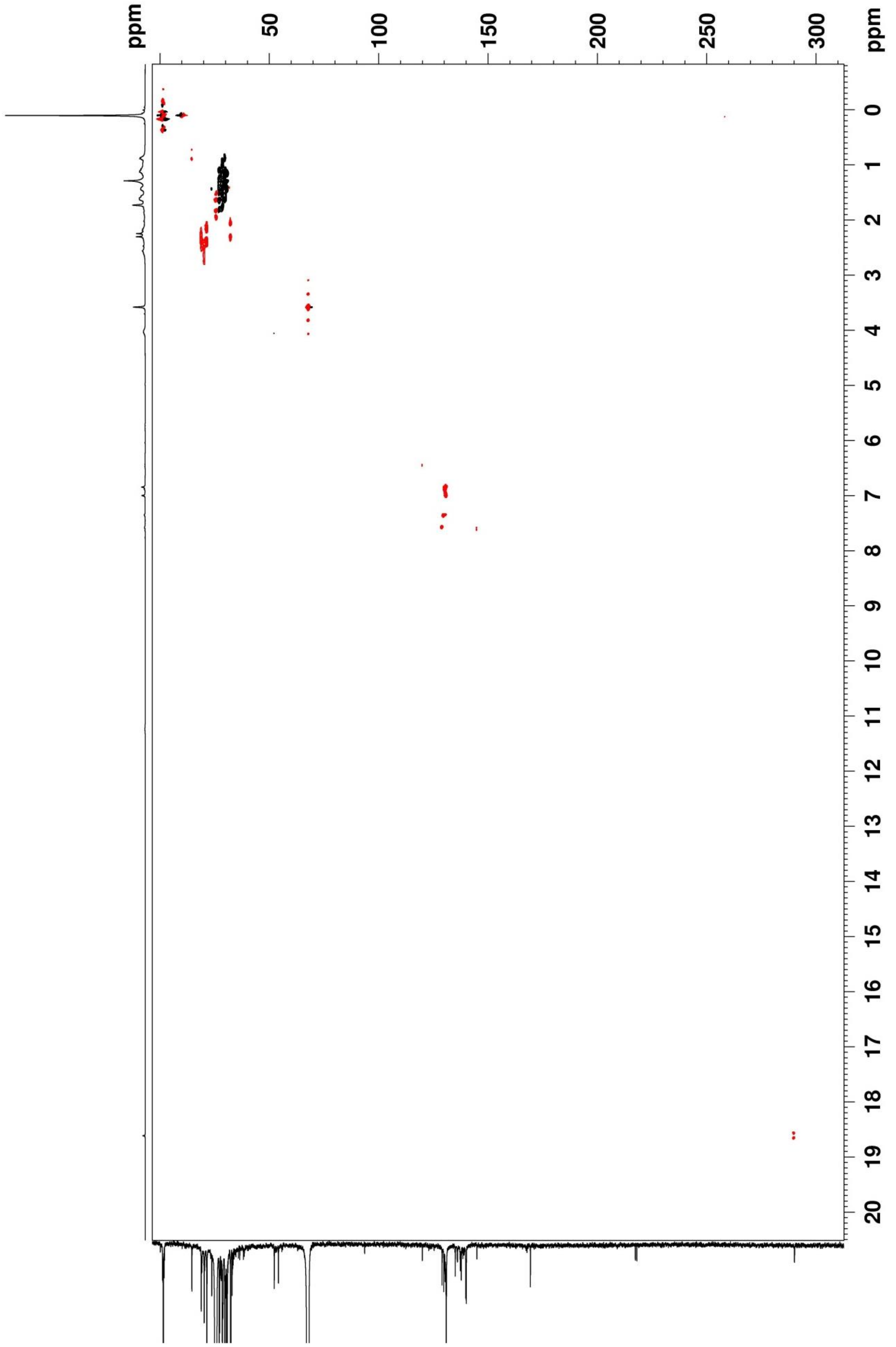

Full ^{1}H-^{13}C HMBC spectrum of **Ru-CHCO$_2$H**

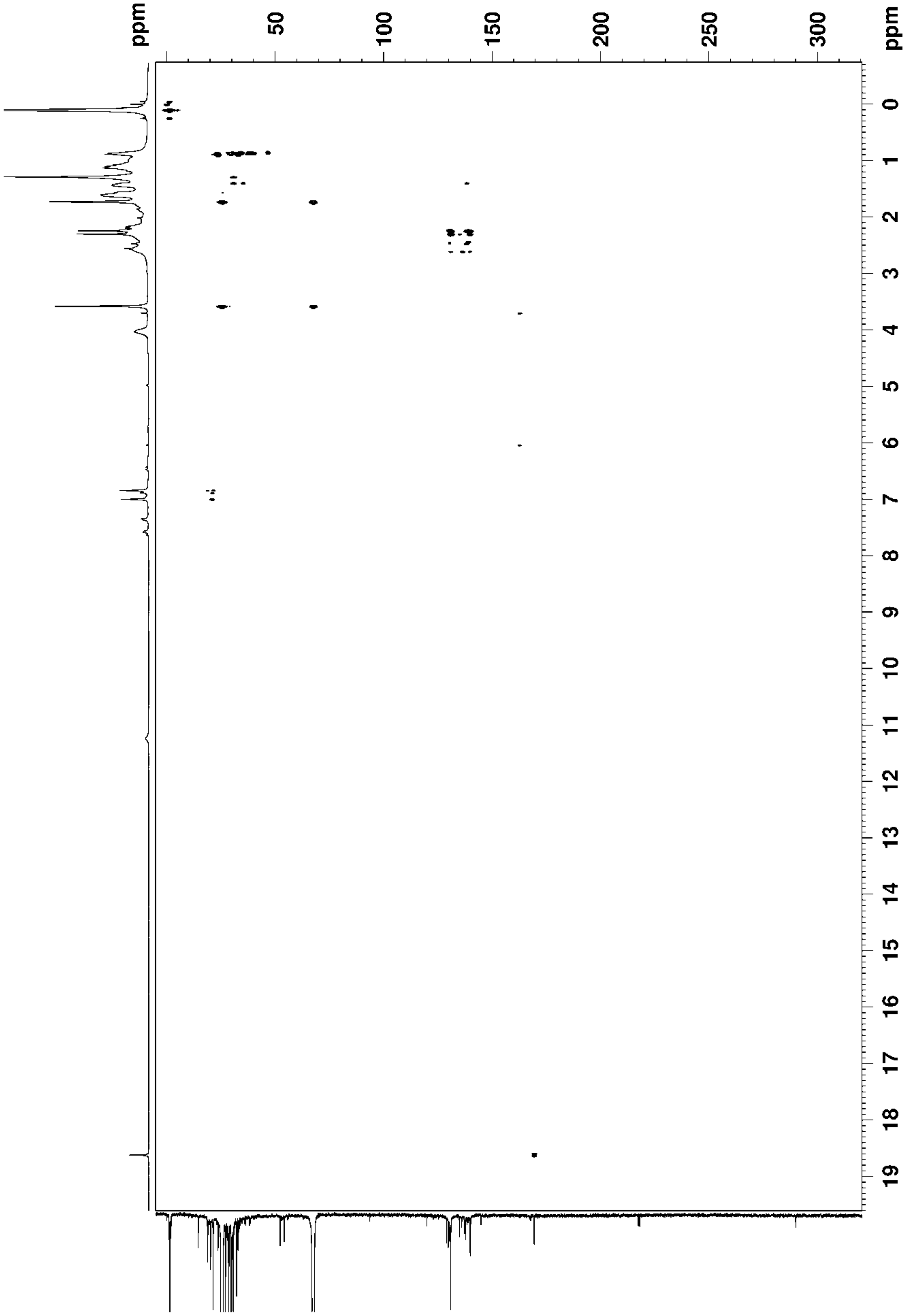

Appendix VI Manuscript published in *Catalysis Science and Technology*

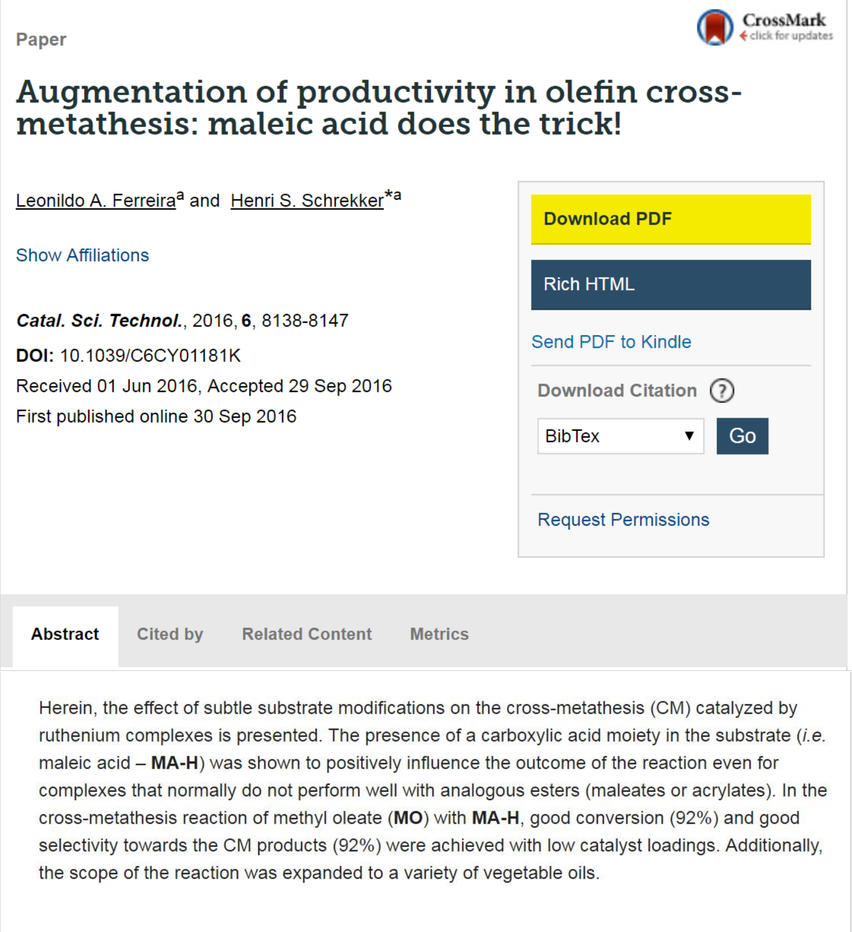
CrossMark
click for updates
Download PDF
Rich HTML
Send PDF to Kindle
Download Citation
BibTex
Go
Request Permissions
Abstract
Cited by
Related Content
Metrics

Paper

Augmentation of productivity in olefin cross-metathesis: maleic acid does the trick!

Leonildo A. Ferreira[a] and Henri S. Schrekker*[a]

Show Affiliations

Catal. Sci. Technol., 2016, **6**, 8138-8147
DOI: 10.1039/C6CY01181K
Received 01 Jun 2016, Accepted 29 Sep 2016
First published online 30 Sep 2016

Herein, the effect of subtle substrate modifications on the cross-metathesis (CM) catalyzed by ruthenium complexes is presented. The presence of a carboxylic acid moiety in the substrate (*i.e.* maleic acid – **MA-H**) was shown to positively influence the outcome of the reaction even for complexes that normally do not perform well with analogous esters (maleates or acrylates). In the cross-metathesis reaction of methyl oleate (**MO**) with **MA-H**, good conversion (92%) and good selectivity towards the CM products (92%) were achieved with low catalyst loadings. Additionally, the scope of the reaction was expanded to a variety of vegetable oils.

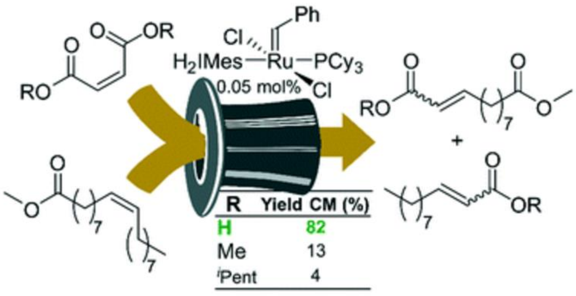
RO
O
O
OR
Cl
Ph
H$_2$IMes—Ru—PCy$_3$
0.05 mol%
Cl
RO
O
O
7
+
O
OR
7
O
O
7
7
R Yield CM (%)
H 82
Me 13
^{i}Pent 4

Catalysis Science & Technology

PAPER

View Article Online
View Journal | View Issue

Published on 30 September 2016. Downloaded by Universidade Federal do Rio Grande do Sul on 17/11/2016 13:12:40.

Cite this: *Catal. Sci. Technol.*, 2016, **6**, 8138

Augmentation of productivity in olefin cross-metathesis: maleic acid does the trick!†

Leonildo A. Ferreira and Henri S. Schrekker*

Received 1st June 2016,
Accepted 29th September 2016

DOI: 10.1039/c6cy01181k

www.rsc.org/catalysis

Herein, the effect of subtle substrate modifications on the cross-metathesis (CM) catalyzed by ruthenium complexes is presented. The presence of a carboxylic acid moiety in the substrate (*i.e.* maleic acid – **MA-H**) was shown to positively influence the outcome of the reaction even for complexes that normally do not perform well with analogous esters (maleates or acrylates). In the cross-metathesis reaction of methyl oleate (**MO**) with **MA-H**, good conversion (92%) and good selectivity towards the CM products (92%) were achieved with low catalyst loadings. Additionally, the scope of the reaction was expanded to a variety of vegetable oils.

Introduction

Olefin metathesis is already a well-established reaction in academia and a growing strategy in the commodity and fine chemicals industries.[1–3] This is the result of years of research on the synthesis of a diversity of (pre-)catalysts, the understanding of the reaction mechanisms, the stability of the (pre-)catalysts and their decomposition/deactivation pathways, allied with the understanding of substrate reactivity.[4–6] Amongst the diversified plethora of homogenous olefin metathesis (pre-)catalysts, the ruthenium-based complexes (*e.g.* those depicted in Fig. 1) have received more attention due to their good activity and higher robustness to varying reaction conditions, allowing the transformation of molecules within a diverse range of complexity.[3,7–9]

A particularly attractive transformation in olefin metathesis is the cross-metathesis (CM) with acrylates, which has grown in importance in recent years as a useful strategy in the preparation of a number of valuable products of commercial interest.[10] These include commodity products from vegetable oils (monomers, surfactants), ingredients for cosmetic uses and compounds with biological applications.[11] For such transformations involving acrylates and other electron deficient olefins, the use of more expensive phosphine-free (pre-)catalysts (*e.g.* **HGII**) generally affords better results.[12] This is the consequence of the decomposition of propagating species due to different pathways (Fig. 1). Within this context, the presence of nucleophilic bases (including PCy_3) has a detrimental influence on the propagating species generated during metathesis.[5a,13,14] For instance, the Ru–methylidene intermediate can be attacked by the dissociated PCy_3 from the **GII** complex, resulting in its decomposition or deactivation (Scheme 1a).[5f] Moreover, in the presence of acrylates, PCy_3 can act as a Michael donor and the resulting adduct participates in the decomposition of the (pre-)catalyst (Scheme 1b).[5a]

Albeit the fate of any (pre-)catalyst is its decomposition/deactivation, any aspect that results in longer catalyst lifetime is of paramount importance.[15] Therefore, changes in the steric/electronic properties of the (pre-)catalysts are commonly pursued to achieve a better performance. Subtle substrate modifications can also result in dramatic improvements in the (pre-)catalyst performance. For instance, the use of methyl crotonate instead of methyl acrylate (**AA-Me**) was found to improve the performance of two ruthenium metathesis (pre-)catalysts in the cross-metathesis with methyl oleate

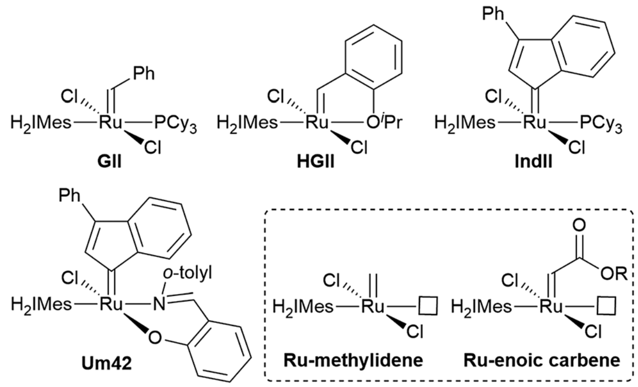

Fig. 1 Selected examples of ruthenium-based olefin metathesis (pre-)catalysts and propagating species (inside the dashed box) formed during the metathesis of terminal and/or α,β-unsaturated carboxylic acid derivatives.

Laboratory of Technological Processes and Catalysis, Institute of Chemistry, Universidade Federal do Rio Grande do Sul, Av. Bento Gonçalves 9500, Porto Alegre, RS, 91501-970, Brazil. E-mail: henri.schrekker@ufrgs.br

† Electronic supplementary information (ESI) available. See DOI: 10.1039/c6cy01181k

This journal is © The Royal Society of Chemistry 2016

Published on 30 September 2016. Downloaded by Universidade Federal do Rio Grande do Sul on 17/11/2016 13:12:40.

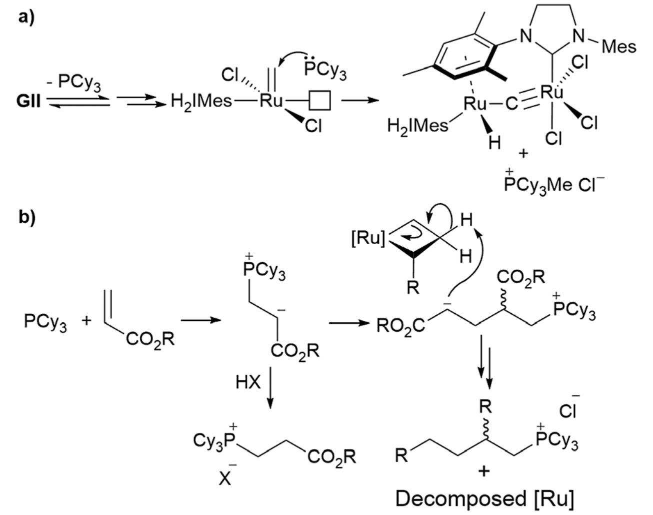

Scheme 1 a) Decomposition of the key Ru–methylidene propagating species formed during metathesis transformations with terminal olefins and b) Michael addition of PCy_3 to the substrate during cross-metathesis with acrylate esters.

(**MO**). This improvement was attributed to the formation of the more stable Ru–ethylidene intermediate, therefore avoiding the formation of Ru–methylidene species.[16a]

It is therefore obvious that any factor that somehow affects the active intermediate species will have a major influence on the outcome of the metathesis reaction. Following this reasoning, the formation of a ruthenium enoic carbene as the sole propagating species (Fig. 1) for the synthesis of α,β-unsaturated carboxylic acids *via* metathesis should have a positive influence on the reaction.[17] Therefore, reported in this paper is the study about the influence on the (pre-)catalyst productivity when maleic acid (**MA-H**) is used as a cross-metathesis partner in the reaction with methyl oleate (**MO**), a model olefin, and the posterior scope expansion to include vegetable oils (Scheme 2).[18]

Experimental

MA-H, **AA-H** (ultrapure), 1,3,5-trimethoxybenzene, **GII**, **HGII**, **IndII** and **Um42** were used as received. THF was distilled over Na/benzophenone and stored over activated molecular sieves under an argon atmosphere. **MA-Me** and **AA-Me** were distilled prior to use. **MO** (>99% purity) was purchased from TRC Inc. Magnesol was purchased from Magnesol® XL Oil Solutions. The vegetable oils were purchased from the local market. Gas chromatogram traces were acquired using a DANI gas chromatograph equipped with a DN-WAX (30 m, 0.32 mm I.D., 0.25 μm film thickness) column and a FID detector. 1,3,5-Trimethoxybenzene was used as internal standard. NMR spectra were recorded on a Bruker (400 MHz) or a Varian Inova 300 (300 MHz) equipment at ambient temperature. The chemical shifts are given in parts per million (ppm) and referenced to the residual solvent signal ($CDCl_3$ = 7.26 (^1H), 77.16 (^{13}C); CD_3OD = 3.31 (^1H), 49.00 (^{13}C)). Infrared spectra were recorded on a Bruker ALPHA FT-IR ATR spectrometer. High-resolution mass spectrometry spectra were recorded on an electrospray ionization (ESI) Micromass Q-Tof Micro™ equipment in the positive mode.

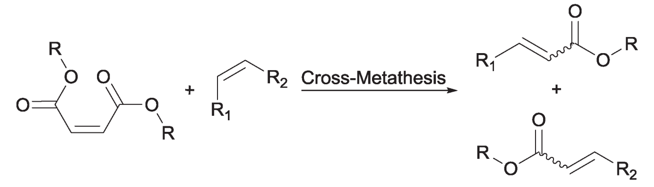

Scheme 2 Cross-metathesis with maleic acid/maleate esters.

General procedure for the cross-metathesis of MO with MA-H

MO, Magnesol (2.5 wt% *vs.* **MO**), Celite (1.5 wt% *vs.* **MO**) and $Ti(O^iPr)_4$ (0 or 2.0 mol% *vs.* **MO**) were transferred to a Schlenk tube and the system was evacuated for 10 minutes before backfilling with argon and stirring for 1 or 12 h at 80 or 50 °C, respectively. The mixture was then passed through a PTFE membrane filter (0.45 μm pore diameter). The vegetable oils were purified using the same approach.

Freshly purified **MO** (0.523 g; 1.77 mmol; 1.0 equiv.), **MA-H** (0.206 g; 1.77 mmol; 1.0 equiv.) and 1,3,5-trimethoxybenzene (0.304 g; 1.80 mmol; internal standard for GC) were transferred to a Schlenk tube, degassed by five consecutive *freeze–pump–thaw* cycles and dissolved in an appropriate amount of dry THF. Then, a freshly prepared solution of the (pre-)catalyst of known concentration (in dry THF) was added to the substrate solution and the Schlenk tube was immersed in a pre-heated oil bath at the reaction temperature. A "time zero" (t_0) aliquot (~250 μL) was taken before the addition of the catalyst solution. Aliquots were taken after determined time intervals and added to test tubes containing 3 drops of a 6.0 mmol L^{-1} KTp methanolic solution (KTp = potassium trispyrazolylborate) to guarantee the quenching of the reaction.[19]

Aliquot derivatization

To each test tube, 1.0 mL of a 2.52 mol L^{-1} methanolic H_2SO_4 solution was added. The tubes were closed with rubber septa and stirred at 63 °C for 2 h. After cooling to 0 °C, hexane (4.0 mL) and deionized water (1.0 mL) were added, and the mixture was centrifuged at 2000 rpm for 8 min. The upper layer was collected and analyzed by GC-FID. Reactions were performed in duplicate and variations in the results are within 1–4% of the average reported values.

Synthesis of MA-^{i}Pent

MA-H (12.37 g; 106.6 mmol; 1.0 equiv.), *p*-toluenesulfonic acid (1.07 g; 6.2 mmol; 0.06 equiv.) and isopentyl alcohol (28.19 g; 334.3 mmol; 3.1 equiv.) were refluxed in toluene (100 mL) using a Dean-Stark apparatus for 18 h. The mixture was then cooled to room temperature, washed with deionized water (3 × 80 mL) and dried over anhydrous magnesium sulfate. After solvent removal, distillation of the crude

Published on 30 September 2016. Downloaded by Universidade Federal do Rio Grande do Sul on 17/11/2016 13:12:40.

mixture under reduced pressure afforded the target compound as a colourless liquid. Yield: 61% (16.62 g; 64.8 mmol). ^{1}H NMR (400 MHz, $CDCl_3$) δ 6.18 (s, 2H, $-C\underline{H}{=}C\underline{H}-$), 4.17 (t, J = 6.9 Hz, 4H, $-C\underline{H_2}O-$), 1.73–1.57 (m, 2H, $-C\underline{H}(CH_3)_2$), 1.52 (q, J = 6.9 Hz, 4H, $-C\underline{H_2}-$), 0.88 (d, J = 6.7 Hz, 12H, $-CH(C\underline{H_3})_2$). ^{13}C NMR (101 MHz, $CDCl_3$) δ 165.3 ($\underline{C}{=}O$), 129.8 ($-\underline{C}H{=}\underline{C}H-$), 63.9 ($-\underline{C}H_2O-$), 37.1 ($-\underline{C}H_2-$), 24.9 ($-\underline{C}H(CH_3)_2$), 22.4 ($-CH(\underline{C}H_3)_2$). Integration revealed the presence of <2% of the fumarate isomer (olefinic singlet at 6.79 ppm). IR (ATR, cm^{-1}) 1728, 1646, 1158. ESI(+)-MS: $C_{14}H_{25}O_4^+$ – calculated: 257.1751, obtained: 257.1753; $C_{14}H_{24}NaO_4^+$ (sodium adduct) – calculated: 279.1567, obtained: 279.1534.

Results and discussion

Influence of the MO purification method

The purification of the substrates (especially those from natural sources) is sometimes an overlooked parameter that is rarely investigated during the optimization of catalytic reactions. Therefore, the purification of the **MO** was the first parameter to be investigated in this study. Based on the literature, four purification methods were investigated. All methods have in common the use of Magnesol/Celite as purifying agents.[20] The initial experiments were performed at 50 °C using a 1 : 1 molar ratio of **MO** : **MA-H** in THF. **GII** was used as a (pre-)catalyst because it was shown to exhibit good activity in the synthesis of carboxy-telechelic polymers *via* the ROMP of cyclooctene with **MA-H** as a chain-transfer agent.[21]

Purification of **MO** over Magnesol (2.5 wt%) and Celite (1.5 wt%) at 40 °C for 12 h (purification method A) prior to use afforded almost a quantitative yield and an excellent selectivity towards the CM products in the reaction with **MA-H**, when applying either 0.4 or 0.2 mol% **GII** (Table 1, entries 1 and 2, respectively). Decreasing the catalyst loading to 0.1 and 0.05 mol% resulted in steadily reducing conversions of 73 and 4%, respectively (Table 1, entries 3 and 4). In both experiments, the reaction occurred only in the initial 10 min (see Fig. S1, ESI†), suggesting catalyst decomposition by remaining impurities.

Purification method B involves treating **MO** with Magnesol (2.5 wt%) and Celite (1.5 wt%) at 80 °C for 1 h. With this procedure, a **MO** conversion of 81% and a yield of CM products of 66% were obtained with a catalyst loading of 0.1 mol% (Table 1, entry 5), being a slight improvement in comparison to purification method A.

With the observed positive temperature effect on the treatment of **MO**, the next step was to determine if pre-drying the Magnesol and Celite could result in further improvement. Nevertheless, when **MO** was treated with dried Magnesol (2.5 wt%) and Celite (1.5 wt%) and subjected to the cross-metathesis reaction, a decrease in both conversion (70%) and yield of CM products (55%) was observed (Table 1, entry 6).

Titanium alkoxides have been used as additives or as co-catalysts in some metathesis transformations of oxygen- and nitrogen-containing substrates.[22–25] Recently, the treatment of natural oils with $Ti(O^iPr)_4$ has been disclosed for use as olefin metathesis substrates.[26] Although the role of $Ti(O^iPr)_4$ in the treatment of **MO** is merely speculative, it may trap nitrogen-containing impurities *via* coordination. Aiming for further improvement in the **MO** conversion, the treatment of **MO** with titanium(IV) isopropoxide was explored. The treatment of **MO** with $Ti(O^iPr)_4$ (2 mol%), Magnesol (2.5 wt%) and Celite (1.5 wt%) resulted in a conversion of 81% and a yield of CM of 69% with 0.1 mol% **GII** as a (pre-)catalyst (Table 1, entry 7). Altogether, purification method D is better than methods A and C and slightly better than method B, showing a slight improvement in the selectivity.

Table 1 Influence of the **MO** purification method on the **GII**-catalysed CM of **MO** with **MA-H**

Entry	GII (mol%)	Purification method	Conv. (%)	Yield (%) CM	Yield (%) SM
1	0.4	A	98	96	1
2	0.2	A	97	94	2
3	0.1	A	73	48	20
4	0.05	A	4	<2	2
5	0.1	B	81	66	14
6	0.1	C	70	55	18
7	0.1	D	81	69	10

Purification method	Magnesol (2.5 mol%)	Celite (1.5 wt%)	Ti (O^{i}Pr)$_4$ (2 mol%)	T (°C)
A[a]	Yes	Yes	No	40[b]
B[a]	Yes	Yes	No	80[c]
C[d]	Yes	Yes	No	80[c]
D[a]	Yes	Yes	Yes	80[c]

Conditions: **MO** : **MA-H** molar ratio = 1 : 1 (**MO** = 1.77 mmol); THF = 7.0 mL; reactions performed at T = 50 °C. Isomerization products complete the mass balance. [a] Magnesol and Celite were used as received. [b] Heated for 12 h. [c] Heated for 1 h. [d] Magnesol and Celite dried at 160 °C for 48 h prior to use.

Interestingly, regardless of the purification method employed and the catalyst loading, all the reactions occurred within the first 25 minutes (see Fig. S1, ESI†), which indicates that despite **MA-H** being electronically deficient, its reactivity is comparable to that of **MO**. Moreover, high selectivity towards the CM products was only obtained with high conversion. This finding is not surprising when the reactivity of the SM and CM products are taken into consideration. The SM products, *E*/*Z* dimethyl 9-octadecenedioate (**P3**) and *E*/*Z* 9-octadecene (**P4**), are type I olefins (*i.e.* homodimerize quickly and are promptly consumed)[27] and have similar reactivity to that of **MO**. As a consequence, the SM is an equilibrium reaction. On the other hand, the CM products, 11-methoxy-11-oxoundec-(2*E*/*Z*)-2-enoic acid (**P1**) and (2*E*/*Z*)-2-undecenoic acid (**P2**), are type IV olefins (*i.e.* are not reactive towards olefin metathesis), and as a consequence, CM with **MA-H** is an irreversible reaction (Scheme 3).

Influence of the MO : MA-H ratio and MO concentration

Purification method D ($Ti(O^iPr)_4$ (2 mol%), Magnesol (2.5 wt%) and Celite (1.5 wt%)) was used to further optimize the

This journal is © The Royal Society of Chemistry 2016

Published on 30 September 2016. Downloaded by Universidade Federal do Rio Grande do Sul on 17/11/2016 13:12:40.

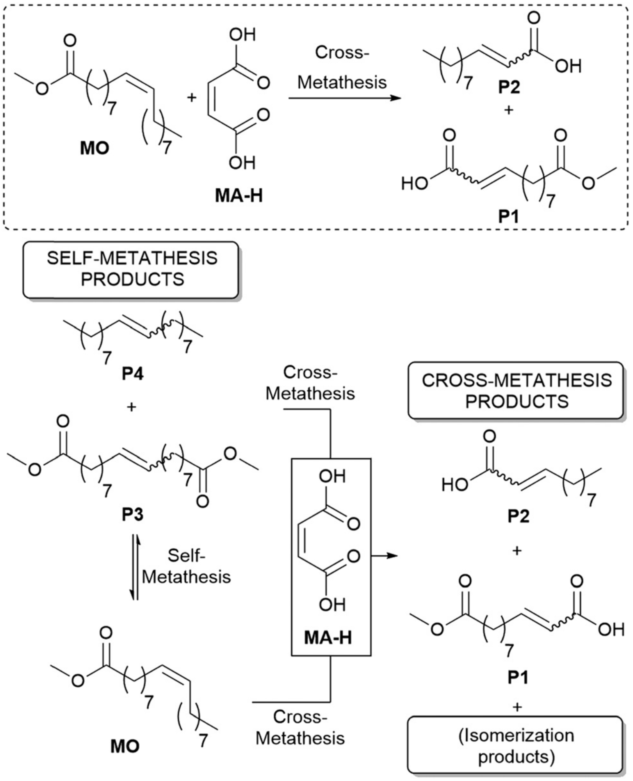

Scheme 3 CM of **MO** with **MA-H**.

reaction conditions. In the next step, the influence of the **MO** : **MA-H** ratio on both the conversion and selectivity was investigated. Increasing the **MO** : **MA-H** molar ratio from 1 : 1 to 1 : 5 resulted in an initial increase in both conversion and yield of CM products, which remained more or less steady for the ratios studied (Table 2, entries 7–11). Only a minor decrease in the conversion was observed when a ratio of 1 : 5 (**MO** : **MA-H**) was used (Table 2, entry 11). Additionally, the effect on the selectivity (yield of CM *vs.* yield of SM) was only evident at the higher ratio of **MO** : **MA-H**. The decrease in both conversion and selectivity by increasing the amount of **MA-H** could be attributed to the decomposition of enoic-carbene species, as the increase in the concentration of **MA-H** would favour the formation of such intermediates. The **MO** : **MA-H** ratio of 1 : 2 was chosen for further optimization and a decrease in the catalyst loading to 0.05 mol% resulted in a conversion of 83% and a 63% yield of the CM products (Table 2, entry 12). A further decrease in the catalyst loading was not pursued as in this scenario it would not be possible to obtain high selectivity[16a] and therefore the reaction would be better described as the inhibition of the **MO** SM by the cross-metathesis partner.[28]

Table 2 Effect of the **MO** : **MA-H** molar ratio on the **GII**-catalysed CM of **MO** with **MA-H**

Entry	MO : MA-H	Conv. (%)	Yield (%)	
			CM	SM
7	1 : 1	81	69	10
8	1 : 2	96	89	4
9	1 : 3	96	90	2
10	1 : 4	95	88	3
11	1 : 5	90	80	7
12[a]	1 : 2	83	63	17

Conditions: THF = 7 mL; **GII** = 0.1 mol% (*vs.* **MO**; **MO** = 1.77 mmol); *T* = 50 °C; purification method D. Isomerization products complete the mass balance. [a] **GII** = 0.05 mol% (*vs.* **MO**).

The decrease in the solvent amount in a reaction is an advantageous parameter for more sustainable processes. Moreover, the amount of the solvent (*i.e.* the concentration of the reactants) does sometimes influence the outcome of metathesis reactions (specifically in ring-closing metathesis reactions). Although the studied reaction cannot be performed under neat conditions due to solubility restrictions inherited by the use of **MA-H**, the amount of solvent was changed in order to observe its influence on the reaction. As summarized in Fig. 2, the concentration of the reactants had just a minor effect on the conversion of **MO**. The increase in the concentration up to 1.2 mol L^{-1} (1.5 mL of THF) resulted in an increase of 10% in the conversion and an increase in the yield of the CM products from 63 to 84%. The increase to higher concentrations was not feasible due to the limited solubility of **MA-H** in THF. At the optimum concentration, high **MO** conversion with good selectivity towards the CM products (84% yield of CM products) was achieved (Fig. 2).

Influence of the temperature and the (pre-)catalyst

Surprisingly, the temperature has just a minor influence on the conversion of the explored reaction using **GII** as a (pre-)catalyst. Only a small variation (4%) was observed in the temperature range of 40 °C to reflux (b.p. THF = 65 °C) (Fig. 3).

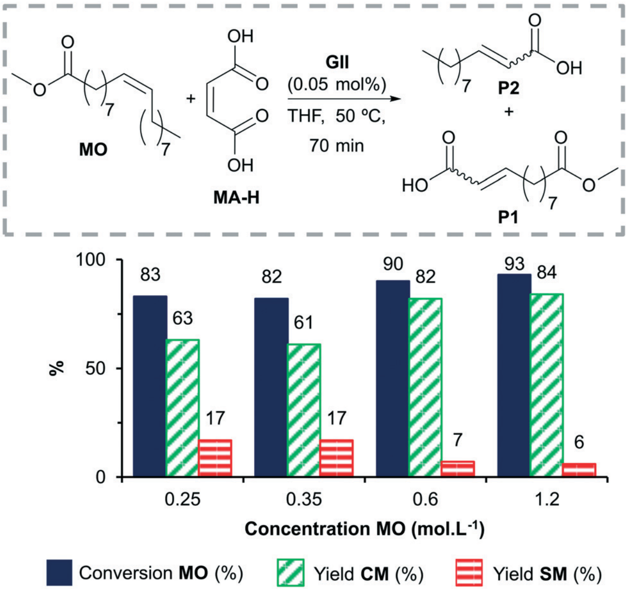

Fig. 2 Effect of the substrate concentration on the cross-metathesis of **MO** with **MA-H** using **GII** as a (pre-)catalyst. Conditions: **MO** : **MA-H** molar ratio = 1 : 2 (**MO** = 1.77 mmol); **GII** = 0.05 mol%; *T* = 50 °C; purification method D. Isomerization products complete the mass balance.

View Article Online

Published on 30 September 2016. Downloaded by Universidade Federal do Rio Grande do Sul on 17/11/2016 13:12:40.

Under refluxing conditions, however, an indication of a detrimental effect on the yield of the CM products was observed, consistent with the thermal decomposition of the catalytic species.

After establishing the optimal purification method, catalyst loading, **MO**:**MA-H** molar ratio, concentration of substrates and temperature, the performance of some (pre-)catalysts was then investigated. Three additional ruthenium-based metathesis (pre-)catalysts were selected. The selection of the complexes was based on the nature (phosphine containing *versus* phosphine-free complexes) and the type (PCy_3, chelating isopropoxybenzylidene and chelating phenoxy-imine) of the departing ligand in the dissociation step and the type of alkylidene (benzylidene, indenylidene or isopropoxybenzylidene) (Fig. 1).

The second-generation Hoveyda–Grubbs metathesis catalyst – **HGII** – is considered the (pre-)catalyst of choice in the cross-metathesis with electron deficient substrates (*e.g.* acrylates). Interestingly, in comparison to **GII**, **HGII** provided a similar conversion under the same conditions, although the CM yield was somewhat lower (Fig. 4). Regarding the temperature, both complexes perform better at 60 °C (see Table S1, ESI†), showing signs of catalyst decomposition at reflux.

The complex **IndII**, an indenylidene analogue of **GII**,[29–31] performed similarly to both **GII** and **HGII**, but as depicted in the time-dependent plots (Fig. 4b and c), the conversion of **MO** was slower in the case of both **HGII** and **IndII**. As seen in Fig. 4b and c, the **GII**-catalyzed reaction occurred within approximately 10 minutes as opposed to the reactions catalysed by **HGII** and **IndII**. For the latter systems, a plateau was reached after approximately 35 minutes.

The fourth complex explored was the phosphine-free, indenylidene-type, **Um42** complex. **Um42** is a "latent" catalyst due to the presence of the non-labile phenoxy-imine chelating ligand. It has been reported that this complex is to be activated thermally or chemically by the use of Brønsted acids or silanes.[32–35] It was therefore envisaged that such a complex could perform well in our system, as **MA-H** could serve as both an activating agent and a substrate. Nevertheless, the CM reaction catalysed by **Um42** under refluxing conditions was less productive and resulted in only 60% conversion with 17% of CM products (Fig. 4a–c).

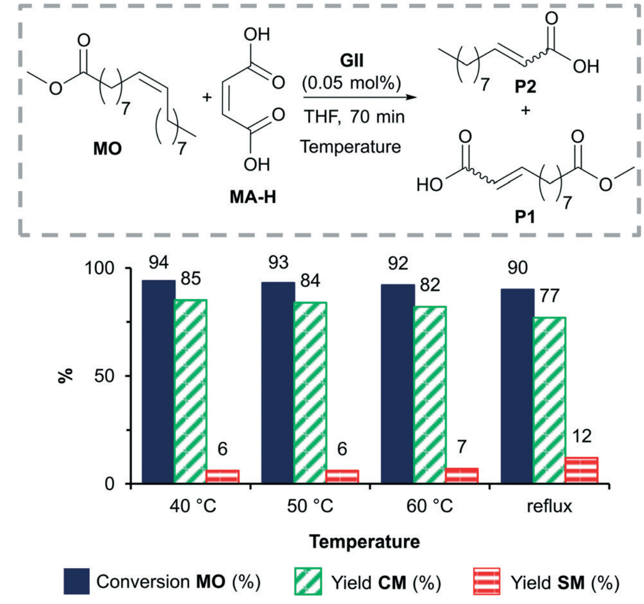

Fig. 3 Effect of the temperature on the CM of **MO** with **MA-H**. Conditions: **MO**:**MA-H** molar ratio = 1:2 (**MO** = 1.77 mmol, [**MO**] = 1.2 mol L^{-1}); **GII** = 0.05 mol%; THF = 1.5 mL; purification method D. Isomerization products complete the mass balance.

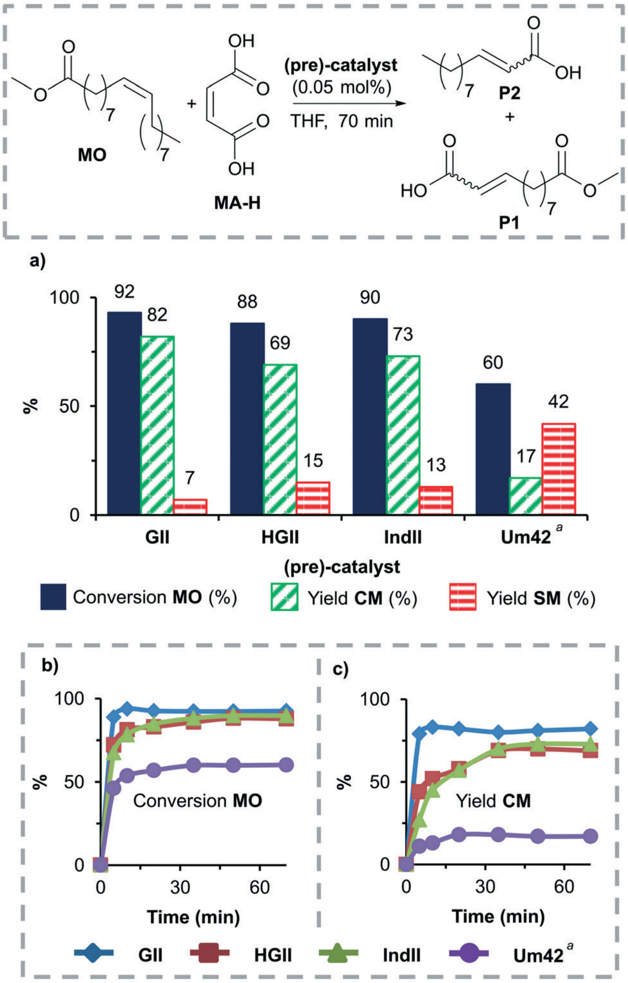

Fig. 4 Influence of the (pre-)catalyst on the CM of **MO** with **MA-H** (a) and time-dependent plots of the conversion of **MO** (b) and the yield of the CM products (c). Lines were added in the time-dependent plots with the only purpose of aiding visualization. Conditions: **MO**:**MA-H** molar ratio = 1:2 (**MO** = 1.77 mmol); THF = 1.5 mL; purification method D; *T* = 60 °C; 0.05 mol% of (pre-)catalyst. Isomerization products complete the mass balance. [a]Reaction performed at reflux.

Maleic acid *vs.* maleates

In an attempt to establish the effect of the structure of the CM partner on the conversion and selectivity, a series of reactions of **MO** with two selected maleate esters were performed. Reactions were performed with both **GII** and **HGII** under the optimized reaction conditions established (*i.e.* purification method D, 0.05 mol% of (pre-)catalyst, 1.2 mol L^{-1} of **MO** and 60 °C) (Fig. 5). The (pre-)catalysts **GII** and **HGII** were

This journal is © The Royal Society of Chemistry 2016

Published on 30 September 2016. Downloaded by Universidade Federal do Rio Grande do Sul on 17/11/2016 13:12:40.

chosen for the continuity of this study due to a number of reasons: a) superior performance in the optimization reactions; b) **HGII** is generally the best (pre-)catalyst when employing electron-deficient olefins; c) **GII** and **HGII** are standard (pre-)catalysts in olefin metathesis; and d) a direct influence of the presence of PCy$_3$ in the reaction media is possible to obtain with this combination, considering that the same propagating species are formed with both (pre-)catalysts.

The use of dimethyl maleate, **MA-Me**, resulted in a decrease in the conversion to about half the conversion obtained with **MA-H** for both **GII** and **HGII** (Fig. 6).[36] The effect on the yield of CM products (*i.e.* on the selectivity) of this substrate is even more pronounced, resulting in less than 15% of the CM products. This decrease in both conversion and selectivity is likely due to the presence of the bulkier methyl group of **MA-Me.**[37] A comparative reaction was performed to check this assumption, using the bulkier di-isopentylmaleate, **MA-$^{\mathrm{i}}$Pent**, as the CM partner. Conversions were similar to those obtained with **MA-Me**, but only traces (>6%) of the target CM products were obtained.[38] Altogether, the outcome of these reactions was mainly governed by the steric bulkiness of the metathesis substrate, regardless of the (pre-)catalyst used. This influence might be associated with the coordination step and/or with the (de)stabilization of intermediate species. Interestingly, the similar (pre-)catalyst performances indicate that the dissociated PCy$_3$ from **GII** had no major influence on the reaction.

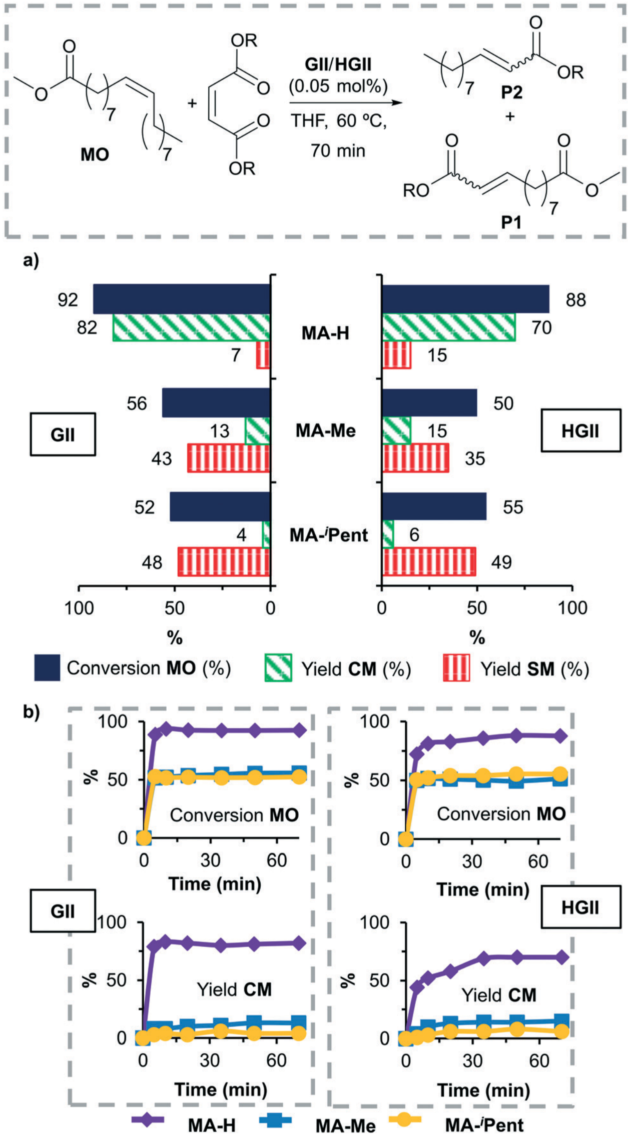

Fig. 6 a) Influence of the CM partner on the conversion (blue bars) and yields of CM (dashed green bars) and SM (dashed red bars) of the reaction with **MO** – **MA-H** *vs.* **MA-Me** and **MA-$^{\mathrm{i}}$Pent**. b) Time-dependent plots using **GII** and **HGII**, respectively. Lines were added in the time-dependent plots with the only purpose of aiding visualization. **MO** : CM partner molar ratio= 1 : 2 (**MO** = 1.77 mmol); THF = 1.5 mL; catalyst: 0.05 mol% (*vs.* **MO**); T = 60 °C; purification method D. Isomerization products complete the mass balance.

Maleic acid *versus* acrylic acid

In order to investigate the effect of a terminal olefin *versus* a di-substituted olefin on the catalytic activity, reactions with acrylic acid, **AA-H**, and methyl acrylate, **AA-Me**, were also investigated. To allow an efficient removal of the co-product ethylene, these reactions were performed under a continuous flow of argon.

In contrast to the use of **MA-H** and maleates, CM of **MO** with **AA-H** and **AA-Me** affords highly distinct results when **GII** and **HGII** are employed (Fig. 7). In the case of **GII**, the conversion and CM yield steadily decreased when the cross-metathesis partner **MA-H** was replaced with **AA-H** and **AA-Me**, respectively. The use of **HGII** instead of **GII** resulted in a different profile. Initially, a slightly higher selectivity was obtained for the CM products when **MA-H** was replaced with **AA-H**, while maintaining a similar **MO** conversion. Next, a decrease in both yield of CM products and **MO** conversion was observed when **AA-Me** was used as a cross-metathesis partner. Comparatively, the use of **AA-Me** as a CM partner resulted in lower conversion and selectivity for both (pre-)catalysts, but **HGII** outperformed **GII.** Although the steric bulkiness of **AA-H** and **AA-Me** also played an important role in the catalytic performance of both **GII** and **HGII**, the catalytic performance was affected by another feature. **HGII** was not negatively affected by the formation of propagating Ru–methylidene species. The detrimental effect on the **GII**-catalysed reaction could be ascribed to PCy$_3$-mediated decomposition/deactivation of propagating Ru–methylidene species. This also signifies that the use of carboxylic acid substrates does not successfully trap the free PCy$_3$ to inhibit the Ru–methylidene decomposition pathway.

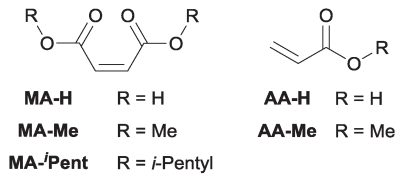

Fig. 5 Cross-metathesis partner scope.

Published on 30 September 2016. Downloaded by Universidade Federal do Rio Grande do Sul on 17/11/2016 13:12:40.

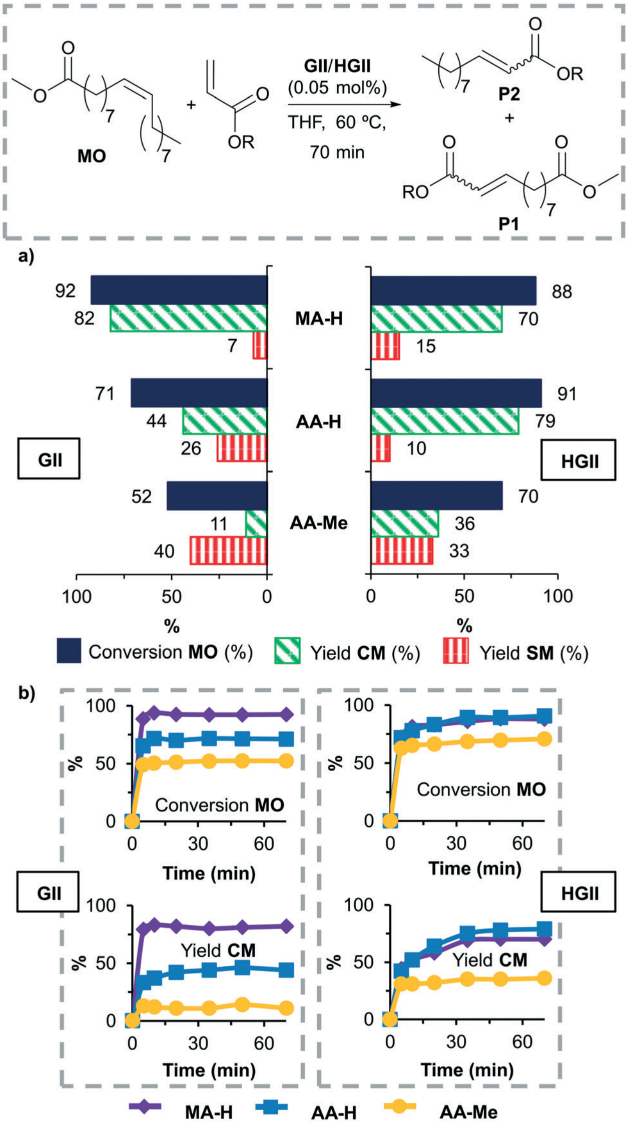

Fig. 7 a) Influence of the CM partner on the conversion (blue bars) and yields of CM (dashed green bars) and SM (dashed red bars) of the reaction with **MO** – **MA-H** *vs.* **AA-H** and **AA-Me**. b) Time-dependent plots using **GII** and **HGII**, respectively. Lines were added in the time-dependent plots with the only purpose of aiding visualization. Conditions: **MO** : **MA-H** molar ratio = 1 : 2 (**MO** = 1.77 mmol); **MO** : **AA-H**/**AA-Me** molar ratio = 1 : 4; THF = 1.5 mL; catalyst: 0.05 mol% (*vs.* **MO**); *T* = 60 °C; purification method D. Isomerization products complete the mass balance.

Altogether, the lower bulkiness of the carboxylic acid substrates accounts predominantly for the higher catalytic productivity when compared to the corresponding esters. For the phosphine-containing (pre-)catalyst **GII**, the avoidance of the formation of Ru–methylidene propagating species is crucial. Thus, when **MA-H** is used as a substrate, the more expensive **HGII** can be substituted by **GII**. If terminal olefins will be used as a substrate, **HGII** remains the (pre-)catalyst of choice.

Use of vegetable oils

To increase the scope of the **MA-H**-based CM, the reaction was also explored using various vegetable oils. Naturally occurring oils and fats (from vegetable and animal origin) are renewable feedstocks of most importance in the chemical industry.[39] For the majority of vegetable oils, most of the side chains in the triglycerides are saturated (C16:0 and C18:0), monounsaturated (C16:1 and C18:1) or polyunsaturated (C18:2 and C18:3) fatty acids (Fig. 8). The content of each of these fatty acid chains depends on a number of factors, including the type of oil (Fig. 9). The use of vegetable oils offers direct advantages compared to the use of **MO**, such as the avoidance of the initial step of transesterification. This also broadens the number of products obtained by enabling the use of vegetable oils with different compositions and may facilitate in the separation of the final product mixture.[40]

CM of several different vegetable oils with **MA-H** under the optimized reaction conditions afforded the results shown in Fig. 9. **GII** was used with a catalyst loading of 0.05 mol% (*versus* C=C bond in the oil). Yields of the CM products were roughly within the observed value for **MO** (82%). A trend in the yield of the CM products *versus* the composition of the oil was not observed, suggesting that none of the major components influence the catalyst productivity. The decrease in the conversion for some of the oils (*e.g.* cottonseed and peanut oils) was more likely due to the presence of residual contaminants not removed during the purification step.

Conclusions

In comparison to the "protected" ester equivalents, the direct use of the carboxylic acid substrates **MA-H** and **AA-H** in the Ru-catalyzed cross-metathesis with **MO** afforded superior

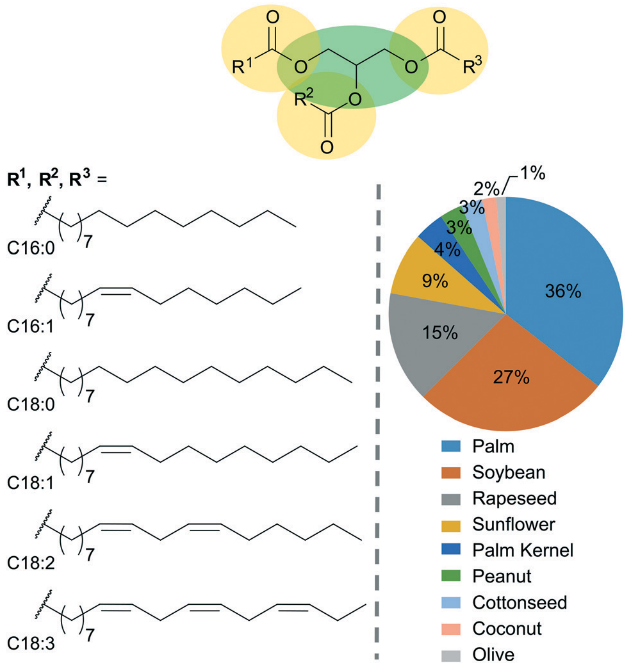

Fig. 8 General structure of a triglyceride with the most common fatty acid side chains and the global market consumption of vegetable oils in 2014–2015 (100% = 175.65 million metric tons).[41]

This journal is © The Royal Society of Chemistry 2016

Published on 30 September 2016. Downloaded by Universidade Federal do Rio Grande do Sul on 17/11/2016 13:12:40.

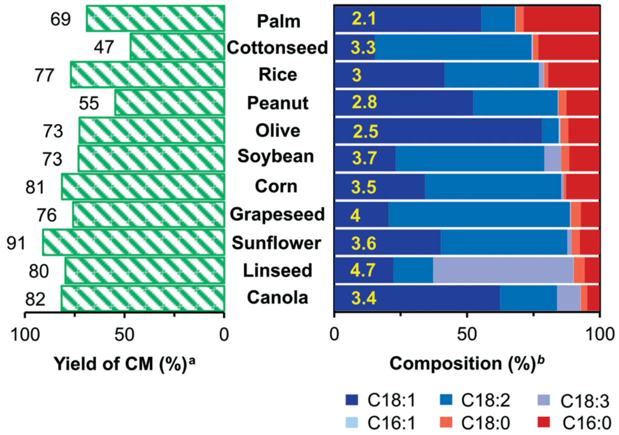

Fig. 9 Effect of the vegetable oil composition on the yield of the CM products. Conditions: oil (C═C) : **MA-H** molar ratio = 1 : 2; THF = 1.5 mL; **GII** = 0.05 mol% (*vs.* C═C); *T* = 60 °C; purification method D; reaction time = 70 min. [a]Yield of CM calculated by ^{1}H NMR. [b]Composition determined by GC. The yellow numbers shown in the blue bars are the number of C═C bonds (calculated by ^{1}H NMR) per triglyceride.

conversions and CM yields. This makes these substrates attractive for the direct synthesis of α,β-unsaturated carboxylic acids, which can be ascribed to the lower steric bulkiness of the $-CO_2H$ group. In the case of a phosphine-containing (pre-)catalyst like **GII**, the avoidance of the formation of Ru–methylidene species is crucial for obtaining good catalytic productivities. This was effectively suppressed by using **MA-H** as an internal olefin, which only leads to the formation of Ru–enoic carbene species. Under these conditions, **GII** can be used as a cheaper alternative for **HGII** in the reaction with **MO** and a variety of vegetable oils. When applying **AA-H** as a substrate, which leads to the formation of Ru–methylidene species, **HGII** remains the (pre-)catalyst of choice. Altogether, these findings have the potential to serve as a rational guideline for determining the reaction conditions in the preparation of α,β-unsaturated carboxylic acid derivatives.

Acknowledgements

The authors are very grateful to Fundação de Amparo à Pesquisa do Estado do Rio Grande do Sul (FAPERGS), Coordenação de Aperfeiçoamento de Pessoal de Nível Superior (CAPES) and Conselho Nacional de Desenvolvimento Científico e Tecnológico (CNPq) for funding and scholarships. H. S. Schrekker is grateful to CNPq for the PQ fellowship.

Notes and references

1 K. Grela, *Olefin Metathesis: Theory and Practice*, John Wiley & Sons Inc, 1st edn, 2014.

2 K. O'Leary Havelka and G. E. Gerhardt, in *Green Polymer Chemistry: Biobased Materials and Biocatalysis*, American Chemical Society, 2015.

3 C. S. Higman, J. A. M. Lummiss and D. E. Fogg, *Angew. Chem., Int. Ed.*, 2016, **55**, 3552–3565.

4 For selected mechanistic studies of ruthenium-based olefin metathesis (pre-)catalysts, see: (*a*) C. Adlhart and P. Chen, *J. Am. Chem. Soc.*, 2004, **126**, 3496–3510; (*b*) J. M. Bates, J. A. M. Lummiss, G. A. Bailey and D. E. Fogg, *ACS Catal.*, 2014, **4**, 2387–2394; (*c*) F. Blanc, R. Berthoud, C. Copéret, A. Lesage, L. Emsley, R. Singh, T. Kreickmann and R. R. Schrock, *Proc. Natl. Acad. Sci. U.S.A.*, 2008, **105**, 12123–12127; (*d*) J. S. Kingsbury and A. H. Hoveyda, *J. Am. Chem. Soc.*, 2005, **127**, 4510–4517; (*e*) K. Paredes-Gil, X. Solans-Monfort, L. Rodriguez-Santiago, M. Sodupe and P. Jaque, *Organometallics*, 2014, **33**, 6065–6075; (*f*) P. E. Romero and W. E. Piers, *J. Am. Chem. Soc.*, 2005, **127**, 5032–5033; (*g*) M. S. Sanford, J. A. Love and R. H. Grubbs, *J. Am. Chem. Soc.*, 2001, **123**, 6543–6554; (*h*) S. Torker, M. J. Koh, R. K. M. Khan and A. H. Hoveyda, *Organometallics*, 2016, **35**, 543–562; (*i*) C. A. Urbina-Blanco, A. Poater, T. Lebl, S. Manzini, A. M. Z. Slawin, L. Cavallo and S. P. Nolan, *J. Am. Chem. Soc.*, 2013, **135**, 7073–7079; (*j*) T. Vorfalt, K.-J. Wannowius and H. Plenio, *Angew. Chem., Int. Ed.*, 2010, **49**, 5533–5536; (*k*) H. Wang and J. O. Metzger, *Organometallics*, 2008, **27**, 2761–2766; (*l*) A. G. Wenzel and R. H. Grubbs, *J. Am. Chem. Soc.*, 2006, **128**, 16048–16049.

5 For selected examples on the decomposition/deactivation of ruthenium-based olefin metathesis (pre-)catalysts, see: (*a*) G. A. Bailey and D. E. Fogg, *J. Am. Chem. Soc.*, 2015, **137**, 7318–7321; (*b*) M. B. Dinger and J. C. Mol, *Eur. J. Inorg. Chem.*, 2003, **2003**, 2827–2833; (*c*) M. B. Dinger and J. C. Mol, *Organometallics*, 2003, **22**, 1089–1095; (*d*) M. B. Herbert, Y. Lan, B. K. Keitz, P. Liu, K. Endo, M. W. Day, K. N. Houk and R. H. Grubbs, *J. Am. Chem. Soc.*, 2012, **134**, 7861–7866; (*e*) S. H. Hong, M. W. Day and R. H. Grubbs, *J. Am. Chem. Soc.*, 2004, **126**, 7414–7415; (*f*) S. H. Hong, A. G. Wenzel, T. T. Salguero, M. W. Day and R. H. Grubbs, *J. Am. Chem. Soc.*, 2007, **129**, 7961–7968; (*g*) B. J. Ireland, B. T. Dobigny and D. E. Fogg, *ACS Catal.*, 2015, **5**, 4690–4698; (*h*) E. M. Leitao, S. R. Dubberley, W. E. Piers, Q. Wu and R. McDonald, *Chem. – Eur. J.*, 2008, **14**, 11565–11572; (*i*) J. A. M. Lummiss, W. L. McClennan, R. McDonald and D. E. Fogg, *Organometallics*, 2014, **33**, 6738–6741; (*j*) A. Poater and L. Cavallo, *Theor. Chem. Acc.*, 2012, **131**, 1–6; (*k*) H. Werner, C. Grünwald, W. Stüer and J. Wolf, *Organometallics*, 2003, 22, 1558–1560.

6 For selected examples on the substrate reactivity in olefin metathesis reactions, see: (*a*) K. Lafaye, L. Nicolas, A. Guérinot, S. Reymond and J. Cossy, *Org. Lett.*, 2014, **16**, 4972–4975; (*b*) M. Ulman and R. H. Grubbs, *Organometallics*, 1998, **17**, 2484–2489.

7 T. M. Trnka and R. H. Grubbs, *Acc. Chem. Res.*, 2001, **34**, 18–29.

8 J. Cossy, S. Arseniyadis and C. Meyer, *Metathesis in Natural Product Synthesis: Strategies, Substrates and Catalysts*, Wiley-VCH Verlag GmbH & Co. KGaA, Weinheim, 2010.

9 R. H. Grubbs, A. G. Wenzel, D. J. O'Leary and E. Khosravi, *Handbook of Metathesis*, Wiley-VCH Verlag GmbH & Co. KGaA, 2nd edn, 2015, vol. 1–3.

10 For selected recent examples on the cross-metathesis with acrylates, see: (*a*) H. Fuwa, S. Matsukida, T. Miyoshi, Y.

View Article Online

Published on 30 September 2016. Downloaded by Universidade Federal do Rio Grande do Sul on 17/11/2016 13:12:40.

Kawashima, T. Saito and M. Sasaki, *J. Org. Chem.*, 2016, **81**, 2213–2227; (*b*) M. H. Nguyen, M. Imanishi, T. Kurogi and Smith A. B., *J. Am. Chem. Soc.*, 2016, **138**, 3675–3678; (*c*) N. Veerasamy, A. Ghosh, J. Li, K. Watanabe, J. D. Serrill, J. E. Ishmael, K. L. McPhail and R. G. Carter, *J. Am. Chem. Soc.*, 2016, **138**, 770–773; (*d*) G. Forcher, N. Clousier, A. Beauseigneur, P. Setzer, F. Boeda, M. S. M. Pearson-Long, P. Karoyan, J. Szymoniak and P. Bertus, *Synthesis*, 2015, **47**, 992–1006; (*e*) G. Luo, L. Chen, C. M. Conway, W. Kostich, J. E. Macor and G. M. Dubowchik, *Org. Lett.*, 2015, **17**, 5982–5985; (*f*) K. Ramakrishna and K. P. Kaliappan, *Org. Biomol. Chem.*, 2015, **13**, 234–240; (*g*) Q. Xiao, K. Young and A. Zakarian, *J. Am. Chem. Soc.*, 2015, **137**, 5907–5910; (*h*) T. T. Ho, T. Jacobs and M. A. R. Meier, *ChemSusChem*, 2009, **2**, 749–754; for examples where acrylic acid was employed as a cross-metathesis partner, see: (*i*) X. Meng, J. B. Matson and K. J. Edgar, *Biomolecules*, 2014, **15**, 177–187; (*j*) J. K. Lee, K.-B. Lee, D. J. Kim and I. S. Choi, *Langmuir*, 2003, **19**, 8141–8143.

11 J. A. M. Lummiss, K. C. Oliveira, A. M. T. Pranckevicius, A. G. Santos, E. N. dos Santos and D. E. Fogg, *J. Am. Chem. Soc.*, 2012, **134**, 18889–18891.

12 (*a*) H. Bonin, A. Keraani, J.-L. Dubois, M. Brandhorst, C. Fischmeister and C. Bruneau, *Eur. J. Lipid Sci. Technol.*, 2015, **117**, 209–216; (*b*) G. Ameh Abel, K. Oliver Nguyen, S. Viamajala, S. Varanasi and K. Yamamoto, *RSC Adv.*, 2014, **4**, 55622–55628; (*c*) X. Miao, C. Fischmeister, P. H. Dixneuf, C. Bruneau, J. L. Dubois and J. L. Couturier, *Green Chem.*, 2012, **14**, 2179–2183; (*d*) X. Miao, R. Malacea, C. Fischmeister, C. Bruneau and P. H. Dixneuf, *Green Chem.*, 2011, **13**, 2911–2919; (*e*) H. Bilel, N. Hamdi, F. Zagrouba, C. Fischmeister and C. Bruneau, *Green Chem.*, 2011, **13**, 1448–1452; (*f*) M. Abbas and C. Slugovc, *Tetrahedron Lett.*, 2011, **52**, 2560–2562; (*g*) R. Malacea, C. Fischmeister, C. Bruneau, J.-L. Dubois, J.-L. Couturier and P. H. Dixneuf, *Green Chem.*, 2009, **11**, 152–155; (*h*) G. B. Djigoué and M. A. R. Meier, *Appl. Catal., A*, 2009, **368**, 158–162; (*i*) A. Rybak and M. A. R. Meier, *Green Chem.*, 2008, **10**, 1099–1104; (*j*) M. Bieniek, A. Michrowska, D. L. Usanov and K. Grela, *Chem. – Eur. J.*, 2008, **14**, 806–818; (*k*) A. Rybak and M. A. R. Meier, *Green Chem.*, 2007, **9**, 1356–1361.

13 P. Compain, *Adv. Synth. Catal.*, 2007, **349**, 1829–1846.

14 Despite primary amines having a deleterious effect on olefin metathesis, the cross-metathesis of Brønsted acid masked alkenylamines with acrylates has been reported recently: N. D. Spiccia, S. Solyom, C. P. Woodward, W. R. Jackson and A. J. Robinson, *J. Org. Chem.*, 2016, **81**, 1798–1805.

15 R. Crabtree, *Chem. Rev.*, 2015, **115**, 127–150.

16 (*a*) P. Vignon, T. Vancompernolle, J.-L. Couturier, J.-L. Dubois, A. Mortreux and R. M. Gauvin, *ChemSusChem*, 2015, **8**, 1143–1146; for a study on the ethenolysis/propenolysis of crotonates, see: (*b*) D. Schweitzer and K. D. Snell, *Org. Process Res. Dev.*, 2015, **19**, 715–720.

17 The stability of Ru-enoic carbenes generated from **GII**/**HGII** is mostly speculative. Nevertheless, evidence points to very reactive species. For analogous complexes of the type $RuCl_2({=}CHCO_2R)(PCy_3)_2$ (R = Me, *p*-tolyl, *t*-butyl; i-propyl, cyclohexyl or 1-adamantyl), second order decomposition constants of the order 0.2–0.6 L mol^{-1} min^{-1} were obtained for C_6D_6 solutions at room temperature. See: M. Ulman, T. R. Belderrain and R. H. Grubbs, *Tetrahedron Lett.*, 2000, **41**, 4689–4693; later, it was shown that the Ru-enoic carbene formed *in situ* from **GII** is very reactive and was applied to open cyclohexene, a substrate generally unreactive in olefin metathesis. See: T.-L. Choi, C. W. Lee, A. K. Chatterjee and R. H. Grubbs, *J. Am. Chem. Soc.*, 2001, **123**(42), 10417–10418.

18 Some Brønsted or Lewis acids (*e.g.* HCl, CuCl) are known to affect the activity of ruthenium metathesis (pre-)catalysts. For selected examples of the effect of HCl on the outcome of metathesis reactions, see: positive effect: (*a*) J. Huang, H.-J. Schanz, E. D. Stevens and S. P. Nolan, *Organometallics*, 1999, **18**, 5375–5380; (*b*) D. M. Lynn, B. Mohr, R. H. Grubbs, L. M. Henling and M. W. Day, *J. Am. Chem. Soc.*, 2000, **122**, 6601–6609; (*c*) negative effect: S. Monsaert, N. Ledoux, R. Drozdzak and F. Verpoort, *J. Polym. Sci., Part A: Polym. Chem.*, 2010, **48**, 302–310; (*d*) for selected examples of the effect of copper salts on the outcome of metathesis reactions, see: K. Voigtritter, S. Ghorai and B. H. Lipshutz, *J. Org. Chem.*, 2011, **76**, 4697–4702; (*e*) M. Rivard and S. Blechert, *Eur. J. Org. Chem.*, 2003, 2225–2228; (*f*) interestingly, H_3PO_4 was found to have no effect on the outcome of the ring-opening metathesis polymerization of cyclooctadiene, catalyzed by the first-generation Grubbs metathesis (pre-)catalyst. See: S. J. P'Pool and H.-J. Schanz, *J. Am. Chem. Soc.*, 2007, **129**, 14200–14212; (*g*) acetic acid has been reported to prevent undesired isomerization during some olefin metathesis reactions catalyzed by **GII**. See: S. H. Hong, D. P. Sanders, C. W. Lee and R. H. Grubbs, *J. Am. Chem. Soc.*, 2005, **127**, 17160–17161.

19 J. M. Blacquiere, T. Jurca, J. Weiss and D. E. Fogg, *Adv. Synth. Catal.*, 2008, **350**, 2849–2855.

20 The use of Magnesol/Celite has been reported to dramatically improve the propenolysis of the soybean oil FAME (fatty acid methyl ester). See: (*a*) A. Nickel, T. Ung, G. Mkrtumyan, J. Uy, C. W. Lee, D. Stoianova, J. Papazian, W.-H. Wei, A. Mallari, Y. Schrodi and R. L. Pederson, *Top. Catal.*, 2012, **55**, 518–523; (*b*) other methods for treating bioderived metathesis feedstocks have also been described. For selected examples, see: J. Bidange, J.-L. Dubois, J.-L. Couturier, C. Fischmeister and C. Bruneau, *Eur. J. Lipid Sci. Technol.*, 2014, **116**, 1583–1589; (*c*) K. D. Uptain, C. Tanger and H. Kaido *US Pat.*, WO 2009020665A1, 2009; (*d*) D. W. Lemke, K. D. Uptain, F. Amore and T. Abraham, *US Pat.*, WO 200902667A1, 2009; (*e*) J.-L. Couturier and J.-L. Dubois, *US Pat.*, WO 2013017786A1, 2013.

21 L. M. Pitet and M. A. Hillmyer, *Macromolecules*, 2011, **44**, 2378–2381.

22 A. Rückert, P. H. Deshmukh and S. Blechert, *Tetrahedron Lett.*, 2006, **47**, 7977–7981.

23 Q. Yang, W.-J. Xiao and Z. Yu, *Org. Lett.*, 2005, **7**, 871–874.

24 M. Michaut, M. Santelli and J.-L. Parrain, *J. Organomet. Chem.*, 2000, **606**, 93–96.

This journal is © The Royal Society of Chemistry 2016

Published on 30 September 2016. Downloaded by Universidade Federal do Rio Grande do Sul on 17/11/2016 13:12:40.

25 A. Fürstner and K. Langemann, *J. Am. Chem. Soc.*, 1997, **119**, 9130–9136.

26 S. A. Cohen, D. R. Anderson, Z. Wang, T. M. Champagne and T. A. Ung, *US Pat.*, WO 2014150470A1, 2014.

27 A. K. Chatterjee, T.-L. Choi, D. P. Sanders and R. H. Grubbs, *J. Am. Chem. Soc.*, 2003, **125**, 11360–11370.

28 Exceptionally low catalyst loadings (**GII**) up to 1.01 ppm (effective TON = 440 000) had been reported for the SM of MO. See: M. B. Dinger and J. C. Mol, *Adv. Synth. Catal.*, 2002, **344**, 671–677.

29 C. A. Urbina-Blanco, S. Guidone, S. P. Nolan and C. S. J. Cazin, in *Olefin Metathesis: Theory and Practice*, John Wiley & Sons, Inc., 2014, pp. 417–436.

30 F. Boeda, H. Clavier and S. P. Nolan, *Chem. Commun.*, 2008, 2726–2740.

31 S. Monsaert, E. De Canck, R. Drozdzak, P. Van Der Voort, F. Verpoort, J. C. Martins and P. M. S. Hendrickx, *Eur. J. Org. Chem.*, 2009, **2009**, 655–665.

32 B. Allaert, N. Dieltiens, N. Ledoux, C. Vercaemst, P. Van Der Voort, C. V. Stevens, A. Linden and F. Verpoort, *J. Mol. Catal. A: Chem.*, 2006, **260**, 221–226.

33 S. Monsaert, A. Lozano Vila, R. Drozdzak, P. Van Der Voort and F. Verpoort, *Chem. Soc. Rev.*, 2009, **38**, 3360–3372.

34 A. Behr and S. Toepell, *J. Am. Oil Chem. Soc.*, 2015, **92**, 603–611.

35 N. Ledoux, R. Drozdzak, B. Allaert, A. Linden, P. Van Der Voort and F. Verpoort, *Dalton Trans.*, 2007, 5201–5210.

36 Cross-metathesis of vegetable oil derivatives with **MA-Me** had been reported previously. See: (*a*) R. Duque, E. Ochsner, H. Clavier, F. Caijo, S. P. Nolan, M. Mauduit and D. J. Cole-Hamilton, *Green Chem.*, 2011, **13**, 1187–1195; (*b*) A. Behr, S. Toepell and S. Harmuth, *RSC Adv.*, 2014, **4**, 16320–16326; (*c*) A. Behr, J. P. Gomes and Z. Bayrak, *Eur. J. Lipid Sci. Technol.*, 2011, **113**, 189–196.

37 No considerable influence of the alkoxy substituent bulkiness was observed in previous reports of the CM reaction with acrylates. Nevertheless, significantly higher catalyst loadings (0.5 or 5 mol% **HGII**) were employed. See ref. 11 and A. F. Newton, S. J. Roe, J.-C. Legeay, P. Aggarwal, C. Gignoux, N. J. Birch, R. Nixon, M.-L. Alcaraz and R. A. Stockman, *Org. Biomol. Chem.*, 2009, **7**, 2274–2277.

38 The carboxylate salt formed in the reaction of **MA-H** + PCy_3 could play a role in catalyst decomposition. A control reaction was conducted to test this hypothesis: 20 equivalents (*versus* **GII**) of disodium maleate were added to the reaction of **MO** with **MA-H** and the **MO** : (**MA-H** + disodium maleate) ratio was kept equal to 1 : 2 (**GII** = 0.05 mol%, 60 °C, 70 min, 1.5 mL of THF). An expressive decrease in both conversion and selectivity was observed (**MO** conversion = 61 %; CM yield = 24 % and SM yield = 36 %). Nevertheless, although the addition of 20 equivalents of the disodium maleate salt represents a maximum 40-fold increase in the concentration of the carboxylate anion, the results obtained under these conditions are still superior to those obtained using **GII** and **MA-Me** (see Fig. 6), confirming the overall positive effect of **MA-H**.

39 U. Biermann, U. Bornscheuer, M. A. R. Meier, J. O. Metzger and H. J. Schäfer, *Angew. Chem., Int. Ed.*, 2011, **50**, 3854–3871.

40 S. Chikkali and S. Mecking, *Angew. Chem., Int. Ed.*, 2012, **51**, 5802–5808.

41 United States Department of Agriculture, *Oil Crops Yearbook, Table 47: World vegetable oils supply and distribution*, 2011/12-2015/16, Accessed on May 18, 2016. http://ers.usda.gov/data-products/oil-crops-yearbook.

7 REFERENCES

1. Kamm, B.; Gruber, P. R.; Kamm, M. **Biorefineries**: Industrial Processes and Products; Vol. 1, Wiley-VCH Verlag GmbH: Weinheim, 2008.

2. van Leeuwen, P. W. N. M. **Homogeneous Catalysis**: Understanding the Art; 1 ed.; Kluwer Academic Publishers: the Netherlands, 2004.

3. **IUPAC Compendium of Chemical Terminology** - *Gold Book*; IUPAC, 2014; Vol. Version 2.3.3.

4. Grela, K. **Olefin Metathesis**: Theory and Practice; John Wiley & Sons, Inc: Hoboken, New Jersey, 2014.

5. Cossy, J.; Arseniyadis, S.; Meyer, C. **Metathesis in Natural Product Synthesis**: Strategies, Substrates and Catalysts; 1 ed.; Wiley-VCH: Germany, 2010.

6. Grubbs, R. H. *Handbook of Metathesis*; 1st ed.; Wiley-VCH: Weinheim, Germany, 2003.

7. Chauvin, Y. *Angew. Chem. Int. Ed.* **2006**, *45*, 3740-3747.

8. Schrock, R. R. *Angew. Chem. Int. Ed.* **2006**, *45*, 3748-3759.

9. Schaverien, C. J.; Dewan, J. C.; Schrock, R. R. *J. Am. Chem. Soc*. **1986**, *108*, 2771-2773.

10. Grubbs, R. H. *Angew. Chem. Int. Ed.* **2006**, *45*, 3760-3765.

11. Trnka, T. M.; Grubbs, R. H. *Acc. Chem. Res.* **2001**, *34*, 18-29.

12. Biermann, U.; Bornscheuer, U.; Meier, M. A. R.; Metzger, J. O.; Schäfer, H. J. *Angew. Chem. Int. Ed.* **2011**, *50*, 3854-3871.

13. Rybak, A.; Meier, M. A. R. *Green Chem.* **2007**, *9*, 1356-1361.

14. Nickel, A.; Pederson, R. L. **Commercial Potential of Olefin Metathesis of Renewable Feedstocks**. In *Olefin Metathesis*; John Wiley & Sons, Inc.: 2014, p 335.

15. Lummiss, J. A. M.; Oliveira, K. C.; Pranckevicius, A. M. T.; Santos, A. G.; dos Santos, E. N.; Fogg, D. E. *J. Am. Chem. Soc.* **2012**, *134*, 18889-18891.

16. Grau, E.; Mecking, S. *Green Chem.* **2013**, *15*, 1112-1115.

17. Mathers, R. T.; McMahon, K. C.; Damodaran, K.; Retarides, C. J.; Kelley, D. J. *Macromolecules* **2006**, *39*, 8982-8986.

18. Pletz, J.; http://www.chicagobusiness.com/article/20130718/BLOGS11/130719823/elevance-cranks-up-worlds-largest-biorefinery: 2013.

19. Bieniek, M.; Michrowska, A.; Usanov, D. L.; Grela, K. *Chem. -Eur. J.* **2008**, *14*, 806-818.

20. Bates, J. M.; Lummiss, J. A. M.; Bailey, G. A.; Fogg, D. E. *ACS Catal.* **2014**, *4*, 2387-2394.

21. Higman, C. S.; Lummiss, J. A. M.; Fogg, D. E. *Angew. Chem. Int. Ed.* **2016**, *55*, 3552-3565.

22. Grubbs, R. H.; Wenzel, A. G.; O'Leary, D. J.; Khosravi, E. **Handbook of Metathesis***;* 2nd ed, Vol. 1-3, Wiley-VCH Verlag GmbH & Co. KGaA, 2015.

23. Guidone, S.; Songis, O.; Nahra, F.; Cazin, C. S. J. *ACS Catal*. **2015**, *5*, 2697-2701.

24. Chatterjee, A. K.; Choi, T. L.; Sanders, D. P.; Grubbs, R. H. *J. Am. Chem. Soc*. **2003**, *125*, 11360-11370.

25. Fogg, D. E.; Foucault, H. **Transition Metal Catalysts in Organic Synthesis**: Ring-Opening Metathesis Polymerization, Vol. 11, Ch. 6.3, pp. 623-652. In Comprehensive Organometallic Chemistry III, editors R.H. Crabtree, D.M.P. Mingos, Elsevier, Oxford, 2007.

26. Schwab, P.; France, M. B.; Ziller, J. W.; Grubbs, R. H. *Angew. Chem., Int. Ed.* **1995**, *34*, 2039-2041.

27. Grela, K.; Harutyunyan, S.; Michrowska, A. *Angew. Chem. Int. Ed*. **2002**, *41* (*21*), 4038-4040.

28. Bieniek, M.; Bujok, R.; Cabaj, M.; Lugan, N.; Lavigne, G.; Arlt, D.; Grela, K. *J. Am. Chem. Soc*. **2006**, *128* (*48*), 13652-13653.

29. Savka, R. D.; Kos, P.; Plenio, H. *Adv. Synth. Catal*. **2013**, *355*, 439-447.

30. Veldhuizen, J. J.; Garber, S. B.; Kingsbury, J. S.; Hoveyda, A. H. *J. Am. Chem. Soc.* **2002**, *124* (*18*), 4954-4955.

31. Veldhuizen, J. J.; Gillinghan, D. G.; Garber, S. B.; Kataoba, O.; Hoveyda, A. H. *J. Am. Chem. Soc.* **2003**, *125* (*41*) 12502-12508.

32. Keitz, B. K.; Endo, K.; Patel, P. R.; Herbert, M. B.; Grubbs, R. H. *J. Am. Chem. Soc*. **2012**, *134* (*1*), 693-699.

33. Torker, S.; Khan, R. K. M.; Hoveyda, A. H. *J. Am. Chem. Soc*. **2014**, *136* (*9*), 3439-3455.

34. Samojłowicz, C.; Bieniek, M.; Grela, K. *Chem. Rev.* **2009**, *109*, 3708-3742.

354. Delaude, L.; Demonceau, A. *Dalton Trans.* **2012**, *41*, 9257-9268.

36. Boeda, F.; Clavier, H.; Nolan, S. P. *Chem. Commun.* **2008**, 2726-2740.

37. Dorta, R.; Kelly, R. A.; Nolan, S. P. *Adv. Synth. Catal.* **2004**, *346*, 917-920.

38. Randl, S.; Gessler, S.; Wakamatsu, H.; Blechert, S. *Synlett* **2001**, *03*, 430-432.

39. Smolen, M.; Kędziorek, M.; Grela, K. *Catal. Commun.* **2014**, *44*, 80-84.

40. Barbasiewicz, M.; Malińska, M.; Błocki, K. *J. Organomet. Chem.* **2013**, *8*, *745-746*.

41. Barbasiewicz, M.; Blocki, K.; Malińska, M.; Pawlowski, R. *Dalton Trans.* **2013**, *42*, 355-358.

42. Savka, R.; Foro, S.; Gallei, M.; Rehahn, M.; Plenio, H. *Chem. – Eur. J.* **2013**, *19*, 10655-10662.

43. Kos, P.; Savka, R.; Plenio, H. *Adv. Synth. Catal.* **2013**, *355*, 439-447.

44. Bantreil, X.; Poater, A.; Urbina-Blanco, C. A.; Bidal, Y. D.; Falivene, L.; Randall, R. A. M.; Cavallo, L.; Slawin, A. M. Z.; Cazin, C. S. J. *Organometallics* **2012**, *31*, 7415-7426.

45. Skowerski, K.; Wierzbicka, C.; Szczepaniak, G.; Gulajski, L.; Bieniek, M.; Grela, K. *Green Chem.* **2012**, *14*, 3264-3268.

46. Skowerski, K.; Szczepaniak, G.; Wierzbicka, C.; Gulajski, L.; Bieniek, M.; Grela, K. *Catal. Sci. Technol.* **2012**, *2*, 2424-2427.

47. Rix, D.; Caijo, F.; Laurent, I.; Boeda, F.; Clavier, H.; Nolan, S. P.; Mauduit, M. *J. Org. Chem.* **2008**, *73*, 4225-4228.

48. Lozano-Vila, A. M.; Monsaert, S.; Bajek, A.; Verpoort, F. *Chem. Rev*. **2010**, *110*, 4865-4909.

49. Shaffer, E. A.; Chen, C. -L.; Beatty, A. M.; Valente, E. J.; Schanz, H. –J. *J. Organomet. Chem*. **2007**, *692*, 5221-5233.

50. Pump, E.; Slugovac, C.; Cavallo, L.; Poater, A. *Organometallics* **2015**, *34*, 3107-3111.

51. O'Leary Havelka, K.; Gerhardt, G. E. **Green Polymer Chemistry: Biobased Materials and Biocatalysis**; American Chemical Society, 2015.

52. Adlhart, C.; Chen, P. *J. Am. Chem. Soc.* **2004**, *126*, 3496-3510.

53. Blanc, F.; Berthoud, R.; Copéret, C.; Lesage, A.; Emsley, L.; Singh, R.; Kreickmann, T.; Schrock, R. R. *P. Natl. Acad. Sci. USA* **2008**, *105*, 12123-12127.

54. Kingsbury, J. S.; Hoveyda, A. H. *J. Am. Chem. Soc.* **2005**, *127*, 4510-4517.

55. Paredes-Gil, K.; Solans-Monfort, X.; Rodriguez-Santiago, L.; Sodupe, M.; Jaque, P. *Organometallics* **2014**, *33*, 6065-6075.

56. Romero, P. E.; Piers, W. E. *J. Am. Chem. Soc.* **2005**, *127*, 5032-5033.

57. Sanford, M. S.; Love, J. A.; Grubbs, R. H. *J. Am. Chem. Soc.* **2001**, 123, 6543-6554.

58. Torker, S.; Koh, M. J.; Khan, R. K. M.; Hoveyda, A. H. *Organometallics* **2016**, *35*, 543-562.

59. Urbina-Blanco, C. A.; Poater, A.; Lebl, T.; Manzini, S.; Slawin, A. M. Z.; Cavallo, L.; Nolan, S. P. *J. Am. Chem. Soc.* **2013**, *135*, 7073-7079.

60. Vorfalt, T.; Wannowius, K.-J.; Plenio, H. *Angew. Chem. Int. Ed*. **2010**, *49*, 5533-5536.

61. Wang, H.; Metzger, J. O. *Organometallics* **2008**, *27*, 2761-2766.

62. Wenzel, A. G.; Grubbs, R. H. *J. Am. Chem. Soc*. **2006**, *128*, 16048-16049.

63. Bailey, G. A.; Fogg, D. E. *J. Am. Chem. Soc.* **2015**, *137*, 7318-7321.

64. Dinger, M. B.; Mol, J. C. *Eur. J. Inorg. Chem.* **2003**, *2003* (*15*), 2827-2833.

65. Dinger, M. B.; Mol, J. C. *Organometallics* **2003**, *22*, 1089-1095.

66. Herbert, M. B.; Lan, Y.; Keitz, B. K.; Liu, P.; Endo, K.; Day, M. W.; Houk, K. N.; Grubbs, R. H. *J. Am. Chem. Soc.* **2012**, *134*, 7861-7866.

67. Hong, S. H.; Day, M. W.; Grubbs, R. H. *J. Am. Chem. Soc.* **2004**, *126*, 7414-7415.

68. Hong, S. H.; Wenzel, A. G.; Salguero, T. T.; Day, M. W.; Grubbs, R. H. *J. Am. Chem. Soc.* **2007**, *129*, 7961-7968.

69. Ireland, B. J.; Dobigny, B. T.; Fogg, D. E. *ACS Catal.* **2015**, *5*, 4690-4698.

70. Leitao, E. M.; Dubberley, S. R.; Piers, W. E.; Wu, Q.; McDonald, R. *Chem. Eur. J.* **2008**, *14*, 11565-11572.

71. Lummiss, J. A. M.; McClennan, W. L.; McDonald, R.; Fogg, D. E. *Organometallics* **2014**, *33*, 6738-6741.

72. Poater, A.; Cavallo, L. *Theor. Chem. Acc.* **2012**, *131*, 1-6.

73. Werner, H.; Grünwald, C.; Stüer, W.; Wolf, J. *Organometallics* **2003**, *22*, 1558-1560.

74. Lafaye, K.; Nicolas, L.; Guérinot, A.; Reymond, S.; Cossy, J. *Org. Lett.* **2014**, *16*, 4972-4975.

75. Ulman, M.; Grubbs, R. H. *Organometallics* **1998**, *17*, 2484-2489.

76. Thiel, V.; Hendann, M.; Wannowius, K. -J.; Plenio, H. *J. Am. Chem. Soc*. **2012**, *134*, 1104-1114.

77. Fuwa, H.; Matsukida, S.; Miyoshi, T.; Kawashima, Y.; Saito, T.; Sasaki, M. *J. Org. Chem.* **2016**, *81*, 2213-2227.

78. Nguyen, M. H.; Imanishi, M.; Kurogi, T.; Smith, A. B. *J. Am. Chem. Soc.* **2016**, *138*, 3675-3678.

79. Veerasamy, N.; Ghosh, A.; Li, J.; Watanabe, K.; Serrill, J. D.; Ishmael, J. E.; McPhail, K. L.; Carter, R. G. *J. Am. Chem. Soc.* **2016**, *138*, 770-773.

80. Forcher, G.; Clousier, N.; Beauseigneur, A.; Setzer, P.; Boeda, F.; Pearson-Long, M. S. M.; Karoyan, P.; Szymoniak, J.; Bertus, P. *Synthesis* **2015**, *47*, 992-1006.

81. Luo, G.; Chen, L.; Conway, C. M.; Kostich, W.; Macor, J. E.; Dubowchik, G. M. *Org. Lett.* **2015**, *17*, 5982-5985.

82. Ramakrishna, K.; Kaliappan, K. P. *Org. Biomol. Chem.* **2015**, *13*, 234-240.

83. Xiao, Q.; Young, K.; Zakarian, A. *J. Am. Chem. Soc.* **2015**, *137*, 5907-5910.

84. Ho, T. T.; Jacobs, T.; Meier, M. A. R. *ChemSusChem* **2009**, *2*, 749-754.

85. Meng, X.; Matson, J. B.; Edgar, K. J. *Biomolecules* **2014**, *15*, 177-187.

86. Lee, J. K.; Lee, K. -B.; Kim, D. J.; Choi, I. S. *Langmuir* **2003**, *19*, 8141-8143.

87. Bonin, H.; Keraani, A.; Dubois, J. -L.; Brandhorst, M.; Fischmeister, C.; Bruneau, C. *Eur. J. Lipid Sci. Technol.* **2015**, *117*, 209-216.

88. Abel, G. A.; Nguyen, K. O.; Viamajala, S.; Varanasi, S.; Yamamoto, K. *RSC Adv.* **2014**, *4*, 55622-55628.

89. Miao, X.; Fischmeister, C.; Dixneuf, P. H.; Bruneau, C.; Dubois, J. -L.; Couturier, J. -L. *Green Chem.* **2012**, *14*, 2179-2183.

90. Miao, X.; Malacea, R.; Fischmeister, C.; Bruneau, C.; Dixneuf, P. H. *Green Chem.* **2011**, *13*, 2911-2919.

91. Bilel, H.; Hamdi, N.; Zagrouba, F.; Fischmeister, C.; Bruneau, C. *Green Chem.* **2011**, *13*, 1448-1452.

92. Abbas, M.; Slugovc, C. *Tetrahedron Lett.* **2011**, *52*, 2560-2562.

93. Malacea, R.; Fischmeister, C.; Bruneau, C.; Dubois, J. -L.; Couturier, J. -L.; Dixneuf, P. H. *Green Chem.* **2009**, *11*, 152-155.

94. Djigoué, G. B.; Meier, M. A. R. *Appl. Catal. A-Gen.* **2009**, *368*, 158-162.

95. Rybak, A.; Meier, M. A. R. *Green Chem.* **2008**, *10*, 1099-1104.

96. Kingsbury, J. S.; Harrity, J. P. A.; Bonitatebus Jr, P. J.; Hoveyda, A. H. *J. Am. Chem. Soc.* **1999**, *121*, 791-799.

97. Vorfalt, T.; Wannowius, K. J.; Thiel, V.; Plenio, H. *Chem. -Eur. J*. **2010**, *16*, 12312−12315.

98. Nuñes-Zarur, F.; Solans-Monfort, X.; Pleixats, R.; Rodríguez-Santiago, L.; Sodupe, M. *Chem. -Eur. J*. **2013**, *19*, 14553−14565.

99. Lummis, J. A. M.; Beach, N. J.; Smith, J.; Fogg, D. E. *Catal. Sci. Technol*. **2012**, *2*, 1630-1632.

100. Ulman, M.; Belderrain, T. R.; Grubbs. *Tetrahedron Lett*. **2000**, *41* (*24*), 4689-4693.

101. Choi, T. -L.; Lee, C. W.; Chatterjee, A. K.; Grubbs, R. H. *J. Am. Chem. Soc.* **2001**, *123* (42), 10417–10418.

102. Randl, S.; Connon, S. J.; Blechert, S. *Chem. Commun*. **2001**, 1796-1797.

103. Fomine, S.; Tlenkopatchev, M. A. Organometallics **2007**, *26* (*18*), 4491-4497.

104. Pitet, L. M.; Hillmyer, M. A. *Macromolecules* **2011**, *44*, 2378-2381.

105. Park, S. –B.; Sakata, N.; Nihiyama, H. *Chem. Eur. J*. **1996**, *2*, 303-306.

106. Baratta, W.; Herrmann, W. A.; Rigo, P.; Schwarz, J. *J. Organomet. Chem.* **2000**, *593-594*, 489-493.

107. Che, C. –M.; Huang, J. –S.; Lee, F. –W.; Li, Y.; Lai, T. –S.; Kwong, H. –L.; Teng, P. –F.; Lee, W. –S.; Lo, W. –C.; Peng, S. –M.; Zhou, Z. –Y. *J. Am. Chem. Soc*. **2001**, *123*, 4119-4129.

108. Shishkov, I. V.; Rominger, F.; Hofmann, P. *Organometallics* **2009,** *28 (4),* 1049-1059.

109. http://www.materia-inc.com/ Accessed on August 27.

110. http://chemistry.umicore.com/Products/#tax_metal_ms=Ruthenium Accessed on August 27.

111. Llevot, A.; Meier, M. A. R. *Green Chem*. **2016**, Editorial. DOI: 10.1039/c6gc90087a.

112. Peng, Y.; Totsingan, F.; Meier, M. A. R.; Steinmann, M.; Wurm, F.; Koh, A.; Gross, R. A. *Eur. J. Lipid. Technol*. **2015**, *117*, 217-228.

113. Peng, Y.; Decatur, J.; Meier, M. A. R.; Gross, R. A. *Macromolecules* **2013**, *46*, 3293-3300.

114. Winkler, M.; Lacerda, T. M.; Mack, F.; Meier, M. A. R. *Macromolecules* **2015**, *48*, 1398-1403.

115. Mathers, R. T.; Shreve, M. J.; Meyler, E.; Damodaran, K.; Iwig, D. F.; Kelley, D. J. *Macromol. Rapid Commun.* **2011**, *32*, 1338-1342.

116. Abbas, M.; Slugovc, C. *Monatsh Chem*. **2012**, *143*, 669–673.

117. Grubbs, R. H.; Trnka, T. M, Sanford, M. S. **Transition Metal-Carbene Complexes in Olefin Metathesis and Related Reactions**. In Current Methods in Inorganic Chemistry, vol 3, 187-231.

118. Herrmann, W. A. *Angew. Chem. Int. Ed.* **2002**, *41*, 1290-1309.

119. Nolan, S. P. **N-Heterocyclic Carbenes**: Effective tools for Organometallic Synthesis. Viley-VCH, Weinhein, Germany, 2014.

120. Glorius, F. **Topics in Organometallic Chemistry** vol 21: H-Heterocyclic Carbenes in Transition Metal Catalysis. Springer-Verlag, Berlin, Germany, 2007.

121. Nickel, A.; Ung, T.; Mkrtumyan, G.; Uy, J.; Lee, C. W.; Stoianova, D.; Papazian, J.; Wei, W.-H.; Mallari, A.; Schrodi, Y.; Pederson, R. L. *Top. Catal*. **2012**, *55*, 518-523.

122. Bidange, J.; Dubois, J. -L.; Couturier, J. -L.; Fischmeister, C.; Bruneau, C. *Eur. J. Lipid. Sci. Technol*. **2014**, *116*, 1583-1589.

123. Uptain, K. D.; Tanger, C.; Kaido, H. US Patent WO 2009020665 A1.

124. Lemke, D. W.; Uptain, K. D.; Amore, F.; Abraham, T. US Patent WO 200902667 A1.

125. Couturier, J. -L.; Dubois, J. -L. US Patent WO 2013017786 A1.

126. Rückert, A.; Deshmukh, P. H.; Blechert, S. *Tetrahedron Lett.* **2006**, *47*, 7977-7981.

127. Yang, Q.; Xiao, W.-J.; Yu, Z. *Org. Lett.* **2005**, *7*, 871-874.

128. Michaut, M.; Santelli, M.; Parrain, J.-L. *J. Organomet. Chem.* **2000**, *606*, 93-96.

129. Fürstner, A.; Langemann, K. *J. Am. Chem. Soc.* **1997**, *119*, 9130-9136.

130. Cohen, S. A.; Anderson, D. R.; Wang, Z.; Champagne, T. M.; Ung, T. A. US Patent WO 2014150470 A1.

131. Vignon, P.; Vancompernolle, T.; Couturier, J.-L.; Dubois, J.-L.; Mortreux, A.; Gauvin, R. M. Che*mSusChem.* **2015**, *8*, 1143-1146.

132. Exceptionally low catalyst loadings (**GII**) up to 1.01 ppm (Effective TON = 440,000) had been reported for the SM of **MO**. See: Dinger, M. B.; Mol, J. C. *Adv. Synth. Catal*. **2002**, *344*, 671-677.

133. Urbina-Blanco, C. A.; Guidone, S.; Nolan, S. P.; Cazin, C. S. J. **Olefin Metathesis**: Theory and Practice; John Wiley & Sons, Inc., 2014, 417-436.

134. Monsaert, S.; De Canck, E.; Drozdzak, R.; van der Voort, P.; Verpoort, F.; Martins, J. C.; Hendrickx, P. M. S. *Eur. J. Org. Chem.* **2009**, *2009* (*5*), 655-665.

135. Allaert, B.; Dieltiens, N.; Ledoux, N.; Vercaemst, C.; van ver Voort, P.; Stevens, C. V.; Linden, A.; Verpoort, F. *J. Mol. Catal. A-Chem.* **2006**, *260*, 221-226.

136. Monsaert, S.; Lozano Vila, A.; Drozdzak, R.; van der Voort, P.; Verpoort, F. *Chem. Soc. Rev.* **2009**, *38*, 3360-3372.

137. Behr, A.; Toepell, S. *J. Am. Oil Chem. Soc.* **2015**, *92*, 603-611.

138. Ledoux, N.; Drozdzak, R.; Allaert, B.; Linden, A.; van der Voort, P.; Verpoort, F. *Dalton Trans.* **2007**, 5201-5210.

139. Duque, R.; Ochsner, E.; Clavier, H.; Caijo, F.; Nolan, S. P.; Mauduit, M.; Cole-Hamilton, D. J. *Green Chem*. **2011**, *13*, 1187-1195.

140. Behr, A.; Toepell, S.; Harmuth, S. *RSC Adv.* **2014**, *4*, 16320-16326.

141. Behr, A.; Gomes, J. P.; Bayrak, Z. *Eur. J. Lipid Sci. Tech.* **2011**, *113*, 189-196.

142. Newton, A. F.; Roe, S. J.; Legeay, J. -C.; Aggarwal, P.; Gignoux, C.; Birch, N. J.; Nixon, R.; Alcaraz, M. -L.; Stockman, R. A. *Org. Biomol. Chem*. **2009**, *7*, 2274-2277.

143. Chikkali, S.; Mecking, S. *Angew. Chem. Int. Ed.* **2012**, *51*, 5802-5808.

144. United States Department of Agriculture, Oil Crops Yearbook, Table 47: World vegetable oils supply and distribution, 2011/12-2015/16. http://ers.usda.gov/data-products/oil-crops-yearbook Accessed on May 18, 2016.

145. Lehman Jr., S. E.; Wagener, K. B. *Organometallics* **2005**, *24*, 1477-1482.

146. Hersh, W. H.; Lam, S. T.; Moskovic, D. J.; Panajiotakis, A. J.; *J. Org. Chem.* **2012**, *77* (*11*), 4968-4979.

147. Ogata, O.; Nakayama, Y.; Nara, H.; Fujiwhara, M.; Kayaki, Y. *Org. Lett*. **2016**, *18*, 3894-3897.

148. Lummiss, J. A. M.; Beach, N. J.; Smith, J. C.; Fogg, D. E. *Catal. Sci. Technol*. **2012**, *2*, 1630-1632.

149. Burling, S.; Mas-Marzá, E.; Valpuesta, J. E. V.; Mahon, M. F.; Whittlesey, M. K. *Organometallics* **2009**, *28*, 6676–6686.

150. Beach, N. J.; Blacquiere, J. M.; Drouin, S. D.; Fogg, D. E. *Organometallics* **2009**, *28,* 441-447.

151. Burling, S.; Paine, B. M.; Nama, D.; Brown, V.S.; Mahon, M. F.; Prior, T. J.; Pregosin, P. S.; Whittlesey, M. K.; Williams, J. M. J.; *J. Am. Chem. Soc*. **2007**, *129*, 1987-1995.

152. Giunta, D.; Hölscher, M.; Lehmann, C. W.; Mynott, R.; Wirtz, C.; Leitner, W. *Adv. Synth. Catal*. **2003**, *345*, 1139-1145.

153. Weskamp, T.; Kohl, F. J.; Herrmann, W. A. *J. Organomet. Chem*. **1999**, *582*, 362-365.

154. Al-Hashimi, M.; Bakar, M. D. A.; Elsaid, K.; Bergbreiterc, D. E.; Bazzi, H. S. *RSC Adv*. **2014**, *4*, 43766-43771.

155. Castarlenas, R.; Vovard, C.; Fischmeister, C.; Dixneuf, P. H. *J. Am. Chem. Soc.* **2006**, *128*, 4079-4089.

156. Ahr, M.; Thieuleux, C.; Copéret, C.; Fenet, B.; Basset, J. -M. *Adv. Synth.Catal.* **2007**, *349*, 1587-1591.

157. Buchmeiser, M. R.; Wang, D.; Zhang, Y.; Naumov, S.; Wurst, K. *Eur. J. Inorg. Chem.* **2007**, *2007* (*25*), 3988-4000.

158. Dragutan, V.; Dragutan, I.; Delaude, L.; Demonceau, A. *Coord. Chem. Rev.* **2007**, *251*, 765-794.

159. Fürstner, A.; Liebl, M.; Lehmann, C. W.; Picquet, M.; Kunz, R.; Bruneau, C.; Touchard, D.; Dixneuf, P. H. *Chem. –Eur. J.* **2000**, *6*, 1847-1857.

160. Ledoux, N.; Allaert, B.; Verpoort, F. *Eur. J. Inorg. Chem.* **2007**, *2007* (*35*), 5578-5583.

161. Bennett, M. A.; Huang, T. N.; Matheson, T. W.; Smith, A. K.; Ittel, S.; Nickerson, W. **Inorganic Syntheses**; John Wiley & Sons, Inc.: 2007; Vol. 21, p 74.

162. Evans, I. P.; Spencer, A.; Wilkinson, G. *J. Chem. Soc. Dalton Trans.* **1973**, 204-209.

163. Alessio, E. *Chem. Rev.* **2004**, *104*, 4203-4242.

164. Alessio, E.; Mestroni, G.; Nardin, G.; Attia, W. M.; Calligaris, M.; Sava, G.; Zorzet, S. *Inorg. Chem.***1988**, *27*, 4099-4106.

165. Alessio, E.; Milani, B.; Bolle, M.; Mestroni, G.; Faleschini, P.; Todone, F.; Geremia, S.; Calligaris, M. *Inorg. Chem.* **1995**, *34*, 4722-4734.

166. Abdallaoui, I. A.; Sémeril, D.; Dixneuf, P. H. *J. Mol. Catal. A: Chem.* **2002**, *182-183*, 577-583.

167. Blacquiere, J. M.; Jurca, T.; Weiss, J.; Fogg, D. E. *Adv. Synth. Catal.* **2008**, *350*, 2849-2855.

168. Arduengo, A. J.; Krafczyk, R.; Schmutzler, R.; Craig, H. A.; Goerlich, J. R.; Marshall, W. J.; Unverzagt, M. *Tetrahedron* **1999**, *55*, 14523-14534.

169. Grasa, G. A.; Viciu, M. S.; Huang, J.; Nolan, S. P. *J. Org. Chem.* **2001**, *66*, 7729-7737.

170. Marciniec, B.; Rogalski, S.; Potrzebowski, M. J.; Pietraszuk, C. *ChemCatChem.* **2011**, *3*, 904-910.

171. Fürstner, A.; Guth, O.; Düffels, A.; Seidel, G.; Liebl, M.; Gabor, B.; Mynott, R. *Chem. –Eur. J.* **2001**, *7*, 4811-4820.

172. Amoroso, D.; Yap, G. P. A.; Fogg, D. E. *Organometallics* **2002**, *21*, 3335-3343.

173. Esteruelas, M. A.; Gómez, A. V.; Lahoz, F. J.; López, A. M.; Oñate, E.; Oro, L. A. *Organometallics* **1996**, *15*, 3423-3435.

174. Esteruelas, M. A.; Gómez, A. V.; López, A. M.; Modrego, J.; Oñate, E. *Organometallics* **1998**, *17*, 5434-5436.

175. Arikawa, Y.; Nishimura, Y.; Kawano, H.; Onishi, M. *Organometallics* **2003**, *22*, 3354-3356.